AD-A064 943 CALIFORNIA UNIV LOS ANGELES SCHOOL OF ENGINEERING A--ETC F/G 20/13
CONVECTIVE HEAT AND MASS TRANSFER TO RE-ENTRY VEHICLES.(U)
DEC 78 A F MILLS AFOSR-76-2931

UNCLASSIFIED UCLA-ENG-7982 AFOSR-TR-79-0030 NL

1 OF 3
AD A064943

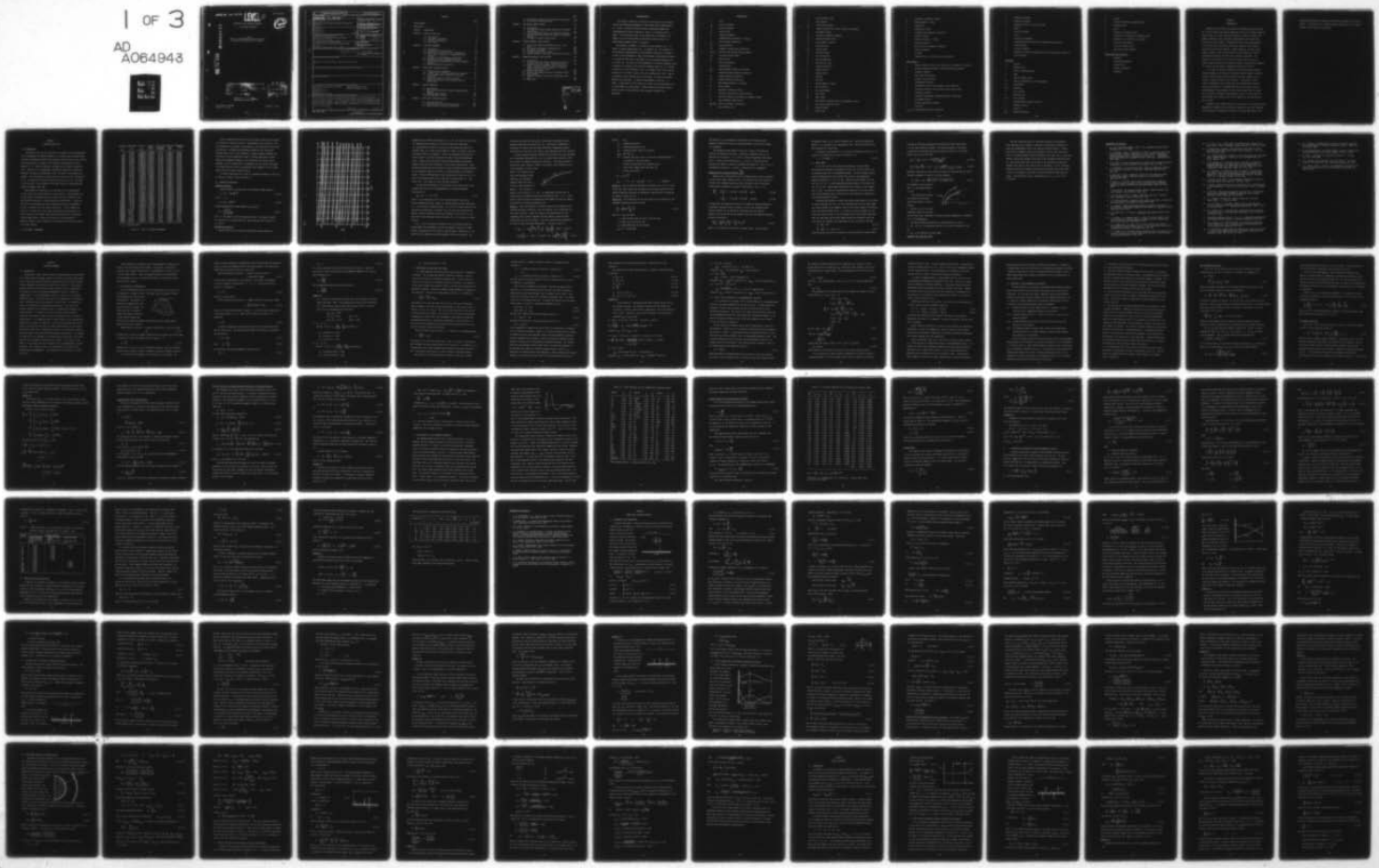

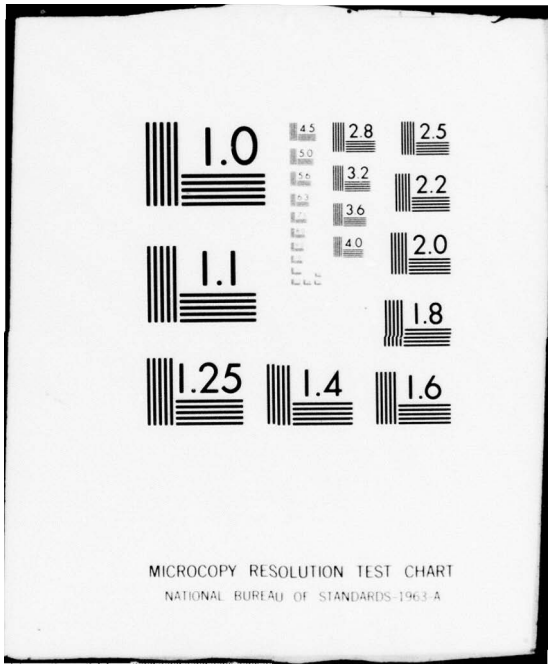
1.0
1.1
1.25
1.4
1.6
1.8
2.0
2.2
2.5
2.8
3.2
3.6
4.0
4.5
5.0
5.6
6.3
MICROCOPY RESOLUTION TEST CHART
NATIONAL BUREAU OF STANDARDS-1963-A

LEVEL II

UCLA-ENG-7892

CONVECTIVE HEAT AND MASS TRANSFER TO RE-ENTRY VEHICLES

A. F. Mills
School of Engineering and Applied Science
University of California, Los Angeles

Final Report on AFOSR
Grant No. 76-2931A

December 1, 1978

SECURITY CLASSIFICATION OF THIS PAGE (When Data Entered)

REPORT DOCUMENTATION PAGE

READ INSTRUCTIONS BEFORE COMPLETING FORM

1. REPORT NUMBER: AFOSR-TR-79-0030	2. GOVT ACCESSION NO.
3. RECIPIENT'S CATALOG NUMBER	
4. TITLE (and Subtitle): CONVECTIVE HEAT AND MASS TRANSFER TO RE-ENTRY VEHICLES.	5. TYPE OF REPORT & PERIOD COVERED: FINAL rept. 1 Oct 75 - 30 Sep 78
	6. PERFORMING ORG. REPORT NUMBER: UCLA-ENG-7982
7. AUTHOR(s): A F MILLS	8. CONTRACT OR GRANT NUMBER(s): AFOSR 76-2931 new
9. PERFORMING ORGANIZATION NAME AND ADDRESS: UNIVERSITY OF CALIFORNIA, SCHOOL OF ENGINEERING & APPLIED SCIENCE, LOS ANGELES, CA 90024	10. PROGRAM ELEMENT, PROJECT, TASK AREA & WORK UNIT NUMBERS: 2307A1, 61102F, A1
11. CONTROLLING OFFICE NAME AND ADDRESS: AIR FORCE OFFICE OF SCIENTIFIC RESEARCH/NA, BLDG 410, BOLLING AIR FORCE BASE, D C 20332	12. REPORT DATE: 1 Dec 78
	13. NUMBER OF PAGES: 254
14. MONITORING AGENCY NAME & ADDRESS (if different from Controlling Office) 255p.	15. SECURITY CLASS. (of this report): UNCLASSIFIED
	15a. DECLASSIFICATION/DOWNGRADING SCHEDULE

16. DISTRIBUTION STATEMENT (of this Report)

Approved for public release; distribution unlimited.

17. DISTRIBUTION STATEMENT (of the abstract entered in Block 20, if different from Report)

18. SUPPLEMENTARY NOTES

19. KEY WORDS (Continue on reverse side if necessary and identify by block number)

CONVECTIVE HEAT AND MASS TRANSFER
DIFFUSION
SURFACE CHEMISTRY
ABLATION
TRANSPIRATION COOLING
LAMINAR BOUNDARY LAYERS
TURBULENT BOUNDARY LAYERS

20. ABSTRACT (Continue on reverse side if necessary and identify by block number)

The analysis of convective heat and mass transfer to re-entry vehicles is reviewed with particular emphasis on relevant basic mass transfer theory. The topics covered include: the inviscid flow field, diffusion phenomena, simple mass transfer analyses, surface chemistry, simple heat transfer analyses, the surface energy balance, laminar boundary layer analysis, and turbulent boundary layer analysis.

404 637

DD FORM 1 JAN 73 1473

UNCLASSIFIED

SECURITY CLASSIFICATION OF THIS PAGE (When Data Entered)

CONTENTS

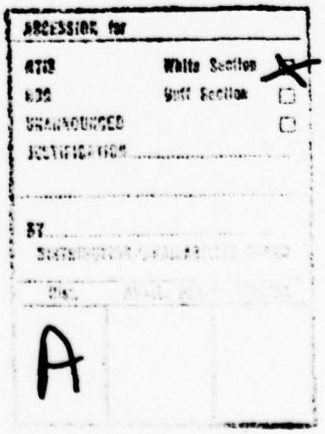

ACKNOWLEDGMENTS

This project started as a series of lectures given in the Missile Systems and Technology Department of TRW Systems Group, Redondo Beach, CA, in 1974. During this lecture series considerable support and encouragement was given by Messers D. Baer, H. R. Wilkinson and A. V. Gomez. In continuing the work at the University of California, Los Angeles, on an Air Force Office of Scientific Research Grant, the AFOSR project manager was Mr. P. Thurston.

The material in Chapter 2 is based on notes prepared by Dr. A. T. Wassel of Science Applications Inc., El Segundo, CA. The treatment of the bifurcation approximation to multicomponent diffusion in Chapter 3, as well as the development of open system chemical equilibrium in Chapter 5, is based on work done in the 1960's by the Aerotherm Corporation of Palo Alto, CA. The review of the fundamentals of turbulent boundary layers in Chapter 9 is based on "The Turbulent Boundary Layer" by F. H. Clauser in *Advances in Applied Mechanics*, Vol. IV, Academic Press, 1956, and the textbook by F. M. White, *Viscous Fluid Flow*, McGraw Hill, 1974. Some of my students at UCLA provided various assistance, in particular Douglas Hatfield and Seung Rhee. A special acknowledgment is due Mr. A. V. Gomez: in many parts of this report are results of work performed by us at TRW Systems as a joint effort. Finally thanks are due Mrs. Phyllis Gilbert and Ms. Lesley Bacha for their competent typing of the manuscript.

NOMENCLATURE

A	area
a_p	particle diameter
B	blowing parameter
B'	driving force
$\mathcal{B}$	bluntness parameter
C	Chapman-Rubesin parameter ($= \rho\mu/\rho_e\mu_e$)
C_F	skin friction coefficient
C_D	drag coefficient
C_d	roughness elements drag coefficient
C_H, C_M	heat and mass transfer Stanton numbers
C_h	sub-layer Stanton number
C_p	specific heat
c	molar concentration
c	atoms/molecule
D_{ij}	multicomponent diffusion coefficient
$\bar{D}$	reference binary diffusion coefficient
$\mathcal{D}$	binary diffusion coefficient
D_i^T	thermal diffusion coefficient
E	Mach number parameter ($= u_e^2/2H_e$)
Ec	Eckert number
F	force/mole; diffusion factor
f	force/lb; dimensionless stream function
h	sensible enthalpy; characteristic roughness height
H	total enthalpy; shape factor
$\Delta H_r, \Delta H_d$	heats of reaction, dissociation
j	mass diffusive flux

J	molar diffusive flux
K	mass fraction
K_p	equilibrium constant
k	thermal conductivity; kinetic energy of turbulence
$\mathcal{k}$	Boltzmann constant
k_s	equivalent sandgrain roughness
k_T	thermal diffusion ratio
Le	Lewis number (= Pr/Sc)
ℓ	mean free path
ℓ_m	mixing length
M	molecular weight
m	mass of molecule
$\dot{m}$	mass transfer rate
n	absolute mass flux
N	absolute molar flux
n	number fraction
N	number density
P	pressure
q	heat flux
Pr	Prandtl number (= $C_p\mu/k$)
R	gas constant/lb
$\mathcal{R}$	gas constant/mole
R_N	nose radius
R_S	shock radius
r	body radius; recovery factor; stoichiometric ratio
$\dot{r}$	mass species generation rate
Re	Reynolds number
S	source term

s	streamwise coordinate; entropy
Sc	Schmidt number (= $\nu/\mathcal{D}_{12}$)
T	temperature
U	oncoming air speed
u,v	streamwise and transverse velocities
v	absolute velocity
v*	friction velocity (= $\sqrt{\tau_w/\rho}$)
$\hat{v}$	diffusion velocity
x	mole fraction; streamwise coordinate
y	normal coordinate
Z	altitude
z	compressibility; z-fraction; axial coordinate

Greek Symbols

α	thermal diffusion factor; mass fraction of an element in a species
β	pressure gradient parameter; Clauser equilibrium parameter
γ	adiabatic exponent
Δ	shock stand-off distance
δ	boundary layer thickness
δ^*	displacement thickness
ε	intermolecular force law parameter; eddy diffusivity
ζ	similarity variable; static density ratio across shock
η	similarity variable
θ	normalized temperature; momentum thickness; body angle
κ	von Karman constant
λ	mixing length model parameter
μ	viscosity
μ_1,μ_2,μ_3	multicomponent mixture properties

ν	kinematic viscosity
ξ	similarity variable
Π	parameter in Cole's "law of the wake"
ρ	density
σ	collision diameter
τ	stress
Φ	mixture rule parameter
ϕ	intermolecular force potential; normalized mass fraction
ψ	stream function
Ω	collision integral
ω	exponent in viscosity-enthalpy power law relationship; normalized stream function

Subscripts

a	ablation
bl	boundary layer
c	char or surface material
D	drag
e	edge of boundary layer
ew	edge gas composition at wall temperature
eq	equilibrium
eff	effective
F	skin friction
g	pyrolysis gas
H,h	heat transfer
i	incompressible, chemical species i
j	chemical species j
k	element k
MN	modified Newtonian

m	mixture
o	reservoir condition; stagnation point
r	reference state
S	shock
t	turbulent, transferred state
u	adjacent to an interface in condensed phase
w	adjacent to an interface in gas phase
x	location along surface
0	zero mass transfer limit
∞	upstream of shock; ambient

Superscripts and Overscores

~	elemental
'	fluctuating component
o	standard state
—	average; normalized
c	conduction

CHAPTER 1

INTRODUCTION

Commencing in the 1950's the analysis of thermal protection systems for re-entry vehicles has been an important activity of aerospace engineers. Various types of re-entry vehicles have been of concern, including, for example, ICBM nose cones, the Apollo command module, and probes into atmospheres of other planets. Such analysis must include consideration of the trajectory, the inviscid flow field, radiative heat transfer, convective heat and mass transfer, surface chemistry, and heat shield thermal response. Each of these aspects of the problem has received considerable attention, and has a vast technical literature. The objective of this report is to review the basic theory of just one aspect, namely convective heat and mass transfer, with particular emphasis on re-entry into the earth's atmosphere of ballistic missiles.

It has been the author's experience that the practicing aerospace engineer engaged in the analysis of re-entry vehicle thermal systems has usually a good training in fluid mechanics and heat transfer, but is lacking in formal training in mass transfer. Furthermore, whereas numerous appropriate and excellent texts on fluid mechanics and heat transfer are available, no appropriate text on mass transfer exists. Correspondingly the development in this report assumes that the reader has an advanced training in fluid mechanics, and to a lesser extent in heat transfer, but requires little prior exposure to the principles of mass transfer.

Perhaps the most notable omission in this report is any mention of the phenomenon of boundary layer transition, despite the fact that knowledge of the location of transition is usually of critical importance to the

successful calculation of convective heat and mass transfer to a re-entry vehicle. The author did not consider himself qualified to write a useful account of this aspect of the subject.

CHAPTER 2

INVISCID FLOW FIELD

2.1 INTRODUCTION

Prediction of the inviscid flow field is essential to the determination of the aerodynamic and thermal response of a re-entry vehicle during flight. In order to determine convective heat and mass transfer rates to the re-entry vehicle heat shield, the edge of the boundary layer properties must be specified, i.e., velocity, pressure, enthalpy and mass species concentrations. Usually the two independent thermodynamic properties, required to determine the edge gas thermodynamic state, are taken to be pressure and entropy. For this purpose we require from the inviscid field a description of (i) the pressure distribution around the vehicle, and (ii) the shape of the bow shock, since curvature of the shock causes an entropy gradient along the boundary layer edge.

Many methods and correlations are available for the determination of the inviscid flow field around a re-entry vehicle. These methods vary in their degree of sophistication and range from exact solutions of the Navier-Stokes equations, to simple engineering correlations. In practice the choice of one method over another depends on accuracy requirements as well as computer time and storage limitations. In this Chapter the intent is to present only some simple engineering correlations for the rapid calculation of boundary layer edge gas conditions for conventional re-entry applications; these can be utilized in later Chapters in numerical examples of the calculation of convective heat and mass transfer to re-entry vehicles.

2.2 THE EARTH'S ATMOSPHERE

Altitude (ft)	Temperature (°F)	Pressure (atm)	Density Ratio (ρ/ρ_o) †	Accel. due to gravity (ft/sec^2)	Mean free path (ft)	Molecular weight
0	59.000	1.00000+0	1.0000+0	32.174	2.1761-7	28.964
500	57.217	9.82063-1	9.8545-1	32.173	2.2082-7	28.964
1000	55.434	9164389-1	9.7107-1	32.171	2.2410-7	28.964
1500	53.651	9.46974-1	9.5684-1	32.169	2.2743-7	28.964
2000	51.868	9.29815-1	9.4278-1	32.168	2.3082-7	28.964
2500	50.086	9.12910-1	9.2887-1	32.166	2.3427-7	28.964
3000	48.303	8.96255-1	9.1513-1	32.165	2.3779-7	28.964
3500	46.521	8.79848-1	9.0154-1	32.163	2.4138-7	28.964
4000	44.738	8.63686-1	8.8811-1	32.162	2.4503-7	28.964
4500	42.956	8.47766-1	8.7483-1	32.160	2.4875-7	28.964
5000	41.173	8.32085-1	8.6170-1	32.159	2.5254-7	28.964
6000	37.609	8.01430-1	8.3590-1	32.156	2.6033-7	28.964
7000	34.045	7.71698-1	8.1070-1	32.152	2.6842-7	28.964
8000	30.482	7.42868-1	7.8609-1	32.149	2.7683-7	28.964
9000	26.918	7.14920-1	7.6206-1	32.146	2.8556-7	28.964
10000	23.355	6.87832-1	7.3859-1	32.143	2.9463-7	28.964
15000	5.546	5.64587-1	6.2946-1	32.128	3.4571-7	28.964
20000	-12.255	4.59912-1	5.3316-1	32.112	4.0816-7	28.964
25000	-30.047	3.71577-1	4.4859-1	32.097	4.8510-7	28.964
30000	-47.831	2.97544-1	3.7473-1	32.082	5.8072-7	28.964
35000	-65.606	2.35962-1	3.1058-1	32.066	7.0067-7	28.964
40000	-69.700	1.85769-1	2.4708-1	32.051	8.8074-7	28.964
45000	-69.700	1.46227-1	1.9449-1	32.036	1.-189-6	28.964
50000	-69.700	1.15116-1	1.5311-1	32.020	1.4213-6	28.964
60000	-69.700	7.13664-2	9.4919-2	31.990	2.2926-6	28.964
70000	-67.424	4.42898-2	5.8565-2	31.959	3.7157-6	28.964
80000	-61.977	2.76491-2	3.6060-2	31.929	6.0347-6	28.964
90000	-56.535	1.73793-2	2.2360-2	31.898	9.7321-6	28.964
100000	-51.098	1.09971-2	1.3960-2	31.868	1.5588-5	28.964
137000	- 0.295	2.24146-3	2.5308-3	31.755	8.5986-5	28.964
150000	19.403	1.34291-3	1.4539-3	31.716	1.4967-4	28.964
197000	0.559	2.20348-4	2.4833-4	31.575	8.7630-4	28.964
200000	- 2.671	1.95371-4	2.2174-4	31.566	9.8140-4	28.964
250000	-107.84	2.0074-5	2.959-5	31.42	7.353-3	28.964
278000	-134.50	4.2751-6	6.819-6	31.33	3.191-2	28.964
300000	-126.77	1.2489-6	1.946-6	31.27	1.118-1	28.96
350000	-24.53	1.1210-7	1.327-7	31.12	1.629+0	28.69
360000	0.70	7.5133-8	8.350-8	31.09	2.572+0	28.57
400000	233.94	2.1071-8	1.522-8	30.97	1.381+1	27.97
450000	734.10	8.3036-9	3.399-9	30.83	6.032+1	27.29
500000	1203.81	4.6117-9	1.333-9	30.68	1.513+2	26.86

† $\rho_o = 0.076474\ lb/ft^3$

Table 2.1. 1962 U.S. Standard Atmosphere

Given a planned trajectory the re-entry vehicle speed U_∞ and altitude Z are known as a function of time; corresponding to the altitude Z, the air temperature T_∞, pressure P_∞ and density ρ_∞ are required for flow field calculations. Although these atmosphere properties are continuously varying, mainly due to solar influence, a single standard atmosphere can be used for re-entry application since (i) during significant re-entry heating the stagnation enthalpy is far larger than the ambient static enthalpy, and (ii) uncertainties in parameters such as density correspond to altitude intervals which are negligibly small compared to the altitude range over which re-entry heating occurs.

In current engineering use is the U.S. Standard Atmosphere of 1962 [1], an abstract of which is given in Table 2.1.

2.3 PRESSURE DISTRIBUTION

Stagnation pressure

For Mach numbers less than unity the isentropic formula applies,

$$P_o = P_\infty\left(1 + \frac{\gamma-1}{2} M_\infty^2\right)^{\frac{\gamma-1}{\gamma}} \qquad (2.3\text{-}1a)$$

or for $\gamma = 1.4$,

$$P_o = P_\infty\left(1 + M_\infty^2/5\right)^{\frac{7}{2}} \qquad (2.3\text{-}1b)$$

To good approximation the Mach number M_∞ is given by

$$M_\infty = \frac{U_\infty(\text{ft/s})}{49.1\sqrt{T_\infty(^\circ\text{R})}} \qquad (2.3\text{-}2)$$

For $M > 1$ the Figure on the next page may be used: this graph is based on calculations of a normal shock for equilibrium air and is valid for $T_\infty < 530$ R.

Pressure distributions

Detailed data for the pressure distributions around sphere-cone

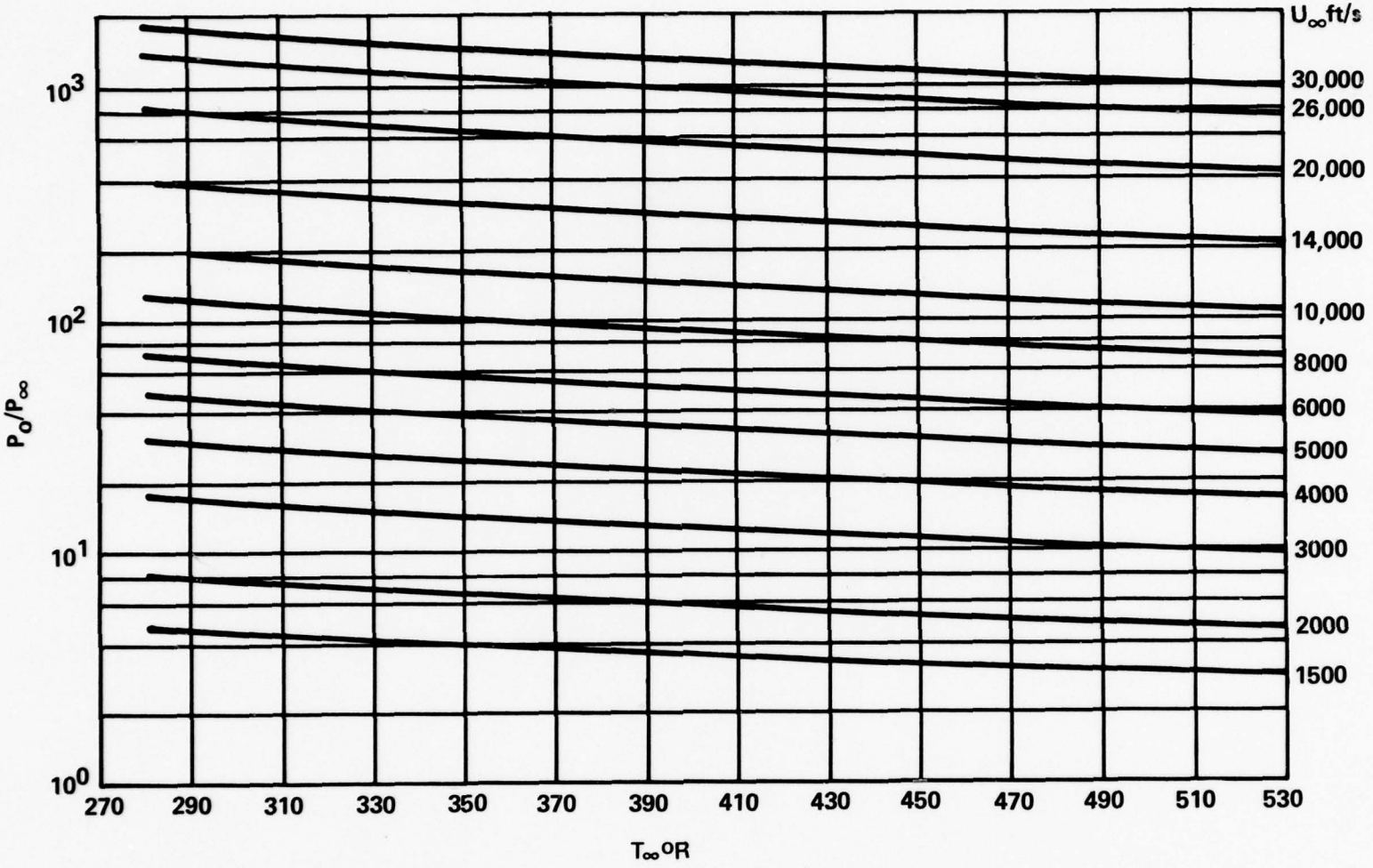
U_∞ ft/s
30,000
26,000
20,000
14,000
10,000
8000
6000
5000
4000
3000
2000
1500
10^3
10^2
10^1
10^0
P_o/P_∞
270
290
310
330
350
370
390
410
430
450
470
490
510
530
T_∞ °R

geometries can be found in References [2, 3, 4]: the ratio of local static to stagnation point pressure, and the local pressure coefficient = $(P - P_\infty)/\frac{1}{2}\rho_\infty U_\infty^2$ can be found as a function of the normalized surface coordinate s/R_N, for a range of Mach number M from 3 to infinity, and cone half-angles from 0 to 40 degrees. Ellett [3] tabulated and plotted the results given in [2] after converting the data to British engineering units. Robert, Lewis and Reed [4] reported Mach numbers and Reynolds numbers around the body in addition to the pressure distribution. These pressure distributions were obtained by using the method of characteristics in the supersonic region, and direct or inverse methods in the subsonic region. Detailed descriptions of these methods may be found in [5, 6, 7]. Most of the reported data are for ideal gas and equilibrium air. Also mostly only a zero angle of attack has been considered.

The pressure distribution in the subsonic region (where most of the pressure drop occurs) can be approximated by a modified-Newtonian distribution as

$$\bar{P}_{MN} = \bar{P}_\infty + (1 - \bar{P}_\infty) \sin^2 \theta \qquad (2.3\text{-}3)$$

where θ is the body angle (90° at the stagnation point) and the bar denotes normalization with respect to pressure behind a normal shock wave, i.e., at the vehicle stagnation point. Eq. (2.3-3) is used extensively for engineering calculations, and agrees very well with exact solutions for spheres, prolate ellipsoids and oblate ellipsoids, for $\theta \leq 30°$ [5, 8, 9]. Note that if the body angle becomes constant, Eq. (2.3-3) gives a constant pressure.

For $\theta < 30°$ the pressure distribution can be calculated using the Prandtl-Meyer flow assumptions, giving the change in pressure (or Mach number) corresponding to the change in surface angle. References [9, 10] show that this approach gives good agreement with exact solutions. On

the conical sections of blunt cones, the pressure distribution can be obtained using blast wave theory [4, 11]; the pressure coefficient is correlated in terms of the nose drag coefficient (integrated pressure coefficient over the nose), nose radius, cone half-angle and axial location.

A useful complete pressure distribution correlation has been developed by the Aerotherm Corporation [12, 13, 14], and has been extensively used for a variety of shapes and degrees of bluntness. The nosetip surface is divided into three regions as shown in the Figure, and a different calculation procedure is used in each region. The location of the sonic point depends on Mach number M_∞, the isentropic exponent behind the shock γ, and the overall bluntness of Region I. The location is always in the vicinity of $\theta = 50°$: its approximate location can be obtained using the modified Newtonian distribution with $\gamma = 1.4$. A more precise location requires accounting for Mach number and real gas effects and involves an iterative preocedure [14].

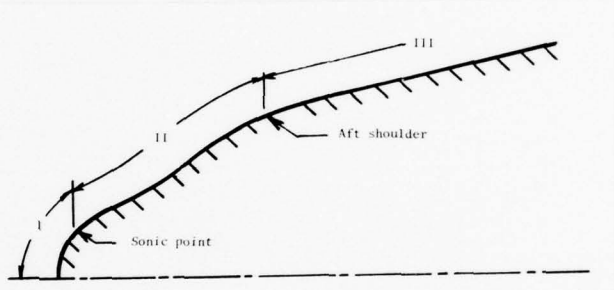

Region I. Love [15] proposed a correlation which was a synthesis of the modified Newtonian correlation, valid for spheres, and a correlation for flat faced cylinders. Dahm [14] improved the representation of the stagnation point velocity gradient, and the subsonic region pressure distribution on very blunt bodies; also the correlation was extended to be valid at lower freestream Mach numbers. The final result was

$$\bar{P} = \bar{P}_{MN} - (1 - \bar{P}_{FD})\left[\frac{\bar{P}_{MN} - \bar{P}^*}{1 - \bar{P}^*}\right] + \left(1 - \frac{R_N}{R_{MAX}}\right)\left\{(1 - \frac{s}{s^*})(1 - \bar{P}_\infty)\cos^2\theta + \frac{1}{2}\frac{s}{s^*}\left[\bar{P}_{FD} - 1 + \frac{s}{s^*}(1 - \bar{P}_\infty)\cos^2\theta + (1 - \bar{P}_{FD})\left(\frac{\bar{P}_{MN} - \bar{P}^*}{1 - \bar{P}^*}\right)\right]\right\} \qquad (2.3\text{-}4)$$

where $\bar{P}$ = P/P_o

P_o = stagnation pressure

$\bar{P}_\infty$ = freestream pressure ratio

R_N = stagnation point radius of curvature

R_{MAX} = max (R_N, R*)

R* = distance from sonic point to body axis, measured normal to the surface at the sonic point

s = surface stream length from stagnation point

θ = angle local tangent makes with body axis

* = denotes sonic point

$$\bar{p}^* = \left(\frac{2}{\gamma + 1}\right)^{\frac{\gamma}{\gamma-1}}$$

$$\bar{P}_{FD} = 1 - e^{-\lambda}(1 - \bar{P}^*) - \frac{1}{16}\left[\left(\frac{s}{s^*}\right)^2 - e^{-\lambda}\right]; \qquad \lambda = 5\sqrt{\ell n(s^*/s)}$$

Region II. Here the modified Newtonian distribution Eq. (2.4-3) is used. If the sonic point angle does not agree with the angle predicted by the modified Newtonian expression an appropriate smoothing must be employed: an example is given in [14].

Region III. The correlation for aft cone pressures was developed at the Aerospace Corporation and has the form

$$\frac{C_p}{\theta_c^2} = f_n\left(\frac{z + R}{R}\frac{\theta_c^2}{\sqrt{C_D}}, \theta_c\right) \tag{2.3-5}$$

where θ_c = cone half angle

z = axial distance from the start of the aft cone

R = radius at start of aft cone

C_D = drag coefficient of the forebody

$C_p = (P - P_\infty)/(\frac{1}{2})\rho_\infty U_\infty^2$

The function f_n was determined by polynomial curve fitting of exact numerical solutions for cones of varying bluntness, with cone half angle as a parameter.

The boundary between Regions II and III is taken to be where the pressure distributions intersect; iteration is required since C_D is a function of its position. Eq. (2.3-5) is based on hypersonic flow theory and is strictly valid only when $M_\infty > 5$. For $M_\infty < 4$ the calculation procedure for Region II should be extended into Region III. For $4 < M_\infty < 5$ interpolation between $M_\infty = 4$ and $M_\infty = 5$ predictions is recommended.

Stagnation Point Velocity Gradient $\left.\frac{du_e}{ds}\right|_o$

Often we are interested only in the stagnation point velocity gradient, for which some simple formulae follow. For subsonic flow over a sphere or cylinder the recommended expressions were developed using the Rayleigh-Janzen method of expansion in powers of Mach number; for $\gamma = 1.4$,

$$\left.\frac{du_e}{ds}\right|_o = \frac{3}{2}\frac{U_\infty}{R_N}\left(1 - 0.252\, M_\infty^2 - 0.0175\, M_\infty^4\right) \quad \text{sphere} \tag{2.3-6a}$$

$$= 2\,\frac{U_\infty}{R_N}\left(1 - 0.416\, M_\infty^2 - 0.164\, M_\infty^4\right) \quad \text{cylinder} \tag{2.3-6b}$$

For supersonic and hypersonic flow over axi-symmetric bodies generated by a hyperbola, parabola, prolate ellipse or circle, the stagnation point velocity gradient can be obtained by combining the Euler equation applied at the outer edge of the boundary layer with the modified Newtonian pressure distribution,

$$\left.\frac{du_e}{ds}\right|_o = \frac{\sqrt{2}}{R_N}\left(\frac{P_o - P_\infty}{\rho_o}\right)^{1/2} \simeq \frac{\sqrt{2}\,U_\infty}{R_N}\,\frac{(\zeta - 1)^{1/2}}{\zeta} \tag{2.3-7}$$

where ζ is the density ratio across the normal shock. For very blunt

axisymmetric bodies, e.g., oblate ellipsoids etc., and three dimensional bodies, it is necessary to use experimental data: Boison and Curtiss [33] have provided some useful data.

A convenient correlation of ζ to be used in conjunction with Eq. (2.3-7) valid for altitudes from sea level to 60,000 ft., is

$$\zeta \simeq 1 + 8.8\ (M_\infty^{\frac{1}{4}} - 1) \tag{2.3-8}$$

2.4 SHOCK SHAPE

As was the case for the pressure distribution, the shock shape associated with supersonic and hypersonic flow over re-entry vehicles can be obtained using exact or approximate methods. The exact methods usually involve determining the full inviscid flow field by some appropriate numerical method [16, 17, 18, 19, 20]. Some analytical methods are also used [21, 22, 23]. A useful approximate method assumes a thin shock layer [11, 14, 24, 25]. Shock shape correlations may be found in, for example, [26, 27, 28]. For practical engineering calculations of re-entry vehicle heat shield response along a trajectory the exact methods are impractical and correlations must be used.

Wilkinson [28] presents a simple correlation method based on the results of several workers [29, 30, 8, 31, 32] which describes the bow shock shape and location ahead of axi-symmetric bodies with various degrees of bluntness. These correlations apply for $M_\infty > 5$, account for real gas properties, and relate the shock directly to the body shape and the free-stream conditions. Both the body shape and the shock shape between the stagnation point and sonic point are assumed to be represented by conic sections of the form

$$r^2 = 2R_N z - Bz^2 \tag{2.4-1}$$

$$r_S^2 = 2R_S(z + \Delta) - B_S(z + \Delta)^2 \tag{2.4-2}$$

where R_N and R_S are radii of curvature of the body and shock respectively;

$\mathcal{B}$ and $\mathcal{B}_S$ are bluntness parameters for the body and shock respectively; Δ is the shock stand-off distance. The relation between Δ, R_S and $\mathcal{B}_S$ is given by two universal functions f_1 and f_2 in terms of ζ, the static density ratio across the shock:

$$\frac{\Delta}{R_S}\left(1 + \frac{\Delta}{R_N}\right) = f_1(\zeta) = \frac{1 + 0.55/(\zeta - 1)^{0.9}}{(1 + \sqrt{8/3\zeta})} \tag{2.4-3a}$$

$$\frac{1}{U_\infty}\frac{\Delta}{1 + \Delta/R}\left.\frac{du_e}{ds}\right|_o = f_2(\zeta) = \frac{0.778}{\zeta(\zeta - 1)^{0.4}[1 + 0.55/(\zeta - 1)^{0.9}]} \tag{2.4-3b}$$

Wilkinson correlated the data of [32] to obtain an expression for the shock bluntness parameter in terms of the body bluntness,

$$\mathcal{B}_S = \frac{1}{2}[\mathcal{B} + 2.232 - \sqrt{(\mathcal{B}+2.232)^2 - 4(2.086\mathcal{B}-0.719)}] \tag{2.4-4}$$

The asymptotic shock bluntness for $\mathcal{B} \to \infty$ *(flat faced bodies)* is 2.09.

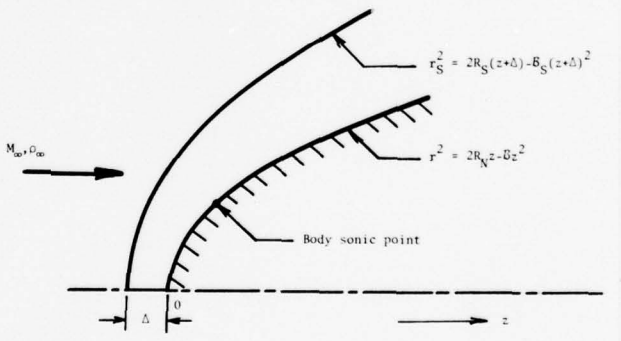

The calculation procedure to determine the bow shock location and shape is then as follows:

1. From Eq. (2.4-1), the body stagnation radius of curvature, and the sonic point coordinates, the body bluntness parameter $\mathcal{B}$ is obtained ($\mathcal{B}$ = 1 for hemispheres).
2. The shock bluntness parameter $\mathcal{B}_S$ is obtained from Eq. (2.4-4).
3. Eq. (2.4-3), in conjunction with Eqs. (2.3-5 and 6) determine Δ and R_S.
4. Eq. (2.4-2) defines the shock shape.

Boundary layer edge gas state

Near the stagnation point an isentropic expansion of the boundary layer edge gas can be assumed, so that once the pressure distribution is known the thermodynamic state of the edge gas follows directly. Further away from the stagnation point the curvature of the bow shock wave gives rise to an entropy gradient along the boundary layer edge. From a simple mass balance between the boundary layer flow at any streamwise location and that of a free-stream shock tube, the entropy of the streamline crossing the boundary layer edge at that location can be determined. Via an isentropic expansion along this streamline from the pressure behind the oblique shock to that at the boundary layer edge, one can determine the edge values h_e and u_e. Then knowing P_e and s_e, such quantities as ρ_e, γ_e etc. can be calculated.

REFERENCES FOR CHAPTER 2

1. ——, U.S. Standard Atmosphere, 1962. U.S. Government Printing Office, Washington D.C., Dec. 1962.

2. P. I. Chushkin, and N. P. Shulishnina, "Tables of supersonic flow about blunted cones" Academy of Sciences, U.S.S.R., Moscow. Computation Center monograph, 1961. [Translated and edited by J. F. Springfield, Research and Advanced Development Division, AVCO Corp., TM RAD-TM-62-63, Sept. 1962.]

3. D. M. Ellett, "Pressure distributions on sphere cones" Sandia Corporation, Albuquerque, N.M. and Livermore, CA, SC-RR-64, 1796, Jan. 1965.

4. J. F. Roberts, C. H. Lewis and M. Reed, "Ideal gas spherically blunted cone flow field solutions at hypersonic conditions" AEDC-TR-66-121, Aug. 1966.

5. H. Lomax and M. Inouye, "Numerical analysis of flow properties about blunt bodies moving at supersonic speeds in an equilibrium gas" NASA-TR-R-204, 1964.

6. M. Inouye, J. V. Rakich, and H. Lomax, "A description of numerical methods and computer programs for two-dimensional and axisymmetric supersonic flow over blunt-nosed and flared bodies" NASA, TN D-2970, 1965.

7. D. Christensen, "An iterative viscous-inviscid computer program with users' manual", USAF RTD-TDR-63-4140, 1965.

8. M. D. Van Dyke, and H. D. Gordon, "Supersonic flow past a family of blunt axisymmetric bodies" NASA TR-R-1, 1959.

9. O. M. Belotserkovskii, "Supersonic flow around blunt bodies, theoretical and experimental investigations" NASA-TT-F453, 1966.

10. C. D. Winant, "Simple approximate method of predicting the pressure distribution on arbitrary axisymmetric blunt bodies at hypersonic speeds" TRW 76-6114.4-33, 1970.

11. W. D. Hayes and R. F. Probstein, Hypersonic Flow Theory Academic Press, 1966.

12. C. B. Moyer, L. W. Anderson and T. J. Dahm, "A coupled computer code for the transient thermal response and ablation of non-charring heat shields and nose tips" NASA CR-1630, 1970.

13. M. J. Abbott and J. E. Davis, Vol. IV, Heat transfer and pressure distribution on ablated shapes, part II: data correlation and analysis" Aerotherm/Acurex Report 74-90 SAMSO-TR-74-86, 1974.

14. T. J. Dahm, et al., "Passive nosetip Technology (part II) program, vol. I, Inviscid flow and heat transfer modeling for re-entry vehicle nosetips" Acurex/Aerotherm Report 76-224, 1976.

15. E. S. Love, et al., "Some topics in hypersonic body shaping" AIAA paper 69-181, AIAA 7th Aerospace Science meeting, NY, Jan 20-22, 1969.

16. S. Vehida and M. Yasuhara, "The rotational field behind a curved shock wave calculated by the method of flux analysis" J. Aero. Sci., Vol. 23 830-845, 1956.

17. O. M. Belotserkovskii, "Flow past a circular cylinder with a detached shock" Dokladi Akad-Nank. SSSR, 113, M. D. Friedman Transl. No. B-131, 509-512, 1957.

18. S. M. Gilinskii, G. F. Telenin, and G. P. Tinyakov, "A method for computing supersonic flow around blunt bodies accompanied by a detached shock wave" Izv. Akad. Nauk. SSR, Otd. Tekhu. Nauk, Mekh. i Mashinostr, 1964, NASA Tech. Transl. No. F-297, 1965.

19. F. G. Gravalos, I. H. Edelfelt, and H. W. Emmons, "The supersonic flow about a blunt body of revolution for gases at chemical equilibrium" Proc. 9th International Astronautical Congress, Amsterdam 1958, Vol. I, Springer, Vienna, 312-332, 1959.

20. G. Moretti and M. Abbot, "A time-dependent computational method for blunt body flows" AIAA Journal, 4, 2136-2141, 1966.

21. W. Chester, "Supersonic flow past a bluff body with a detached shock" J. Fluid Mechanics, 1, part 4, 353-363, 1956 and 1, part 5, 490-496, 1956.

22. M. Van Dyke, "The blunt body problem revisited" Proc. International Symposium on Fundamental Phenomena in Hypersonic Flow, Cornell University Press, Ithaca, NY, 52-65, 1966.

23. R. J. Swigart, "A theory of asymetric hypersonic blunt-body flows" AIAA J., 1, 1034-1042, 1963.

24. J. D. Cole and J. J. Brainerd, "Slender wings at high angles of attack in hypersonic flow" Hypersonic Flow Research, Academic Press, NY, 321-343, 1962.

25. H. K. Cheng, et al., "Boundary layer displacement and leading edge bluntness effects in high temperature hypersonic flow" J. Aero Sci, 28, 353-381, 1961.

26. "Hardening Technology Studies - III, Vol. I, Combined thermochemistry and thermomechanical response in nosetips" SAMSO-TR-69-181, 1967.

27. R. A. Berry, et al., "Interim Report - Passive Nosetip Technology (PANT) program, Vol. XVI - Investigation of erosion mechanics on re-entry materials" SAMSO-RE-74-86, 1975.

28. H. R. Wilkinson, "Simple method of predicting the shape and location of detached shock ahead of arbitrary axisymmetric blunt bodies at hypersonic speed" TRW 70-6114.2-19, 1970.

29. S. C. Traugott, "An approximate solution of the direct supersonic blunt body problem for arbitrary axisymmetric shape" J. Aero. Sci., 27, 361-370, 1960.

30. O. M. Belotserkovskii, "Flow field around a symmetric profile with a detached shock wave" Prikl. Matem i Mekhan., 22, No. 2, 1958.

31. H. Serbin, "Supersonic flow around blunt bodies", J. of Aero. Sci., 25, 58-66, 1958.

32. M. D. Van Dyke, "The supersonic blunt body problem - review and extension" IAS Reprint No. 801, 26th Annual meeting, Jan. 1958.

33. J. C. Boison, and H. A. Curtiss, "An experimental investigation of blunt body stagnation point velocity gradient" ARS Journal, 29, 130-135, 1959.

CHAPTER 3

DIFFUSION PHENOMENA

3.1 INTRODUCTION

The analysis of mass transfer requires an understanding of the movement of a chemical species through a mixture or solution, and across phase boundaries. There are a number of physical mechanisms which cause mass transfer, the most important being *ordinary diffusion* and *convection*. The essential features of these two mechanisms of mass transfer are well illustrated if we consider a crystal of potassium permanganate placed in a beaker of stagnant water. As the permanganate dissolves it may be seen to diffuse through the water. The local concentration of permanganate is indicated by color, the deepest purple being adjacent to the crystal. The diffusion is always in the direction of decreasing concentration. This process of *ordinary diffusion* occurs whenever there is a concentration gradient in a liquid solution: it occurs also in solid solutions and gas mixtures. According to the kinetic theory of gases, gas molecules are in a state of random motion. If an imaginary plane is placed normal to the concentration gradient of the species in question, it follows that more molecules of that species cross from the side with the higher concentrations of that species than from the other side. Consequently, there is a net transfer of species across the plane in the direction of decreasing concentration. This transfer is simply due to the difference in concentrations on each side of the plane: there may be no movement of the mixture as a whole. If the water in the beaker is now stirred, the rate of dispersion of the permanganate is greatly increased. This increase is due to the bulk motion of the water bodily transporting the permanganate; such transfer due to bulk motion is called *convection*.

Other mechanisms of diffusion result from gradients of temperature or pressure, and from external force fields. In addition, concentration gradients cause energy transport due to interdiffusion of species, as well as by the Dufour effect. Apart from energy transport by interdiffusion, these phenomena give rise to second order effects in the present context, and are usually ignored.

3.2 DEFINITIONS OF CONCENTRATION

In a multicomponent mixture the local concentration of a species can be expressed in a number of ways. The Figure shows an elemental volume dV surrounding the location under consideration: the problem is to describe the composition of the material within the volume. One method would be to determine somehow the number of molecules of each species present and divide by dV to obtain the number of molecules per unit volume; hence a *number density* can be defined.

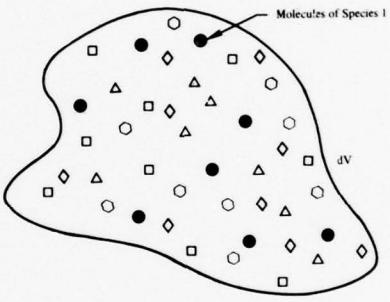

Number density of species i = number of molecules of i per unit volume

$$= N_i \qquad (3.2\text{-}1)$$

Alternatively, if the total number of molecules of all species per unit volume is denoted as N, then the *number fraction* of species i is

$$n_i = \frac{N_i}{N} \qquad (3.2\text{-}2)$$

Equations (3.2-1) and (3.2-2) are *microscopic* concepts; they are essential when the kinetic theory of gases is employed to describe transport processes.

It is usually more convenient to treat matter as a continuum; the

smallest volume considered is sufficiently large so that *macroscopic* properties such as pressure and temperature have their usual meaning. Thus macroscopic definitions are required, first on a mass basis:

Mass concentration of species i = *partial density* of species i

$$= \rho_i \text{ mass/unit volume} \tag{3.2-3}$$

The total mass concentration is the density $\rho = \Sigma\rho_i$, where the summation is over all species in the mixture, i = 1, 2,...n. The *mass fraction* of species i is defined as

$$K_i = \frac{\rho_i}{\rho} \tag{3.2-4}$$

Second, on a molar basis:

Molar concentration of species i = number of moles of i per unit volume

$$c_i = \frac{\rho_i}{M_i} \text{ moles/unit volume} \tag{3.2-5}$$

where M_i is the molecular weight of species i. The total molar concentration is the molar density $c = \Sigma c_i$. Then the *mole fraction* of species i is defined as

$$x_i = \frac{c_i}{c} \tag{3.2-6}$$

A number of important relations follow directly from these definitions and are listed below. The mean molecular weight of the mixture is denoted M and is given by:

$$M = \frac{\rho}{c} = \Sigma x_i M_i \tag{3.2-7}$$

$$\text{also,} \qquad \frac{1}{M} = \Sigma \frac{K_i}{M_i} \tag{3.2-8}$$

By definition the following summation rules hold true:

$$\Sigma K_i = 1 \tag{3.2-9}$$

$$\Sigma x_i = 1 \tag{3.2-10}$$

It is often necessary to have the mass fraction of species i expressed explicitly in terms of mole fractions and molecular weights; this relation may be derived to be

$$K_i = \frac{x_i M_i}{\Sigma x_j M_j} \tag{3.2-11}$$

The corresponding expression for mole fraction is

$$x_i = \frac{K_i/M_i}{\Sigma K_j/M_j} \tag{3.2-12}$$

Example 3.1

(a) A mixture of noble gases contains equal mole fractions of helium, argon, and xenon. What is the composition in terms of mass fractions?

(b) If the mixture contains equal mass fractions of He, A, and Xe, what are the corresponding mole fractions?

$M_{He} = M_1 = 4.003$

$M_A = M_2 = 39.95$ $\quad \Sigma M_j = 175.3$

$M_{Xe} = M_3 = 131.30$ $\quad \Sigma 1/M_j = 0.283$

a) $x_1 = x_2 = x_3$

From Eq. (3.2-11) $K_i = \frac{x_i M_i}{\Sigma x_j M_j} = \frac{M_i}{\Sigma M_j}$ for equal x_i's

$K_1 = 4.003/175.3 = 0.023$

$K_2 = 39.95/175.3 = 0.228$

$K_3 = 131.3/175.3 = 0.749$

b) $K_1 = K_2 = K_3$

From Eq. (3.2-12), $x_i = \frac{K_i/M_i}{\Sigma K_j/M_j} = \frac{1/M_j}{\Sigma 1/M_j}$ for equal K_i's.

$x_1 = (1/4.003)/(0.283) = 0.884$

$x_2 = (1/39.95)/(0.283) = 0.088$

$$x_3 = (1/131.30)/(0.283) = 0.028$$

3.3 DEFINITIONS OF VELOCITIES AND FLUXES

In a multicomponent system the various species may move at different velocities. Let $\underline{v}_i$ denote the absolute velocity of species i, that is, the velocity relative to stationary coordinate axes. In this sense the velocity is not that of an individual molecule of species i, but rather it is the local average of the species, that is, the sum of the velocities of molecules of species i within an elemental volume divided by the number of such molecules. Then the local *mass-average velocity*, $\underline{v}$, is defined as

$$\underline{v} = \frac{\Sigma \rho_i \underline{v}_i}{\Sigma \rho_i} = \frac{\Sigma \rho_i \underline{v}_i}{\rho} = \Sigma K_i \underline{v}_i \tag{3.3-1}$$

The quantity $\rho\underline{v}$ is the local mass flux; that is, the rate at which mass passes through a unit cross-section placed normal to the velocity vector $\underline{v}$. From Eq. (3.3-1), $\rho\underline{v} = \Sigma\rho_i\underline{v}_i$; that is, the local mass flux is the sum of the local species mass fluxes. The velocity $\underline{v}$ is the velocity which would be measured by a Pitot tube, and corresponds to the velocity $\underline{v}$ used when considering pure fluids. Of particular importance is that velocity $\underline{v}$ is the velocity field described by the Navier-Stokes equations and thus originates in Newton's second law of motion.

The local *molar-average velocity*, $\underline{v}^*$, is defined in an analogous manner:

$$\underline{v}^* = \frac{\Sigma c_i \underline{v}_i}{\Sigma c_i} = \Sigma x_i \underline{v}_i \tag{3.3-2}$$

The quantity $c\underline{v}^*$ is the local molar flux; that is, the rate at which moles pass through a unit area placed normal to the velocity $\underline{v}^*$. In general $\underline{v}^* \neq \underline{v}$; in particular one of these average velocities may be zero when the other is not. The question then arises as to how to define a stationary mixture.

The velocity of a particular species relative to the mass or molar-

average velocity is termed a *diffusion* velocity. We define two such velocities:

$$\underline{v}_i - \underline{v} = \text{diffusion velocity of species i relative to } \underline{v} \qquad (3.3\text{-}3)$$

$$= \hat{\underline{v}}_i$$

$$\underline{v}_i - \underline{v}^* = \text{diffusion velocity of species i relative to } \underline{v}^* \qquad (3.3\text{-}4)$$

We shall see that a species can have a velocity relative to $\underline{v}$ or $\underline{v}^*$ only if diffusion is taking place.

Next we turn to definitions of fluxes. The mass (or molar) flux of species i is a vector quantity given by the mass (or moles) of species i that passes per unit time through a unit area normal to the vector. Such fluxes may be defined relative to stationary coordinate axes, or to either of the two local average velocities. We define the *absolute* mass and molar fluxes, that is, relative to stationary coordinate axes, as

$$\text{mass flux} \quad \underline{n}_i = \rho_i \underline{v}_i \qquad (3.3\text{-}5)$$

$$\text{molar flux} \quad \underline{N}_i = c_i \underline{v}_i \qquad (3.3\text{-}6)$$

The mass flux relative to the mass average velocity $\underline{v}$ is

$$\underline{j}_i = \rho_i (\underline{v}_i - \underline{v}) = \rho_i \hat{\underline{v}} \qquad (3.3\text{-}7)$$

The molar flux relative to the mole-average velocity v* is

$$\underline{J}_i^* = c_i (\underline{v}_i - \underline{v}^*) \qquad (3.3\text{-}8)$$

From a mathematical viewpoint any one of these flux definitions is adequate for all diffusion situations; however, in a given situation there is usually one definition which, when employed, leads to minimum algebraic complexity. The most important such situation is when the convective transport present requires a solution of the conservation of momentum equation; the solution yields the mass-average velocity field, and it is then most convenient to use the mass flux relative to the mass-average velocity, that is, $\underline{j}_i$. Conditions of constant pressure and temperature, often encountered by chemical engineers, have usually led to the choice of the absolute molar flux $\underline{N}_i$ to

take advantage of the constant molar density c which results in such situations.

The definitions of fluxes lead directly to a number of useful relations as follows:

$$\underline{n} = \Sigma \underline{n}_i = \rho \underline{v} \tag{3.3-9}$$

$$\underline{N} = \Sigma \underline{N}_i = c \underline{v}^* \tag{3.3-10}$$

$$\Sigma \underline{j}_i = \Sigma \underline{J}_i^* = 0 \tag{3.3-11}$$

$$\underline{N}_i = \frac{\underline{n}_i}{M_i} \tag{3.3-12}$$

$$\underline{n}_i = \rho_i \underline{v} + \underline{j}_i = K_i \underline{n} + \underline{j}_i \tag{3.3-13}$$

$$\underline{N}_i = c_i \underline{v}^* + \underline{J}_i^* = x_i \underline{N} + \underline{J}_i^* \tag{3.3-14}$$

Example 3.2

A gas mixture at 1 atm pressure and 300°F contains 20% H_2, 40% O_2, and 40% H_2O by weight. The absolute velocities of each species are -10 ft/sec, -2 ft/sec, and 12 ft/sec, respectively, all in the direction of the z-axis. Calculate $\underline{v}$ and $\underline{v}^*$ for the mixture. For each species calculate $\underline{n}_i$, $\underline{j}_i$, $\underline{N}_i$, and $\underline{J}_i^*$.

$$\underline{v} = \Sigma K_i \underline{v}_i = (0.2)(-10) + (0.4)(-2) + (0.4)(12) = 2 \text{ ft/sec}$$

$$x_i = \frac{K_i/M_i}{\Sigma K_j/M_j}, \quad x_{H_2} = \frac{0.2/2}{0.2/2 + 0.4/32 + 0.4/18} = 0.75$$

Similarly $x_{O_2} = 0.09$, $x_{H_2O} = 0.16$.

$$v^* = \Sigma x_i \underline{v}_i = (0.75)(-10) + (0.09)(-2) + (0.16)(12) = 5.7 \text{ ft/sec}$$

$$\rho = \frac{PM}{RT} = \frac{P}{RT}(\Sigma x_i M_i) = \frac{(14.7)(144)}{(1545)(760)}(0.75(2) + 0.09(32) + 0.16(18))$$

$$= 0.013 \text{ lb/ft}^3$$

$$\underline{n}_i = \rho_i \underline{v}_i = K_i \rho \underline{v}_i$$

$$\underline{n}_{H_2} = (0.2)(1.3\times10^{-2})(-10) = -0.026 \text{ lb/ft}^2 \text{ sec}$$

Similarly, $\underline{n}_{O_2} = -0.0104$ lb/ft^2 sec; $\underline{n}_{H_2O} = 0.0625\times10^{-2}$ lb/ft^2 sec

$$\underline{j}_i = \rho_i(\underline{v}_i - \underline{v}) = K_i\rho(\underline{v}_i - \underline{v})$$

$$\underline{j}_{H_2O} = (0.2)(0.013)(-10-2) = -.031 \text{ lb/ft}^2 \text{ sec}$$

Similarly, $\underline{j}_{O_2} = -.021$ lb/ft^{2}sec; $\underline{j}_{H_2O} = 0.052$ lb/ft^{2}sec

$$\underline{N}_i = c_i\underline{v}_i = \underline{n}_i/M_i$$

$$\underline{N}_{H_2} = -0.026/2 = -0.013 \text{ lb-mole/ft}^2 \text{ sec}$$

Similarly, $\underline{N}_{O_2} = -3.2\text{x}10^{-3}$ lb-mole/ft^2 sec; $\underline{N}_{H_2O} = 3.5\text{x}10^{-3}$ lb-mole/ft^2 sec

$$\underline{J}_i^* = c_i(\underline{v}_i - \underline{v}^*) = \frac{K_i\rho}{M_i}(\underline{v}_i - \underline{v}^*)$$

$$\underline{J}^*_{H_2} = \frac{(0.2)(0.013)}{2}(-10+5.7) = -5.6\text{x}.0^{-3} \text{ lb-mole/ft}^2 \text{ sec}$$

Similarly, $\underline{J}^*_{O_2} = 0.60\text{x}10^{-3}$ lb-mole/ft^2 sec; $\underline{J}^*_{H_2O} = 5.0\text{x}10^{-3}$ lb-mole/ft^2 sec

3.4 FICK'S LAW OF DIFFUSION AS A PHENOMENOLOGICAL RELATION

It is convenient to introduce Fick's law of diffusion as a phenomenological relation, and defer examination of its physical basis. In 1855 Adolph Fick proposed a linear relation between the rate of diffusion and the local concentration gradient. The concept of a linear relation between a flux and the corresponding driving force had already been introduced by Newton in his law of viscosity, by Fourier in his law of heat conduction, and by Ohm in his law of electrical conduction.

We have noted how a chemical species may be transported by convection and diffusion. Convection is of its nature a *bulk* motion and thus transports the mixture as a whole. A given species can be transported relative to this bulk motion by *ordinary diffusion* only if concentration gradients exist. Thus a precise definition of Fick's law must describe diffusion relative to an average velocity of the mixture. For a binary mixture of species 1 and 2 we now propose that the law should be written as

$$\underline{j}_1 = -\rho\mathcal{D}_{12}\nabla K_1 \tag{3.4-1}$$

where the measure of concentration has been chosen to be the mass fraction of species 1 and the diffusive flux is relative to the mass average velocity.

The constant of proportionality has been separated into a product of local mixture density and a coefficient $\mathcal{D}_{12}$, called the *binary diffusion coefficient* with dimensions of (length)^2/time. The corresponding law written for species 2 is

$$\underline{j}_2 = -\rho\mathcal{D}_{21}\nabla K_2 \tag{3.4-2}$$

Since $\nabla K_1 = -\nabla K_2$, and from Eqn. (3.3-11) $\underline{j}_1 + \underline{j}_2 = 0$, it follows immediately that

$$\mathcal{D}_{12} = \mathcal{D}_{21} \tag{3.4-3}$$

The equivalent law on a molar basis may be obtained by algebra as follows. By definition, $\underline{j}_1 = \rho_1\hat{\underline{v}}_1 = \rho_1(\underline{v}_1 - \underline{v})$

$$= \rho_1(\underline{v}_1 - K_1\underline{v}_1 - K_2\underline{v}_2)$$

$$= \rho_1\left(\underline{v}_1 - \frac{x_1M_1}{M}\underline{v}_1 - \frac{x_2M_2}{M}\underline{v}_2\right)$$

$$\frac{M}{M_2}\underline{j}_1 = \rho_1\left(\underline{v}_1\frac{M}{M_2} - \frac{x_1M_1}{M_2}\underline{v}_1 - x_2\underline{v}_2\right)$$

$$= \rho_1\left(\underline{v}_1\frac{x_1M_1 + (1-x_1)M_2}{M_2} - x_1\frac{M_1}{M_2}\underline{v}_1 - x_2\underline{v}_2\right)$$

$$= \rho_1(\underline{v}_1 - x_1\underline{v}_1 - x_2\underline{v}_2)$$

$$= \rho_1(\underline{v}_1 - \underline{v}^*)$$

$$= \underline{j}_1^*$$

But $\underline{J}_1^* = \underline{j}_1^*/M_1$, $\underline{J}_1^* = \frac{M}{M_1M_2}\underline{j}_1$ (3.4-4)

Also $\nabla x_1 = \nabla\left(\frac{K_1/M_1}{K_1/M_1 + K_2/M_2}\right)$

$$= \frac{M^2}{M_1M_2}\nabla K_1 \tag{3.4-5}$$

Substituting the results in Eqn. (3.4-1), with $c = \frac{\rho}{M}$, gives

$$\underline{J}_1^* = -c\mathcal{D}_{12}\nabla x_1 \tag{3.4-6}$$

Notice that $\underline{J}_1^*$ is the molar flux relative to the *molar average velocity*.

It is now possible to give a correct interpretation of what we mean by a stationary medium. If we are working in mass units, we require that the mass

average velocity be zero; if we are working in molar units, we require that the molar average velocity be zero. Since a Pitot tube or anemometer measures the mass average velocity, the interpretation of stationary as zero mass average velocity is more in accord with our physical intuition.

It cannot be demonstrated in a simple manner that Eq. (3.4-1) is the most appropriate mathematical statement of Fick's law. There is no single physical mechanism of ordinary diffusion; in particular there are radical differences between the mechanisms in gases, liquids, and solids. However the kinetic theory of gases shows that this expression is appropriate for gas mixtures at low pressures, while experiment has shown it is valid for dilute liquid solutions as well.

Substitution of Fick's law into Eqs. (3.3-13) and (3.3-14) written for a binary system, yields two important relations:

$$\underset{\sim}{n}_1 = \rho_1 \underset{\sim}{v} - \rho \mathcal{D}_{12} \nabla K_1 = K_1 (\underset{\sim}{n}_1 + \underset{\sim}{n}_2) - \rho \mathcal{D}_{12} \nabla K_1 \tag{3.4-7}$$

$$\underset{\sim}{N}_1 = c_1 \underset{\sim}{v}^* - c \mathcal{D}_{12} \nabla x_1 = x_1 (\underset{\sim}{N}_1 + \underset{\sim}{N}_2) - c \mathcal{D}_{12} \nabla x_1 \tag{3.4-8}$$

We see that the absolute flux of a species can always be conveniently expressed as the sum of two components, one due to convection, and the other due to diffusion.

Binary diffusion coefficient of gases at low pressures are composition independent, increase with temperature, and vary inversely with pressure. Liquid and solid diffusion coefficients are markedly concentration dependent and increase exponentially with temperature.

Strictly speaking, Fick's law is valid only in binary systems, however it is often applied in an approximate manner to multicomponent mixtures. For example, for water vapor diffusing through air the oxygen and nitrogen are considered to be a single "air" species: since O_2 and N_2 molecules are physically not too different the error incurred is small. Alternatively, when a number of species are in small concentration in nearly pure species 1,

than an *effective binary diffusion coefficient* for species i is simply $\mathcal{D}_{il}$. If appreciable error can be tolerated in an engineering calculation involving a mixture of many species of not too different molecular weights, then we might simply assume *equal diffusion coefficients* for all species pairs, at some average value.

3.5 TRANSPORT IN MULTICOMPONENT GAS MIXTURES

For gas mixtures at low pressures the Chapman-Enskog kinetic theory of gases yields results which have proven satisfactory over a wide range of conditions. Not only does this theory rigorously describe multicomponent diffusion, and provide accurate formulae for the transport properties, that is, viscosity, thermal conductivity and diffusion coefficients, but also it exhibits the following additional physical phenomena:

(i) Thermal diffusion or Soret effect which is a movement of species resulting from a temperature gradient in the mixture.

(ii) Pressure diffusion which is a movement of species resulting from a pressure gradient.

(iii) Forced diffusion, which results from force fields acting on the molecules of the mixture.

(iv) The diffusion thermo or Dufour effect (also called diffusional conduction) which is an energy transport resulting from concentration gradients in the mixture.

The most suitable reference work from which the results of the Chapman-Enskog theory may be obtained is the treatise authored by J. O. Hirschfelder, C. F. Curtiss and R. B. Bird entitled "Molecular Theory of Gases and Liquids" [1], and hereafter referred to as H.C.B. In particular we first require the diffusion and energy flux vectors, but before presenting these it is of importance to discuss some aspects of the physical model so as to indicate possible restrictions on the validity of the results.

1.) The density of the mixture must be low enough for three body collisions to occur with negligible frequency.

2.) The model assumes monatomic molecules but little error is introduced by applying the results to polyatomic gases. The momentum flux and diffusion flux are not appreciably affected by the internal degrees of freedom. The heat flux vector on the other hand contains both the translational energy and the energy of the internal degrees of freedom; the so called "Eucken correction" will be introduced to take this into account.

3.) The flux vectors are general in the sense that they do not explicitly contain the force law which is assumed to characterize the molecular interaction. The various transport coefficients do however depend on the particular force law.

4.) The solution of the Boltzman Equation involves an expansion in terms of Sonine polynomials. Chapman and Cowling [2] in their solution used an infinite series of these polynomials with the result that the transport coefficients are expressed in terms of ratios of infinite determinants. However to obtain numerical values it is necessary to consider only a few elements of the determinants since convergence is rapid as additional rows and columns are included. For viscosity, thermal conductivity and ordinary diffusion one term gives a good approximation. For ordinary diffusion however, one term does not describe the dependence of the coefficient on concentration, two terms show a slight dependence. Thermal diffusion and the diffusion thermo-effect only appear when the second term is included, indicating that they are usually second order effects.

5.) The expressions for the flux vectors contain only the first spatial derivatives of temperature, pressure, concentration, and so on. Thus the results are inapplicable when gradients change abruptly, for example, within a shock wave.

The Diffusion Flux Vector

H.C.B. Eqn. (8.1-1) gives the mass flux vector relative to the mass average velocity for the i'th species in a mixture of n components as:

$$\underset{\sim}{j}_i = N_i m_i \hat{\underset{\sim}{v}}_i$$

$$= \frac{N^2}{\rho} \sum_{j=1}^{n} m_i m_j D_{ij} \underset{\sim}{d}_j - D_i^T \nabla \ell n T \qquad (3.5\text{-}1)$$

where $\underset{\sim}{d}_j$ includes the gradients of the number fraction N_j/N, pressure P and also the external forces $\underset{\sim}{X}_k$ acting on the molecules,

$$\underset{\sim}{d}_j = \nabla \frac{N_j}{N} + \left(\frac{N_j}{N} - \frac{N_j m_j}{\rho}\right) \nabla \ell n P - \frac{N_j m_j}{P\rho} \left[\frac{\rho}{m_j} \underset{\sim}{X}_j - \sum_{k=1}^{n} N_k \underset{\sim}{X}_k\right] \qquad (3.5\text{-}2)$$

The mass of a molecule of species i is m_i while $\underset{\sim}{X}_k$ is the external force per molecule: thus $\underset{\sim}{X}_k = m_k \underset{\sim}{f}_k$ where $\underset{\sim}{f}_k$ is the force per unit mass. For a gravitational force field the force per unit mass is constant: substitution in the last term of Eqn. (3.5-2) gives

$$\frac{N_j m_j}{P\rho} \left[\rho \underset{\sim}{f}_j - \sum_{k=1}^{n} \rho_k \underset{\sim}{f}_k\right] = 0 \text{ if } \underset{\sim}{f}_i \text{ is a constant.}$$

However a gravitational field does produce a pressure gradient and thus indirectly yields a contribution to the diffusion flux as pressure diffusion.

The D_{ij} are *multicomponent diffusion coefficients*. Except in binary mixtures, for which $D_{12} = \mathcal{D}_{12}$, $D_{ij} \neq D_{ji}$, and $D_{ii} = 0$. The D_{ij} are concentration dependent. The D_{ij} satisfy the following summation rule:

$$\sum_i \left[M_i M_h D_{ih} - M_i M_k D_{ik}\right] = 0 \qquad (3.5\text{-}3)$$

H.C.B. relates the D_{ij} to the binary diffusion coefficients $\mathcal{D}_{ij}$; as mentioned above, for a binary mixture, $D_{12} = \mathcal{D}_{12}$, while for a ternary mixture,

$$D_{12} = \mathcal{D}_{12} \left[1 + \frac{N_3 \left(\frac{m_3}{m_2} \mathcal{D}_{13} - \mathcal{D}_{12}\right)}{N_1 \mathcal{D}_{23} + N_2 \mathcal{D}_{13} + N_3 \mathcal{D}_{12}}\right] \qquad (3.5\text{-}4)$$

with similar relations for $\mathcal{D}_{21}$, $\mathcal{D}_{23}$, $\mathcal{D}_{32}$, $\mathcal{D}_{13}$ and $\mathcal{D}_{31}$. The calculation of the binary diffusion coefficients will be dealt with in §3.6.

The D_i^T are the multicomponent thermal diffusion coefficients and depend in a complex manner on temperature, concentration, molecular weights and the force law of the molecular interaction. For a binary mixture it is important to note that the D_i^T defined here does not reduce to the coefficients of Chapman and Cowling [2], but the difference arises only due to a difference in definitions.

Because the D_{ij} are concentration dependent it is convenient in some situations to replace the n relations given by Eqn. (3.5-1) by a set of (n-1) independent equations:

$$\sum_{j=1}^{n} \frac{N_i N_j}{N^2 \mathcal{D}_{ij}} (\underset{-}{v}_j - \underset{-}{v}_i) = \underset{-}{d}_i - \nabla \ell n T \sum_{j=1}^{n} \frac{N_i N_j}{N^2 \mathcal{D}_{ij}} \left(\frac{D_j^T}{N_j m_j} - \frac{D_i^T}{N_i m_i} \right) \tag{3.5-5}$$

These are the so called Stefan-Maxwell equations in their most general form; their derivation is presented in H.C.B. §7.4.

The Energy Flux Vector

H.C.B. Eqn. (8.1-23) gives the energy flux relative to the mass average velocity in a multicomponent mixture as:

$$\underset{-}{q} = -k\nabla T + \frac{5}{2} kT \sum_{i=1}^{n} N_i \hat{\underset{-}{v}}_i + \frac{kT}{N} \sum_{i=1}^{n} \sum_{j=1}^{n} \frac{N_j D_i^T}{m_i \mathcal{D}_{ij}} (\underset{-}{v}_i - \underset{-}{v}_j) \tag{3.5-6}$$

The first term is ordinary thermal conduction. The second term is the interdiffusion energy flux since $N_i \hat{\underset{-}{v}}_i$ is the diffusion flux of species i relative to the mass average velocity in molecules/unit time-unit area, and each monatomic molecule carries, on an average, a quantity of thermal energy equal to $\frac{5}{2} kT$. For polyatomic molecules the interdiffusion term becomes $\sum_{i=1}^{n} N_i m_i h_i \hat{\underset{-}{v}}_i$, where h_i is the enthalpy per unit mass of species i. H.C.B. §7.6b

presents a description of this modification for polatomic molecules which is part of the so called "Eucken correction". The last term in Eqn. (3.5-6) is the Dufour effect.

Example 3.3

The relation $\sum_{i=1}^{n} \underline{j}_i = 0$ is easily proven. For a multicomponent system show that similar summation rules are valid for the ordinary, pressure, forced and thermal diffusion components separately.

Sum Eqn. (3.5-1) over all species,

$$\sum_{i=1}^{n} \underline{j}_i = \frac{N^2}{\rho} \sum_{i=1}^{n} \sum_{j=1}^{n} m_i m_j D_{ij} \underline{d}_j - \sum_{i=1}^{n} D_i^T \nabla \ell nT$$

$$= \frac{N^2}{\rho} \sum_{j=1}^{n} \underline{d}_j \sum_{i=1}^{n} m_i m_j D_{ij} - \sum_{i=1}^{n} D_i^T \nabla \ell nT$$

$$= \frac{N^2}{\rho} \sum_{j=1}^{n} \underline{d}_j \left(\sum_{i=1}^{n} m_i m_h D_{ih} \right) - \sum_{i=1}^{n} D_i^T \nabla \ell nT \quad \text{using Eq. (3.5-3)}$$

$$= \frac{N^2}{\rho} \left(\sum_{i=1}^{n} m_i m_h D_{ih} \right) \sum_{j=1}^{n} \underline{d}_j - \sum_{i=1}^{n} D_i^T \nabla \ell nT$$

Now consider each term in $\sum_{j=1}^{n} \underline{d}_j$ in turn:

$$\sum_j \nabla \frac{N_j}{N} = \sum_j \nabla x_j = 0, \text{ since } \sum_j x_j = 1.$$

$$\sum_j \left(\frac{N_j}{N} - \frac{N_j m_j}{\rho} \right) \nabla \ell nP = \nabla \ell nP \left[\sum_j x_j - \sum_j K_j \right]$$

$$= \nabla \ell nP \, [1 - 1]$$

$$= 0$$

$$\sum_j \frac{N_j m_j}{P\rho} \left[\frac{\rho}{m_j} \underline{X}_j - \sum_k N_k \underline{X}_k \right] = \frac{1}{P} \left[\sum_j N_j \underline{X}_j - \sum_k N_k \underline{X}_k \sum_j \frac{\rho_j}{\rho} \right]$$

$$= \frac{1}{P} \left[\sum_j N_j \underline{X}_j - \sum_k N_k \underline{X}_k \right]$$

$$= 0$$

Thus summation rules have been proven for ordinary, pressure and forced diffusion in turn. For thermal diffusion the rules follows immediately from the relation $\sum_i D_i^T = 0$, or by subtraction.

Simplifications for a Binary Mixture

While still dealing with the flux vectors expressed in terms of microscopic parameters it is useful to write down some ot the simplified forms which obtain for a binary system. The diffusion flux Eq. (3.5-1) reduces to:

$$\underline{j}_1 = N_1 m_1 \hat{\underline{v}}_1$$

$$= \frac{N^2}{\rho} m_1 m_2 \mathcal{D}_{12} \underline{d}_2 - D_1^T \nabla \ell n T \tag{3.5-7}$$

while Eq. (3.5-2) reduces to:

$$\underline{d}_2 = \nabla \frac{N_2}{N} + (\frac{N_2}{N} - \frac{N_2 m_2}{\rho}) \nabla \ell n P - \frac{N_1 N_2}{P\rho} [m_1 \underline{X}_2 - m_2 \underline{X}_1] \tag{3.5-8}$$

The coefficient of $\nabla \ell n P$ in this equation is simply the difference between the mole fraction and the mass fraction, hence it follows that

$$\underline{d}_1 = -\underline{d}_2 \tag{3.5-9}$$

Also, since $\underline{j}_1 = -\underline{j}_2$, it follows that

$$\mathcal{D}_{12} = \mathcal{D}_{21} \text{ and } D_1^T = -D_2^T \tag{3.5-10}$$

By writing Eqns. (3.5-7) for $\underline{j}_1$ and $\underline{j}_2$ respectively and subtracting, the Stefan-Maxwell equations become

$$(\underline{v}_1 - \underline{v}_2) = - \frac{N^2}{N_1 N_2} \mathcal{D}_{12} [\underline{d}_1 + k_T \nabla \ell n T] \tag{3.5-11}$$

where the thermal diffusion ratio k_T has been introduced, and is defined as

$$k_T = \frac{\rho}{N^2 m_1 m_2} \frac{D_1^T}{\mathcal{D}_{12}} \tag{3.5-12}$$

Thus k_T is a measure of the relative importance of thermal and ordinary diffusion.

The Flux Vectors for a Binary Mixture Expressed in Continuum Parameters

The foregoing flux vectors contain microscopic parameters such as the mass of a molecule and number density. For purposes of engineering analysis we prefer to have these vectors expressed in terms of appropriate continuum parameters. The microscopic parameters can be eliminated from Eqs. (3.5-7), (3.5-8) and (3.5-12) by introducing Avogadro's number, $\mathcal{A}$, in the following identities:

$$m_1 = M_1/\mathcal{A}; \quad N = \mathcal{A}c$$

The three equations become, respectively,

$$\underline{j}_1 = \rho_1 \hat{\underline{v}}_1 = \frac{c^2}{\rho} M_1 M_2 \mathcal{D}_{12} \underline{d}_2 - D_1^T \nabla \ell n T \tag{3.5-13}$$

$$\underline{d}_2 = \nabla x_2 - (x_2 - K_2)\nabla \ell n P - \frac{K_1 K_2}{RT}(\underline{f}_2 - \underline{f}_1) = -\underline{d}_1 \tag{3.5-14}$$

$$k_T = \frac{\rho}{c^2 M_1 M_2} \frac{D_1^T}{\mathcal{D}_{12}} = \frac{M^2}{M_1 M_2 \rho} \frac{D_1^T}{\mathcal{D}_{12}} \tag{3.5-15}$$

where $R = \mathcal{R}/M$ and $\frac{1}{M} = \frac{K_1}{M_1} + \frac{K_2}{M_2}$. If Eqn. (3.5-14) is written for $\underline{d}_1$ and substituted in Eq. (3.5-13), then after some manipulation,

$$\underline{j}_1 = -\rho \mathcal{D}_{12} \left[\nabla K_1 + \frac{M_2}{M}\left(1 - \frac{M_1}{M}\right) K_1 \nabla \ell n P - \frac{M_1 M_2}{M} \frac{K_1 K_2}{RT}(\underline{f}_1 - \underline{f}_2) + \frac{M_1 M_2}{M^2} k_T \nabla \ell n T\right] \tag{3.5-16}$$

By using Eqn. (3.4-4) the equivalent molar form is obtained,

$$\underline{J}_1^* = -c \mathcal{D}_{12} \left[\nabla x_1 + \left(1 - \frac{M_1}{M}\right) x_1 \nabla \ell n P - \frac{x_2 x_1}{M^2 RT}(M_2 \underline{F}_1 - M_1 \underline{F}_2) + k_T \nabla \ell n T\right] \tag{3.5-17}$$

where $\underline{F}$ is the external force per mole.

To obtain the binary mixture energy flux vector in terms of continuum parameters, the first step is to rewrite Eq. (3.5-6) for a binary system, and then replace the microscopic parameters by their macroscopic counterparts, yielding final forms in terms of either mass or molar units. For a polyatomic gas Eqn. (3.5-6) becomes

$$\underline{q} = -k\nabla T + \underline{j}_1(h_1-h_2) + \frac{kT}{N}\frac{D_1^T}{\mathcal{D}_{12}}\left[\frac{N_2}{m_1}(\hat{\underline{v}}_1-\hat{\underline{v}}_2) + \frac{N_1}{m_2}(\hat{\underline{v}}_2-\hat{\underline{v}}_1)\right] \tag{3.5-18}$$

where the relations $\underline{j}_1 = N_1 m_1 \hat{\underline{v}}_1 = -\underline{j}_2$, and $D_1^T = -D_2^T$ have been used. If further the relation $k = R/A = RM/A$ is introduced, after some manipulation Eqn. (3.5-18) in terms of mass becomes

$$\underline{q} = -k\nabla T + \underline{j}_1 (h_1 - h_2) + \underline{j}_1 k_T RT \frac{\rho^2}{\rho_1\rho_2} \tag{3.5-19}$$

or

$$\underline{q} = -k\nabla T + \underline{j}_1 (h_1 - h_2) + \underline{j}_1 \frac{k_T RT}{K_1 K_2} \tag{3.5-20}$$

An alternative form is obtained by introducing the *thermal diffusion factor* $\alpha_{12} = k_T/x_1x_2$. With 1 denoting the heavier species, α_{12} is positive, i.e., the heavier species diffuses down the temperature gradient. Substitution in Eq. (3.5-19) gives

$$\underline{q} = -k\nabla T + \underline{j}_1 (h_1 - h_2) + \underline{j}_1 \alpha_{12} RT \frac{M^2}{M_1M_2} \tag{3.5-21}$$

The merit of this last equation is that whereas k_T is strongly dependent on composition, α_{12} is essentially independent of composition. Thus data for thermal diffusion coefficients are more conveniently expressed in terms of α_{12}.

In molar terms Eq. (3.5-21) becomes

$$\underline{q} = -k\nabla T + \left(\frac{M_2}{M} H_1 - \frac{M_1}{M} H_2\right) \underline{J}_1^* + \alpha_{12} RT \underline{J}_1^* \tag{3.5-22}$$

where H is the enthalpy per mole.

Example 3.4

Two bulbs are connected by a small diameter tube and filled with a helium-air mixture with 60% by volume helium. One bulb is maintained at 60°F while the other is at 580°F. If convection is entirely suppressed estimate the steady state difference in composition for the two bulbs. Take $\alpha_{12} = 0.51$.

Eqn. (3.5-17) reduces to $J_{-1}^{*} = -c\mathcal{D}_{12}\left[\frac{dx_1}{dz} + k_T \frac{d\ell nT}{dz}\right]$ with coordinate z taken along the connecting tube. At steady state $J_1^{*} = 0$, thus

$$\frac{dx_1}{dz} = -k_T \frac{d\ell nT}{dz}$$

Integrating, $x_{1,H} - x_{1,C} = -k_T \ell n \frac{T_H}{T_C}$ for k_T constant, where subscripts H and C refer to the hot and cold bulbs respectively. With $k_T = x_1 x_2 \alpha_{12}$, the separation is

$$x_{1,H} - x_{1,C} = -(0.4)(0.6)(0.51)\ell n \frac{1040}{520}$$

$$= -0.085$$

i.e., the mole fraction of air in the hot bulb is 0.085 less than in the cold bulb. Note that k_T should be evaluated at a suitable average temperature composition for an accurate result.

3.6 CALCULATION OF GAS TRANSPORT PROPERTIES

The Chapman-Enskog kinetic theory of gases described in 3.5 gives formulae for the transport properties of pure gases as well as for multi-component mixtures. In order to calculate these properties a potential energy of interaction ϕ must be chosen to characterize the forces acting on a pair of molecules during a collision. A realistic model should embody a weak attractive force between the two molecules at distances several times the distance at which strong repulsive forces start to come into action. The weak forces will cause a noticeable effect on two relatively slowly moving molecules, but will have a negligible effect on two relatively fast moving ones: the shorter range repulsive forces remain effective for the fast pairs. The potential energy ϕ is the integral of the interaction force F, thus $F = -d\phi/dr$, where r is the separation distance. To the left of minimum in the potential energy curve the molecules repel each other, while to the

right there is an attractive force. An empirical representation of the potential energy function which has proven fairly successful, is the Lennard-Jones 6-12 potential model,

$$\phi(r) = 4\varepsilon[(\frac{\sigma}{r})^{12} - (\frac{\sigma}{r})^{6}] \quad (3.6\text{-}1)$$

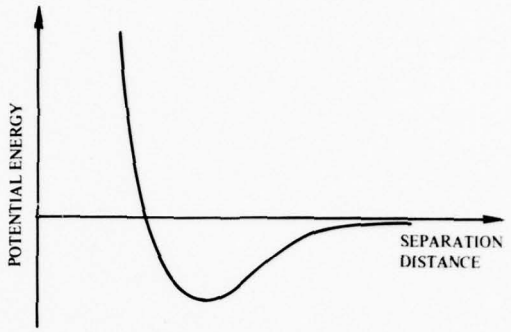

where σ, the *collision diameter*, is the value of r for which $\phi(r) = 0$, and ε is the maximum energy of attraction between a pair of molecules. This model exhibits the required weak attraction, due to London dispersion forces, at large separations (like r^{-6}) and strong repulsion, due to electron cloud overlapping, at small separations (nearly like r^{-12}). Table 3.1 lists values of σ and ε for a number of pertinent chemical species.

The Lennard-Jones model describes a spherically symmetrical force field and hence is intended for use with nonpolar, nearly symmetrical molecules (for example, O_2, He, CO). Indeed, the Chapman-Enskog theory is, strictly speaking, only valid for molecules with spherically symmetrical force fields. Molecules with appreciable dipole moments (for example, H_2O, NH_3) or which are highly elongated (for example, C_3H_6, n - C_6H_{14}) interact with potentials which are angle dependent. For polar molecules the Stockmayer potential model, which adds an angle dependent factor to the Lennard-Jones expression, has been successfully used. However, polar interactions have little effect at high temperatures, and for many practical purposes it has been found adequate to use the Lennard-Jones potential even for polar and elongated molecules. The usual practice is to determine the parameters σ and ε by matching theoretical viscosity predictions with experimental data. In this way experimental viscosity data are extrapolated outside the original temperature range; also the same

Table 3.1. Force Constants for the Lennard-Jones Potential Model[†]

Species	σ Å	ε/κ K	Species	σ Å	ε/κ K	Species	σ Å	ε/κ K
Al	2.655	2750	CH_3CCH	4.761	252	Li_2O	3.561	1827
AlO	3.204	542	C_3H_8	5.118	237	Mg	2.926	1614
Al_2	2.940	2750	n-C_3H_7OH	4.549	577	N	3.298	71
Air	3.711	79	n-C_4H_{10}	4.687	531	NH_3	2.900	558
A	3.542	93	iso-C_4H_{10}	5.278	330	NO	3.492	117
C	3.385	31	n-C_5H_{12}	5.784	341	N_2	3.798	71
CCl_2	4.692	213	C_6H_{12}	6.182	297	N_2O	3.828	232
CCl_2F_2	5.25	253	n-C_6H_{14}	5.949	399	Na	3.567	1375
CCl_4	5.947	323	Cl	3.613	131	NaCl	4.186	1989
CH	3.370	69	Cl_2	4.217	316	NaOH	3.804	1962
$CHCl_3$	5.389	340	H	2.708	37	Na_2	4.156	1375
CH_3OH	3.626	482	HCN	3.630	569	Ne	2.820	33
CH_4	3.758	149	HCl	3.339	345	O	3.050	107
CN	3.856	75	H_2	2.827	60	OH	3.147	80
CO	3.690	92	H_2O	3.737	32	O_2	3.467	107
CO_2	3.941	195	H_2O_2	4.196	289	S	3.839	847
CS_2	4.483	467	H_2S	3.623	301	SO	3.993	301
C_2	3.913	79	He	2.551	10	SO_2	4.112	335
C_2H_2	4.033	232	Hg	2.969	750	Si	2.910	3036
C_2H_4	4.163	225	I_2	5.160	474	SiO	3.374	569
C_2H_6	4.443	216	Kr	3.655	179	SiO_2	3.706	2954
C_2H_5OH	4.530	363	L8	2.850	1899	UF_6	5.967	237
C_2N_2	4.361	349	LiO	3.334	450	Xe	4.047	231
$C_2H_2CHCH_3$	4.678	299	Li_2	3.200	1899	Zn	2.284	1393

[†]Taken largely from R. A. Svehla, NASA TR R-132, 1962.

values of σ and ε usually prove to be the best available for the estimation of thermal conductivity and mass diffusivity.

Formulae Based on the Lennard-Jones Potential

Use of the Lennard-Jones potential in the Chapman-Enskog kinetic theory of gases gives the viscosity of a pure monatomic gas as

$$\mu = C_1 \frac{\sqrt{MT}}{\sigma^2 \Omega_\mu} \tag{3.6-2}$$

With T in kelvins, $C_1 = 2.67 \times 10^{-6}$ gives μ in N s/m^2. With T in °R, $C_1 = 4.16 \times 10^{-8}$ gives μ in lb_f sec/ft^2 and σ is in Angstrom units (1 Å = 10^{-10}m). The quantity Ω_μ is the *collision integral* and is tabulated in Table 3.2; it is a weak function of temperature, becoming very nearly constant at high temperatures.

The Chapman-Enskog kinetic theory shows that, for a monatomic gas, the relation between thermal conductivity and viscosity is

$$k = \frac{5}{2} c_V \mu \; ; \; (c_V = \frac{3}{2} \frac{R}{M}) \tag{3.6-3}$$

thus

$$k_{monatomic} = C_{12} \frac{\sqrt{T/M}}{\sigma^2 \Omega_k} \tag{3.6-4}$$

With T in kelvins, $C_2 = 8.32 \times 10^{-2}$ gives k in W/mK; with T in °R, $C_2 = 3.58 \times 10^{-2}$ gives k in Btu/hr ft °F, and again σ is in Å. The collision integral for thermal conductivity is identical to that for viscosity, $\Omega_k = \Omega_\mu$. For polyatomic gases the *modified Eucken correction* is recommended,

$$k = k_{monatomic} + 1.32 \left(c_p - \frac{5}{2} \frac{R}{M}\right) \mu \tag{3.6-5}$$

we see that data for specific heats is required for the calculation of thermal conductivity in polyatomic gases.

The binary diffusion coefficient is given by

Table 3.2. Collision integrals for the Lennard-Jones Potential Model

$\frac{kT}{\varepsilon}$	$\Omega_\mu = \Omega_k$	Ω_D	$\frac{kT}{\varepsilon}$	$\Omega_\mu = \Omega_k$	Ω_D	$\frac{kT}{\varepsilon}$	$\Omega_\mu = \Omega_k$	Ω_D
0.30	2.785	2.662	1.60	1.279	1.167	3.80	0.9811	0.8942
0.35	2.628	2.476	1.65	1.264	1.153	3.90	0.9755	0.8888
0.40	2.492	2.318	1.70	1.248	1.140	4.00	0.9700	0.8836
0.45	2.368	2.184	1.75	1.234	1.128	4.10	0.9649	0.8788
0.50	2.257	2.066	1.80	1.221	1.116	4.20	0.9600	0.8740
0.55	2.156	1.966	1.85	1.209	1.105	4.30	0.9553	0.8694
0.60	2.065	1.877	1.90	1.197	1.094	4.40	0.9507	0.8652
0.65	1.982	1.798	1.95	1.186	1.084	4.50	0.9464	0.8610
0.70	1.908	1.729	2.00	1.175	1.075	4.60	0.9422	0.8568
0.75	1.841	1.667	2.10	1.156	1.057	4.70	0.9382	0.8530
0.80	1.780	1.612	2.20	1.138	1.041	4.80	0.9343	0.8492
0.85	1.725	1.562	2.30	1.122	1.026	4.90	0.9305	0.8456
0.90	1.675	1.517	2.40	1.107	1.012	5.0	0.9269	0.8422
0.95	1.629	1.476	2.50	1.093	0.9996	6.0	0.8963	0.8124
1.00	1.587	1.439	2.60	1.081	0.9878	7.0	0.8727	0.7896
1.05	1.549	1.406	2.70	1.069	0.9770	8.0	0.8538	0.7712
1.10	1.514	1.375	2.80	1.058	0.9672	9.0	0.8379	0.7556
1.15	1.482	1.346	2.90	1.048	0.9576	10.0	0.8242	0.7424
1.20	1.452	1.320	3.00	1.039	0.9490	20.0	0.7432	0.6640
1.25	1.424	1.296	3.10	1.030	0.9406	30.0	0.7005	0.6232
1.30	1.399	1.273	3.20	1.022	0.9328	40.0	0.6718	0.5960
1.35	1.375	1.253	3.30	1.014	0.9256	50.0	0.6504	0.5756
1.40	1.353	1.233	3.40	1.007	0.9186	60.0	0.6335	0.5596
1.45	1.333	1.215	3.50	0.9999	0.9120	70.0	0.6194	0.5464
1.50	1.314	1.198	3.60	0.9932	0.9058	80.0	0.6076	0.5352
1.55	1.296	1.182	3.70	0.9870	0.8998	90.0	0.5973	0.5256
						100.0	0.5882	0.5170

For $4 < (\frac{kT}{\varepsilon}) < 400$; $\Omega_D \simeq 1.07\ (\frac{kT}{\varepsilon})^{-0.159}$

Taken from J. O. Hirschfelder, R. B. Bird and E. L. Spotz, Chem. Revs., Vol. 44, p. 205, 1949.

$$\mathcal{D}_{12} = C_3 \frac{\sqrt{T^3\left(\frac{1}{M_1} + \frac{1}{M_2}\right)}}{\sigma_{12}^2 \Omega_{\mathcal{D}} P} \tag{3.6-7}$$

With T in kelvins, $C_3 = 1.86 \times 10^{-7}$ gives $\mathcal{D}_{12}$ in m^2/s; with T in °R, $C_3 = 8.28 \times 10^{-7}$ gives $\mathcal{D}_{12}$ in ft^2/sec, P is in atm, and σ is in Å. The intermolecular potential field for a pair of unlike molecules, species 1 and species 2, is approximated as

$$\phi_{12}(r) = 4\varepsilon_{12} \left[\left(\frac{\sigma_{12}}{r}\right)^{12} - \left(\frac{\sigma_{12}}{r}\right)^{6}\right] \tag{3.6-8}$$

The collision integral for mass diffusion $\Omega_{\mathcal{D}}$ differs from Ω_{μ}; values for $\Omega_{\mathcal{D}}$ are given in Table 3.2. The Lennard-Jones parameters σ_{12} and ε_{12} must be obtained from the empirical relations

$$\sigma_{12} = \frac{1}{2}(\sigma_1 + \sigma_2) \tag{3.6-9a}$$

$$\varepsilon_{12} = \sqrt{\varepsilon_1 \varepsilon_2} \tag{3.6-9b}$$

where, as was mentioned before, the values of σ and ε for the individual species have usually been estimated from viscosity data.

Mixture Rules

The rigorous kinetic theory of Chapman and Enskog gives a prescription of how to calculate the viscosity and thermal conductivity of a gas mixture from the values for the pure species. C. R. Wilke simplified the rigorous result by introducing elements of the rigid sphere model; the resulting formulae are simple and adequate.

$$\mu_{mix} = \sum_{i=1}^{n} \frac{x_i \mu_i}{\sum_{j=1}^{n} x_j \Phi_{ij}} \tag{3.6-10}$$

$$k_{mix} = \sum_{i=1}^{n} \frac{x_i k_i}{\sum_{i=1}^{n} x_j \Phi_{ij}} \qquad (3.6\text{-}11)$$

where

$$\Phi_{ij} = \frac{\left[1 + \left(\frac{\mu_i}{\mu_j}\right)^{1/2} \left(\frac{M_j}{M_i}\right)^{1/4}\right]^2}{\sqrt{8}\left[1 + \left(\frac{M_i}{M_j}\right)\right]^{1/2}} \qquad (3.6\text{-}12)$$

The important feature of these mixture rules is that the weighting is essentially with mole (number) fraction, as we would expect from simple kinetic theory.

Example 3.5

Determine the binary diffusion coefficient of methane in air at 80°F and 1 atm pressure.

For methane $M_1 = 16$, $\sigma_1 = 3.758$, $\varepsilon_1/k = 148$ K.

For air $M_2 = 29$, $\sigma_2 = 3.711$, $\varepsilon_2/k = 79$ K.

$\varepsilon_{12}/k = (149 \times 79)^{1/2} = 108.5$, $kT/\varepsilon_{12} = (540/1.8 \times 108.5) = 2.77$

$\Omega_D = 0.970$; $\left(\frac{1}{M_1} + \frac{1}{M_2}\right)^{1/2} = 0.311$; $\sigma_{12}^2 = \frac{1}{4}(3.758+3.711)^2 = 13.95$

thus $D_{12} = 0.86$ ft^2/hr.

3. THE BIFURCATION APPROXIMATION FOR MULTICOMPONENT DIFFUSION

A convenient approximate treatment of multicomponent diffusion has been used extensively for re-entry vehicle boundary layer analysis. The idea was first suggested by Bird [3], and was successfully implemented by Bartlett, Kendall and Rindal [4]. The approximation is developed as follows. Eqns. (3.5-1 and 2) may be rewritten in terms of macroscopic parameters as:

$$j_i + D_i^T \frac{\partial \ell n T}{\partial y} = \frac{\rho}{M^2} \sum_{j \neq i} M_i M_j D_{ij} \frac{\partial x_j}{\partial y} \qquad (3.7\text{-}1)$$

or in the Stefan-Maxwell form,

$$\frac{\partial x_i}{\partial y} = \sum_j \frac{x_i x_j}{\rho \mathcal{D}_{ij}} \left[\frac{j_j + D_j^T \frac{\partial \ell n T}{\partial y}}{K_j} - \frac{j_i + D_i^T \frac{\partial \ell n T}{\partial y}}{K_i} \right] \tag{3.7-2}$$

where pressure and forced diffusion have been ignored, and the ∇ operator has been replaced by $\partial/\partial y$ in anticipation of application to re-entry vehicle boundary layer analysis. Each of the (n-1)n multicomponent diffusion coefficients D_{ij} depend on local concentrations and upon the (1/2)(n-1)n symmetric binary diffusion coefficients $\mathcal{D}_{ij}$. In terms of the Lennard-Jones potential model,

$$\mathcal{D}_{ij} = \frac{2.628 \times 10^{-3} \, T^{3/2} \left(\frac{M_i + M_j}{2 M_i M_j} \right)^{1/2}}{P \sigma_{ij}^2 \Omega_{\mathcal{D}}(ij)} \quad cm^2/s \tag{3.7-3}$$

R. B. Bird first showed that a bifurcation of the effects of species i and species j in Eq. (3.7-2) permits explicit solution of the Stefan-Maxwell relations for j_i in terms of gradients and properties of species i and the system as a whole. The approximation is used in the form

$$\mathcal{D}_{ij} = \frac{\bar{D}}{F_i F_j} \tag{3.7-4}$$

where

$\bar{D}$: reference diffusion coefficient

F_i: diffusion factor for species i

Eq. (3.7-4) is exact for ternary systems, but approximate for n > 3; it should be viewed as a correlation equation for the actual binary diffusion coefficient data. One method to obtain this correlation is as follows. First $\bar{D}$ is defined:

$$\bar{D} = 2.6280 \times 10^{-3} \frac{T (T/M_r)^{\frac{1}{2}}}{P \sigma_r^2 \Omega_{\mathcal{D}}(rr)} \quad cm^2/s \tag{3.7-5}$$

where r refers to a reference species, often chosen to be O_2; $\bar{D}$ is thus the self diffusion coefficient of that species. The F_i are then determined by a

least-squares correlation for the $\mathcal{D}_{ij}$ for all diffusing pairs in the chemical system of interest. With this approach the pressure dependence and the majority of the temperature dependence of the $\mathcal{D}_{ij}$ is absorbed into $\bar{D}$ so that the F_i are independent of pressure and have only a slight secondary temperature dependence. All species are weighted equally in the correlation; hence the F_i are independent of concentration and can be determined a priori for a given set of chemical species. In fact to take F_i independent of both temperature and chemical system has proven to be a good approximation in many ablation problems.

Substituting Eqn. (3.7-4) in Eqn. (3.7-2) and eliminating mole fractions in favor of mass fractions on the r.h.s. gives

$$\frac{\partial x_i}{\partial y} = \frac{M^2}{\rho \bar{D}} \left(\frac{K_i F_i}{M_i} \sum_j \frac{j_j^{od} F_j}{M_j} - \frac{F_i j_i^{od}}{M_i} \sum_j \frac{K_j F_j}{M_j} \right) \tag{3.7-6}$$

where

$$j_j^{od} = j_j + D_j^T \partial \ell n T / \partial y$$

Multiplying Eq. (3.7-6) by M_i/F_i and summing over i, and noting that the sum of diffusive fluxes is zero, and the sum of mass fractions is unity,

$$\sum_j \frac{j_j^{od} F_j}{M_j} = \frac{\rho \bar{D}}{M^2} \sum_i \frac{M_i}{F_i} \frac{\partial x_i}{\partial y} \equiv \frac{\rho \bar{D}}{M^2} \sum_j \frac{M_j}{F_j} \frac{\partial x_j}{\partial y} \tag{3.7-7}$$

Substituting back in Eq. (3.7-6) gives

$$\frac{\partial x_i}{\partial y} = \frac{K_i F_i}{M_i} \sum_j \frac{M_j}{F_j} \frac{\partial x_j}{\partial y} - \frac{M^2}{\rho \bar{D}} \frac{F_i j_i^{od}}{M_i} \sum_j \frac{K_j F_j}{M_j} \tag{3.7-8}$$

Now define

$$z_i \equiv \frac{M_i x_i}{F_i \mu_2} \qquad \mu_2 \equiv \sum_j \frac{M_j x_j}{F_j}$$

$$\mu_1 \equiv \sum_j x_j F_j \qquad \mu_4 \equiv \sum_j \frac{K_j}{F_j^2} \frac{dF_j}{dT}$$

then

$$\frac{\partial}{\partial y}(z_i \mu_2) = \mu_2 \frac{\partial z_i}{\partial y} + z_i \frac{\partial \mu_2}{\partial y} = \frac{M_i}{F_i}\frac{\partial x_i}{\partial y} - \frac{M_i x_i}{F_i^2}\frac{\partial F_i}{\partial y} \tag{3.7-9}$$

Substituting in Eq. (3.7-8), noting $\sum_j z_j = 1$ and $F_i = F_i(T)$ only, then

$$j_i + \frac{D_i^T}{T}\frac{\partial T}{\partial y} = -\frac{\rho \bar{D}}{\mu_1}\left[\frac{\mu_2}{M}\frac{\partial z_i}{\partial y} + \frac{(z_i - K_i)}{M}\frac{\partial \mu_2}{\partial y} + K_i\left(\frac{1}{F_i^2}\frac{dF_i}{dT} - \mu_4\right)\frac{\partial T}{\partial y}\right] \tag{3.7-10}$$

which is the desired explicit relation for j_i in terms of gradients and properties of species i and of the system as a whole. The z_i is a quantity relating to species i which sums to unity and has between the mass and the mole fraction; μ_1, μ_2 and μ_4 are properties of the system as a whole. If we further assume the F_i to be independent of temperature, Eq. (3.7-10) reduces to

$$j_i + \frac{D_i^T}{T}\frac{\partial T}{\partial y} = -\frac{\rho \bar{D} \mu_2}{\mu_1 M}\left[\frac{\partial z_i}{\partial y} + \frac{(z_i - K_i)}{\mu_2}\frac{\partial \mu_2}{\partial y}\right] \tag{3.7-11}$$

Finally, if we assume thermal diffusion is negligible, and assume $\partial z_i/\partial y$ large compared to $[(z_i - K_i)/\mu_2]\partial \mu_2/\partial y$, Eq. (3.7-11) becomes

$$j_i = -\frac{\rho \bar{D} \mu_2}{\mu_1 M}\frac{\partial z_i}{\partial y} \tag{3.7-12}$$

Eq. (3.7-12) suggests that the driving potential for multicomponent diffusion is the z-fraction, rather than the mass or mole fraction.

In order to establish the adequacy of the correlation of binary diffusion coefficients, a number of different chemical systems have been investigated including the C-N-O, C-H-N-O and H-O systems [4]. The results show average absolute errors in the $\mathcal{D}_{ij}$ (defined as the value calculated from Eq. (3.7-3) minus the value calculated from Eq. (3.7-4), ranging from 1.3 to 10.8 percent. Additional calculations have shown that to assume the F_i to be temperature independent introduces a largest single error of 0.7 percent and average absolute error of 0.13 percent; hence, it is consistent with the level of

approximation to assume the F_i temperature independent. Table 3.3 shows typical F_i values. For use in crude calculations a simple correlation of these F_i values is

$$F_i = \left(\frac{M_i}{26}\right)^{0.461} \tag{3.7-13}$$

Table 3.3. Diffusion factors F_i for three chemical systems as calculated by Bartlett, Kendall and Rindal [4], at 12,000°R, 1 atm.

Chemical Species	Chemical System		
	OXYGEN-NITROGEN-CARBON-HYDROGEN Force data, Ref. [5,6]	OXYGEN-NITROGEN-CARBON Force data, Ref. [5]	OXYGEN-HYDROGEN Force data, Ref. [6]
O	0.739	0.740	0.732
O_2	1.000	1.000	1.000
N	0.791	0.738	
N_2	1.076	1.033	
CO	1.065	1.022	
CO_2	1.308	1.270	
C	0.722	0.664	
C_3	1.129	1.093	
CN	1.082	1.035	
H	0.203		0.221
H_2	0.296		0.303
H_2O	0.810		0.836
OH	0.777		0.819
CH_4	0.999		
C_2H	1.187		
HCN	1.201		

3.8 THERMAL DIFFUSION COEFFICIENTS

To complete our treatment of transport in gas mixtures we need to provide methods for the calculation of thermal diffusion coefficient D_i^T: for binary mixtures we could equivalently calculate k_T or α_{12}. To first approximation α_{12} depends on the (1, 2) force law, the molecular weight and mole fraction ratios, M_1/M_2 and x_1/x_2, and the temperature T.

Chapman [7] has noted that in the simplest case where the (1, 2) force law is an inverse power law Kr^{-s}, α_{12} is independent of T and contains the

factor (s-5)/(s-1), the reminder of the expression being negative when suffix 1 refers to the heavier species. Thus for $s > 5$, α_{12} and k_T are positive for $s < 5$ the opposite is true. When $s = 5$, $\alpha_{12} = 0$ and there is no thermal diffusion: this is the force law of "Maxwellian" molecules. For the rigid elastic sphere model $s = \infty$ and the above factor has its maximum value of 1. Usually $s > 5$ except in a completely ionized gas. When the molecular weights of two species are nearly equal the larger molecule will tend to diffuse down the temperature gradient, though in some cases α_{12} can change sign with concentration variations. The Lennard-Jones force law shows a temperature dependence for α_{12}, and the weak attractive field slightly increases α_{12}.

The calculation of multicomponent diffusion coefficients from the rigorous kinetic theory formulae is algebraically complex, and the results of such calculations are of questionable accuracy owing to the sensitive dependence on the molecular interaction force law. Furthermore experimental data for these coefficients are sparse, and are mainly for binary mixtures of noble gases. Since thermal diffusion and diffusional conduction are invariably second order effects in re-entry vehicle boundary layer analysis, simple approximate formulae for D_i^T are desirable. Bartlett, Kendall and Rindal [4] have developed such formulae in the following manner.

It is postulated that the mean thermal diffusion velocity of a statistical molecule set, $\hat{\underset{\sim}{v}}_i^T$ must result from some characteristic of this molecule set as it relates to the system as a whole,

$$\hat{\underset{\sim}{v}}_i^T \alpha (G_i - \bar{G}) \tag{3.8-1}$$

where $\bar{G}$ is some mean value of the property G_i for the system as a whole; thus

$$D_i^T \alpha \rho k_i (G_i - \bar{G}) \tag{3.8-2}$$

Since it is required that $\sum_i D_i^T = 0$, it follows that

$$\bar{G} = \sum_j K_j G_j \tag{3.8-3}$$

and we can write

$$D_i^T = \bar{D}^T \rho K_i \left(G_i - \sum_j K_j G_j\right) \tag{3.8-4}$$

where $\bar{D}^T$ is some property of the system as a whole. By analogy to the diffusion factors F_i the G_i are called thermal diffusion factors. For a binary system, Eq. (3.8-4) reduces to

$$D_1^T = \bar{D}^T \rho K_1 K_2 (G_1 - G_2) \tag{3.8-5}$$

and

$$\alpha_{12} = \frac{\bar{D}^T}{\bar{D}} (G_1 - G_2) F_1 F_2 \tag{3.8-6}$$

where the exact relation $\mathcal{D}_{12} = \bar{D}/F_1 F_2$ has been introduced, and species 1 is the heavier molecule.

In order to determine a suitable expression for the thermal diffusion factors it was first noted that an expression of the form

$$\alpha_{12} = c_t \frac{1 - (F_1/F_2)}{\{1 - x_1[1 - (F_1/F_2)]\}} \tag{3.8-7}$$

with c_t is a constant, allowed considerable simplification of the diffusion flux vector. Using the results of exact calculations by Mason [8] for several binary gas mixtures it was found that Eq. (3.8-7) with $c_t = -0.5$ provided a reasonable correlation above about 1800°R. Comparison of Eqn. (3.8-7) with Eq. (3.8-6) indicates

$$G_1 = \frac{1}{F_1} \; ; \; G_2 = \frac{1}{F_2} \; ; \; \bar{D}^T = \frac{c_t \bar{D}}{x_1 F_1 + x_2 F_2} \tag{3.8-8}$$

The particular form of Eqn. (3.8-8) suggests the *ad hoc* extension to multicomponent systems as

$$G_i = \frac{1}{F_i} \; ; \; \bar{D}_T = \frac{c_t \bar{D}}{\sum_j x_j F_j} \tag{3.8-9}$$

and the theoretical work of Laranjeira [9] appears to support this generalization. Substituting into Eqn. (3.8-4) gives

$$D_i^T = \frac{c_t \rho \bar{D} K_i \left[1/F_i - \sum_j K_j/F_j\right]}{\sum_j x_j F_j} \qquad (3.8\text{-}10)$$

Using the definitions of μ_1, μ_2 and z_i given in §3.7 gives

$$D_i^T = \frac{c_t \rho \bar{D} \mu_2}{\mu_1 M} \left(z_i - K_i\right) \qquad (3.8\text{-}11)$$

Also, substitution into Eqn. (3.7-11) gives for the diffusive flux of species i,

$$j_i = \frac{\rho \bar{D} \mu_2}{\mu_1 M} \left[\frac{\partial z_i}{\partial y} - (z_i - K_i)\left(\frac{\partial \ell n \mu_2}{\partial y} + c_t \frac{\partial \ell n T}{\partial y}\right)\right] \qquad (3.8\text{-}12)$$

which is particularly simple to use.

Example 3.6

Estimate the thermal diffusion coefficients for the components of equilibrium dissociated steam at 3500 K and 1 atm pressure.

From Eqn. (3.8-11), $D_i^T = \frac{c_t \rho \bar{D} \mu_2}{\mu_1 M} (z_i - K_i)$,

where $\mu_1 = \sum_j x_j F_j$; $\mu_2 = \sum_j \frac{x_j M_j}{F_j}$; $z_i = \frac{x_i M_i}{F_i \mu_2}$

The equilibrium composition and thermodynamic properties may be obtained from Reference [6], and the diffusion factors F_i from Table 3.3. In particular

$\rho = (14.7 \times 144 \times 11.18 / 1545 \times 3500 \times 1.8) = 0.00243$ lb/ft^3

$\bar{D} = 4.98 \times 10^{-2}$ ft^2/s from Table 3.3 and Eq. (3.7-5).

$c_t = -0.5$.

The calculations are summarized in the Table below.

Species	M	x_i	F_i	$x_i M_i$	$x_i F_i$	$\frac{x_i M_i}{F_i}$	K_i	z_i	D_i^T $ft^2/s \times 10^6$
H	1	.253	.221	.253	.0559	1.145	.023	.076	-7.5
H_2	2	.185	.303	.370	.0561	1.221	.033	.081	-6.8
H_2O	18	.234	.836	4.212	.1956	5.038	.376	.336	+5.6
O	16	.118	.732	1.888	.0864	2.579	.169	.172	- .4
O_2	32	.059	1.000	1.888	.0590	1.888	.169	.126	+6.1
OH	17	.151	.819	2.567	.1237	3.134	.230	.209	+3.0

also, $\Sigma x_i M_i = 11.8 = M$

$\Sigma x_i F_i = .5767 = \mu_1$

$\Sigma x_i M_i / F_i = 15.0 = \mu_2$

Notice how the z_i are inbetween the corresponding x_i and K_i. Negative values of D_i^T imply diffusion up the temperature gradient.

REFERENCES FOR CHAPTER 3

1. J. O. Hirschfelder, C. F. Curtiss, and R. B. Bird, "Molecular Theory of Gases and Liquids", John Wiley, NY 1954.

2. S. Chapman and T. G. Cowling "The Mathematical Theory of Non-Uniform Gases" Cambridge University Press, 1961.

3. R. B. Bird, "Diffusion in multicomponent gas mixtures", Kagaku Kogaku, 26, 718-721 (1962).

4. E. P. Bartlett, R. M. Kendall and R. A. Rindal, "An analysis of the coupled chemically reacting boundary layer and charring ablator, Part IV: A unified approximation for mixture transport properties for multicomponent boundary layer applications", NASA CR-1063 (1968).

5. R. A. Svehla, "Estimated viscosities and thermal conductivities of gases at high temperatures" NASA TR R-132 (1962).

6. R. A. Svehla, "Thermodynamics and transport properties for the Hydrogen-Oxygen system" NASA SP-3011 (1964).

7. S. Chapman, "Thermal Diffusion" Lecture Series No. 19, The Institute for Fluid Dynamics and Applied Mathematics, University of Maryland (1952).

8. E. A. Mason, "Forces between unlike molecules and the properties of gaseous mixtures" J. Chem. Phys., 23, 49-56 (1955).

9. M. F. Laranjeira "Experimental and Theoretical Thermal Diffusion Factors in Binary and Tertiary Mixtures" Klein Offsetdrukkerij, Poortpers N.V., (1959).

CHAPTER 4

SIMPLE MASS TRANSFER ANALYSES

4.1 EVAPORATION AND SUBLIMATION

A Couette flow model, of the mass transfer processes involved in the evaporation or sublimation of a material into an air-stream, is relatively simple to analyze, and illustrates some of the essential features of ablative and transpiration cooling. We consider flow of air over a porous plate, the surface of which is kept wet by a supply of water through the plate. Let species 1 be water vapor and species 2, air. The mass fraction of water vapor in the air-stream is $K_{1,e}$, while adjacent to the wetted plate it is $K_{1,w}$. Conservation of species applied to a control volume dy thick, cross-sectional area A, requires that at steady state

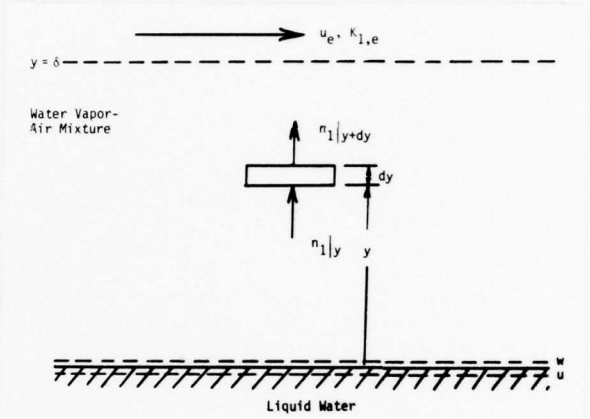

$$\begin{matrix}\text{outflow of} \\ \text{species 1}\end{matrix} - \begin{matrix}\text{inflow of} \\ \text{species 1}\end{matrix} = \begin{matrix}\text{production of} \\ \text{species 1}\end{matrix} = 0 \qquad \text{(species 1 is inert)}$$

or $\quad An_1|_{y+dy} - An_1|_y = 0$

divide by volume Ady $\quad (n_1|_{y+dy} - n_1|_y)/dy = 0$

let dy → 0 $\quad \dfrac{d}{dy}(n_1) = 0 \qquad (4.1\text{-}1)$

similarly $\quad \dfrac{d}{dy}(n_2) = 0 \qquad (4.1\text{-}2)$

adding $\quad \dfrac{d}{dy}(n_1+n_2) = \dfrac{d}{dy}(n) = \dfrac{d}{dy}(\rho v) = 0 \qquad (4.1\text{-}3)$

Of course, Eq. (4.1-3) is simply the one-dimensional form of the steady continuity equation. Now integrate Eq. (4.1-1),

n_1 = constant = $n_{1,w}$, the value of n_1 at y = 0

But the absolute flux n_1 can be expressed in terms of its convective and diffusive components as

$$n_1 = K_1 n - \rho D_{12} \frac{dK_1}{dy}$$

thus $$K_1 n - \rho D_{12} \frac{dK_1}{dy} = n_{1,w} \qquad (4.1\text{-}4)$$

Next integrate Eq. (4.1-3) $$n = \text{constant} = n_w \equiv \dot{m} \qquad (4.1\text{-}5)$$

We give the total absolute mass flux across the w-surface the special distinguishing symbol m since it is the all-important *mass transfer rate*. Substitute Eq. (4.1-5) in (4.1-4),

$$K_1 \dot{m} - \rho D_{12} \frac{dK_1}{dy} = n_{1,w}$$

rearrange as $$\frac{dK_1}{K_1 \dot{m} - n_{1,w}} = \frac{dy}{\rho D_{12}}$$

and integrate $$\frac{1}{\dot{m}} \int_{K_{1,w}}^{K_1} \frac{dK_1}{K_1 - (n_{1,w}/\dot{m})} = \int_0^y \frac{dy}{\rho D_{12}}$$

Assuming the exchange coefficient ρD_{12} is independent of y we obtain

$$\frac{K_1 - (n_{1,w}/\dot{m})}{K_{1,w} - (n_{1,w}/\dot{m})} = \exp\left(\frac{\dot{m} y}{\rho D_{12}}\right) \qquad (4.1\text{-}6)$$

Now $(n_{1,w}/\dot{m})$ = (absolute flux of species 1 across w-surface/total absolute mass flux across w-surface); if we view the mass transfer processes as a stream of matter crossing the w-surface, then $(n_{1,w}/\dot{m})$ is the fraction of the stream which is species 1, and properly might be called the mass fraction of species 1 in the *transferred state*. For our water evaporation problem intuition tells us that the only species being transferred is water, so that the mass fraction of H_2O in the transferred state must be unity, i.e., $n_{1,w}/\dot{m} = 1$. However we should rather obtain this result by a formal

deductive approach: integrating Eq. (4.1-2) gives

$$n_2 = \text{constant} = n_{2,w}$$

But air is negligibly soluble in water so that $n_{2,w} = 0$, then

$$\dot{m} = n_w = n_{1,w} + n_{2,w} = n_{1,w}$$

or $$\frac{n_{1,w}}{\dot{m}} = 1 \qquad \text{as required}$$

Substituting in Eq. (4.1-6) gives

$$\frac{K_1 - 1}{K_{1,w} - 1} = \exp\left(\frac{\dot{m}y}{\rho D_{12}}\right) \tag{4.1-7}$$

which is the equation for the concentration profile $K_1(y)$. In particular, at $y = \delta$, $K_1 = K_{1,e}$, so that

$$\frac{K_{1,e} - 1}{K_{1,w} - 1} = \exp\left(\frac{\dot{m}\delta}{\rho D_{12}}\right)$$

or $$1 + \frac{K_{1,e} - K_{1,w}}{K_{1,w} - 1} = \exp\left(\frac{\dot{m}\delta}{\rho D_{12}}\right) \tag{4.1-8}$$

In order to calculate $K_{1,w}$ we need to know the water surface temperature T_w; usually we may safely assume thermodynamic equilibrium and hence use steam tables to find the saturation partial pressure of water vapor $P_{H_2O,sat}(T_w)$. Then assuming an ideal gas mixture,

mole fraction of water vapor $$x_{H_2O} = \frac{P_{H_2O}}{P}$$

mass fraction of water vapor $$K_{H_2O} = x_{H_2O} \frac{M_{H_2O}}{M}$$

where $P = \sum_i P_i$ is the total pressure, and $M = \sum_i x_i M_i$ is the mean molecular weight of the mixture. Hence

$$K_{H_2O} = \frac{P_{H_2O}}{P_{H_2O} + \frac{29}{18}(P - P_{H_2O})} \tag{4.1-9}$$

Equation (4.1-8) is the solution to our problem: given T_w and δ we can calculate the mass transfer rate $\dot{m}$, which is the rate of evaporation since $n_{1,w} = \dot{m}$ in this problem. However it is instructive to further rearrange Eq. (4.1-8). First we define the mass transfer Stanton number as

$$C_M = \frac{j_{1,w}}{\rho_e u_e (K_{1,w} - K_{1,e})} \tag{4.1-10}$$

Note C_M is a dimensionless form of the *diffusive* rather than the absolute component of the flux of species 1 across the w-surface. Then since

$$n_{1,w} = K_{1,w} n_w + j_{1,w}$$

and $n_{1,w} = n_w = \dot{m}$ since only water is transferred,

$$\dot{m} = K_{1,w} \dot{m} + j_{1,w}$$

or

$$\dot{m} = \frac{j_{1,w}}{1 - K_{1,w}} \tag{4.1-11}$$

Substituting Eq. (4.1-10) in (4.1-11),

$$\dot{m} = \rho_e u_e C_M \frac{K_{1,e} - K_{1,w}}{K_{1,w} - 1} \tag{4.1-12}$$

$\rho_e u_e C_M \equiv$ *mass transfer conductance*, units $lb/ft^2 s$

$\frac{K_{1,e} - K_{1,w}}{K_{1,w} - 1} \equiv B'$, the driving force, dimensionless

Thus

$$\dot{m} = \rho_e u_e C_M B' \tag{4.1-13}$$

or

$$B' = \frac{\dot{m}}{\rho_e u_e C_M} \tag{4.1-14}$$

Substituting in Eq. (4.1-8) $\quad 1 + B' = \exp\left(\frac{\dot{m}\delta}{\rho D_{12}}\right)$,

and solving for m gives $\quad \dot{m} = \frac{\rho D_{12}}{\delta} \ell n(1+B')$

or

$$\dot{m} = \frac{\rho D_{12}}{\delta} \frac{\ell n(1+B')}{B'} B' \tag{4.1-15}$$

Comparing Eqs. (4.1-12) and (4.1-15), we can identify

$$\rho_e u_e C_M = \frac{\rho D_{12}}{\delta} \frac{\ell n(1+B')}{B'} \tag{4.1-16}$$

We will find it useful to normalize the Stanton number with its value in the limit of zero mass transfer rate. To obtain this limit we note from Eq. (4.1-15) that $\dot{m} \to 0$ as $B' \to 0$, and that

$$\lim_{B' \to 0} \frac{\ell n(1+B')}{B'} = \frac{B' - \frac{1}{2} B'^2 + \ldots.}{B'} = 1$$

which upon substitution into Eq. (4.1-16) gives

$$\lim_{\dot{m} \to 0} (\rho_e u_e C_M) = \frac{\rho D_{12}}{\delta} \equiv \rho_e u_e C_{MO} \tag{4.1-17}$$

Notice from the definition of $B' = (K_{1,e}-K_{1,w})/(K_{1,w}-1)$ that $B' \to 0$ as $K_{1,w} \to K_{1,e}$ i.e., as the concentration gradients go to zero, and intuition tells us that this corresponds to the limit $\dot{m} \to 0$. It is also instructive to see that as $\dot{m} \to 0$ the concentration profiles are linear. For $\dot{m} \to 0$, $n \to 0$ so that Eq. (4.1-1) is

$$\frac{d}{dy}(j_1) = 0$$

integrating $\qquad j_1 = -\rho D_{12} \frac{dK_1}{dy} = \text{constant} = C_1$

integrating again $\qquad -\rho D_{12} K_1 = C_1 y + C_2$

Apply boundary conditions $K_1 = K_{1,w}$ at $y = 0$ and $K_1 = K_{1,e}$ at $y = \delta$, and solve for C_1 and C_2 to obtain

$$\frac{K_1-K_{1,w}}{K_{1,e}-K_{1,w}} = \frac{y}{\delta} \qquad \text{(a linear concentration profile)} \tag{4.1-18}$$

and $$j_{1,w} = -\rho D_{12} \left.\frac{dK_1}{dy}\right|_{y=0} = \frac{\rho D_{12}}{\delta} (K_{1,w}-K_{1,e}) \tag{4.1-19}$$

hence $$\rho_e u_e C_{MO} = \frac{j_{1,w}}{K_{1,w}-K_{1,e}} = \frac{\rho D_{12}}{\delta}$$, as before

with the relationship $\rho_e u_e C_{MO} = \rho D_{12}/\delta$ established, we choose to write Eq. (4.1-15) as

$$\dot{m} = \underbrace{\rho_e u_e C_{MO}}_{\text{conductance in limit of zero mass transfer}} \quad \underbrace{\frac{\ell n(1+B')}{B'}}_{\text{"blowing correction"}} \quad \underbrace{B'}_{\text{driving force}} \tag{4.1-20}$$

$$B' = \frac{K_{1,e}-K_{1,w}}{K_{1,w}-1} \tag{4.1-21}$$

Equation (4.1-20) is simply an alternate form of our original solution to the problem, Eq. (4.1-8); given $\rho_e u_e C_{MO}$, $K_{1,e}$ and T_w, we can calculate $\dot{m}$. The advantage of Eq. (4.1-20) is that it is in a form suitable for application to real boundary layer flows. Recall our Couette flow is only intended to be a *model* of a real boundary layer flow, which we analyze to obtain the effect of mass transfer. We have isolated this effect in Eq. (4.1-20) as the blowing correction, $\ell n(1+B')/B'$, and we now postulate that this blowing correction is approximately correct for real boundary layer flows, laminar or turbulent. Thus for real boundary layer flows we will use Eq. (4.1-20) but with the Stanton number C_{MO} calculated from a correlation appropriate to the wall geometry and flow condition.

Finally we look at concentration profiles plotted from Eq. (4.1-7) as shown in the figure on the following page. With evaporation ($\dot{m} > 0$), the effect of mass transfer into the flow (blowing) is to reduce the concentration gradient of H_2O at the w-surface. Since

$$\rho_e u_e C_M = \frac{j_{1,w}}{K_{1,w}-K_{1,e}} = \frac{-\rho D_{12} \left.\frac{dK_1}{dy}\right|_w}{K_{1,w}-K_{1,e}}$$

it follows that C_M decreases with increasing m; in fact from Eqs. (4.1-15)

and (4.1-17),

$$\frac{C_M}{C_{MO}} = \frac{\ell n(1+B')}{B'} \qquad (4.1\text{-}22)$$

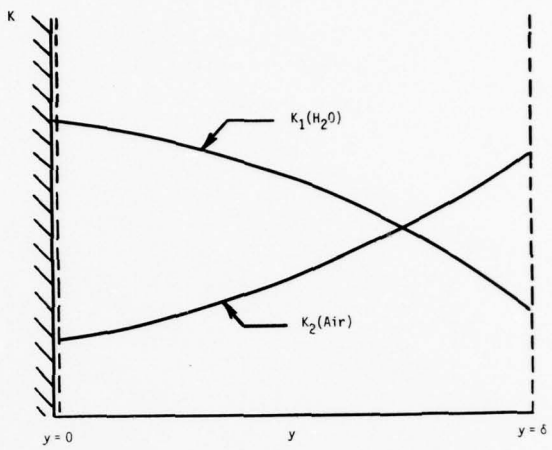

Also, since $K_1+K_2 = 1$ for this binary system, the concentration profile for species 2, air, is as shown. We see that the air is diffusing towards the water surface: but the water surface is impermeable to air so is there not a contradiction somewhere? The explanation is as follows: we have shown that $n_2 \equiv 0$, thus

$$n_2 = K_2 n - \rho D_{12} \frac{dK_2}{dy} = 0$$

and $$K_2 n = \rho D_{12} \frac{dK_2}{dy}$$

which states that the convective flux of air, $K_2 n$, is everywhere equal (and in the opposite direction) to the diffusive flux, $-\rho D_{12} dK_2/dy$, resulting in the air being exactly stationary. On the other hand, the convective flux of water vapor is in the same direction as its diffusive flux so that the convection augments the diffusion. This convection is sometimes called the *Stefan flow* in the chemical engineering literature.

Example 4.1

At a particular location on a transpiration cooled flat porous wall, the wall is maintained at 190°F by injection of water at a rate just sufficient to wet the wall. Dry air at 1000°F and 1 atm pressure flows past the wall at 300 ft/s, and dry wall heat transfer experiments for the same geometry indicate a local Stanton number $C_{HO} = 0.0046$. Calculate the water supply rate.

We need to use Eq. (4.1-20). For ρ_e we take the density of air at 1000°F = 0.0272 lb/ft^3. Next we obtain C_{MO} from C_{HO}: the data suggest a turbulent boundary layer for which

$$C_{HO} = 0.0296 Re^{-0.2} Pr^{-0.4}$$

$$C_{MO} = 0.0296 Re^{-0.2} Sc^{-0.4}$$

thus $$\frac{C_{MO}}{C_{HO}} = \left(\frac{Pr}{Sc}\right)^{0.4} = Le^{0.4}$$

To approximately account for variable property effects Pr and Sc should be evaluated at an appropriate reference state; although not well established, the 1/3 rule is the best available. Mixture rules (Chapter 3) are then used to calculate ρ, C_p, μ and k for the mixture, and also ρD_{12} must be evaluated; hence $Pr = C_p\mu/k$ and $Sc = \mu/\rho D_{12}$ are obtained. At 190°F, P_{H_2O} = 9.34 psia. For 1 atm total pressure,

$$K_{H_2O,w} = \frac{9.34}{9.34 + \frac{29}{18}(14.7-9.34)} = 0.52$$

$$\therefore \quad K_{1,r} = 0.52 + \frac{1}{3}(0-0.52) = 0.35$$

and $$T_r = 190 + \frac{1}{3}(1000-190) = 460°F$$

Hence Pr_r and Sc_r may be calculated to be 0.85 and 0.56, respectively, and

$$\frac{C_{MO}}{C_{HO}} = \left(\frac{0.85}{0.56}\right)^{0.4} = 1.517^{0.4} = 1.18$$

and $$C_{MO} = (1.18)(0.0046) = 0.0054$$

Also $$B' = \frac{K_{H_2O,e} - K_{H_2O,w}}{K_{H_2O,w} - 1} = \frac{0-0.52}{0.52-1} = 1.09$$

Substituting in Eq. (4.1-20),

$$\dot{m} = \rho_e u_e C_{MO} \frac{\ell n(1+B')}{B'} B'$$

$$\dot{m} = \left(0.0272 \frac{lb}{ft^3}\right)\left(300 \frac{ft}{s}\right)(0.0054)\frac{\ell n(1+1.09)}{1.09}(1.09)$$

$$= (0.044)(0.67)(1.09)$$

$$= 0.032, \text{ the required water supply rate.}$$

Note that the blowing correction $\ell n(1+B')/B'$ is only exact for a constant property Couette flow. The answer obtained above could be refined by using a blowing correction appropriate to a variable property turbulent boundary layer. Such matters will be discussed in Chapter 9.

4.2 A SIMPLE CASE OF DIFFUSION CONTROLLED OXIDATION

Many ablation processes involve diffusion controlled oxidation. One simple example is tungsten according to the reaction

$$3W + 4\,\frac{1}{2}\,O_2 \rightarrow W_3O_9$$

where the free-stream contains undissociated oxygen, the surface is metal tungsten, and temperatures are high enough for chemical equilibrium to exist at the w-surface with $K_{O_2,w} \simeq 0$. Another simple example is graphite according to the reaction

$$2C + O_2 \rightarrow 2CO$$

where again the free-stream contains undissociated oxygen, but temperatures are high enough for chemical equilibrium to exist at the w-surface with $K_{O_2,w} \simeq 0$, and no formation of carbon dioxide in the boundary layer.

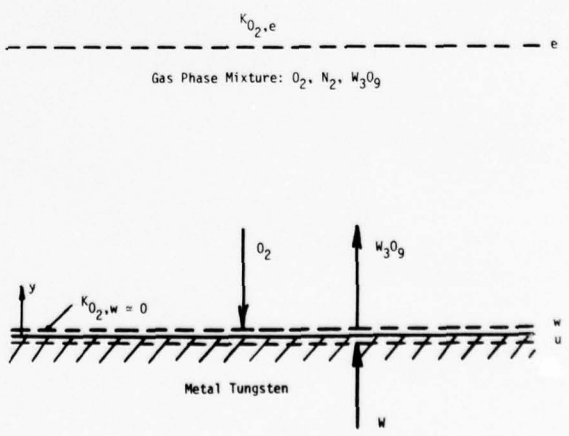

In both these examples the reaction is *heterogeneous*: the reaction takes place only at the wall since O_2 is inert in the gas phase. Thus if we choose to

model the real boundary layer with a Couette flow, the governing species conservation equations are identical to those derived in §4.1 for water evaporation as H_2O was, of course, also inert. Denoting O_2 as species 1,

conservation of O_2, $$\frac{d}{dy}(n_1) = 0 \qquad (4.2\text{-}1)$$

conservation of mass, $$\frac{d}{dy}(n) = 0 \qquad (4.2\text{-}2)$$

Integrate Eq. (4.2-2), $$n = \text{constant} = n_w = \dot{m} \qquad (4.2\text{-}3)$$

Integrate Eq. (4.2-1), $$n_1 = \text{constant} = n_{1,w}$$

or, expressing the absolute flux of species 1 in terms of its convective and diffusive components,

$$K_1 n = \rho D_{1m} \frac{dK_1}{dy} = K_1 \dot{m} - \rho D_{1m} \frac{dK_1}{dy} = n_{1,w}$$

where D_{1m} is the effective binary diffusion coefficient of O_2 in the mixture of O_2, N_2 and W_3O_9. Rearranging and integrating,

$$\int_{K_{1,w}}^{K_1} \frac{dK_1}{K_1 - n_{1,w}/\dot{m}} = \dot{m} \int_0^y \frac{dy}{\rho D_{1m}}$$

hence $$\ell n \frac{K_1 - n_{1,w}/\dot{m}}{K_{1,w} - n_{1,w}/\dot{m}} = \frac{\dot{m}y}{\rho D_{1m}} \qquad \text{if } \rho D_{1m} \text{ is assumed constant.}$$

For $y = \delta$, $$\frac{K_{1,e} - n_{1,w}/\dot{m}}{K_{1,w} - n_{1,w}/\dot{m}} = \exp\left(\frac{\dot{m}\delta}{\rho D_{1m}}\right)$$

or $$1 + B' = \exp\left(\frac{\dot{m}\delta}{\rho D_{1m}}\right) \; ; \quad \ell n(1+B') = \frac{\dot{m}\delta}{\rho D_{1m}} \qquad (4.2\text{-}4)$$

where again $$B' \equiv \frac{K_{1,e} - K_{1,w}}{K_{1,w} - n_{1,w}/\dot{m}} \qquad (4.2\text{-}5)$$

We see that the algebra involved is identical to that for the water evaporation problem of §4.1; we need only to evaluate $K_{1,w}/\dot{m}$ for the oxidation

problem. Recall that this ratio was unity for the water evaporation problem, and was identified as the transferred state mass fraction of species 1. In that case we used the fact that air is negligibly soluble in water, i.e., $n_{2,w} = 0$, to evaluate $n_{1,w}/\dot{m}$: we used a *physical fact* to evaluate a *boundary condition*. For tungsten oxidation the physical fact we use comes from the stoichiometry of the reaction occurring at the boundary,

$$3W + 4\tfrac{1}{2}O_2 \rightarrow W_3O_9$$

$$3\text{x}184 + 4.5\text{x}32$$

1 lb W* + 0.26 lb O_2 (W* denotes metal tungsten)

i.e., the stoichiometric ratio r is 0.26. By looking at the u-surface we see that only tungsten is transferred, so that $\dot{m} = n_{W^*,u}$ and, from the stoichiometry, for every 1 lb of tungsten transferred, 0.26 lb of O_2 crosses the w-surface in the negative y-direction. Thus $n_{O_2,w} = -0.26\ \dot{m}$, or $(n_{1,w}/\dot{m}) = (n_{O_2,w}/\dot{m}) = -0.26 = -r$. Substitute in Eq. (4.2-5),

$$B' = \frac{K_{1,e} - K_{1,w}}{K_{1,w} + r} \tag{4.2-6}$$

Now Eqs. (4.2-4) and (4.2-6) describe transfer between the e- and w-surfaces, and apply irrespective of the rate at which the reaction of the interface proceeds. If the reaction is slow, then the mass fraction of O_2 at the w-surface, $K_{1,w}$, is determined partly by chemical kinetics considerations. However, often the temperature and pressure are high enough for reactions to be very fast and for chemical equilibrium to prevail: then the concentration $K_{1,w}$ may be determined from thermodynamic considerations only. If, in addition, the backward reaction rate is very small, a thermodynamics calculation will show that the equilibrium concentration of O_2 at the w-surface is a very small value indeed. Thus $K_{i,w}$ can be set equal to zero in Eq. (4.2-6) to obtain

$$B' = \frac{K_{1,e}}{r} \tag{4.2-7}$$

For an air free-stream $K_{1,e} = 0.232$ and $B' = 0.89$. Notice that if the reaction product were W_2O_6 or WO_3, B' is unchanged since r is unchanged (provided thermodynamics again indicates $K_{1,w} = 0$).

Similarly, for the carbon reaction,

$$C + \frac{1}{2} O_2 \rightarrow CO$$

$$12 + 16 \rightarrow$$

$$1\ lb + \frac{4}{3}\ lb \rightarrow \qquad \therefore \quad r = \frac{4}{3}$$

Again, for $K_{1,e} = 0.232$, $B' = (0.232)/(4/3) = 0.174$.

As was the case for the water evaporation problem we can rearrange Eq. (4.2-4) to read

$$\dot{m} = \frac{\rho D_{1m}}{\delta} \frac{\ell n(1+B')}{B'} B' \tag{4.2-8}$$

and then, recognizing that we have a Couette flow model of a real boundary layer flow, identify $\rho D_{1m}/\delta = \rho_e u_e C_{MO}$ and write

$$\dot{m} = \rho_e u_e C_{MO} \frac{\ell n(1+B')}{B'} B' \tag{4.2-9}$$

When we apply Eq. (4.2-9) to real boundary layers we assume that the blowing correction $\ell n(1+B')/B'$ developed for the Couette flow is a good approximation for the real flow. Equation (4.2-9) is easier to use for this oxidation problem than was the case for the water evaporation problem inasmuch B' has a fixed value, rather than being dependent on surface temperature. For example, in the case of tungsten oxidation Eq. (4.2-9) reduces to $\dot{m} = 0.64\rho_e u_e C_{MO}$.

Notice that it is the rate at which O_2 can diffuse from the free-stream to the wall which determines the rate of reaction, hence the characterization as a *diffusion controlled* reaction. Also note that we did not use the species conservation equation governing transport of the reaction product away from the wall. If we were to do so, there would again result Eq. (4.2-9)

but with $B' = K_{W_3O_9,w}/(K_{W_3O_9,w}-(1+r))$. Since we cannot specify $K_{W_3O_9,w}$ we cannot use this form of B' to calculate $\dot{m}$; in fact, knowing $\dot{m}$, Eq. (4.2-9) allows us to determine $K_{W_3O_9,w}$. In physical terms the concentration of product at the w-surface adjusts itself to the value required for transfer away from the wall at the required rate: diffusion of the product away from the wall does *not* control the rate of reaction in this situation.

Example 4.2

Develop an expression for the rate of combustion of carbon ejecta in the flow over the aft heatshield of a missile. The ejecta have sizes between 1 and 10 μ and temperatures in the range 3000-6000°R.

In this temperature range oxidation to CO and negligible O_2 dissociation may be assumed. Since C_{MO} increases inversely proportional to particle size chemical kinetics limitations may be important for very small particles: for the C-O_2 reaction such chemical kinetics effects are negligible for particle sizes greater than 10^{-1} μ. Thus the carbon combustion rate is given by Eq. (4.2-8)

$$\dot{m} = \rho_e u_e C_{MO} \frac{\ell n(1+B')}{B'} B' \qquad \text{where} \qquad B' = \frac{K_{O_2,e}-K_{O_2,w}}{K_{O_2,w}+r}$$

For diffusion control $K_{O_2,w} \simeq 0$, and for the reaction $C + O_2 \rightarrow 2CO$, $r = 4/3$ and $B' = \frac{3}{4} K_{O_2,e}$. However now $K_{O_2,e}$ is the oxygen concentration some distance away from the particle, of the order of a few particle diameters. We cannot set $K_{O_2,e} = 0.232$, the O_2 concentration in the free-stream, since the O_2 concentration will vary from 0.232 at the boundary layer edge to zero at the heatshield surface (the heatshield itself will be oxidizing in the diffusion controlled limit). To evaluate the conductance $\rho_e u_e C_{MO}$ we will assume that the particles follow the flow and use the result for a sphere

in stagnant infinite surrounds, $\rho_e u_e C_{MO} = 2\rho D_{O_2 m}/a_p$, where a_p is the particle diameter. This conductance expression will be more accurate for the smallest particles, and will underestimate the conductance for larger particles, owing to their longer persisting initial velocity; however, it is the smallest particles which are more important owing to their higher combustion rates. The result is thus

$$\dot{m} = \frac{2\rho D_{O_2 m}}{a_p} \ell n(1 + \frac{3}{4} K_{O_2,\text{ambient}})$$

where the subscript e has been replaced by "ambient" as a reminder that it is the *local* concentration of O_2 in the boundary layer. The strongly dependent temperature product $\rho D_{O_2 m}$ must be evaluated at some reference state dependent on particle and ambient temperatures: the 1/3 rule is probably adequate.

We might also be interested in estimating the life-time of an ejecta particle: a mass balance on a spherical particle is

$$\frac{d}{dt} (\rho_p \frac{1}{6} \pi a_p^3) = \pi a_p^2 \dot{m}$$

$$\text{or} \quad \frac{da_p}{dt} = \frac{2\dot{m}}{\rho_p} = \frac{4\rho D_{O_2 m}}{a_p \rho_p} \ell n(1 + \frac{3}{4} K_{O_2,\text{ambient}})$$

A lower limit on the particle life can be estimated by setting $K_{O_2,\text{ambient}} = 0.232$; then $\ell n(1+B') = 0.160$, and integrating from t = 0 with initial size a_{pO}, to $t = \tau$ when $a_p = 0$, gives

$$\tau = 0.32 \rho_p a_{pO}^2 / \rho D_{O_2 m}$$

where $\rho D_{O_2 m}$ has been taken to be constant, and chemical kinetics limitations near the end of the particle lifetime have been ignored.

Example 4.3

In contrast to a solid graphite or carbon-carbon heatshield the carbonaceous surface of a charring ablator is porous, and through the pores percolates pyrolysis gas. For steady state ablation determine the effect of the pyrolysis gas on the diffusion controlled surface oxidation rate. Assume that the pyrolysis gases are inert with respect to the boundary layer gases.

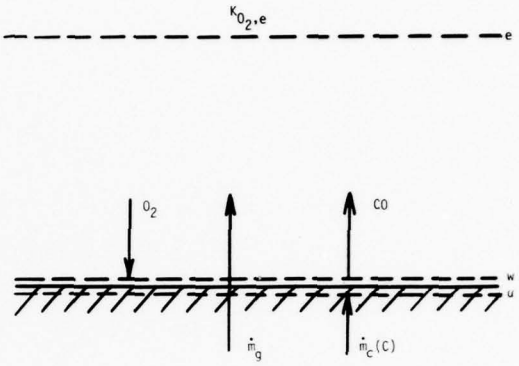

We will again simplify the analysis by assuming that the freestream contains undissociated oxygen, and that thermodynamic equilibrium prevails at the w-surface with $K_{O_2,w} = 0$. The mass transfer driving force is, from Eq. (4.2-5),

$$B' = \frac{K_{1,e} - K_{1,w}}{K_{1,w} - n_{1,w}/\dot{m}} \qquad \text{where species 1 is } O_2$$

$$= \frac{0.232}{-n_{1,w}/\dot{m}}$$

For steady state ablation the mass loss rate of pyrolysis gas and char are equal, $\dot{m}_g = \dot{m}_c$, and thus $\dot{m} = \dot{m}_c + \dot{m}_g = 2\dot{m}_c$. Also for the reaction $C + O_2 \rightarrow 2CO$ the stoichiometric ratio r is again 4/3, i.e., for each 1 lb of char crossing the u-surface, 4/3 lb of O_2 crosses the w-surface, in the negative direction,

$$\frac{n_{1,w}}{\dot{m}_c} = -\frac{4}{3}, \qquad \text{or} \qquad \frac{n_{1,w}}{\dot{m}} = -\frac{n_{1,w}}{2\dot{m}_c} = -\frac{2}{3}$$

and $$B' = \frac{0.232}{2/3} = 0.348$$

From Eq. (4.2-9), $$\dot{m} = \rho_e u_e C_{MO} \frac{\ell n(1+B')}{B'} B'$$

$$\dot{m} = \rho_e u_e C_{MO}(0.858)(0.348)$$

$$= 0.299\rho_e u_e C_{MO}$$

and $\dot{m}_c = \frac{1}{2}\dot{m} = 0.150\rho_e u_e C_{MO}$

For a solid carbon surface we have already shown that $B' = 0.174$ and $\dot{m} = \rho_e u_e C_{MO}(0.922)(0.174) = 0.160\rho_e u_e C_{MO}$. Hence the reduction in oxidation rate due to the pyrolysis gas is $(0.160-0.150)/0.160 = 7\%$.

4.3 A MORE COMPLEX CASE OF DIFFUSION CONTROLLED OXIDATION

We now consider oxidation of a graphite surface when significant reactions might occur in the gas phase, for example: (i) If the free-stream is at a high enough temperature for O_2 to dissociate, and if the surface is much cooler, there may be recombination $2O \rightarrow O_2$ occurring in the boundary layer. (ii) If the surface temperature is in the range 2000-4000°F, and the free-stream is cool, the surface reaction is $C + CO_2 \rightarrow 2CO$, and there is a gas phase reaction $2CO + O_2 \rightarrow 2CO_2$, as shown above.

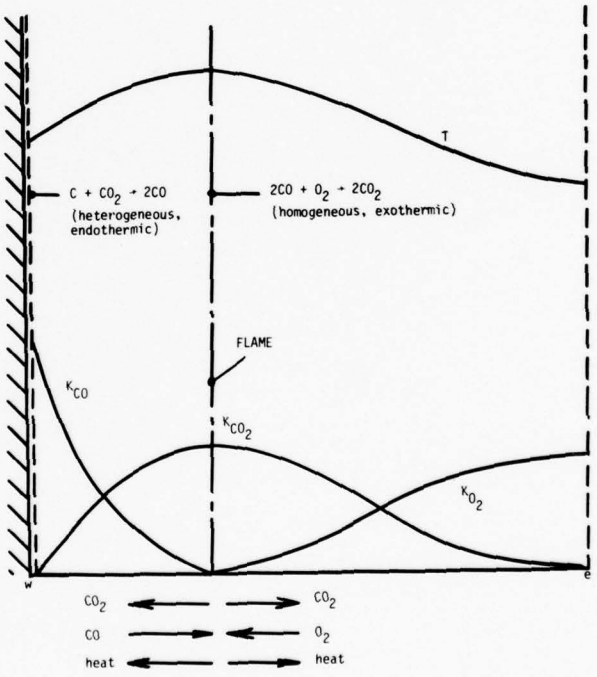

Let us analyze the latter problem. Again we will use a Couette flow model: conservation of species i in a control volume dy thick, cross-sectional area A requires that at steady state

$$\begin{matrix}\text{outflow of} \\ \text{species i}\end{matrix} - \begin{matrix}\text{inflow of} \\ \text{species i}\end{matrix} = \begin{matrix}\text{production of species i} \\ \text{due to chemical reactions}\end{matrix}$$

$$An_i\big|_{y+dy} - An_i\big|_y = \dot{r}_i A dy$$

$$(n_i\big|_{y+dy} - n_i\big|_y)/dy = \dot{r}_i$$

let $dy \to 0$, $$\frac{d}{dy}(n_i) = \dot{r}_i \qquad (4.3\text{-}1)$$

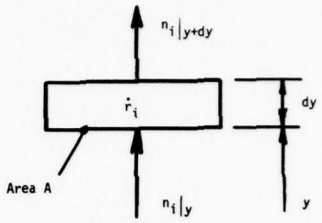

Here $\dot{r}_i$ is the mass rate of production of species i due to chemical reactions, and has dimensions mass/unit volume - unit time. Species i may be O_2, CO_2, CO or N_2, thus

$$\frac{d}{dy}(n_{O_2}) = \dot{r}_{O_2} \qquad (4.3\text{-}2a)$$

$$\frac{d}{dy}(n_{CO_2}) = \dot{r}_{CO_2} \qquad (4.3\text{-}2b)$$

$$\frac{d}{dy}(n_{CO}) = \dot{r}_{CO} \qquad (4.3\text{-}2c)$$

$$\frac{d}{dy}(n_{N_2}) = \dot{r}_{N_2} = 0 \qquad \text{since } N_2 \text{ is inert} \qquad (4.3\text{-}2d)$$

The $\dot{r}_i$'s are given by complex expressions involving reaction rates and equilibrium relations. However, we can solve a problem to determine the carbon oxidation rate without knowing the $\dot{r}_i$ expressions, provided we are prepared to assume all the species diffusion coefficients equal, which for this chemical system is quite realistic. We first multiply Eq. (4.3-2a) by the mass fraction of element oxygen in O_2, α_{OO_2}, Eq. (4.3-2b) by α_{OCO_2}, Eq. (4.3-2c) by α_{OCO}, and then add,

$$\frac{d}{dy}(\alpha_{OO_2} n_{O_2} + \alpha_{OCO_2} n_{CO_2} + \alpha_{OCO} n_{CO}) = \alpha_{OO_2}\dot{r}_{O_2} + \alpha_{OCO_2}\dot{r}_{CO_2} + \alpha_{OCO}\dot{r}_{CO}$$

or $$\frac{d}{dy} \sum_i \alpha_{O_i} n_i = \sum_i \alpha_{O_i} \dot{r}_i \qquad (4.3\text{-}3)$$

Now the first term on the right hand side of Eq. (4.3-3) is the rate at which element O appears (or disappears) in the form of O_2 as O_2 is produced (or consumed) by chemical reactions; the second term is the rate at which

O appears in the form of CO_2; etc. Since there cannot be a net creation or destruction of a chemical element, these terms must sum to zero, $\sum_i \alpha_{Oi} r_i = 0$. Or, more generally

$$\sum_i \alpha_{ki} \dot{r}_i = 0 , \qquad \text{any element } k \tag{4.3-4}$$

The absolute flux of *element* O, $\tilde{n}_O = \sum \alpha_{Oi} n_i$, so Eq. (4.3-3) becomes

$$\frac{d}{dy} (\tilde{n}_O) = 0 \tag{4.3-5}$$

integrate, $$\tilde{n}_O = \text{constant} = \tilde{n}_{O,w} \tag{4.3-6}$$

or $$\sum_i \alpha_{Oi} (K_i n - \rho D_{im} \frac{dK_i}{dy}) = \tilde{n}_{O,w} \tag{4.3-7}$$

If we now assume all the D_{im} equal, i.e., $D_{O_2m} = D_{CO_2m} = D_{CO_m} = D$, then

$$n \sum \alpha_{Oi} K_i - \rho D \frac{d}{dy} \sum \alpha_{Oi} K_i = \tilde{n}_{O,w}$$

or $$n\tilde{K}_O - \rho D \frac{d\tilde{K}_O}{dy} = \text{constant} = \tilde{n}_{O,w} \tag{4.3-8}$$

where $\tilde{K}_O \equiv \sum_i \alpha_{Oi} K_i$ is the mass fraction of element oxygen in the mixture, irrespective of which chemical species it is contained. At this point the problem has been reduced to a mathematical form identical to those of §4.1 and §4.2, and we need not repeat the algebra of the previous analyses from this point forward. The result is

$$\dot{m} = \rho_e u_e C_{MO} \frac{\ell n(1+B')}{B'} B' \tag{4.3-9}$$

$$B' = \frac{\tilde{K}_{O,e} - \tilde{K}_{O,w}}{\tilde{K}_{O,w} - \tilde{n}_{O,w}/\dot{m}} \tag{4.3-10}$$

Notation for the transferred state mass fraction. The quantity $\tilde{n}_{O,w}/\dot{m}$ has been previously identified as the *transferred state* mass fraction, i.e., is the fraction of the stream of mass crossing the w-surface which is element oxygen. To introduce notation for this quantity first go back to

§4.1 where we were dealing with transfer of an inert species, H_2O, denoted species 1, and define $n_{1,w}/\dot{m} \equiv K_{1,tw}$; $n_{1,u}/\dot{m} \equiv K_{1,tu}$. Then since H_2O is inert, $n_{1,w} = n_{1,u}$, and $K_{1,tw} = K_{1,tu} \equiv K_{1,t}$ i.e., the subscripts tw and tu may be replaced by t without ambiguity. In §4.2 we dealt with species i which could react at the surface, then if $n_{i,w}/\dot{m} \equiv K_{i,tw}$ and $n_{i,tu}/\dot{m} = K_{i,tu}$, in general $K_{i,tw} \neq K_{i,tu}$. For example $K_{W,tu} = 1$, while $K_{W,tw} = 0$ since only metal tungsten crosses the u-surface, while only O_2 and W_3O_9 cross the w-surface. In the present problem $\tilde{n}_{O,w} = \tilde{n}_{O,u}$ since a chemical element cannot be created or destroyed between the u- and w-surfaces, thus we define $\tilde{n}_{O,w}/\dot{m} \equiv K_{O,t}$ without ambiguity. Since $\Sigma n_i = n$, and $\Sigma \tilde{n}_k = n$ it follows that the sums of mass fractions in the transferred state of species or elements are unity. But in contrast to mixture mass fractions, transferred state mass fractions may take on any value between $-\infty$ and $+\infty$.

Thus Eq. (4.3-10) becomes $$B' = \frac{\tilde{K}_{O,e} - \tilde{K}_{O,w}}{\tilde{K}_{O,w} - \tilde{K}_{O,t}} \qquad (4.3\text{-}11)$$

Now recall that $\rho_e u_e C_{MO}$ is simply a property of the flow and is straightforward to calculate. Thus if we can evaluate B' we can determine $\dot{m}$. Lets look at each term in B' in turn:

$\tilde{K}_{O,e} = K_{O_2,e}$, and is known from the free-stream composition

$$\tilde{K}_{O,w} = \Sigma \alpha_{O_i} K_{i,w} = K_{O_2,w} + \frac{32}{44} K_{CO_2,w} + \frac{16}{28} K_{CO,w}$$

But at the surface temperatures under consideration the forward reaction of carbon with oxidizing species are very rapid, and thus the concentrations of O_2 and CO_2 at the w-surface may be taken to be zero, then

$$\tilde{K}_{O,w} = \frac{16}{28} K_{CO,w}$$

Carbon monoxide is the product of the oxidation reactions and its concen-

tration is finite at the w-surface, and is *a priori* unknown. So we cannot use Eq. (4.3-11) directly to evaluate B'. Instead we first perform a little algebraic manipulation. Rewrite Eq. (4.3-9) as

$$B' = \exp(\dot{m}/\rho_e u_e C_{MO}) - 1$$

and substitute from Eq. (4.3-11) to obtain

$$\tilde{K}_{O,e} - \tilde{K}_{O,w} = (\tilde{K}_{O,w} - \tilde{K}_{O,t})[\exp(\dot{m}/\rho_e u_e C_{MO}) - 1] \tag{4.3-12}$$

Now recognize that we could have equally well done our analysis for element carbon, which would have given

$$\tilde{K}_{C,e} - \tilde{K}_{C,w} = (\tilde{K}_{C,w} - \tilde{K}_{C,t})[\exp(\dot{m}/\rho_e u_e C_{MO}) - 1] \tag{4.3-13}$$

Multiply Eq. (4.3-12) by ζ and Eq. (4.3-13) by ξ, add and rearrange,

$$\dot{m} = \rho_e u_e C_{MO} \frac{\ell n(1+B')}{B'} B'$$

$$B' = \frac{(\zeta\tilde{K}_O + \xi\tilde{K}_C)_e - (\zeta\tilde{K}_O + \xi\tilde{K}_C)_w}{(\zeta\tilde{K}_O + \xi\tilde{K}_C)_w - (\zeta\tilde{K}_O + \xi\tilde{K}_C)_t} \tag{4.3-14}$$

We are free to choose any values for the multipliers ζ and ξ: lets see if we can choose values such that we can evaluate the terms in Eq. (4.3-14) from given data. Clearly the e-state gives no problem. For the w-state:

$$(\zeta\tilde{K}_O + \xi\tilde{K}_C)_w = \zeta(K_{O_2,w} + \frac{32}{44} K_{CO_2,w} + \frac{16}{28} K_{CO,w}) + \xi(\frac{12}{44} K_{CO_2,w} + \frac{12}{28} K_{CO,w})$$

$$= K_{CO,w}(\frac{16}{28}\zeta + \frac{12}{28}\xi) \qquad \text{since} \qquad K_{O_2,w} = K_{CO_2,w} = 0$$

So if we choose $\zeta = 12/16$ and $\xi = -1$, then $(\frac{12}{16}\tilde{K}_O - \tilde{K}_C)_w = 0$ and we need not know $K_{CO,w}$. Also then $(\frac{12}{16}\tilde{K}_O - \tilde{K}_C)_e = \frac{12}{16} K_{O_2,e}$, and $(\frac{12}{16}\tilde{K}_O - \tilde{K}_C)_t = -1$ since looking at the u-surface, $\tilde{n}_O = 0$, $\tilde{n}_C = \dot{m}$ so $\tilde{K}_{O,t} = 0$ and $\tilde{K}_{C,t} = 1$. Substituting in Eq. (4.3-14),

$$B' = \frac{\frac{3}{4} K_{O_2,e} - 0}{0-(-1)} = \frac{3}{4} K_{O_2,e} = 0.174$$

which is the same value as was obtained in §4.2. Notice, however, we have made the additional assumption that all the diffusion coefficients of species containing C or O are equal, and thus our value of B' may be less accurate. In fact binary diffusion coefficients for the chemical system C-O-N are not too different, and the assumption is quite justified.

Example 4.4

As an example of the analysis technique used above, let us investigate the effect of adding water vapor to an air-stream flowing over combusting carbon. The technological problem might concern heatshield performance during reentry through a rainstorm.

Relative to carbon, water vapor is an oxidizer and, at temperatures of concern, chemical equilibrium shows that $K_{H_2O,w} \simeq 0$. Again we use a B' based on the combination $(\frac{12}{16}\tilde{K}_O - \tilde{K}_C)$ as follows.

$$\tilde{K}_C = \frac{12}{44} K_{CO_2} + \frac{12}{28} K_{CO}$$

$$\tilde{K}_O = K_{O_2} + \frac{32}{44} K_{CO_2} + \frac{16}{28} K_{CO} + \frac{16}{18} K_{H_2O}$$

thus $$(\frac{12}{16}\tilde{K}_O - \tilde{K}_C) = \frac{12}{16} K_{O_2} + \frac{12}{44} K_{CO_2} + \frac{12}{18} K_{H_2O}$$

As before $$(\frac{12}{16}\tilde{K}_O - \tilde{K}_C)_w = 0 \; ; \quad (\frac{12}{16}\tilde{K}_O - \tilde{K}_C)_t = -1$$

and now $$(\frac{12}{16}\tilde{K}_O - \tilde{K}_C)_e = \frac{12}{16} K_{O_2,e} + \frac{12}{44} K_{CO_2,e} + \frac{12}{18} K_{H_2O,e} = B'$$

We see that water vapor serves to increase the driving force B' and hence the carbon oxidation rate. For an increase of 10 percent in B' over the value for dry air (0.174) the required H_2O concentration is calculated to be $\tilde{K}_{H_2O,e} = 0.026$.

Note that the carbon-steam reaction is highly endothermic: the analysis has assumed that the heat supply requirements of this reaction do not markedly change the carbon surface temperature. A much lower temperature would

significantly alter the conductance through the transport properties, or could even cause a change to the kinetics controlled oxidation regime. In the case of a heatshield the convective heating usually dominates and T_w is little affected by the oxidation reactions; however for small ejecta particles combusting in the boundary layer the particle temperature can be significantly lowered.

Example 4.5

A solid propellant rocket motor has a graphite lined throat. The propellant gases contain oxidizing species which cause the throat to enlarge at an appreciable rate. If the elemental composition of the propellant is $\tilde{K}_O = 0.560$, $\tilde{K}_C = 0.256$, $\tilde{K}_H = 0.028$ and $\tilde{K}_N = 0.156$, estimate the mass transfer driving force B'.

We can safely assume that the surface temperature is high enough for thermodynamic equilibrium, and that CO is the only oxygen containing species having an appreciable concentration at the w-surface. Thus, as before, the driving force may be based on the combination $(\frac{12}{16}\tilde{K}_O - \tilde{K}_C)$ to obtain

$$B' = \frac{12}{16}\tilde{K}_{O,e} - \tilde{K}_{C,e}$$

However, in contrast to the previous problems, we do not know the molecular species composition at the e-surface: typically the mixture will be quite complex. Thus we cannot express $\tilde{K}_{C,e}$ and $\tilde{K}_{O,e}$ in terms of the $\tilde{K}_{i,e}$. But fortunately we do not have to since the elemental composition at the e-surface must be the same as that of the propellant. Hence

$$B' = \frac{12}{16}(0.560) - (0.256) = 0.164$$

To obtain the rate of enlargement of the throat we would obtain $\rho_e u_e C_{MO}$ from an appropriate turbulent boundary layer correlation and determine $\dot{m}$ using Eq. (4.3-9).

4.4 FLAME SHEET MODEL FOR CARBON OXIDATION

The method of analysis presented in §4.3 allowed determination of the mass transfer rate, but does not give the concentration profiles, and, in particular, the location of the flame. We will now re-analyze the problem assuming that the homogeneous reactions occur at an infinitely thin flame "sheet" as depicted in the Figure for a carbon sphere of radius R_s located in stagnant air. Region I lies between the particle and the flame, while region II lies between the flame of radius R_f and infinity. The mass transfer rate across the w-surface is $\dot{m}_I$, while across the uf-and wf-surfaces it is $\dot{m}_{II}$. The reactions are as described in §4.3.

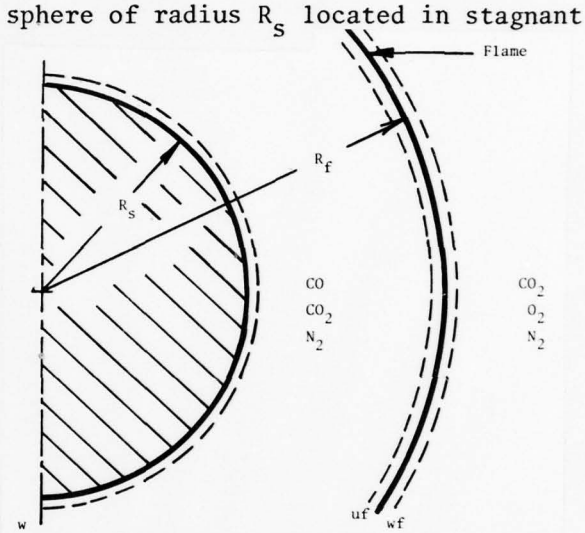

Solution of species conservation equations follows the procedure given in §4.2, except that the spherical geometry must be accounted for. With equal diffusion coefficients $\mathcal{D}_{im} = \mathcal{D}$,

$$\dot{m}_I = \frac{\rho\mathcal{D}}{R_s} \frac{R_f}{R_f - R_s} \ln(1+B'_I) \tag{4.4-1}$$

$$\dot{m}_{II} = \frac{\rho\mathcal{D}}{R_f} \ln(1+B'_{II}) \tag{4.4-2}$$

where in region I the integration is from R_f to R_s, while in region II it is from R_f to infinity. For region I B' may be based on CO or CO_2,

$$B'_I = \frac{K_{CO,uf} - K_{CO,w}}{K_{CO,w} - K_{CO,tw}} = \frac{K_{CO_2,uf} - K_{CO_2,w}}{K_{CO_2,w} - K_{CO_2,tw}}$$

But $K_{CO,uf} = 0$, $K_{CO_2,w} = 0$, and stoichiometry at the w-surface requires

$$CO_2 + C \rightarrow 2CO$$

$$11\ \text{lb} + 3\ \text{lb} \rightarrow 14\ \text{lb} \qquad \text{or} \qquad K_{CO,tw} = \frac{14}{3}\ ;\quad K_{CO_2,tw} = -\frac{11}{3}$$

Thus $$B'_I = \frac{K_{CO,w}}{\frac{14}{3} - K_{CO,w}} = \frac{3}{11} K_{CO_2,uf} \tag{4.4-3,4}$$

For region II B' may be based on O_2 and CO_2,

$$B'_{II} = \frac{K_{O_2,e} - K_{O_2,wf}}{K_{O_2,wf} - K_{O_2,twf}} = \frac{K_{CO_2,e} - K_{CO_2,wf}}{K_{CO_2,wf} - K_{CO_2,twf}}$$

But $K_{O_2,wf} = 0$, $K_{CO_2,e} = 0$, thus

$$B'_{II} = \frac{0.232}{-K_{O_2,twf}} = \frac{K_{CO_2}}{K_{CO_2,twf} - K_{CO_2,wf}} \tag{4.4-5,6}$$

Continuity of mass flux at the flame requires

$$\dot{m}_{II} = n_{CO_2,uf} + n_{CO,uf} = n_{CO_2,wf} + n_{O_2,wf} \tag{4.4-7,8}$$

while stoichiometry at the flame requires

$$2CO_2 + O_2 \rightarrow 2CO_2$$

$$7\ \text{lb} + 4\ \text{lb} \rightarrow 11\ \text{lb}\ ; \quad \text{thus} \quad n_{CO,uf} = -\frac{7}{4} n_{O_2,wf} \tag{4.4-9}$$

Also mass conservation requires $$\dot{m}_I = \frac{R_f^2}{R_s^2} \dot{m}_{II} \tag{4.4-10}$$

while the CO_2 concentration is continuous, $$K_{CO_2,uf} = K_{CO_2,wf} \tag{4.4-11}$$

Lastly $n_{CO_2,uf} = (R_s^2/R_f^2) n_{CO_2,w}$ is related to $\dot{m}_I$ through stoichiometry as

$$\frac{11}{3} \dot{m}_I = -\frac{R_f^2}{R_s^2} n_{CO_2,uf} \tag{4.4-12}$$

There are 12 equations in the 12 unknowns $\dot{m}_I$, $\dot{m}_{II}$, R_f, B'_I, B'_{II}, $K_{CO,w}$, $K_{CO_2,uf}$, $K_{CO_2,wf}$, $n_{O_2,wf}$, $n_{CO,uf}$, $n_{CO_2,uf}$ and $n_{CO_2,wf}$. The solution proceeds as follows.

From Eqs. (4.4-12) and (4.4-10), $\frac{11}{3} \dot{m}_{II} = -n_{CO_2,uf}$, and substituting in Eq. (4.4-7) gives

$$\dot{m}_{II} = -\frac{11}{3}\dot{m}_I + n_{CO,uf} \; ; \quad \text{thus} \qquad n_{CO,uf} = \frac{14}{3}\dot{m}_{II} \; .$$

From Eq. (4.4-9): $$n_{O_2,wf} = -(\tfrac{4}{7})(\tfrac{14}{3})\dot{m}_{II} = -\frac{8}{3}\dot{m}_{II} \; .$$

From Eq. (4.4-5): $$B'_{II} = \frac{0.232}{8/3} = 0.087 \; .$$

From Eq. (4.4-8): $$\dot{m}_{II} = n_{CO_2,wf} - \frac{8}{3}\dot{m}_{II} \; , \quad \text{thus} \qquad n_{CO_2,wf} = \frac{11}{3}\dot{m}_{II}$$

From Eq. (4.4-6): $$B'_{II} = 0.087 = \frac{K_{CO_2,wf}}{\frac{11}{3} - K_{CO_2,wf}} \; , \quad \text{thus} \quad K_{CO_2,wf} = 0.293$$

From Eq. (4.4-4): $$B'_I = (3/11)(0.293) = 0.080$$

From Eq. (4.4-3): $$0.080 = \frac{K_{CO,w}}{\frac{14}{3} - K_{CO,w}} \; , \quad \text{thus} \qquad K_{CO,w} = 0.346$$

From Eqs. (4.4-1,2 and 10),

$$\frac{\dot{m}_I}{\dot{m}_{II}} = \frac{R_f/R_s)/(R_f-R_s)}{(1/R_f)} \frac{\ell n(1+0.080)}{\ell n(1+0.087)} = \frac{R_f^2}{R_s^2}$$

Solving, $$\frac{0.922}{R_f-R_s} = \frac{1}{R_s} \qquad \text{or} \qquad R_f/R_s = 1.922$$

From Eq. (4.4-1),

$$\dot{m}_I = \frac{\rho\mathcal{D}}{R_s} \frac{1}{1-(1/1.922)} \ell n(1+0.080) = 0.160 \frac{\rho\mathcal{D}}{R_s}$$

which is exactly the result obtained in §4.3. Since the assumptions made in each analysis were identical (particularly that of equal diffusion coefficients) the result should indeed be identical. Notice that the flame radius is slightly less than twice the particle radius. If the analysis is carried out neglecting radial convection, then $\dot{m}_I = 0.174\ \rho\mathcal{D}/R_s$ and $R_f/R_s = 2.0$, i.e., the flame has exactly twice the radius of the particle.

4.5 COUETTE FLOW ANALYSIS WITH UNEQUAL DIFFUSION COEFFICIENTS

A number of new concepts were introduced with the bifurcation approximation for multicomponent diffusion introduced in §3.7. In order to become more

familiar with these concepts let us analyze simple diffusion controlled oxidation of carbon in a high temperature stream of argon and dissociated oxygen, i.e., the reaction is

$$C + O \rightarrow CO$$

where at the e-surface we have A and O. The carbon surface temperature is high enough to ensure that O does not recombine in the flow, and for chemical equilibrium to exist at the w-surface with $K_{O,w} \cong 0$. Three species are thus present in the gas phase: O, A and CO, species 1, 2 and 3, respectively.

mass conservation

$$\frac{d}{dy}(n) = 0$$

integrating

$$n = \text{constant} = \dot{m} \qquad (4.5\text{-}1)$$

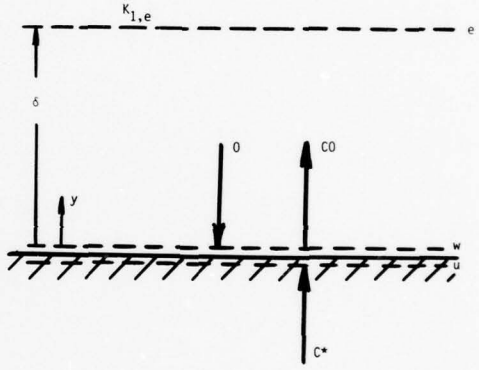

species 1 conservation

$$\frac{d}{dy}(n_1) = 0$$

integrating

$$n_1 = \text{constant} = n_{1,w}$$

or

$$K_1 n + j_1 = n_{1,w} \qquad (4.5\text{-}2)$$

Substituting for n from Eq. (4.5-1) and for j_1 from Eq. (3.7-12)

$$K_1\dot{m} - \frac{\rho\bar{D}\mu_2}{\mu_1 M}\frac{dz_1}{dy} = n_{1,w} \qquad (4.5\text{-}3)$$

Since $z_1 \equiv M_1 x_1/F_1\mu_2$, and $K_1 \equiv M_1 x_1/M$, we have $K_1 = F_1\mu_2 z_1/M$, and substituting in Eq. (4.5-3) gives

$$z_1 - \frac{\rho\bar{D}}{\dot{m}\mu_1 F_1}\frac{dz_1}{dy} = \frac{M}{F_1\mu_2}\frac{n_{1,w}}{\dot{m}} = \frac{M}{F_1\mu_2}K_{1,tw}$$

Now $K_{1,tw}$, the mass fraction in the transferred state, is fixed since it depends only on the stoichometry of the reaction, as is F_1, a property of species 1. However M, the mixture molecular weight, and $\mu_2 \equiv \sum_j M_j x_j/F_j$ vary with

composition across the flow. In order to obtain an analytical solution to our problem, we will now assume the mixture property M/μ_2 to be constant across the flow and define $z_{1,tw} = MK_{1,tw}/F_1\mu_2$, then

$$z_1 - \frac{\rho\bar{D}}{\dot{m}\mu_1 F_1}\frac{dz_1}{dy} = z_{1,tw} \tag{4.5-4}$$

The analysis now proceeds in a similar fashion to that of §4.2:

$$\int_{z_{1,w}}^{z_{1,e}} \frac{dz_1}{z_1 - z_{1,tw}} = \frac{\dot{m}F_1}{\bar{D}} \int_0^{\delta} \frac{\mu_1}{\rho}\, dy$$

$$\ell n\left(1 + \frac{z_{1,e} - z_{1,w}}{z_{1,w} - z_{1,tw}}\right) = \frac{\dot{m}\delta F_1 \mu_1}{\rho\bar{D}} \qquad \text{if } \rho/\mu_1 \text{ is taken constant.}$$

$$\dot{m} = \frac{\rho\bar{D}}{F_1\mu_1\delta}\ell n(1+B'_z) \qquad \text{where} \qquad B'_z = \frac{z_{1,e} - z_{1,w}}{z_{1,w} - z_{1,tw}} \tag{4.5-5}$$

In order to assess the effect of unequal diffusion coefficients on mass loss rate $\dot{m}$, let us compare this result with the result obtained if effective binary diffusion is assumed; then we would approximate $\mathcal{D}_{1m}$ as $\mathcal{D}_{O,A}$ and write

$$\dot{m} = \frac{\rho\mathcal{D}_{O,A}}{\delta}\ell n(1+B')$$

Now if the reference diffusion coefficient is chosen to be that of argon, then $\mathcal{D}_{O,A} = \bar{D}/F_1F_2 = \bar{D}/F_1$, and

$$\dot{m} = \frac{\rho\bar{D}}{F_1\delta}\ell n(1+B') \tag{4.5-6}$$

Comparing Eqs. (4.5-5) and (4.5-6),

$$\frac{\dot{m}_{\text{unequal}}}{\dot{m}_{\substack{\text{effective}\\ \text{binary}}}} = \phi = \frac{\ell n(1+B'_z)}{\mu_1 \ell n(1+B')} \tag{4.5-7}$$

Example 4.6

Compare the mass loss rate for diffusion controlled oxidation of carbon in a high temperature stream of 80 percent argon and 20 percent atomic oxygen,

by volume, calculated (i) for unequal diffusion coefficients, and (ii) effective binary diffusion.

First we calculate the F_i's:

Species	M_i	F_i
1. O	16	$(16/40)^{0.461} = 0.655$
2. A	40	1
3. CO	28	$(28/40)^{0.461} = 0.848$

where we have taken $\bar{D}$ as the self-diffusion coefficient of argon. Next we calculate the edge gas properties we need.

$$\mu_{1,e} = \Sigma x_i F_i = (0.2)(0.655) + (0.8)(1) = 0.931$$

$$\mu_{2,e} = \Sigma \frac{M_i x_{i,e}}{F_i} = \frac{(16)(0.2)}{0.655} + \frac{(40)(0.8)}{1} = 36.89$$

$$z_{1,e} = \frac{M_1 x_{1,e}}{F_1 \mu_{2,e}} = \frac{(16)(0.2)}{(0.655)(36.89)} = 0.1324$$

$$K_{1,e} = \frac{x_{1,e} M_1}{M} = \frac{(0.2)(16)}{(0.2)(16)+(0.8)(40)} = 0.0909$$

$$(z_1/K_1)_e = 1.456.$$

(Note how the z fraction lies between the mole and mass fractions.) Next we simplify Eq. (4.5-7) by evaluating the driving forces B' and B'_z.

$$B' = \frac{K_{1,e} - K_{1,w}}{K_{1,w} - K_{1,tw}} = \frac{0.0909-0}{0+4/3} = 0.0682$$

$$B'_z = \frac{z_{1,e} - z_{1,w}}{z_{1,w} - z_{1,tw}} = \frac{0.1324-0}{0-z_{1,tw}}$$

but $$z_{1,tw} = \frac{M}{F_1 \mu_2} K_{1,tw} = -\frac{4}{3}\left(\frac{M}{F_1 \mu_2}\right) = -\frac{4}{3}\left(\frac{z_1}{K_1}\right)_{1/3}$$

where the subscript 1/3 indicates that we will evaluate this variable property at a 1/3 rule reference state (1/3 e-surface value + 2/3 w-surface value). Recall that in the analysis we assumed M/μ_2 to be constant across the flow in

taking $z_{1,tw}$ to be constant. Thus

$$B'_z = \frac{0.0324-0}{0 + \frac{4}{3}(z_1/K_1)_{1/3}} = 0.0993\ (K_1/z_1)_{1/3}$$

Substituting in Eq. (4.5-7) then gives

$$\frac{\dot{m}_{unequal}}{\dot{m}_{\substack{effective\\binary}}} = \phi = \frac{(15.16)\ (1+0.0993(K_1/z_1)_{1/3})}{(\mu_1)_{1/3}}$$

where we have also evaluated the variable property μ_1 at a 1/3 rule reference state.

We cannot calculate the w-surface composition for unequal diffusion coefficients until we have $\dot{m}_{unequal}$; hence an iterative calculation is required, and as a first guess we will use the composition corresponding to the effective binary solution.

$$\dot{m}_{\substack{effective\\binary}} = \frac{\rho\mathcal{D}_{12}}{\delta} \ln\left(1 + \frac{K_{1,e}-K_{1,w}}{K_{1,w}-K_{1,tw}}\right) = \frac{\rho\mathcal{D}_{32}}{\delta} \ln\left(1 + \frac{K_{3,e}-K_{3,w}}{K_{3,w}-K_{3,tw}}\right)$$

or $$\frac{1}{F_1} \ln(1 + 0.0682) = \frac{1}{F_3} \ln\left(1 + \frac{-K_{3,w}}{K_{3,w}-7/3}\right)$$

solving, $K_{3,w} \simeq 0.19$; $x_{3,w} \simeq 0.25$.

$$\mu_{1,w} = (0.25)(0.848)+(0.75)(1) = 0.962$$

$$\mu_{2,w} = \frac{(0.25)(28)}{(0.848)} + \frac{(0.75)(40)}{1} = 38.25$$

$$(\mu_2)_{1/3} = (2/3)(38.25)+(1/3)(36.89) = 37.80$$

$$(K_1)_{1/3} = (2/3)(0)+(1/3)(0.0909) = 0.0303$$

$$(x_1)_{1/3} = (2/3)(0)+(1/3)(0.2) = 0.0667$$

$$(z_1)_{1/3} = \frac{(16)(0.0667)}{(0.655)(37.80)} = 0.04308 \quad \text{and} \quad (K_1/z_1)_{1/3} = 0.7033$$

$$(\mu_1)_{1/3} = (2/3)(0.962)+(1/3)(0.931) = 0.9516$$

then $$\phi = \frac{(15.16)\ (1+(0.0993)(0.7033))}{0.9516} = 1.0754$$

Let us check our guess for $x_{3,w}$. We have

$$\frac{1}{F_1} \ln(1+B'_{z_1}) = \frac{1}{F_3} \ln(1+B'_{z_3})$$

$$\frac{1}{0.655} \ln(1+0.06984) = \frac{1}{0.848} \ln(1+B'_{z_3}) \ , \quad \text{solving, } B'_{z_3} = 0.09133$$

But $$z_{3,t} = (28/12)(z_1/K_1)_{1/3} = (28/12)(1/0.7033) = 3.318$$

thus $$B'_{z_3} = 0.09133 = \frac{0-z_{3,w}}{z_{3,w}-3.318} \ , \quad \text{solving, } z_{3,w} = 0.277$$

and $$x_{3,w} = \frac{F_3 \mu_{2,w} z_{3,w}}{M_3} = \frac{(0.848)(38.25)(0.277)}{28} = 0.321$$

So we see that our first guess of $x_{3,w} = 0.25$ was a little low. If the calculation is now repeated for $x_{3,w} = 0.321$, it is found that the new value of ϕ is 1.0748. So within sufficient accuracy we can take $\phi = 1.075$.

Note that in this simple problem we are able to carefully choose an appropriate effective binary diffusion coefficient by recognizing that the argon concentration was large throughout the flow; thus for diffusion of atomic oxygen, $\mathcal{D}_{O,A}$ was used. In general this is a superior procedure to assuming all effective binary diffusion coefficients equal, as has been done in most computer codes developed for engineering use.

CHAPTER 5

SURFACE CHEMISTRY

5.1 INTRODUCTION

In Chapter 4 we treated mass transfer problems for which the essential details of the w-surface molecular composition were known. For example, in the water evaporation problem of §4.1, $K_{H_2O,w}$ was obtained from $P_{H_2O,sat}(T_w)$, an equilibrium relation tabulated in steam tables. In the tungsten oxidation problem of §4.2, $K_{O_2,w} \simeq 0$, again an equilibrium relation: in the temperature range considered the reaction $3W^* + 4.5O_2 \rightleftharpoons W_3O_9$ is in equilibrium, and the equilibrium constant is

$$K_{P\,W_3O_9}(T) = P_{W_3O_9}/P_{O_2}^{4.5} >> 1 \qquad (5.1\text{-}1)$$

But how did we know that the reaction product was W_3O_9? At higher temperatures we would expect W_2O_6 and WO_3 to appear, and finally even WO_2 and WO. If all these products are to be considered we have numerous equilibrium relations, of the form of Eq. (5.1-1), to consider simultaneously, and the problem of determining the w-surface composition becomes quite complex.

As another example consider graphite ablation at high temperatures. In the stagnation region of a missile at peak heating the freestream temperatures are usually very high, and at values of the wall temperature greater than about 3000°R the reactions are

$$C + O \rightarrow CO \quad \text{and} \quad 2C + O_2 \rightarrow 2CO,$$

and are diffusion controlled with $K_{O,w}$ and $K_{O_2,w} \simeq 0$. If T_w is increased to about 5500°R the carbon surface begins to sublime yielding vapor species such as C_1, C_2, C_3, etc. Also reactions between carbon and nitrogen take place and, for example, the cyano radical CN is formed. The figure on the following page shows the typical mass loss behavior, plotted as the dimen-

sionless ratio $\dot{m}/\rho_e u_e C_M (=B')$.

Recall from §4.3,

$$\dot{m} = \rho_e u_e C_M B' \quad \text{(exact)} \qquad (5.1\text{-}2)$$

$$\frac{C_M}{C_{MO}} = \frac{\ell n(1+B')}{B'} \quad \text{(Couette flow model)} \qquad (5.1\text{-}3)$$

$$B' = \frac{\tilde{K}_{k,e} - \tilde{K}_{k,w}}{\tilde{K}_{k,w} - \tilde{K}_{k,t}} \quad \text{(equal } D\text{'s)} \qquad (5.1\text{-}4)$$

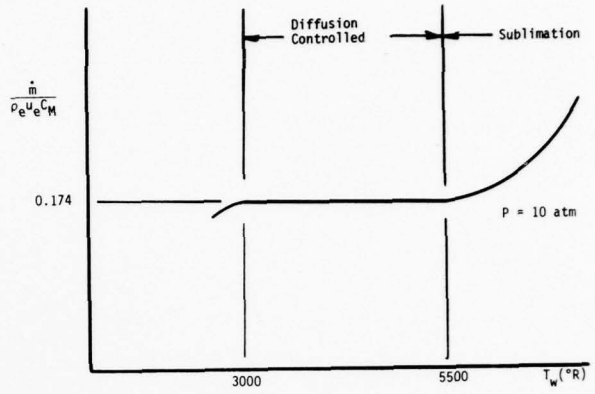

In order to calculate the mass transfer rate $\dot{m}$ we must evaluate B'. $\tilde{K}_{C,e} = 0$ of course, and since only species carbon crosses the u-surface, $\tilde{K}_{C,t} = 1$, so it remains to evaluate $\tilde{K}_{C,w} = \Sigma_i \alpha_{C_i} K_{i,w}$, and we see that we require the molecular composition at the w-surface. If we knew the $K_{i,w}$'s we could evaluate B' and hence $\dot{m}$. At these high temperatures and pressures the assumption of chemical equilibrium is good so that we can use chemical equilibrium relations to determine the $K_{i,w}$'s. In fact, we shall see that is convenient to determine B' directly, and since $K_{i,w} = K_{i,w}(T_w,P)$, we obtain $B'(T_w,P) = \dot{m}/\rho_e u_e C_M$, i.e., a graph of the kind shown in the figure above.

5.2 OPEN SYSTEM EQUILIBRIUM (WITHOUT CONDENSED PHASE REMOVAL)

Texts on chemical thermodynamics usually discuss chemical equilibrium in the context of a closed system. A closed system equilibrium calculation involves specification of the relative amounts of each chemical element, together with two independent thermodynamic variables (e.g., T and P), and the result is the molecular composition K_i. On the other hand the w-surface is an open system where the elemental composition depends on various mass transfer and material degradation rates, and surface constraints. Thus in ablation analysis we are primarily interested in open systems and we focus attention here on the calculation of open system chemical equilibrium.

We will develop the theory for boundary layer flow over an ablating surface and will assume (i) no material is removed from the surface as a condensed phase, i.e., no melt layer removal, erosion or mechanical fail removal, and (ii) equal diffusion coefficients for all species. These restrictions will be removed in a later section. The figure shows a control volume bounded by the w- and u-surfaces, and the fluxes of chemical elements. Subscript c refers to surface material (often char) and g refers to gas (often pyrolysis gas) which may be percolating through the surface material. The fluxes $\dot{m}_c\tilde{K}_{k,c}$ and $\dot{m}_g\tilde{K}_{k,g}$ are fluxes across the u-surface and strictly speaking should be subscripted u. Mass conservation applied to the control volume requires

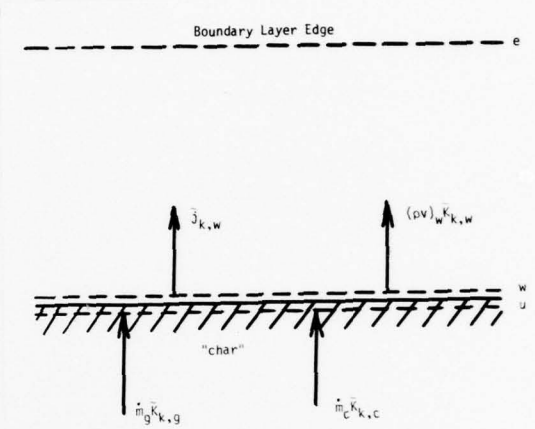

$$\dot{m}_g + \dot{m}_c = \dot{m} = (\rho v)_w \tag{5.2-1}$$

by definition
$$\tilde{K}_{k,w} = \sum_{i=1}^{I} \alpha_{ki} K_{i,w} \tag{5.2-2}$$

and
$$\tilde{j}_{k,w} = \sum_{i=1}^{I} \alpha_{ki} j_{i,w} \tag{5.2-3}$$

where I is the number of gaseous species. The figure shows the total element flux $\tilde{n}_{k,w}$ divided into its convective component $(\rho v)_w \tilde{K}_{k,w}$, and its diffusive component $\tilde{j}_{k,w}$. Conservation of chemical elements in the control volume requires

$$\tilde{j}_{k,w} + (\rho v)_w \tilde{K}_{k,w} = \dot{m}_g \tilde{K}_{k,g} + \dot{m}_c \tilde{K}_{k,c} \tag{5.2-4}$$

Now the mass transfer Stanton number for species i is defined as

$$\rho_e u_e C_{Mi} \equiv j_{i,w}/(K_{i,w}-K_{i,e}) \tag{5.2-5}$$

thus $$\tilde{j}_{k,w} = \sum_{i=1}^{I} \alpha_{ki} j_{i,w}$$

$$= \sum_{i=1}^{I} \alpha_{ki} \rho_e u_e C_{Mi} (K_{i,w}-K_{i,e})$$

In general, $C_{Mi} = C_{Mi}(Re,Sc_i)$ and $Sc_i = \mu/\rho D_{im}$, so for equal diffusion coefficients all the C_{Mi} are equal, $C_{Mi} = C_M$ say, and

$$\tilde{j}_{k,w} = \rho_e u_e C_M (\Sigma\alpha_{ki} K_{i,w} - \Sigma\alpha_{ki} K_{i,e})$$

$$= \rho_e u_e C_M (\tilde{K}_{k,w}-\tilde{K}_{k,e}) \tag{5.2-6}$$

or $$\rho_e u_e C_M = \tilde{j}_{k,w}/(\tilde{K}_{k,w}-\tilde{K}_{k,e}) \tag{5.2-7}$$

Substitute Eq. (5.2-7) in (5.2-4),

$$\rho_e u_e C_M (\tilde{K}_{k,w}-\tilde{K}_{k,e}) + (\rho v)_w K_{k,w} = \dot{m}_g \tilde{K}_{k,g} + \dot{m}_c \tilde{K}_{k,c} \tag{5.2-8}$$

We now define dimensionless pyrolysis, char and mass transfer rates as

$$B'_g \equiv \frac{\dot{m}_g}{\rho_e u_e C_M} \; ; \quad B'_c \equiv \frac{\dot{m}_c}{\rho_e u_e C_M} \; ; \quad B' = \frac{(\rho v)_w}{\rho_e u_e C_M}$$

and solve Eq. (5.2-8) for $K_{k,w}$,

$$\tilde{K}_{k,w} = \frac{B'_g \tilde{K}_{k,g} + B'_c \tilde{K}_{k,c} + \tilde{K}_{k,e}}{1+B'} \tag{5.2-9}$$

which constrains the elemental composition at the w-surface: Eq. (5.2-9) gives the relative amounts of chemical elements at the w-surface in terms of the known elemental compositions of the freestream, pyrolysis gas and char, and two of B'_g, B'_c or B' ($B'_g + B'_c = B'$) from Eq. (5.2-1)).

Example 5.1

Determine the form taken by Eq. (5.2-9) for graphite ablation into air.

In this situation $B'_g = 0$ so $B' = B'_c$. Also $\tilde{K}_{C,c} = 1$, $\tilde{K}_{O,e} = 0.232$, $\tilde{K}_{N,e} = 0.768$; $\tilde{K}_{C,e} = \tilde{K}_{O,c} = \tilde{K}_{N,c} = 0$. Thus

$$\tilde{K}_{C,w} = \frac{B'}{1+B'} \; ; \quad \tilde{K}_{O,w} = \frac{0.232}{1+B'} \; ; \quad \tilde{K}_{N,w} = \frac{0.768}{1+B'}$$

So we see that the elemental concentrations at the w-surface are unique functions of the dimensionless mass transfer rate $B' = \dot{m}/\rho_e u_e C_M$.

Note that if we lump the pyrolysis gas and char streams into a single stream, it will have an elemental composition $\tilde{K}_{k,t}$ given by,

$$\dot{m}\tilde{K}_{k,t} = \dot{m}_g \tilde{K}_{k,g} + \dot{m}_c \tilde{K}_{k,c}$$

substituting in Eq. (5.2-9), $\tilde{K}_{k,w} = \dfrac{B'\tilde{K}_{k,t}+\tilde{K}_{k,e}}{1+B'}$ (or $B' = \dfrac{\tilde{K}_{k,e}-\tilde{K}_{k,w}}{\tilde{K}_{k,w}-\tilde{K}_{k,t}}$)

With the elemental composition $\tilde{K}_{k,w}$ specified by Eq. (5.2-9), we proceed to develop the relations required to calculate the equilibrium molecular composition $K_{i,w}$. For reactions of gaseous monatomic species with the ablating surface we write

$$\sum_{k=1}^{K} c_{k\ell} N_k \rightarrow N_\ell \tag{5.2-10}$$

where $c_{k\ell}$ is the number of atoms of element k in condensed phase species ℓ, and N_k represents the symbol for gaseous element k, k = 1,2,...,K. Similarly, for reactions between the gaseous species i, an independent set will be the formation reactions from the gaseous monatomic species,

$$\sum_{k=1}^{K} c_{ki} N_k \rightarrow N_i \qquad i = 1,2,\ldots,I-K \tag{5.2-11}$$

We have chosen the monatomic gaseous species as *base* species for convenience in developing the theory; in practice these species might be in too small a concentration, and to avoid numerical problems another set of base species should be used. The number of independent equations in the set Eq. (5.2-11)

is equal to the number of gaseous species minus the number of elements. An exception to this rule is when two or more elements are in the same ratio in all molecules of a system, e.g., NO_2, N_2O_4.

For thermally perfect gaseous species the equilibrium relations corresponding to Eqs. (5.2-11) are

$$P_i / \prod_{k=1}^{K} P_k^{c_{ki}} = K_{Pi}(T) \qquad i = 1,2,\ldots,I-K \tag{5.2-12}$$

$$\text{or} \quad \ell n P_i - \sum_{k=1}^{K} c_{ki} \ell n P_k = \ell n K_{Pi}(T) \qquad i = 1,2,\ldots,I-K \tag{5.2-13}$$

where $K_{Pi}(T)$ is the equilibrium constant for the reaction and is available in tabulated form or may be calculated from thermodynamic data. The equilibrium relation corresponding to Eq. (5.2-10) are, if ℓ is the surface species (assuming only one is present),

$$-\sum_{k=1}^{K} c_{k\ell} \ell n P_k = \ell n K_{P\ell}(T) \tag{5.2-14}$$

and for all other candidate condensed phase species,

$$-\sum_{k=1}^{K} c_{k\ell} \ell n P_k < \ell n K_{P\ell}(T) \tag{5.2-15}$$

if work of compression for condensed phases is assumed to be negligible. The partial pressures of the gaseous species must add to the total pressure,

$$\sum_{i=1}^{I} P_i = P \tag{5.2-16}$$

and finally we must relate the $\tilde{K}_{k,w}$ to P_i as follows:

molar concentration of species i, $c_i = cP_i/P$

molar concentration of element k, $\tilde{c}_k = \Sigma_i c_{ki} cP_i/P$

partial density of element k, $\tilde{\rho}_k = \tilde{c}_k M_k$

mass fraction of element k, $\tilde{K}_k = \tilde{\rho}_k/\rho$

AD-A064 943 CALIFORNIA UNIV LOS ANGELES SCHOOL OF ENGINEERING A--ETC F/G 20/13
CONVECTIVE HEAT AND MASS TRANSFER TO RE-ENTRY VEHICLES.(U)
DEC 78 A F MILLS AFOSR-76-2931

UNCLASSIFIED UCLA-ENG-7982 AFOSR-TR-79-0030 NL

2 OF 3
AD A064943

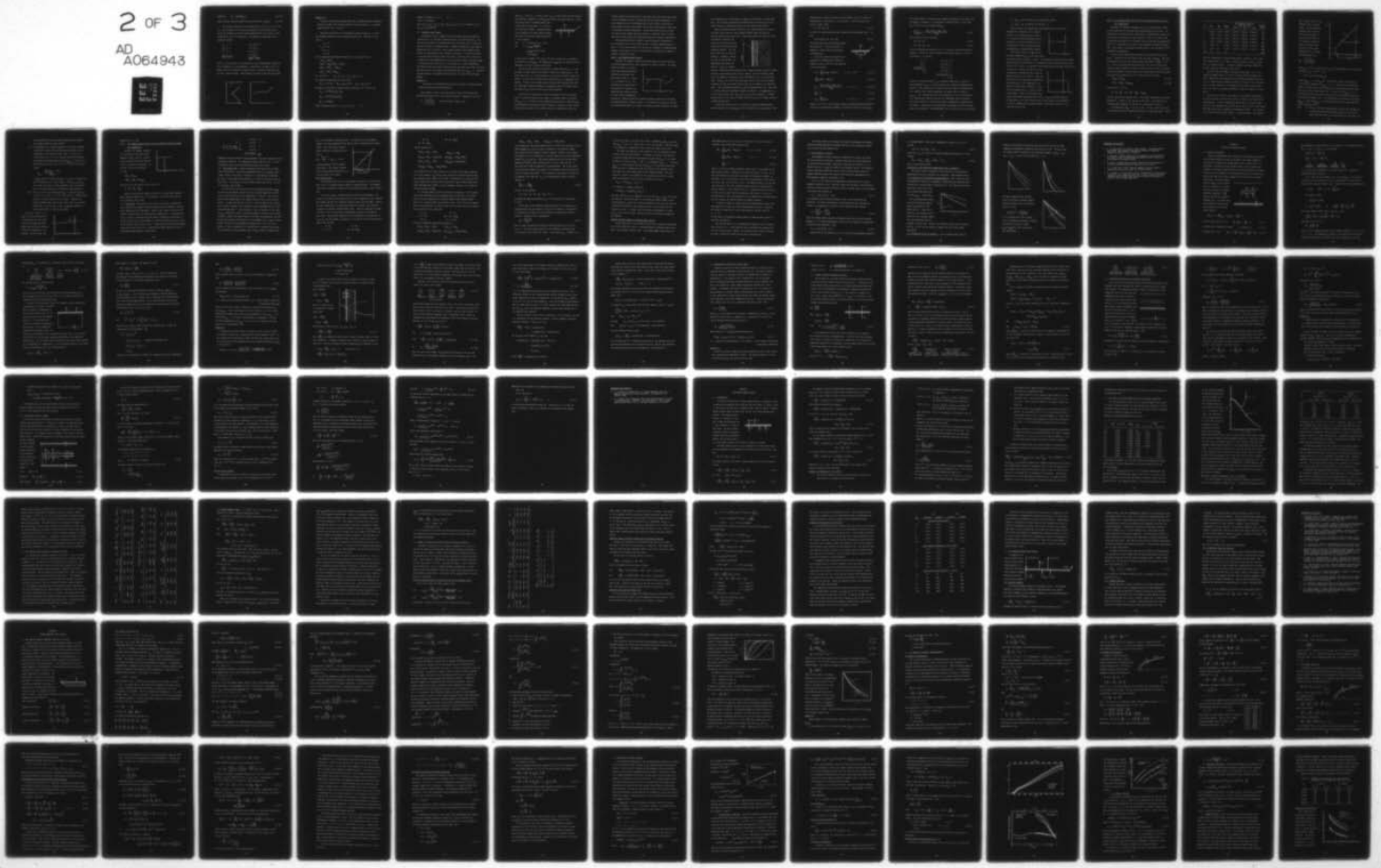

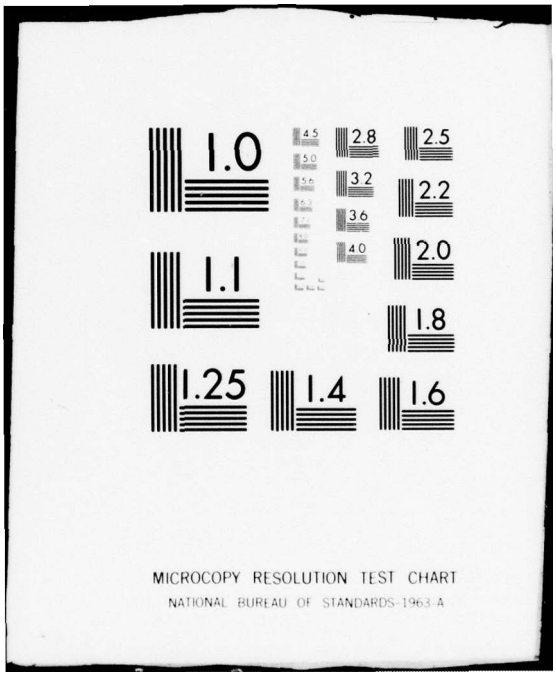
1.0
1.1
1.25
1.4
1.6
1.8
2.0
2.2
2.5
2.8
3.2
3.6
4.0
4.5
5.0
5.6
MICROCOPY RESOLUTION TEST CHART
NATIONAL BUREAU OF STANDARDS-1963-A

combining, $$\tilde{K}_k = (M_k/PM)\sum_i c_{ki} P_i \qquad (5.2\text{-}17)$$

where the mean molecular weight of the gas mixture $$M = \sum_i M_i P_i / P \qquad (5.2\text{-}18)$$

The system of equations to be solved are Eqs. (5.2-9, 13, 14, 16 and 17). We can regard P to be known and B_g' and B_c' to be specified (these latter two variables are often varied parametrically for a given P); then T_w and the P_i are to be determined. The unknowns and equations can be counted as follows:

P_i	I	(5.2-13)	I-K
$\tilde{K}_{k,w}$	K	(5.2-14)	1
M	1	(5.2-9)	K
T_w	1	(5.2-16)	1
Total	I+K+2	(5.2-17)	K
		Total	I+K+2

With P_i, P and T_w known, the calculation of other thermodynamic properties, such as enthalpy, is straightforward. Alternatively we might treat T_w as known and B_c' as an unknown, an approach which is necessary when the B_c'-T_w plot has a plateau region. Some examples are shown in the following figure.

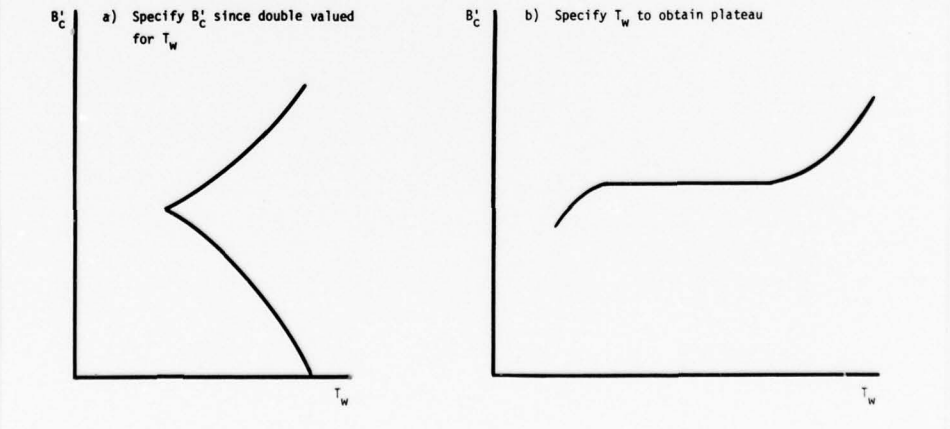

Example 5.2

Illustrate the theory presented above for a simplified model of graphite ablation in argon, with chemical species C* (solid carbon), C, C_3 (carbon vapor species), CO, O, O_2 and A.

Taking the base species as the monatomic gaseous species C_1, O, and A, the formation reactions for the remaining species are, from Eqs. (5.2-10 and 11),

$$C_1 \rightarrow C^*$$

$$C_1 + O \rightarrow CO$$

$$3C_1 \rightarrow C_3$$

$$2O \rightarrow O_2$$

the corresponding equilibrium relations Eqs. (5.2-13 and 14) are

$$-\ell n P_{C_1} = \ell n K_{P\,C^*}$$

$$\ell n P_{CO} - (\ell n P_{C_1} + \ell n P_O) = \ell n K_{P\,CO}$$

$$\ell n P_{C_3} - 3\ell n P_{C_1} = \ell n K_{P\,C_3}$$

$$\ell n P_{O_2} - 2\ell n P_O = \ell n K_{P\,O_2}$$

Eq. (5.2-16) is $P_{O_2} + P_O + P_{C_1} + P_{C_3} + P_{CO} + P_A = P$

the elemental constraints, Eq. (5.2-9) are

$$\tilde{K}_{C,w} = B'/(1+B') \; ; \quad \tilde{K}_{O,w} = \tilde{K}_{O,e}/(1+B') \; , \quad \tilde{K}_{A,w} = \tilde{K}_{A,e}/(1+B')$$

element mass fractions in terms of partial pressures, Eq. (5.2-17) are

$$\tilde{K}_{C,w} = (12/PM)(P_{CO}+P_{C_1}+3P_{C_3})$$

$$\tilde{K}_{O,w} = (16/PM)(P_{CO}+P_O+2P_{O_2})$$

$$\tilde{K}_{A,w} = (40/PM)P_A$$

number of gaseous species: C_1, C_3, O, O_2, CO I = 5

number of elements: C, O, A K = 3

I+K+2 = 11 equations

P_{CO}, P_O, P_{O_2}, P_{C_1}, P_{C_3}, P_A, $\tilde{K}_{C,w}$, $\tilde{K}_{O,w}$, $\tilde{K}_{A,w}$, M, T_w = 11 unknowns (P, B', $K_{O_2,e}$, $K_{A,e}$ specified).

5.3 CONDENSED PHASE REMOVAL

The analysis of §5.2 assumes that all the mass leaving the ablating surface does so in the form of gaseous species, the flux being $(\rho v)_w$. We now wish to consider the situation where some of the mass loss is caused by material leaving as a condensed phase. Examples include melt layer removal, mechanical fail, or erosion. Mass transfer problems with condensed phase removal are encountered in many industrial processes. A well known example is oxy-acetylene cutting of sheet steel where, after the steel is heated to a sufficiently high temperature by the oxy-acetylene flame, the oxygen supply is increased and the steel burns in the oxygen jet. At the temperatures involved the oxides are mostly molten and flow away under the action of gravity and shear forces; also chemical equilibrium prevails with $K_{O_2,w} \simeq 0$. The mass transfer problem is straightforward to analyze, as shown in the following example.

Example 5.3

Iron burns in a stream of 99% O_2 and 1% N_2 by mass. Calculate the mass transfer driving force and burning rate.

Since oxygen is inert in the gas phase we can use the driving force expression developed in §4.2 for tungsten oxidation. Equation (4.2-5) was

$$B' = \frac{K_{1,e} - K_{1,w}}{K_{1,w} - n_{1,w}/\dot{m}} \qquad \text{where subscript 1 refers to } O_2$$

Here $K_{1,e} = 0.99$, $K_{1,w} = 0$ and $n_{1,w}/\dot{m} = K_{1,tw}$ is unity since the only species crossing the w-surface is O_2 and n_{O_2} and $\dot{m}$ are in the same direction. Since the oxides leave as condensed phases they do not enter the gas phase, i.e., they do not cross the w-surface. Condensed phases can be thought of as being removed through the side of the control volume between the w- and u-surfaces.

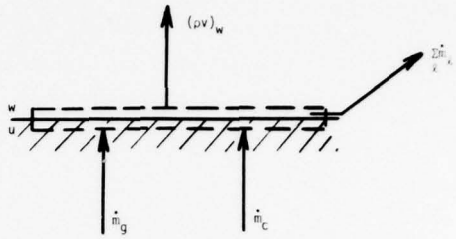

thus $B' = (0.99-0)/(0-1) = -0.99$

and $$\dot{m} = \rho_e u_e C_{MO} \frac{\ell n(1+B')}{B'}$$

$$= \rho_e u_e C_{MO}(4.651)(-0.99)$$

$$= -4.60\rho_e u_e C_{MO}$$

If the oxide is assumed to be Fe_2O_3, the rate at which iron is consumed is $(112/48)\dot{m}$ or $10.74\rho_e u_e C_{MO}$. The conductance $\rho_e u_e C_{MO}$ must be evaluated for an impinging jet using a suitable correlation.

Notice that the "blowing correction" is greater than unity, i.e., the gas phase is under suction, and indeed is under very strong suction. The lower limit of B' is -1 and corresponds to an infinite velocity towards the surface. We see that the Couette flow formula gives $C_M = 4.65C_{MO}$ for this problem. In fact, exact boundary layer solutions and experiment show that the logarithmic formula underpredicts C_M/C_{MO} when there is strong suction, and values of C_M as much as 50% greater can be expected.

Our ability to calculate $\dot{m}$ in the above example rests on two assumptions. Firstly the chemistry was simple: no gaseous oxides were formed, and $K_{O_2,w} \simeq 0$. If either of these conditions were not met, a detailed equilibrium chemistry calculation would be required. Secondly, we have assumed that the heat evolved in the oxidation process is sufficient to melt the

oxides, supply the sensible heat to the virgin iron, and balance heat losses to the environment to give a steady state at the process temperature. If this condition is met, the burning rate is truly limited by the rate at which oxygen can get to the surface, and we are not particularly interested in the precise surface temperature. On the other hand we shall see that, for oxide or melt removal from heat shields, a transient state is usually involved, and the coupled heat transfer problem also requires consideration.

The equilibrium surface chemistry codes developed by Aerotherm [1] have an option, the so-called "FAIL" option, to handle condensed phase removal. It will prove convenient to discuss the treatment of condensed phase removal in the context of use of the FAIL option as applied to a number of specific situations in turn.

Case 1. One condensed phase species.

Consider, for example, tungsten and ignore details at other than near the melting temperature for metal tungsten, W*, which is 3681°K. The figure shows the result of a conventional open system equilibrium chemistry calculation, with prescribed T_w and P, to obtain B' as a function of T_w. The calculation also shows that, at the pressures of interest, no condensed phase oxides are present near the melt temperature.

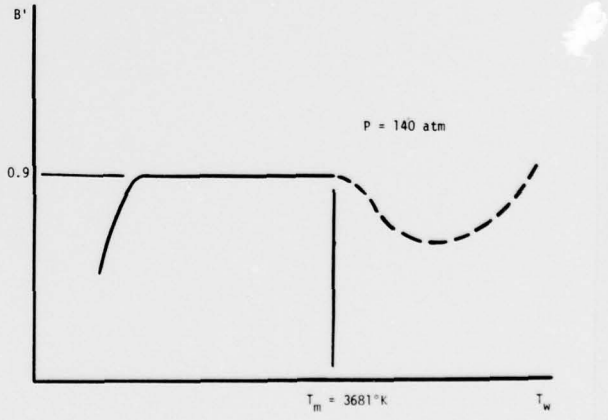

So below T_m = 3681°K we have the relatively simple situation of solid tungsten being oxidized to gaseous oxides. As the values of T_w input to the code are increased from below T_m to above we continue to obtain solutions, as shown

by the dashed curve in the figure, but above T_m the surface is liquid tungsten. The solutions indicated by the dashed curve are quite valid, but of little interest to heatshield analysis for the reasons which follow.

When the tungsten surface reaches T_m, the liquid tungsten will form a film which flows along the solid tungsten surface under the action of pressure gradient and shear forces. Since these forces are large in a typical ablation situation, the film will be very thin and the liquid will flow back along the heatshield rapidly. The film may be very wavy, or even may break up. Assuming a continuous film for the present, the temperature drop across the film $\Delta T = T_w - T_m$ is a complex function of the shear and pressure forces, thermal transport processes across the film, and the melting rate itself. However, since the thermal conductivity of tungsten is relatively large (~100 Btu/hr ft F) ΔT is relatively small. Analysis [2] of the film flow shows that for usual missile reentry conditions ΔT does not exceed 20°R and thus can be assumed to be negligibly small. Thus for modeling purposes, T_w may be approximated by T_m. Then there is a unique chemical equilibrium solution of interest: corresponding to T_m we have unique values of B', $\tilde{K}_{k,w}$ and $P_{i,w}$ for a given pressure. A higher heating rate will not lead to a higher value of T_w, but will simply result in a higher melting rate.

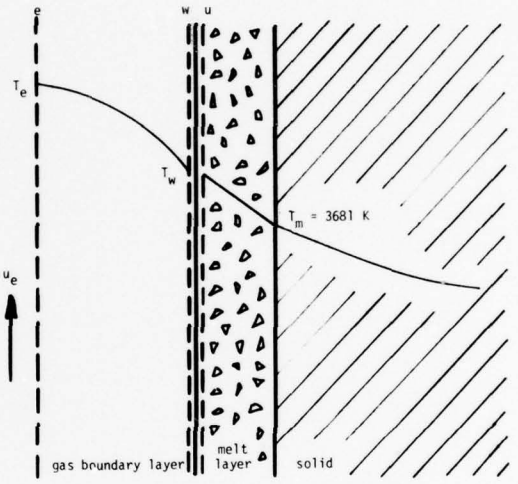

In the FAIL option a new B' is defined to represent condensed phase material removal, $B'_\ell \equiv \dot{m}_\ell/\rho_e u_e C_M$, and if we retain $B'_c = \dot{m}_c/\rho_e u_e C_M$ then, when

melting occurs, we have a choice as how to define a total B', usually unsubscripted, or subscripted 'a' for ablation. In the FAIL option the choice is made to have

$$B' = B'_a = B'_g + B'_c \tag{5.3-1}$$

so that B' no longer described mass transfer into the boundary layer. In fact

$$(\rho v)_w/\rho_e u_e C_M = B'_a - B'_\ell = B'_{b1} \tag{5.3-2}$$

The figure shows the relationships between the various B's. Notice that the $\dot{m}$ in Example 5.2 should strictly speaking be subscripted $\dot{m}_w$.

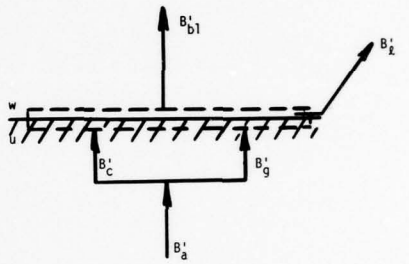

Since the counting of equations and unknowns for condensed phase removal is somewhat tricky we will list the equations to be solved again:

$$\ell n P_i - \sum_{k=1}^{K} c_{ki} \ell n P_k = \ell n K_{Pi}(T) \qquad i = 1,2,\ldots(I-K) \tag{5.2-13}$$

$$-\sum_{k=1}^{K} c_{k\ell} \ell n P_k = \ell n K_{P\ell}(T) \tag{5.2-14}$$

$$\tilde{K}_{k,w} = \frac{B'_g \tilde{K}_{k,g} + B'_c \tilde{K}_{k,c} - B'_\ell \tilde{K}_{k,\ell} + \tilde{K}_{k,e}}{1+B'_{b1}} \qquad k = 1,2,\ldots,K \tag{5.2-9†}$$

$$\sum_{i=1}^{I} P_i = P \tag{5.2-16}$$

$$\tilde{K}_{k,w} = \frac{M_k}{PM} \sum_i c_{ki} P_i \qquad k = 1,2,\ldots,K \tag{5.2-17}$$

where Eq. (5.2-9†) is the original element constraint equation modified to account for condensed phase removal, and the fact that $B'_a \neq (\rho v)_w/\rho_e u_e C_M$

in the FAIL option. For purposes of comparing the number of equations with the number of unknowns it is convenient to substitute Eqs. (5.2-17) into Eq. (5.2-9†) so as to eliminate the $\tilde{K}_{k,w}$,

$$\frac{M_k}{PM}\sum_{i=1}^{I} c_{ki}P_i = \frac{B'_g\tilde{K}_{k,g}+B'_c\tilde{K}_{k,c}-B'_\ell\tilde{K}_{k,\ell}+\tilde{K}_{k,e}}{1+B'_{b1}} \tag{5.3-3}$$

and to add the trivial relations,

$$B'_a = B'_c + B'_g \tag{5.3-4}$$

$$B'_c + B'_g = B'_{b1} + B'_\ell \tag{5.3-5}$$

Now let us examine the equation set as it is used to calculate melting of tungsten. Pressure is always regarded as specified, and $B'_g = 0$; then if we specify $T_w = T_m$ and B'_a,

P_i	I	(5.2-13)	I-K
M	1	(5.2-14)	1
B'_c, B'_{b1}, B'_ℓ	3	(5.3-3)	K
		(5.2-16)	1
		(5.3-4 and 5)	2
	I+4		I+4

Actually, in the FAIL option, T_w is determined implicitly as follows. A fail temperature $T_{fail-\ell}$ is pre-assigned to any candidate condensed phase species ℓ; this species will be removed from the surface in condensed form at a rate $\dot{m}_\ell$ if the surface temperature is greater than, or equal to, $T_{fail-\ell}$. For a melting solid the fail temperature is just the melt point; for a mechanically failing solid the fail temperature may be related to the stress situation. Also one can specify a maximum fail temperature for all species: physically this maximum might correspond to the fail temperature of the substrate. The determination of T_w is then via the restrictions:

$T_w < T_{fail}$ for the surface (solid substrate) species

$T_w > T_{fail}$ for any species for which $\dot{m}_\ell > 0$.

Thus in the case of tungsten the code determines T_w to be the pre-assigned fail temperature of W*, 3681°K, since W* is the surface species and $\dot{m}_\ell$ is > 0 in order to obtain B'_a greater than 0.9. Of course, if we did not specify $B'_a > 0.9$ we would not be able to obtain solutions corresponding to condensed phase removal.

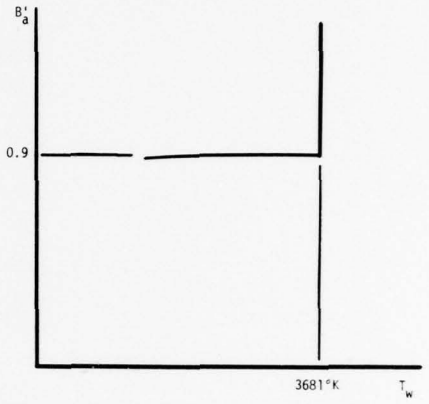

Notice that in this case B'_{bl} and the gas phase composition $K_{i,w}$ do not vary along the vertical leg of the B'_a vs. T_w plot. The equilibrium relations being solved are equivalent to those solved in a conventional open system equilibrium calculation, with P and $T_w = T_m$ specified, which would give the lowermost point on the vertical leg. Indeed, we could use the B'_c so obtained to calculate B'_ℓ for a given B'_a directly from Eqs. (5.3-4 and 5). Note also that we are free to prescribe a temperature lower than T_m as a fail temperature, say based on a solid stress criterion. In the case of tungsten the B'_a - T_w plot is shown in the figure. Again, a conventional open system equilibrium calculation with P and $T_w = T_{fail}$ specified would give the B'_{bl} and $K_{i,w}$'s at the lowermost point of the vertical leg; provided W* is the only condensed phase species present, these quantities do not vary along the vertical leg.

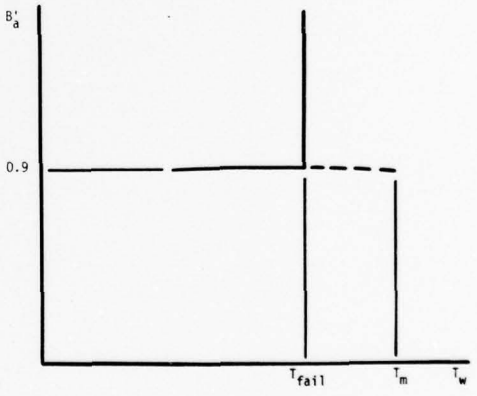

Case 2. Two condensed phase species with the substrate having the lower fail temperature.

Consider, for example, molybdenum close to its melting point 2892°K. At usual pressures the condensed phase dioxide MoO_2^* may be present. The dioxide has no liquid phase and, additionally, a decomposition temperature of the solid has evidently not been observed. Since it is unlikely that the dioxide could maintain its integrity once the substrate molybdenum had melted, it is reasonable to assign a fail temperature of 2892°K to MoO_2^* as well. This choice is equivalent to having input to the code 2892°K as the maximum fail temperature.

Clearly we have added another unknown to the problem considered in Case 1. Instead of one B'_ℓ (= B'_{W^*}) we have two, B'_{Mo^*} and $B'_{MoO_2^*}$. Thus from a mathematical point of view we know we must add another equation to our set. Since we envisage both failing species to be at the surface (even though our model assumes that they are removed as fast as they are formed) it seems reasonable to require both to be in equilibrium with the gas phase. Thus we have two equations (5.2-14), rather than one as before

$$-\ell n P_{Mo} = \ell n K_{P\,Mo^*} \qquad (5.2\text{-}14a)$$

$$-2\ell n P_O - \ell n P_{Mo} = \ell n K_{P\,MoO_2^*} \qquad (5.2\text{-}14b)$$

and write Eq. (5.3-5) as

$$B'_c + B'_g = B'_{b1} + \Sigma B'_\ell = B'_{b1} + B'_{Mo^*} + B'_{MoO_2^*}$$

and our equations and unknowns tally. The surface temperature restrictions determine T_w = 2892°K in the same way as for Case 1. The table on the following page summarizes the results of a calculation at 100 atm.

By interpolation $B'_{Mo^*} = 0$ at $B'_a = 0.687$. For $B'_a > 0.687$ we have two failing species and the mathematical problem is as described above. Notice

B'_a	B'_{b1}	B'_{Mo*}	$B'_{MoO_2^*}$	Base Species w-Surface Mole Fractions			Surface Species
				Mo	O_2	N_2	
5	-.1646	4.3133	0.8514	4.097-07	6.891-05	9.809-01	Mo*
2	-.1646	1.3133	0.8514	4.097-07	6.891-05	9.809-01	Mo*
1	-.1646	0.3133	0.8514	4.097-07	6.891-05	9.809-01	Mo*
0.7	-.1646	0.0133	0.8514	4.097-07	6.891-05	9.809-01	Mo*
0.6	.0687	0.0	0.5323	1.473-08	1.916-03	9.223-01	MoO_2^*
0.5	.320	0.0	0.1758	4.703-09	6.00-03	8.647-01	MoO_2^*
0.46	.46	0.0	0.0				MoO_2^*

that the concentration of gaseous molybdenum is constant in this regime: this confirms that Eq. (5.2-14a) is being satisfied, since $K_p = K_p(T_w)$ and T_w is fixed at 2892°K. In fact the complete gas phase composition, as well as B'_{b1} are invariant for $B'_a > 0.687$.

For $B'_a < 0.687$ only MoO_2^* is failing and since $B'_{Mo*} = 0$, it is no longer an unknown, and Eq. (5.2-14a) is deleted from the equation set. Again, inspection of the concentration of gaseous molybdenum shows that it is no longer constant confirming that Eq. (5.2-14a) is not being satisfied. For this reason Mo* is not output as the surface species since, if Eq. (5.2-14a) is not being satisfied Mo* cannot be exposed to the gas phase.

The values of B' given in the table are conveniently represented in what may be called a *failing phase diagram* as shown in the figure on the following page. In such a diagram B'_{b1} and the B'_ℓ's are plotted cumulatively vs. B'_a, together with B'_a itself (which gives a line of unity slope). The figure shows such a diagram for molybdenum at 2892°K. It is instructive to look at how the value of $B'_{b1} = -0.165$ comes about. The quantity

B'_{b1} is simply the B' of our elementary mass transfer theory. We can assume the boundary layer inert and no dissociated oxygen in the free stream since we are looking at equal diffusion coefficient calculations for which these assumptions have no effect. Then basing B'_{b1} on O_2,

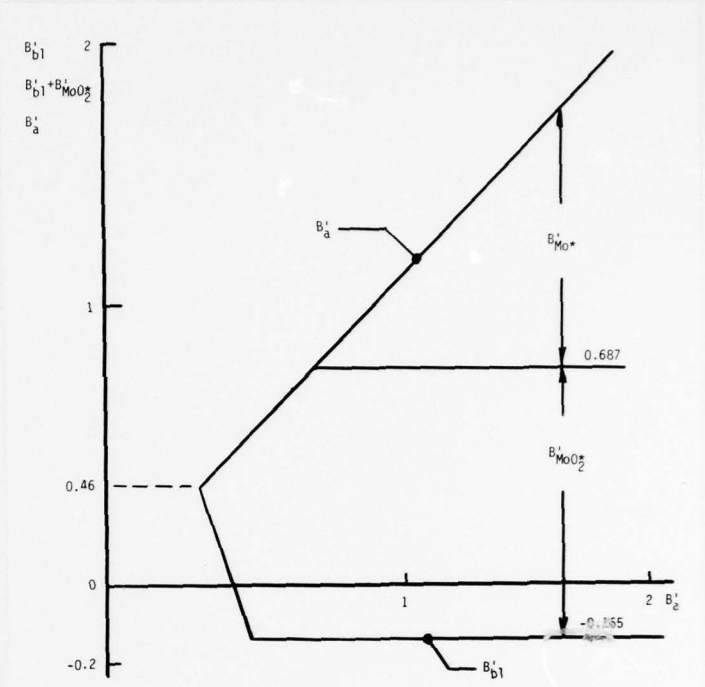

$$B'_{b1} = \frac{K_{O_2,w} - K_{O_2,w}}{K_{O_2,w} - K_{O_2,tw}}$$

Now $K_{O_2,e} = 0.232$; we would expect $K_{O_2,w}$ to be approximately zero (the code calculates $K_{O_2,w} = 7\times10^{-5}$). Thus

$$-0.165 = (0.232-0)/(0-K_{O_2,tw})$$

so that $K_{O_2,tw} = 1.41$ $(=n_{O_2,w}/\dot{m})$. Notice that a lower limit for B'_{b1} is -0.232 which corresponds to $K_{O_2,tw} = 1$, i.e., when the only transferred species is oxygen and all this oxygen goes to form condensed phase oxides which do not enter the boundary layer. In fact we have $K_{O_2,tw} = 1.41$ which indicates that part of the oxygen goes to form gaseous oxides which do reenter the boundary layer. The code printout indicates mass fractions $K_{MoO_3,w} = 0.059$ and $K_{MoO_2,w} = 0.024$ showing that there is appreciable formation of gaseous oxides.

Note: (i) For $B'_a > 0.687$ both condensed phase species Mo* and MoO_2^* are in equilibrium with the gas phase; however, we have not required that they both be in equilibrium with each other. We

have regarded each as pure condensed phase species which do not interact with each other directly.

(ii) The dependence of w-surface composition on the mass transfer situation in an open system equilibrium calculation is well illustrated by the behavior of $B'_a > 0.687$. As B'_a is increased from, say, 0.5 to 0.6, the mass fraction of the dominant gaseous oxide MoO_3 decreases from $K_{MoO_3,w} = 0.39$ to 0.27. The reason can be seen if Eq. (5.2.9^T) is written for element oxygen,

$$\tilde{K}_{O,w} = \frac{-\frac{32}{128} B'_{MoO_2^*} + 0.232}{1+B'_{b1}}$$

As $B'_{MoO_2^*}$ increases so $\tilde{K}_{O,w}$ decreases, in order to increase the rate of diffusion of $\tilde{O}$ to the surface. Since $K_{O_2,w}$ and $K_{O,w}$ are already very small at this temperature, $\tilde{K}_{O,w}$ can decrease only if the concentrations of the gaseous oxides decrease.

(iii) For $B'_a < 0.687$ we have noted that $B'_{Mo^*} = 0$ and that hence Eq. (5.2.14a) is not used. It follows that only *one* condensed phase species is actually present on the surface. However, the second condensed phase species does play a role via the "char" composition: here the char is Mo*; a completely different result would obtain if the char were MoO_2^*.

The B'_a vs. T plot is as shown. At lower pressures the w-surface gaseous oxide concentrations are higher and hence higher values of B'_a are attained as the melt temperature is approached: the plot shows this

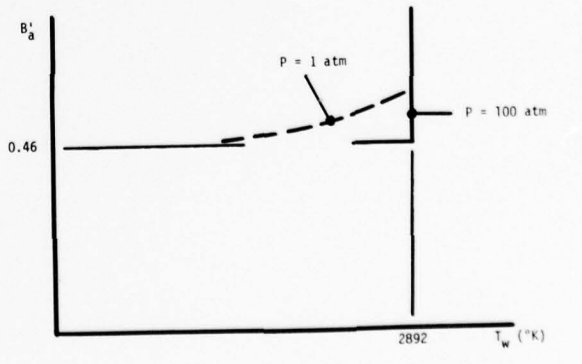

behavior for P = 1 atm.

Case 3. Two condensed phase species with the substrate having the higher fail temperature.

Consider, for example, tungsten in the vicinity of the melting temperature of WO_3^*, 1745.2°K. Calculations using the FAIL option indicate a B_a' vs. T_w plot as shown below. As in Case 2 we have two equations (5.2-14),

$$-\ell n P_W = \ell n K_{P\,W^*}$$

$$-3\ell n P_O - \ell n P_W = \ell n K_{P\,WO_3^*}$$

but now we only have one B_ℓ', so Eq. (5.3-5) is

$$B_c' + B_g' = B_{b1}' + B_{WO_3^*}'$$

There are two distinct regimes of the B_a' vs. T_w plot where condensed phase removal of WO_3^* occurs, (i) the plateau, and (ii) the vertical leg. Let us consider each in turn.

(i) The Plateau. The plateau in this case is not truly a constant B_a' curve, B_a' does vary slightly along the plateau owing to changes in the gas phase composition with temperature. However, this regime can only be calculated by specifying T_w to avoid numerical difficulties. A specification of $T_w > 1745$°K is consistent with the surface temperature restrictions in the FAIL option, but is not determined by these restrictions as was the case on the vertical legs in Cases 1 and 2. Consistent with the specified temperature option of the code no B' is specified and indeed need not be as the following unknowns-equations count shows:

P_i	I	(5.2-13)	I-K
M	1	(5.2-14)	2
B'_a, B'_c, B'_{b1}, $B'_{WO_3^*}$	4	(5.3-3)	K
	I+5	(5.2-16)	1
		(5.3-4 and 5)	2
			I+5

Somewhere along the plateau the WO_3^* disappears, the exact temperature being dependent on pressure. For temperatures higher than this, $B'_\ell = 0$, and a conventional open system equilibrium calculation can be made.

(ii) The Vertical Leg. Consider approaching the melting point of WO_3^*, 1745.2°K from below. Below this temperature there is no condensed phase removal and the calculation is identical to a conventional calculation: $B'_a = B'_{b1}$ is prescribed and the unknown T_w is found as one advances up the B'_a-T_w curve. Since WO_3^* is the only surface species only one Eq. (5.2-14) is satisfied, that for WO_3^*.

At 1745.2°K the FAIL option allows for an additional unknown, $B'_{WO_3^*}$, but need not add another equation since the surface temperature restrictions in the FAIL option fix the temperature at 1745.2°K. For this purpose the code regards WO_3^* as the surface species as well as the failing species. So again the only Eq. (5.2-14) is that for WO_3^* and the vertical leg is exactly analogous to the vertical leg of molybdenum for $B'_a < 0.687$, discussed under Case 2. Thus similarly, as B'_a is increased, so the value of $K_{O_2,w}$ decreases in order to allow more oxygen to diffuse to the surface in order to supply the oxygen content of the WO_3^*; correspondingly the value of B'_{b1} drops (becomes more negative) as the boundary layer is under suction because the oxides are predominantly condensed and do not cross the w-surface. If B'_a is increased still further there is reached a point where the concentration of O_2 approaches zero, and B'_{b1} reaches a minimum value;

this is the diffusion controlled limit. In contrast to the molybdenum example, the lower temperature here implies small concentrations of gaseous oxides. Thus simple mass transfer theory would give a minimum value of B'_{b1} as

$$B'_{b1} = \frac{K_{O_2,e}{}^{-0}}{0-1} = -K_{O_2,e} = -0.232$$

in good agreement with FAIL option calculations. The general features of the failing phase diagram for this case are shown in the figure.

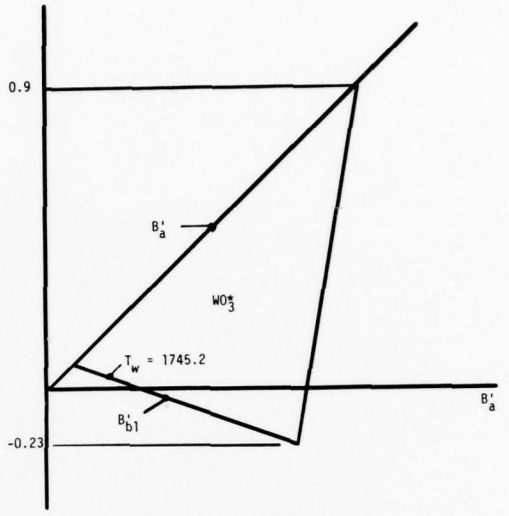

More complex cases.

One can deduce from our set of equations considered by the FAIL option that there is a maximum allowable number of condensed phases. Two examples follow which illustrate a number of interesting implications of this restriction.

As a first example, consider again the ablation of molybdenum. Previously we considered only behavior near the melt temperature of Mo* (2892°K) and assumed that the only candidate condensed phase oxide was MoO_2^*. However, at lower temperatures, we would expect MoO_3^* to be present, and should be allowed as a candidate condensed phase oxide. The melt temperature of MoO_3^* is 1074°K. Let us see how many condensed phase species are allowed for this sytem. The gas phase chemistry will be simplified by allowing only O, O_2, N, N_2, NO, Mo and MoO_3. Equations (5.2-13 and 14) for the system correspond to the reactions

$$2N \rightarrow N_2 \qquad Mo \rightarrow Mo^*$$

$$N + O \rightarrow NO \qquad Mo + 2O \rightarrow MoO_2^*$$

$$2O \rightarrow O_2 \qquad\qquad Mo + 3O \rightarrow MoO_3^*$$

$$Mo + 3O \rightarrow MoO_3$$

and the equations are,

$$\ell nK_{P\,N_2} = \ell nP_{N_2} - 2\ell nP_N \qquad \ell nK_{P\,Mo^*} = -\ell nP_{Mo}$$

$$\ell nK_{P\,NO} = \ell nP_{NO} - (\ell nP_N + \ell nP_O) \qquad \ell nK_{P\,MoO_2^*} = -(\ell nP_{Mo} + 2\ell nP_O)$$

$$\ell nK_{P\,O_2} = \ell nP_{O_2} - 2\ell nP_O \qquad \ell nK_{P\,MoO_3^*} = -(\ell nP_{Mo} + 3\ell nP_O)$$

$$\ell nK_{P\,MoO_3^*} = \ell nP_{MoO_3} - (\ell nP_{Mo} + 3\ell nP_O)$$

If we examine the last three equations we see that we have three equations in only two unknowns, P_{Mo} and P_O; hence one must be discarded implying that only condensed phase species are allowed. Aerotherm [3], in using the FAIL option, handled this problem rather arbitrarily; they eliminate MoO_2^* below 2400°K and MoO_3^* above 2400°K, based on arguments related to an estimate of the boiling point of MoO_3^*.

As a second example consider the ablation of aluminum. Since nitrogen reacts with aluminum to form a condensed phase nitride AlN*, it is found that at the melt temperature of aluminum (934°K) three condensed phase species Al*, $Al_2O_3^*$ and AlN* are expected to form. Also at this low temperature the concentrations of gaseous oxides are very small and can be ignored. The reactions for this system are

$$2N \rightarrow N_2 \qquad\qquad Al \rightarrow Al^*$$

$$N + O \rightarrow NO \qquad\qquad 2Al + 3O \rightarrow Al_2O_3^*$$

$$2O \rightarrow O_2 \qquad\qquad Al + N \rightarrow AlN^*$$

and the corresponding equilbrium relations are

$$\ell nK_{P\,N_2} = \ell nP_{N_2} - 2\ell nP_N \qquad \ell nK_{P\,Al^*} = -\ell nP_{Al}$$

$$\ell nK_{P\,NO} = \ell nP_{NO} - (\ell nP_N + \ell nP_O) \qquad \ell nK_{P\,Al_2O_3^*} = -(2\ell nP_{Al} + 3\ell nP_O)$$

$$\ell nK_{P\,O_2} = \ell nP_{O_2} - 2\ell nP_O \qquad \ell nK_{P\,AlN^*} = -(\ell nP_{Al} + \ell nP_N)$$

If we examine the last three equations we see we have three equations in the three unknowns P_{Al}, P_O and P_N, and in contrast to the previous example, these equations do not appear to cause a problem. However, if we examine the complete set of six equations we see that there are only three additional unknowns P_{O_2}, P_{N_2} and P_{NO}. Thus these equations would fix the gas phase composition without using (satisfying) Eq. (5.2-16), which was $\sum_i P_i = P$. Thus again the system of equations is overconstrained. But we can remedy this particular situation very simply if we recognize that a freestream of real air contains some argon. If we introduce a small amount of argon into the boundary layer edge gas, $K_{A,e}$, the corresponding element constraint equation is

$$\frac{M_A}{PM} P_{A,w} = \frac{K_{A,e}}{1+B'_{b1}} \tag{5.3-6}$$

and Eq. (5.2-16) becomes

$$P_{Al} + P_{N_2} + P_N + P_O + P_{O_2} + P_{NO} + P_A = P$$

By adding the additional unknown $P_{A,w}$ it is now possible to satisfy Eq. (5.3-16).

Notice that in the diffusion controlled limit for the formation of $Al_2O_3^*$ and AlN*, the gas adjacent to the wall (w-surface) is calculated to be essentially all argon, as can be explained by simple mass transfer analysis. Equation (5.3-6) rearranged is

$$B'_{b1} = \frac{K_{A,e} - K_{A,w}}{K_{A,w}} \tag{5.3-7}$$

which is what we would expect from our original definition of B' since $K_{A,t} = 0$. The value of B'_{b1} obtained in the diffusion controlled limit is calculated by the code to be -0.999. If we choose $K_{A,e} = 0.00999$ (i.e.,

a little less than 1 per cent) then $-0.999 = (0.00999-K_{A,w})/K_{A,w}$, and solving, $K_{A,w} = 0.99$, i.e., 99 per cent. So we see that only 1 per cent argon in the edge gas is sufficient to give 99 per cent argon at the wall.

Of course this problem is quite similar to the oxy-acetylene cutting of sheet steel discussed earlier. In Example 5.3 we had 1 per cent N_2 in a stream of oxygen and we were prepared to assume that $K_{O_2,w} = 0$ in order to obtain our result of $B'_{b1} = -0.99$. As a consequence $K_{N_2,w} = 1$. In reality $K_{O_2,w}$ is a little greater than zero and $K_{N_2,w}$ is a little less than unity. Physically what is happening is that the suction on the boundary layer is very large due to the oxygen going to form condensed oxides. The inert nitrogen is swept to the surface by this convective flux, but at steady state the absolute flux of N_2 at the w-surface must be zero.

$$n_{N_2,w} = (\rho v)_w K_{N_2,w} + j_{N_2,w} = 0$$

or in terms of a transfer coefficient

$$(\rho v)_w K_{N_2,w} + \rho_e u_e C_M (K_{N_2,w} - K_{N_2,e}) = 0$$

The mass velocity $(\rho v)_w$ is negative, so we see that $K_{N_2,w} > K_{N_2,e}$ to satisfy the equation. Notice that there is the strong non-linear effect; as the concentration $K_{2,w}$ builds up to allow the diffusive flux away from the wall to balance the convective flux towards the wall, so the convective flux increases as well. At steady state the solution corresponds to a value of $K_{N_2,w}$ very close to unity. One can think of the nitrogen "blanketing" the surface.

Maximum allowable number of condensed phase species

As mentioned before, we can deduce from the set of equations considered by the FAIL option that there is a maximum number of condensed phases allowable. We now deduce a general rule. The maximum number follows from the

requirement that Eqs. (5.2-13), (5.2-14) and (5.2-16) are not overconstrained. Recall that these equations are:

$$\ell n P_i - \sum_{k=1}^{K} c_{ki} \ell n P_k = \ell n K_{Pi}(T) \; ; \qquad i = 1,2,\ldots(I-K) \tag{5.2-13}$$

$$- \sum_{k=1}^{K} c_{k\ell} \ell n P_k = \ell n K_{P\ell}(T) \; ; \qquad = 1,2,\ldots,L \tag{5.2-14}$$

$$\sum_{i=1}^{I} P_i = P \tag{5.2-16}$$

where I is the total number of gaseous species and L is the number of condensed phase species. Looking first at the sub-set Eqs. (5.2-14), we see that the unknowns are the partial pressures of the gaseous elements, P_k, and hence $L \leq K$ if the sub-set is not to be overconstrained. Next look at the sub-set Eqs. (5.2-13) and (5.2-16): the unknowns appear to be the partial pressures of the (I-K) remaining gaseous species P_i (excluding the gaseous elements). Since there are (I-K) + 1 equations and only (I-K) P_i's, at least one of P_k must also be an unknown if the sub-set is not to be overconstrained. These considerations can be summarized in a simple general rule for counting the required number of chemical elements:

"A chemical element is required for each condensed phase species and must appear in at least one of the condensed phase species; in addition, one element is required for the gas phase species, giving a total of $K = L + 1$."

In this manner the maximum allowable number of condensed phase species is implicitly determined.

Note that the phase rule of thermodynamics applied to this situation simply states $L \leq K - 1$ and cannot be used to determine the maximum value of L for a given system. However, the reasoning we have used to develop our rule is identical to that used to derive the phase rule.

The reader should now re-examine the tungsten, molybdenum and aluminum ablation problems previously described, and see if the conclusions reached are in accord with the general rule.

5.4 MULTICOMPONENT DIFFUSION

The assumption of equal diffusion coefficients is accurate and useful for most ablation calculations. However, when there are large differences in species molecular weights, significant errors may be incurred, e.g., if species such as H or W_3O_9 are present in air boundary layers. The Aerotherm surface equilibrium chemistry codes [1] have an option which allows for unequal diffusion coefficients based on the bifurcation approximation for multicomponent diffusion introduced in §3.7.

In §3.7 it was shown that an appropriate driving potential for multicomponent diffusion is the z fraction, rather than the mass or mole fraction. Thus for a purely diffusive situation, such as a Couette flow, we could attempt to correlate mass transfer as

$$j_{i,w} = \rho_e u_e C_M (z_{i,w} - z_{i,e}) \tag{5.4-1}$$

In a boundary layer flow mass transport is due to both convection and diffusion; the former contribution is characterized by mass fractions K_i, so that it is appropriate to define a new z* fraction by the relation

$$z_i^* = \frac{z_i^\gamma K_i^{1-\gamma}}{\Sigma z_j^\gamma K_j^{1-\gamma}} = \frac{K_i/F_i^\gamma}{\Sigma K_j/F_j^\gamma} \tag{5.4-2}$$

where the Schmidt number exponent in boundary layer flows of binary mixtures suggests $\gamma = 2/3$ should approximately account for the respective contributions of convection and diffusion. Then

$$j_{i,w} = \rho_e u_e C_M (z^*_{i,w} - z^*_{i,e}) \tag{5.4-3}$$

Modification of the analysis of §5.2 to allow for multicomponent diffusion

is straightforward. Since C_M is independent of species, Eq. (5.2-7) becomes

$$\rho_e u_e C_M = \tilde{j}_{k,w} / (\tilde{z}^*_{k,w} - \tilde{z}^*_{k,e}) \tag{5.4-4}$$

where $\tilde{z}^*_k = \sum_i \alpha_{ki} z^*_i$, while the w-surface elemental constraint Eq. (5.2-9) becomes

$$\tilde{z}^*_{k,w} + B' \tilde{K}_{k,w} = B'_g \tilde{K}_{k,g} + B'_c \tilde{K}_{k,c} + \tilde{z}^*_{k,e} \tag{5.4-5}$$

which is the desired result.

Evaluation of the bifurcation approximation and z* potential

Data which allow an evaluation of the accuracy of the bifurcation approximation and the z* potential are available. Some examples follow.

(i) Evaluation of the bifurcation approximation. Exact solutions of the Stefan-Maxwell equations in axisymmetric stagnation point flow have been obtained for a limited range of conditions [4]. The Figure which follows shows exact results for injection of helium and xenon into air with $K_{He,t} = 0.25$ and $K_{Xe,t} = 0.75$, and approximate results using the bifurcation approximation calculated with the BLIMP code [5]. Since the bifurcation, in principle, can be made exact for a ternary system, this case admittedly does not represent a severe test. However, the diffusion factors were calculated from Eq. (3.7-13) and the results do support the use of this simple correlation.

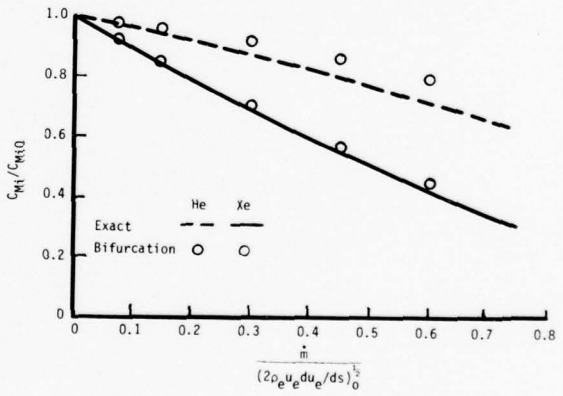

(ii) Evaluation of the z* potential. The two Figures below show the

results of calculations for multiple species injection into air in high temperature axisymmetric stagnation point flow of air [5]. The mass transfer Stanton number is defined in the conventional manner, $\rho_e u_e C_{Mi} = j_{i,w} / (K_{i,w} - K_{i,e})$. For all the injectants $K_{i,t} = 1/3$.

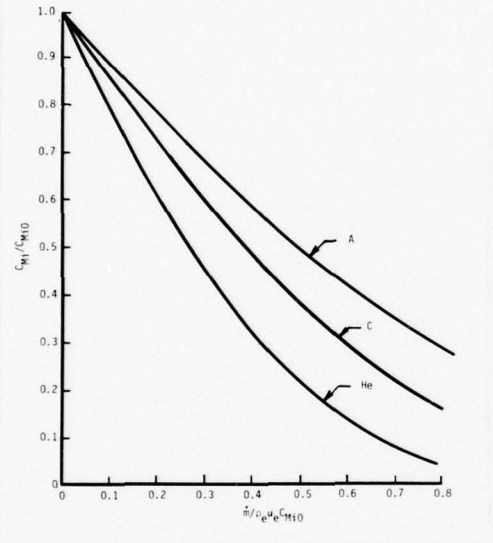

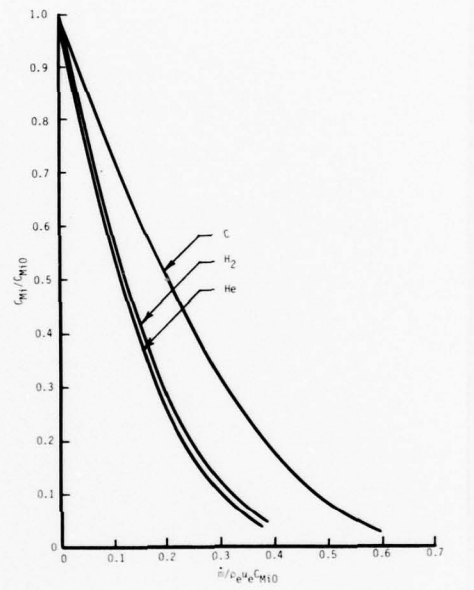

The Figure opposite shows the data recast in the form of Stanton numbers defined in terms of the z* potential; from Eq. (5.4-4),

$$\rho_e u_e C_{Mi}(z^*) = \frac{j_{i,w}}{(z^*_{i,w} - z^*_{i,e})}$$

It is seen that use of the z* potential is reasonably successful in collapsing the curves to give a single $C_{Mi}(z^*)/C_{MiO}(z^*)$, for a given injectant composition.

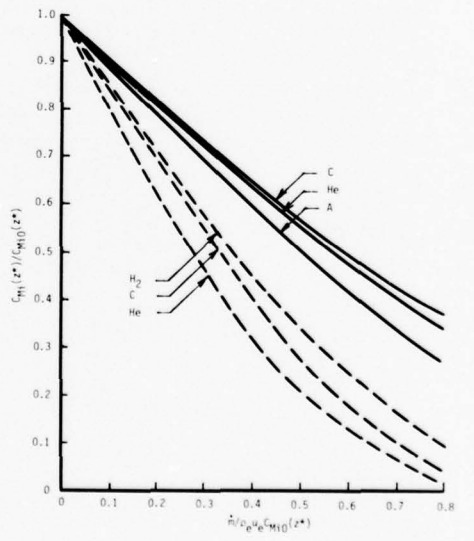

REFERENCES FOR CHAPTER 5

1. A. C. Powers and R. M. Kendall, "User's Manual: Aerotherm Chemical Equilibrium (ACE) Computer Program" Rept. UM-69-70, Aerotherm Corporation, Mountain View, CA (1969).

2. B. Bluestein, "Liquid layer flow over axisymmetric melting ablators" M.S. Thesis, School of Engineering and Applied Science, University of California, Los Angeles (1978).

3. K. Clark, A. Shimazu and W. Bonnett, "Metal ablation" Document C/N 7100.59, Aerotherm Corporation, Mountain View, CA (1974).

4. P. A. Libby and P. Sepri, "Laminar boundary layer with complex composition" Physics of Fluids, 10, 2138-2146 (1967).

5. A. V. Gomez, A. F. Mills and D. Curry, "Correlations of heat and mass transfer for the stagnation region of a re-entry vehicle with multi-component mass addition" Space Systems and Thermal Technology for the 70's, Part II, ASME, June 1970.

CHAPTER 6

SIMPLE HEAT TRANSFER ANALYSES

6.1 INERT GAS INJECTION

Some of the fundamental ideas involved in calculating heat transfer to an ablating surface are well illustrated by the simple problem of injection of a single inert foreign species into a Couette flow. In particular, the analysis of this problem shows us how to define heat transfer to a surface through which mass is being transferred, and demonstrates the roles played by the inter-diffusion term in the energy flux vector, the unity Lewis number assumption, and the choice of enthalpy base states. The figure shows a control volume, cross-sectional area A, thickness dy. Energy can flow in and out the control volume by conduction, $-k\frac{dT}{dy}$, and each species can transport enthalpy, $n_i h_i$. At steady state the principle of energy conservation applied to the control volume requires

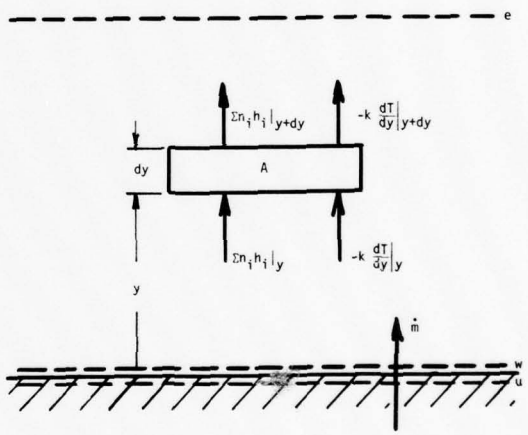

$$A\left(\sum_i n_i h_i - k\frac{dT}{dy}\right)_{y+dy} - A\left(\sum_i n_i h_i - k\frac{dT}{dy}\right)_y = 0$$

divide by Ady, and let dy → 0,

$$\frac{d}{dy}\left(\sum_i n_i h_i - k\frac{dT}{dy}\right) = 0 \qquad (6.1\text{-}1)$$

as before mass conservation requires

$$n = \text{constant} = \dot{m} \qquad (6.1\text{-}2)$$

integrate Eq. (6.1-1),

$$\sum_i n_i h_i - k\frac{dT}{dy} = \left(\sum_i n_i h_i - k\frac{dT}{dy}\right)_w \equiv \dot{m} h_t \qquad (6.1\text{-}3)$$

The integration constant defines h_t, *the enthalpy in the transferred state*. Now $n_i = K_i m + j_i$, thus Eq. (6.1-3) becomes

$$\sum_i (K_i \dot{m} + j_i) h_i - k \frac{dT}{dy} = \dot{m} h_t$$

$$\dot{m} \sum_i K_i h_i + \sum_i j_i h_i - k \frac{dT}{dy} = \dot{m} h_t$$

$$\underbrace{\dot{m}h}_{\text{convection}} + \underbrace{\Sigma j_i h_i}_{\text{interdiffusion}} - \underbrace{k \frac{dT}{dy}}_{\text{conduction}} = \underbrace{\dot{m} h_t}_{\text{total}} \qquad (6.1\text{-}4)$$

i.e., we have three components of the total energy flux: convection, interdiffusion and conduction.

If we assume the Lewis numbers, $Le_i = (k/C_p)/(\rho \mathcal{D}_{im})$, to be unity for all species, we can simplify Eq. (6.1-4) and integrate to obtain the enthalpy profile and heat transfer rate. Consider the following manipulation:

$$h = \sum_i K_i h_i \qquad \text{where} \quad h_i \equiv h_i^{\,o} + \int_{T^o}^{T} C_{pi} dT$$

$$dh = \sum_i K_i dh_i + \sum_i h_i dK_i$$

$$= \sum_i K_i C_{pi} dT + \sum_i h_i dK_i$$

$$dh = C_p dT + \sum_i h_i dK_i \qquad \text{and} \qquad \frac{k}{C_p} \frac{dh}{dy} = k \frac{dT}{dy} + \frac{k}{C_p} \sum_i h_i \frac{dK_i}{dy}$$

Unity Lewis numbers require $k/C_p = \rho \mathcal{D}_{im}$ for i, thus

$$\frac{k}{C_p} \frac{dh}{dy} = k \frac{dT}{dy} + \sum h_i \rho \mathcal{D}_{im} \frac{dK_i}{dy} = k \frac{dT}{dy} - \sum j_i h_i$$

substitute in Eq. (6.1-4),

$$\dot{m} h - \frac{k}{C_p} \frac{dh}{dy} = \dot{m} h_t$$

which is to be integrated subject to the boundary conditions $y = 0$, $h = h_w$; $y = \delta$, $h = h_e$. The mathematical problem is now identical to that solved already for diffusion in a Couette flow, with h replacing K_1, and k/C_p

replacing $\rho\mathcal{D}_{12}$. On assuming k/C_p is constant across the flow, the result is

$$\dot{m} = \underbrace{\frac{k/C_p}{\delta}}_{\substack{\text{conductance for} \\ \text{limit of zero} \\ \text{mass transfer}}} \times \underbrace{\frac{\ell n(1+B_h')}{B_h'}}_{\substack{\text{"blowing} \\ \text{correction"}}} \times \underbrace{B_h'}_{\substack{\text{driving} \\ \text{force}}} \quad \text{where } B_h \equiv \frac{h_e - h_w}{h_w - h_t} \qquad (6.1\text{-}5)$$

or, generalizing to a boundary layer

$$\dot{m} = \rho_e u_e C_{HO} \frac{\ell n(1+B_h')}{B_h'} B_h' \qquad (6.1\text{-}6)$$

As was the case in the mass transfer problem, the Stanton number C_{HO} is just a property of the flow, so use of Eq. (6.1-6) requires further consideration of only the evaluation of B_h'.

To look at the evaluation of B_h' let us consider a model transpiration cooling problem. Helium is injected from a reservoir at temperature T_o into a hot air-stream, and it is required to maintain the wall temperature at T_w. In the figure the o-surface is located far enough back in the reservoir so that temperature gradients are negligible there. Recall that h_t was defined as the integration constant in Eq. (6.1-3); hence evaluation of h_t, and hence B_h', requires specification of an additional physical fact: here we specify that the helium in the reservoir has enthalpy h_o, corresponding to a temperature T_o. Then an energy balance on the control volume located between the w- and o-surfaces gives

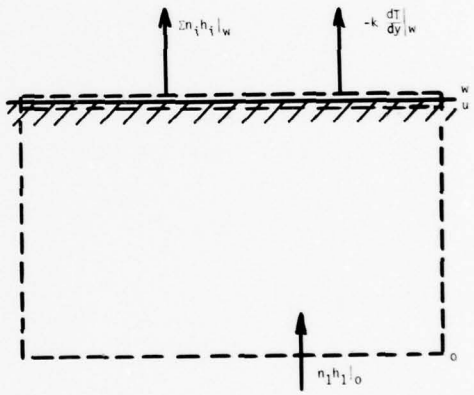

$$\sum_i n_i h_i\Big|_w - k\,\frac{dT}{dy}\Big|_w - n_1 h_1\Big|_o = 0$$

where species 1 is helium. But from Eq. (6.1-3),

$$\dot{m}h_t = \sum_i n_i h_i\Big|_w - k\left.\frac{dT}{dy}\right|_w$$

thus $\dot{m}h_t = n_1 h_{1,o} = \dot{m}h_{1,o}$, or $h_t = h_{1,o} = h_o$, i.e., for this simple case the enthalpy in the transferred state proves to be equal to the enthalpy of the injectant at the reservoir temperature, and

$$B'_h = \frac{h_e - h_w}{h_w - h_o} \tag{6.1-7}$$

Now $h_e = h_{2,e}$ since the free-stream is pure air, and $h_w = \sum_i K_i h_i\big|_w = K_{1,w}h_{1,w} + K_{2,w}h_{2,w}$. So to evaluate h_w we apparently need the composition at the w-surface as well. However we can circumvent this problem through use of the following manipulation. For an inert mixture we are free to choose the enthalpy base state for each species, helium and air, such that the enthalpy of each is zero at T_w, then

$$B'_h = h_e^{\,T_w} - h_o^{\,T_w} \tag{6.1-8}$$

but $$h_o^{\,T_w} = h_{1,o}^{\,T_w} = 0 + \int_{T_w}^{T_o} C_{p1}\,dT = h_{1,o} - h_{1,w}$$

where the last equality holds *irrespective* of datum state, so that the superscript T_w has disappeared. Also

$$h_e^{\,T_w} = \sum_i K_{i,e} h_{i,e}^{\,T_w}$$

$$= \sum_i K_{i,e}(h_{i,e} - h_{i,w}) \qquad \text{irrespective of datum state}$$

$$= \sum_i K_{i,e} h_{i,e} - \sum_i K_{i,e} h_{i,w}$$

$$= h_e - h_{ew}$$

where h_{ew} is the enthalpy of a mixture of e-composition at the w-temperature,

then

$$B'_h = \frac{h_e - h_{ew}}{h_{1,w} - h_{1,o}} = \frac{h_{2,e} - h_{2,w}}{h_{1,w} - h_{1,o}} \tag{6.1-9}$$

If the specific heats of species 1 and 2 are independent of temperature, then

$$B'_h = \frac{C_{p2}(T_e - T_w)}{C_{p1}(T_w - T_o)} = \frac{C_{p\,air}(T_e - T_w)}{C_{p\,He}(T_w - T_o)} \tag{6.1-10}$$

To gain insight into the significance of B'_h, substitute in $\dot{m} = \rho_e u_e C_H B'_h$, and rearrange,

$$\dot{m} C_{p\,He}(T_w - T_o) = \rho_e u_e C_{p\,air} C_H (T_e - T_w) \tag{6.1-11}$$

i.e., (injection rate)x(coolant enthalpy rise) = (heat transfer coefficient) x (temperature difference)

Notice that the heat transfer coefficient is obtained by multiplying C_H by $\rho_e u_e C_{p\,air}$. Had we used intuition to write down Eq. (6.1-11) we would probably have thought some average C_p was appropriate; since $C_{p\,air} = 0.24$ Btu/lb and $C_{p\,He} = 1.24$ Btu/lb, the difference is substantial. We shall see that the appearance of $C_{p\,air}$ in Eq. (6.1-11) is related to the role played by the interdiffusion term.

Example 6.1

A transpiration cooled surface is exposed to an air stream at 3000°F. The coolant is helium and is supplied from a plenum chamber at 100°F. If the surface must be maintained at 800°F calculate the coolant supply rate at a location where the impermeable wall heat transfer conductance $\rho_e u_e C_{HO}$ is 120 lb/ft^2 hr.

From Eq. (6.1-10) $B'_h = \dfrac{C_{p\,air}(T_e - T_w)}{C_{p\,He}(T_w - T_o)} = \dfrac{0.24(3000-800)}{1.24(800-100)} = 0.608$

From Eq. (6.1-6) $\dot{m} = \rho_e u_e C_{HO} \frac{\ell n(1+B_h')}{B_h'} B_h'$

$= (120)(0.781)(0.608)$

$= 57.0 \text{ lb/ft}^2 \text{ hr}$

In order to see what we mean by "heat transfer to the wall" in this sort of situation, let us look at an energy balance on a control volume located between the w- and u-surfaces,

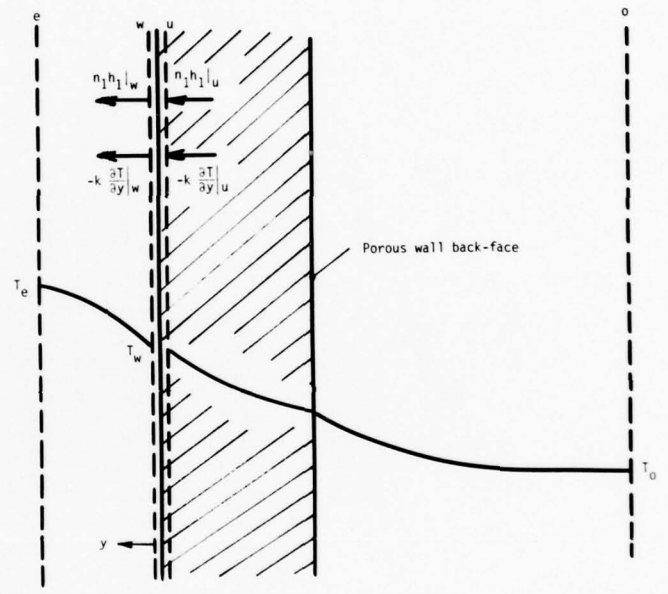

$$(\Sigma_i h_i h_i - k \frac{dT}{dy})_w = (\Sigma n_i h_i - k \frac{dT}{dy})_u$$

but $n_2 = 0$ since no air is transferred at steady state, thus

$$(n_1 h_1 - k \frac{dT}{dy})_w = (n_1 h_1 - k \frac{dT}{dy})_u$$

since helium is inert, and $T_w = T_u$; $h_{1,w} = h_{1,u}$, so

$$-k \left.\frac{dT}{dy}\right|_w = -k \left.\frac{dT}{dy}\right|_u \qquad (6.1\text{-}12)$$

Now $-k \left.\frac{dT}{dy}\right|_u$, the conduction into the wall is what we usually think of as the "heat transfer". To further illustrate this, consider an energy balance between the u- and the o-surfaces; without introducing any assumptions we have

$$n_1 h_{1,u} - k \left.\frac{dT}{dy}\right|_u = n_1 h_{1,o} + 0 \qquad \text{and since } n_1 = \dot{m},$$

$$k \left.\frac{dT}{dy}\right|_u = \dot{m}(h_{1,u} - h_{1,o}) = \dot{m} C_{p1} (T_w - T_o)$$

i.e., $k \left.\frac{dT}{dy}\right|_u$ is equal to the product of $\dot{m}$ and the enthalpy rise of the coolant as it flows from the reservoir to the surface, surely what our intuition tells us should be regarded as the heat transfer. Note then that Eq. (6.1-12) states that it is the conductive component of the energy flux at the w-surface which is to be regarded as the heat transfer.

From Eqs. (6.1-3 and 4) we have two alternative forms of the total energy flux across the w-surface:

$$\underbrace{\dot{m}h_w}_{\text{bulk convection}} + \underbrace{\underbrace{\sum_i j_i h_i|_w}_{\text{inter-diffusion}} - \underbrace{k \left.\frac{dT}{dy}\right|_w}_{\text{conduction}}}_{\text{total diffusion}} = \underbrace{\sum_i n_i h_i|_w}_{\text{absolute convection}} - \underbrace{k \left.\frac{dT}{dy}\right|_w}_{\text{conduction}} \qquad (6.1\text{-}13)$$

Many workers regard the total diffusive flux to the "wall value of the energy flux" or the "convective heat flux to the wall". But we have seen that the total diffusive flux is not really of interest since the "heat transfer" is given by the conduction component alone. Nevertheless there is merit to combining the interdiffusion and conduction fluxes for correlation purposes. Equation (6.1-5), written at the wall is

$$k \left.\frac{dT}{dy}\right|_w - \sum_i j_i h_i|_w = \frac{k}{C_p} \left.\frac{dh}{dy}\right|_w = \dot{m}(h_w - h_t)$$

and $$\dot{m} = \rho_e u_e C_H B_h' = \rho_e u_e C_H (h_e - h_w)/(h_w - h_t)$$

thus $$k \left.\frac{dT}{dy}\right|_w - \sum_i j_i h_i|_w = \frac{k}{C_p} \left.\frac{dh}{dy}\right|_w = \rho_e u_e C_H (h_e - h_w) \qquad (6.1\text{-}14a)$$

or $$C_H = \frac{k \left.\frac{dT}{dy}\right|_w - \sum_i j_i h_i|_w}{\rho_e u_e (h_e - h_w)} \qquad (6.1\text{-}14b)$$

Thus, for unity Lewis number, the appropriate driving force for the total diffusive flux is the enthalpy difference across the boundary layer. But

let us once again exploit our freedom to choose the enthalpy base state of each inert species, and set the enthalpy of each equal to zero at T_w, then Eq. (6.1-14a) becomes

$$k \left.\frac{dT}{dy}\right|_w = \frac{k}{C_p} \left.\frac{dh}{dy}^{T_w}\right|_w = \rho_e u_e C_H (h_e^{T_w} - 0) = \rho_e u_e C_H (h_e - h_{ew}) \qquad (6.1\text{-}15a)$$

$$\text{or} \quad C_H = \frac{k \left.\frac{dT}{dy}\right|_w}{\rho_e u_e (h_e - h_{ew})} \qquad (6.1\text{-}15b)$$

i.e., the appropriate driving force for the conductive heat flux is the difference between the free stream enthalpy and the enthalpy of gas of free-stream composition at the wall temperature. We see now why $C_{p\,air}$ appears in Eq. (6.1-11), and not some average C_p. Use of an average C_p would approximate the right hand side of Eq. (6.1-14a), and give the total diffusive flux. Use of $C_{p\,air}$ gives the conduction component, which we have already seen is the required "heat transfer".

The use of choice of base states to derive Eq. (6.1-15) from Eq. (6.1-14) is a convenient, but not necessary, method. A purely algebraic derivation proceeds as follows. From Eq. (6.1-15),

$$k \left.\frac{dT}{dy}\right|_w - \Sigma j_i h_i \Big|_w = \rho_e u_e C_H (h_e - h_w)$$

$$= \rho_e u_e C_H (h_e - h_{ew}) + \rho_e u_e C_H (h_{ew} - h_w)$$

but for unity Lewis number, $C_H = C_M$, thus

$$\rho_e u_e C_H (h_{ew} - h_w) = \rho_e u_e C_M (\Sigma_i K_{i,e} h_{i,w} - \Sigma_i K_{i,w} h_{i,w})$$

$$= \Sigma_i \rho_e u_e C_M (K_{i,e} - K_{i,w}) h_{i,w}$$

$$= -\Sigma_i j_{i,w} h_{i,w}$$

hence $k \left.\frac{dT}{dy}\right|_w = \rho_e u_e C_H (h_e - h_{ew})$ as desired.

Another point to note is that caution must be exercised when working with numerical values of the total diffusive flux, since the values depend on the choice of enthalpy base state. Let us look at the values which obtain in Example 6.1.

$$k \left.\frac{dT}{dy}\right|_w = \dot{m} C_{p\,He} (T_w - T_o) = (57.0)(1.20)(800-100) = 49{,}500 \text{ Btu/ft}^2 \text{ hr}$$

$$\left.\sum_i j_i h_i\right|_w = j_1 (h_1 - h_2)_w \qquad \text{since } j_2 = -j_1$$

If we choose enthalpy base states such that the enthalpies of helium and air are both zero at T = 0°R, and if we assume constant species specific heats, then

$$\sum_i j_i h_{i\,w} = j_{1,w} T_w (C_{p1} - C_{p2}) = j_{1,w} T_w (1.24 - 0.24) = j_{1,w} T_w$$

To evaluate $j_{1,w}$ we note that since the Lewis number is unity, $B' = B'_h$ so

$$\frac{0 - K_{1,w}}{K_{1,w} - 1} = 0.606 \; ; \quad \text{solving,} \quad K_{1,w} = 0.377$$

Also $$\dot{m} K_{1,w} + j_{1,w} = \dot{m} K_{1,t} = \dot{m}$$

solving, $$j_{1,w} = \dot{m}(1 - K_{1,w}) = 57.0(1-0.377) = 35.5 \text{ lb/ft}^2 \text{ hr}$$

Thus $$\left.\sum_i j_i h_i\right|_w = j_{1,w} T_w = (35.5)(800+460) = 42{,}600 \text{ Btu/ft}^2 \text{ hr}$$

The total diffusive flux is then

$$\left.\sum_i j_i h_i\right|_w - k \left.\frac{dT}{dy}\right|_w = 42{,}600 - 49{,}500 = -6{,}900 \text{ Btu/ft}^2 \text{ hr}$$

On the other hand if T^o = 800°F had been chosen as the enthalpy base state then the interdiffusion flux would have been zero, and the total diffusive flux would have been equal to the conduction, -49,500 Btu/ft^2 hr.

6.2 TRANSPIRATION COOLING WITH PHASE CHANGE

Consider now the use of water instead of helium as a coolant, with an injection rate just sufficient to keep the wall wet. Let water be species 1 and air species 2, and again the water is supplied from a reservoir at temperature T_o. The analysis of §6.1 leading to Eq. (6.1-6) considers only the transport processes occurring between the e- and w-surfaces, and thus is not altered by a phase change taking place between the w- and u-surfaces. Furthermore, the analysis leading to Eq. (6.1-7), based on an energy balance on a control volume located between the w- and o-surfaces, is also unaffected by a phase change taking place within the control volume, since enthalpies rather than temperatures were used. Finally the manipulation leading to Eq. (6.1-9) is unaffected since H_2O is inert. Thus

$$B_h' = \frac{h_e - h_{ew}}{h_{1,w} - h_{1,o}} \tag{6.2-1}$$

where $h_{1,w}$ is the enthalpy of water vapor at temperature T_w and $h_{1,o}$ is the enthalpy of liquid water at temperature T_o. Equation (6.2-1) can be rewritten assuming constant specific heats, as

$$B_h' = \frac{C_{p\,air}(T_e - T_w)}{h_{fg} + C_{p\,water}(T_w - T_o)} \tag{6.2-2}$$

Substituting in $\dot{m} = \rho_e u_e C_H B_h'$ and rearranging gives

$$\dot{m}[h_{fg} + C_{p\,water}(T_w - T_o)] = \rho_e u_e C_H C_{p\,air}(T_e - T_w) \tag{6.2-3}$$

i.e., (injection rate)x(enthalpy rise of coolant) = (heat transfer coefficient) x (temperature difference)

Example 6.2

Rework the previous example with helium replaced by water as the coolant, and a required wall temperature of 400°F. The ambient pressure is 20 atm, and thus boiling does not occur within the wall.

From Eq. (6.2-2) $B'_h = \frac{0.24(3000-400)}{825+1(400-100)} = 0.555$

From Eq. (6.1-6) $\dot{m} = (120)(0.795)(0.555) = 53.0 \text{ lb/ft}^2 \text{ hr}$

6.3 SIMPLE DIFFUSION CONTROLLED OXIDATION

We now return to the simple diffusion controlled oxidation problem for which the mass transfer analysis was done in §4.2. Specifically consider tungsten being oxidized by an air-stream containing undissociated oxygen, with wall temperatures high enough for chemical equilibrium to exist at the w-surface with $K_{O_2,w} \simeq 0$. The reaction is assumed to be $3W + 4\,\frac{1}{2}\,O_2 \rightarrow W_3O_9$, and we found that $B' = K_{O_2,e}/r = 0.232/0.26 = 0.893$. For the heat transfer analysis we can again use Eq. (6.1-6) with the heat transfer driving force given by

$$B'_h = \frac{h_e - h_w}{h_w - h_t}$$

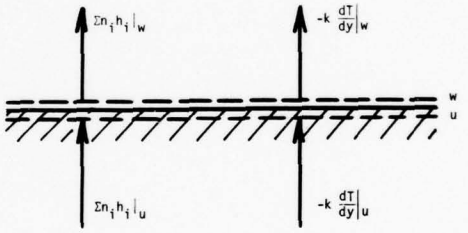

$$\dot{m}h_t = \sum_i n_i h_i\Big|_w - k\,\frac{dT}{dy}\Big|_w$$

$$= \sum_i n_i h_i\Big|_u - k\,\frac{dT}{dy}\Big|_u$$

thus
$$B'_h = \frac{h_e - h_w}{h_w - (1/\dot{m})\left(\sum_i n_i h_i\Big|_u - k\,\frac{dT}{dy}\Big|_u\right)} \qquad (6.3\text{-}1)$$

If we assume quasi-steady state heat conduction in the tungsten, the evaluation of B'_h is straightforward. As was the case with transpiration cooling, we locate an o-surface far enough back in the tungsten for temperature gradients to be negligible, and an energy balance on the control volume lying between the u- and o-surfaces gives

$$n_{W^*}h_{W^*}\Big|_u - k\,\frac{dT}{dy}\Big|_u = n_{W^*}h_{W^*}\Big|_o + 0$$

but $n_{W^*} \equiv \dot{m}$, so $\quad k\,\frac{dT}{dy}\Big|_u = \dot{m}(h_{W^*,u} - h_{W^*,o})$

substitute in Eq. (6.3-1), $$B_h' = \frac{h_e - h_w}{h_w - h_{W^*,o}} \tag{6.3-2}$$

Equation (6.3-2) cannot be further simplified unless we are prepared to make use of the assumption that the O_2 and W_3O_9 are inert in the gas phase. However the steady state ablation solution is of limited interest: it was presented mainly to show that a result analogous to those obtained in §6.1 and §6.2 could be obtained for the oxidation problem. In practice we more often encounter time-wise unsteady state heat conduction in a heat shield and proceed as follows. Since $\dot{m} = \rho_e u_e C_H B_h'$, Eq. (6.3-1) can be rearranged as

$$\dot{m}h_w - \sum_i n_i h_i\big|_u + k \left.\frac{\partial T}{\partial y}\right|_u = \rho_e u_e C_H (h_e - h_w)$$

or $$k \left.\frac{\partial T}{\partial y}\right|_u = \rho_e u_e C_H (h_e - h_w) - \dot{m}h_w + \sum_i n_i h_i\big|_u \tag{6.3-3}$$

where we have replaced dT/dy by ∂T/∂y to remind us that now T = T(y,t). The l.h.s. of Eq. (6.3-3) is the conduction heat flux into the heat shield, and serves as a boundary condition for the heat coneuction equation governing the temperature distribution in the heat shield. We would like to see a term on the r.h.s. of Eq. (6.3-3) which could be identified as a "heat of reaction". In order to proceed we need to assume, as in §4.2 that the boundary layer is inert: then we can use the manipulation following Eq. (6.1-15) to obtain

$$k \left.\frac{\partial T}{\partial y}\right|_u = \rho_e u_e C_H (h_e - h_{ew}) - \sum_i j_i h_i\big|_w - \dot{m}h_w + \sum n_i h_i\big|_u$$

but $\dot{m}h + \sum j_i h_i = \sum n_i h_i$, thus

$$\underbrace{k \left.\frac{\partial T}{\partial y}\right|_u}_{\text{conduction flux into heatshield}} = \underbrace{\rho_e u_e C_H (h_e - h_{ew})}_{\text{conduction flux across w-surface}} - \underbrace{\left(\sum n_i h_i\big|_w - \sum n_i h_i\big|_u\right)}_{\text{heat release between w- and u-surface due to surface reactions}} \tag{6.3-4}$$

Referring back to our previous examples notice that the "surface reaction" term is zero for an inert injectant, and equal to the latent heat of vaporization for a water injectant. Also in the latter case $(\Sigma n_i h_i|_w - \Sigma n_i h_i|_u) = \dot{m}(h_{l,w} - h_{l,u}) = \dot{m}h_{fg}$, and we see that the conduction into the heatshield is less than the conduction across the w-surface by the amount $\dot{m}h_{fg}$.

Let us evaluate the surface reaction term for the tungsten oxidation problem:

$$\Sigma n_i h_i|_u = n_{W^*,u} h_{W^*,u} = \dot{m} h_{W^*,u}$$

$$\Sigma n_i h_i|_w = n_{W_3O_9,w} h_{W_3O_9,w} + n_{O_2,w} h_{O_2,w} \qquad (n_{N_2,w} = 0)$$

Since $T_w = T_u$ all the species enthalpies are to be evaluated at temperature T_w;

$$\Sigma n_i h_i|_w - \Sigma n_i h_i|_u = \dot{m}[(n_{W_3O_9,w}/\dot{m}) h_{W_3O_9,w} + (n_{O_2,w}/\dot{m}) h_{O_2,w} - h_{W^*,w}]$$

$$= \dot{m}[(1+r) h_{W_3O_9} - r h_{O_2} - h_{W^*}]_w$$

But $$(1+r) h_{W_3O_9} - r h_{O_2} - h_{W^*} = \Delta H_{r(W^*)}$$

thus $$\Sigma n_i h_i|_w - \Sigma n_i h_i|_u = \dot{m} \Delta H_{r(W^*)}^{T_w} \qquad (6.3\text{-}5)$$

where $\Delta H_{r(W^*)}^{T_w}$ is the heat of reaction per lb of tungsten at temperature T_w; for this exothermic reaction ΔH_r is negative. Notice that Eq. (6.3-5) can be rewritten as

$$\Sigma n_i h_i|_w - \Sigma n_i h_i|_u = (r\dot{m})(\Delta H_{r(W^*)}^{T_w}/r)$$

$$= -n_{O_2,w} \Delta H_{r(O_2)}^{T_w} \qquad (6.3\text{-}6)$$

where $\Delta H_{r(O_2)}^{T_w}$ is the heat of reaction per lb of O_2. Substituting Eq. (6.3-6) in Eq. (6.3-4) gives the surface energy balance in the familiar form,

$$k \left.\frac{\partial T}{\partial y}\right|_u = \rho_e u_e C_H (h_e - h_{ew}) + n_{O_2,w} \overset{T_w}{\Delta H_{r(O_2)}} \qquad (6.3\text{-}7)$$

conduction flux into heatshield — conduction flux across w-surface — heat release in oxidation reaction

6.4 TRANSPIRATION COOLING WITH INJECTANT DISSOCIATION

We first look at the situation where the injectant dissociates in the boundary layer and investigate the effect of dissociation on the surface heat transfer. For simplicity consider a dimer A_2 injected into a high temperature flow of an inert gas with temperatures such that no dissociation of A_2 occurs below the wall temperature, i.e., the dissociation takes place wholly within the boundary layer and not in the porous wall. As for inert gas injection (§6.1) the A_2 is supplied from a reservoir at temperature T_o. Let species 1 be A_2, species 2 be A and species 3 the inert gas. Our analysis of §6.1 leading to Eq. (6.1-7) is valid for a chemically reacting system provided that the Lewis number is unity for all reacting species. Thus

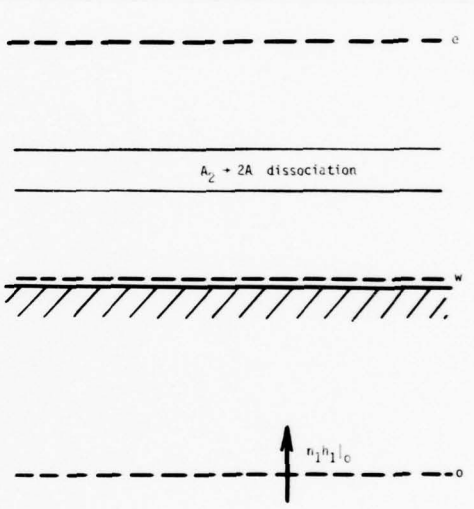

$$\dot{m} = \rho_e u_e C_H \frac{\ell n(1+B'_h)}{B'_h} B'_h \; ; \quad B'_h = \frac{h_e - h_w}{h_w - h_o} \qquad (6.4\text{-}1)$$

In general we can write for the species and mixture enthalpies, respectively,

$$h_i = h_i^o + \int_{T^o}^{T} C_{pi} dT \; ; \quad h = \Sigma_i K_i h_i \; ;$$

and we are free to choose $T^o = T_w$ and $h_i(T_o) = 0$ for species 1 (A_2) and 3 (inert), then

$$h_1 = \int_{T_w}^{T} C_{p1} dT \; ; \qquad h_2 = h_2^{oT_w} + \int_{T_w}^{T} C_{p2} dT \; ; \qquad h_3 = \int_{T_w}^{T} C_{p3} dT \; ;$$

and we evaluate the mixture enthalpies as follows:

$$h_e = \sum_i K_{i,e} h_{i,e} = (1)(h_{3,e}) = \int_{T_w}^{T} C_{pe} dT = h_e - h_{ew} \simeq C_{p3}(T_e - T_w)$$

$h_w = 0$ (since $K_{2,w} = 0$)

$$h_o = \int_{T_w}^{T} C_{p1} dT = h_{1,o} - h_{1,w} \simeq C_{p1}(T_o - T_w)$$

Substitute in Eq. (6.4-1)

$$B_h' = \frac{h_e - h_{ew}}{h_{1,w} - h_{1,o}} \simeq \frac{C_{p3}(T_e - T_w)}{C_{p1}(T_w - T_o)} \qquad (6.4\text{-}2)$$

which is identical to the result obtained for an inert injectant, Eq. (6.1-10). Thus we conclude that dissociation of a transpirant in the boundary layer has no direct effect on the surface heat transfer. Of course, dissociation does lower temperatures in the boundary layer and there are second order effects on the heat transfer via temperature dependent transport properties. The above result was first obtained in the early paper by Cohen, Bromberg and Lipkis [1].

We now look at the situation where dissociation takes place within the wall, i.e., we postulate that the A_2 dissociation takes place wholly below the wall temperature so that no A_2 is present at the w-surface. Equation (6.4-1) still applies and again we choose $T^o = T_w$, but now we put $h_i^o(T^o) = 0$ for species 2 (A) and 3 (inert),

$$h_1 = h_1^{oT_w} + \int_{T_w}^{T} C_{p1} dT \; ; \qquad h_2 = \int_{T_w}^{T} C_{p2} dT \; ; \qquad h_3 = \int_{T_w}^{T} C_{p3} dT$$

Then $h_e = C_{p3}(T_e - T_w)$ again,

$$h_w = 0 \quad (\text{since } K_{1,w} = 0)$$

$$h_o = h_1^{\,oT_w} + \int_{T_w}^{T_o} C_{p1}\,dT = h_1^{\,oT_w} + C_{p1}(T_o - T_w)$$

substitute in Eq. (6.4-1)

$$B_h' = \frac{C_{p3}(T_e - T_w)}{C_{p1}(T_w - T_o) - h_1^{\,oT_w}}$$

Now $h_1^{\,oT_w}$ is just $\Delta H_d^{\,T_w}$ where $\Delta H_d^{\,T_w}$ is the heat of dissociation of A_2 at T_w; to the level of approximation of the analysis we can ignore the temperature dependence of ΔH_d and then

$$B_h' = \frac{C_{p3}(T_e - T_w)}{C_{p1}(T_w - T_o) + \Delta H_d}\,; \quad (\Delta H_d \text{ is positive}) \tag{6.4-3}$$

Heats of dissociation are often large; in such cases B_h' calculated from Eq. (6.4-3) will be much less than the value calculated from Eq. (6.4-2).

Example 6.3

A candidate passive transpiration cooling system is the combination of a copper fluoride infiltrant and a tungsten matrix. Evaluate the effect of dissociation on the capacity of the infiltrant to absorb heat.

We must determine the effect of heat of dissociation on the enthalpy difference $(h_{CuF_2,w} - h_{CuF_2,o})$. Take T_w to be the melt temperature of tungsten (6624°R), then the required thermodynamic data are (JANAF tables):

100 atm boiling temperature = 4266°R

Enthalpy increase from solid at 536°R to vapor at 4266°R = 2056 Btu/lb

Enthalpy increase of vapor from 4266°R to 6624°R = 369 Btu/lb

Heat of dissociation, $CuF_2 \rightarrow Cu + 2F$, = 3324 Btu/lb

a) without dissociation

$$h_{CuF_2,w} - h_{CuF_2,o} = 2056 + 269 = 2425 \text{ Btu/lb}$$

b) Assuming dissociation to be complete at T_w (quite a good assumption)

$h_{CuF_2,w} - h_{CuF_2,o} = 2056+369+3324 = 5749$

$\therefore$ percentage improvement $= \frac{5749-2425}{2425} \times 100 = 137\%$

Note however that passive transpiration cooling system operation is usually strongly transient in nature, thus the expression for $\dot{m}$ in Eq. (6.4-1) is not appropriate for this situation.

6.5 THE RECOVERY ENTHALPY CONCEPT

We now use a Couette flow model to introduce the concept of recovery enthalpy and recovery factor. Previously we assumed a low speed flow where viscous dissipation effects are negligible; in order to include such effects we will now have our e-surface at a plate, temperature T_e and moving with velocity u_e. For simplicity we will consider a pure fluid of constant specific heat. Conservation equations are derived by applying the principles of mass, momentum and total (mechanical plus thermal) energy conservation to an elementary control volume Ady; the figure shows details for total energy.

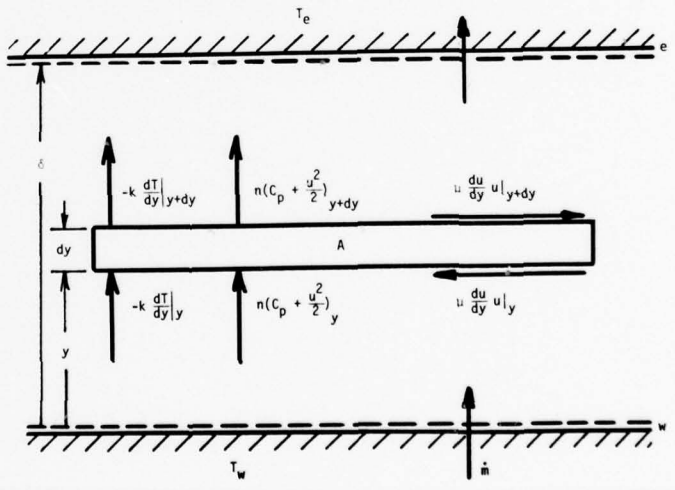

mass: $\frac{d}{dy}(n) = 0$ (6.5-1)

momentum: $\frac{d}{dy}(nu - \mu \frac{du}{dy}) = 0$ (6.5-2)

total energy: $\frac{d}{dy}(n(C_pT + u^2/2) - k\frac{dT}{dy} - \mu u \frac{du}{dy}) = 0$ (6.5-3)

We will first obtain a solution for the simple case of zero mass transfer ($n = \dot{m} = 0$); then the momentum equation is easily integrated to give a linear velocity profile,

$$\frac{u}{u_e} = \frac{y}{\delta} \tag{6.5-4}$$

The energy equation integrated once is

$$k \frac{dT}{dy} + \mu u \frac{du}{dy} = \text{constant},$$

but $u = u_e(y/\delta)$ and $du/dy = u_e/\delta$, thus

$$\frac{dT}{dy} + \frac{\mu u_e^2 y}{k\delta^2} = \text{constant} \tag{6.5-5}$$

It is now useful to introduce dimensionless variables $T^* = (T-T_w)/(T_e-T_w)$ and $y^* = y/\delta$, then

$$\frac{dT^*}{dy^*} = 2 \frac{C_p \mu}{k} \frac{u_e^2/2}{C_p(T_w-T_e)} y^* + C_1 = 2\text{PrEc}y^* + C_1$$

where Pr is the Prandtl number, $C_p\mu/k$ and Ec is the Eckert number, $(u_e^2/2)/C_p(T_w-T_e)$. Integrating again gives

$$T^* = \text{PrEc}y^{*2} + C_1 y^* + C_2$$

The boundary conditions to be satisfied are:

$$y = 0,\ T = T_w \quad \text{or} \quad y^* = 0,\ T^* = 0$$

$$y = \delta,\ T = T_e \quad \text{or} \quad y^* = 1,\ T^* = 1$$

hence $$T^* = \text{PrEc}y^{*2} + (1-\text{PrEc})y^* \tag{6.5-6}$$

The heat transfer to the wall is given by Fourier's law,

$$q_w = -k \frac{dT}{dy}_w$$

$$= -\frac{k(T_e-T_w)}{\delta} \left.\frac{dT^*}{dy^*}\right|_{y=0}$$

$$q_w = -\frac{k(T_e-T_w)}{\delta}(2PrEcy^* + 1-PrEc)_{y^*=0}$$

$$= -\frac{k(T_e-T_w)}{\delta}(1-PrEc)$$

$$q_w = -\frac{k}{\delta}\left[\left(T_e+Pr\frac{u_e^2}{2C_p}\right) - T_w\right] \qquad (6.5\text{-}7)$$

In a low speed flow with negligible viscous dissipation the wall heat transfer is simply the conduction through a slab δ thick,

$$q_w = -\frac{k}{\delta}(T_e-T_w) \qquad (6.5\text{-}8)$$

Thus we see that the effect of viscous dissipation can be accounted for by replacing T_e by the "recovery" temperature $T_r = T_e + Pr(u_e^2/2C_p)$ in the driving potential for heat transfer. The temperature T_r is the temperature corresponding to the enthalpy $h_r = C_pT_r$ recovered from the total enthalpy of a unit mass of fluid at the e-surface, $C_pT_e + \frac{1}{2}u_e^2$, when the wall is adiabatic. In other words, when $q_w = 0$, $T_w = T_r$.

More generally it is convenient to work in terms of enthalpy and

$$h_r = h_e + Pr\frac{u_e^2}{2} \qquad (6.5\text{-}9)$$

The Couette flow is of course a simple model of real flows; we may further generalize our result by writing

$$h_r + r(Pr)\frac{u_e^2}{2} \qquad (6.5\text{-}10)$$

where the recovery factor $r = Pr$ for a Couette flow, $r \cong Pr^{1/2}$ for laminar flow, and $r \cong Pr^{1/3}$ for a turbulent flow, all for an impermeable wall ($\dot{m} = 0$).

Effect of mass transfer

To determine the effect of blowing or suction on the recovery factor we now obtain the solution to Eqs. (6.5-1) through (6.5-3) for $\dot{m} \neq 0$.

Eq. (6.5-1) $\quad n = \text{constant} = \dot{m}$

Eq. (6.5-2) $\quad \dot{m}u = \mu \frac{du}{dy} + \text{constant}$

or $\quad \frac{du}{dy} - \frac{\dot{m}}{\mu} u = C_1$

Integrate subject to the boundary conditions $u = 0$ at $y = 0$, and $u = u_e$ at $y = \delta$ to obtain the velocity profile

$$\frac{u}{u_e} = \frac{e^{(\dot{m}/\mu)y} - 1}{e^{(\dot{m}/\mu)\delta} - 1} \tag{6.5-11}$$

Since we now have transport of mechanical energy by the transverse mass flux it is convenient to solve the thermal energy equation to obtain the temperature field. We multiply the momentum equation by u and subtract the resulting mechanical energy equation from the total energy equation, Eq. (6.5-3) to obtain, after some algebra,

$$k \frac{d^2T}{dy^2} - \dot{m}C_p \frac{dT}{dy} + \mu\left(\frac{du}{dy}\right)^2 = 0 \tag{6.5-12}$$

The viscous dissipation term is evaluated from Eq. (6.5-11),

$$\frac{du}{dy} = \frac{u_e(\dot{m}/\mu)e^{(\dot{m}/\mu)y}}{(e^{(\dot{m}/\mu)\delta} - 1)}$$

$$\mu\left(\frac{du}{dy}\right)^2 = \frac{\mu u_e^2(\dot{m}/\mu)^2 e^{2(\dot{m}/\mu)y}}{(e^{(\dot{m}/\mu)\delta} - 1)^2}$$

Substituting Eq. (6.5-12)

$$\frac{d^2T}{dy^2} - \frac{\dot{m}}{\mu} Pr \frac{dT}{dy} = \frac{-(\mu/k)u_e^2(\dot{m}/\mu)^2 e^{2(\dot{m}/\mu)y}}{(e^{(\dot{m}/\mu)\delta} - 1)^2}$$

or $\quad \frac{d^2T}{dy^2} - \alpha Pr \frac{dT}{dy} = -\phi e^{2\alpha y} \; ; \quad \phi = \frac{(Pr/C_p)u_e^2\alpha^2}{(e^{\alpha\delta} - 1)^2}$

solving $$T = \frac{-\phi}{2\alpha^2(2-Pr)} e^{2\alpha y} + \frac{C_1}{\alpha Pr} e^{\alpha Pry} + C_2 \qquad (6.5\text{-}13)$$

To obtain the recovery temperature we can simply obtain a solution for an adiabatic wall at y = 0.

$$\left.\frac{dT}{dy}\right|_o = \frac{-\phi}{\alpha(2-Pr)} + C_1 = 0 \quad \text{hence} \quad C_1 = \frac{\phi}{\alpha(2-Pr)}$$

$$T = \frac{\phi}{\alpha^2(2-Pr)Pr} e^{\alpha Pry} - \frac{\phi}{2\alpha^2(2-Pr)} e^{2\alpha y} + C_2$$

$$= \frac{\phi}{2\alpha^2(2-Pr)Pr} (2e^{\alpha Pry} - Pre^{2\alpha y}) + C_2$$

Apply a second boundary condition, $T = T_e$ at $y = \delta$, giving

$$T_e = \frac{\phi}{2\alpha^2(2-Pr)Pr} (2e^{\alpha Pr\delta} - Pre^{2\alpha\delta}) + C_2 \ , \quad \text{hence } C_2.$$

Finally the temperature distribution is

$$T-T_e = \frac{\phi}{2\alpha^2(2-Pr)Pr} [2(e^{\alpha Pry}-e^{\alpha Pr\delta}) - Pr(e^{2\alpha y}-e^{2\alpha\delta})] \qquad (6.5\text{-}14)$$

and the adiabatic wall temperature results on putting y = 0 in Eq. (6.5-14) to obtain

$$T_{aw}-T_e = \frac{\phi}{2\alpha^2(2-Pr)Pr} [2(1-e^{\alpha Pr\delta}) - Pr(1-e^{2\alpha\delta})]$$

Substituting for ϕ and rearranging gives

$$T_{aw}-T_e = \frac{u_e^2}{2C_p} \left[\frac{2(1-e^{\alpha Pr\delta}) - Pr(1-e^{2\alpha\delta})}{(2-Pr)(e^{\alpha\delta}-1)^2}\right] = \frac{u_e^2}{2C_p} F(\alpha\delta) \qquad (6.5\text{-}15)$$

Now $\alpha\delta = \frac{\dot{m}}{\mu}\delta$, and to see more clearly the effect of mass transfer we obtain a solution for small $\dot{m}$ (small $\alpha\delta$) by expanding $F(\alpha\delta)$ in a Taylor series about $\alpha\delta = 0$,

$$F = F(0) + (\alpha\delta)F'(0) + \ldots$$

Repeated use of L'Hopital's rule together with considerable algebra yields

$$F(0) = Pr$$

$$F'(0) = \frac{1}{3} Pr(Pr-1)$$

$$T_{aw}-T_e = \frac{u_e^2 Pr}{2C_p} \left[1 + \frac{1}{3} \frac{\dot{m}\delta}{\mu} (Pr-1) + \ldots\right] \qquad (6.5\text{-}16)$$

a result which was obtained by Knuth [2]. For gases $Pr < 1$, so that the effect of blowing is seen to be a decrease in the adiabatic wall temperature.

REFERENCES FOR CHAPTER 6

1. C. B. Cohen, R. Bromberg and R. P. Lipkis, "Boundary layers with chemical reactions due to mass addition", Jet Propulsion, 28, 659-668 (1958).

2. E. L. Knuth, "Use of reference states and constant property solutions in predicting mass-, momentum-, and energy-transfer rates in high speed laminar flows", Int. J. Heat Mass Transfer 6, 1-22 (1963).

CHAPTER 7

THE SURFACE ENERGY BALANCE

7.1 INTRODUCTION

In ablation calculations a surface energy balance is required in order to evaluate the conduction heat flux into the heat shield, $-k\ \partial T/\partial y|_u$, which is then used as an input into a conduction code. Thus we require a surface energy balance similar in form to Eq. (6.3-1), but of more general applicability. The surface energy balance is a balance on a control volume located between the w- and u-surfaces, as shown in the Figure. We shall consider stagnation regions, and ignore thermal radiation and mechanical removal, for the time being so as to focus more clearly on the effects of chemical reactions.

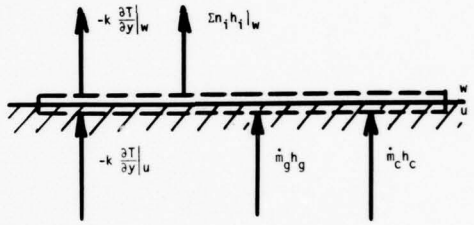

Following common practice we will separate the u-surface mass fluxes into two components, corresponding to the pyrolysis gas and the char, such that

$$\dot{m}_g + \dot{m}_c = \sum_i n_{i,u} = \sum_i n_{i,w} = \dot{m} \tag{7.1-1}$$

The energy balance on the control volume bounded by the w- and u-surfaces is then

$$k\left.\frac{\partial T}{\partial y}\right|_u = k\left.\frac{\partial T}{\partial y}\right|_w - \sum_i n_i h_i\Big|_w + \dot{m}_g h_g + \dot{m}_c h_c \tag{7.1-2}$$

or, since $\sum_i n_i h_i = \dot{m} h + \sum_i j_i h_i$

$$k\left.\frac{\partial T}{\partial y}\right|_u = k\left.\frac{\partial T}{\partial y}\right|_w - \sum_i j_i h_i\Big|_w - \dot{m} h_w + \dot{m}_g h_g + \dot{m}_c h_c \tag{7.1-3}$$

The approach used by Aerotherm/Acurex Corporation [1,2] in rearranging Eq. (7.1-3) is typical of good current practice and is as follows. First, for a Lewis number of unity, we have the exact result that

$$k \left.\frac{\partial T}{\partial y}\right|_u = \rho_e u_e C_H (h_e - h_w) - \dot{m} h_w + \dot{m}_g h_g + \dot{m}_c h_c \qquad (7.1\text{-}4)$$

then adding and subtracting $\rho_e u_e C_H h_{ew}$,

$$k \left.\frac{\partial T}{\partial y}\right|_u = \rho_e u_e C_H (h_e - h_{ew}) + \rho_e u_e C_H (h_{ew} - h_w) - \dot{m} h_w + \dot{m}_g h_g + \dot{m}_c h_c$$

but for Le = 1, $C_H = C_M$; also $h_{ew} \equiv \sum_i K_{i,e} h_{i,w}$, thus

$$k \left.\frac{\partial T}{\partial y}\right|_u = \rho_e u_e C_H (h_e - h_{ew}) + \rho_e u_e C_M \sum_i (K_{i,e} - K_{i,w}) h_{i,w} - \dot{m} h_w + \dot{m}_g h_g + \dot{m}_c h_c \qquad (7.1\text{-}5)$$

and this equation holds irrespective of whether or not reactions occur within the boundary layer.

For all species diffusion coefficients assumed equal but Le $\neq$ 1, Aeroterm recommends use of Eq. (7.1-5) but with $C_M/C_H = Le^{2/3}$, i.e.,

$$k \left.\frac{\partial T}{\partial y}\right|_u = \rho_e u_e C_H (h_e - h_{ew}) + \rho_e u_e Le^{2/3} C_H \sum_i (K_{i,e} - K_{i,w}) h_{i,w} - \dot{m} h_w + \dot{m}_g h_g + \dot{m}_c h_c \qquad (7.1\text{-}6)$$

For unequal diffusion coefficients, Eq. (7.1-5) is replaced by

$$k \left.\frac{\partial T}{\partial y}\right|_u = \rho_e u_e (h_e - h_{ew}) + \rho_e u_e C_M \sum_i (z^*_{i,e} - z^*_{i,w}) h_{i,w} - \dot{m} h_w + \dot{m}_g h_g + \dot{m}_c h_c \qquad (7.1\text{-}7)$$

Equations (7.1-4, 6 and 7) are the three forms of the surface energy balance in general use by Aerotherm.

Comments on Equations (7.1-4, 6 and 7)

1. Use of these equations requires various quantities which may be calculated by, for example, the ACE code [3].

For Eq. (7.1-4): h_w, and the surface thermochemistry calculation is sufficient.

For Eq. (7.1-6): h_w, $h_{ew} = \Sigma K_{i,e} h_{i,w}$, so that in addition we now require a frozen edge gas calculation.

For Eq. (6.1-7): h_w, h_{ew}, $\Sigma z^*_{i,w} h_{i,w}$, $\Sigma z^*_{i,e} h_{i,w}$ and again the frozen edge gas calculation is required.

Thus clearly Eq. (7.1-4) is the simplest of the three to use in practice.

2. When Le = 1 the three equations will give identical values for the conduction flux into the heat shield.

3. We have seen that for Le = 1 there are two equivalent heat transfer Stanton number definitions, Eqs. (6.1-14b) and (6.1-15b). For Le $\neq$ 1 these heat transfer Stanton numbers are no longer equal. When applying Eq. (7.1-4) the consistent definition of Stanton number is

$$C_H = \frac{k \left.\frac{\partial T}{\partial y}\right|_w - \Sigma j_i h_i|_w}{\rho_e u_e (h_e - h_w)} \qquad (7.1\text{-}8)$$

while applying Eqs. (7.1-6) or (7.1-7) the consistent definition is

$$C_H = \frac{k \left.\frac{\partial T}{\partial y}\right|_w}{\rho_e u_e (h_e - h_{ew})} \qquad (7.1\text{-}9)$$

Unless $T^o = T_w$, these Stanton numbers will have different numerical values when Le $\neq$ 1. In addition C_H defined by Eq. (7.1-8) will depend on the choice of enthalpy datum state when Le $\neq$ 1.

4. For engineering analysis, Eqs. (7.1-4), (7.1-6) and (7.1-7) should be viewed as alternative correlation schemes, and the merits of

each should only be judged according to their success in correlating numerical or experimental data.

5. It is quite incorrect to use a Stanton number formed out of the numerator of Eq. (7.1-8) and the denominator of Eq. (7.1-9), or vice versa. Such an error was made by, for example, Meroney and Giedt [4].

6. Notice that the use of $\rho_e u_e C_M (z^*_{i,e} - z^*_{i,w})$ to describe transport of species i to the surface in Eq. (7.1-7) is only practical for an inert boundary layer. But in line with Comment No. 4 above, there is little to be gained from attempting to refine this representation if Eq. (7.1-7) satisfactorily correlates the data in question.

7. Blowing corrections in the form C_H/C_{HO} developed from experimental or numerical data for real ablation problems will differ according to whether Eq. (7.1-8) or Eq. (7.1-9) is used to define C_H. Care must be taken when obtaining correlations from the literature.

In ablation situations where the surface chemistry is dominated by a single oxidation reaction, the surface energy balance has been often written in the form

$$k \left.\frac{\partial T}{\partial y}\right|_u = \rho_e u_e C_H (h_e - h_w)_{\substack{\text{equilibrium} \\ \text{air}}} + n_{O_2,w} \Delta H_{r_{(O_2)}}^{T_w} ; \quad (\Delta H_r \text{ is negative}) \qquad (7.1\text{-}10)$$

where $n_{O_2,w}$ is calculated assuming equal diffusion coefficients for O and O_2. The implied model includes the assumptions that (i) the only reactions in the boundary layer are those involving air species, and (ii) the wall temperature is low enough for O recombination to be complete. The question again arises as to the appropriate definition of C_H. As before we should regard Eq. (7.1-10) as an engineering correlation scheme and evaluate its

suitability by examining the ability of the scheme to correlate numerical or experimental data.

7.2 THE EFFECT OF STANTON NUMBER DEFINITION ON BLOWING CORRECTIONS

For inert foreign gas injection into a laminar boundary layer numerical data is readily available for investigating the consequences of choice of Stanton number definition. We shall use here data of Mills and Wortman [5] for axi-symmetric stagnation point flow.

Case (i). H_2 into air injection, $T_w/T_e = 0.1$

$-f_w$	$(k\frac{\partial T}{\partial y} - \Sigma j_i h_i^{0°R})_w$	$k\frac{\partial T}{\partial y}\Big\|_w$	$K_{H_2,w}$	C_H/C_{HO} Eq. (7.1-8)	C_H/C_{HO} Eq. (7.1-9)
0.0	0.6509	0.6509	0.0	1.0	1.0
0.05	0.5773	0.6403	0.0459	0.950	0.984
0.1	0.4534	0.5699	0.1171	0.842	0.876
0.15	0.3302	0.4841	0.2231	0.754	0.744
0.2	0.2295	0.3969	0.3661	0.763	0.610
0.25	0.1597	0.3120	0.5492	1.265	0.479
0.3	0.1219	0.2398	0.7021	negative	0.368
0.35	0.0994	0.1761	0.8341	"	0.271
0.4	0.0812	0.1237	0.9195	"	0.190
0.45	0.0625	0.0831	0.9653	"	0.128
0.5	0.0444	0.0533	0.9866	"	0.082

In the Table and Figure f_w is the wall value of the dimensionless stream function and is directly proportional to the mass transfer rate $\dot{m}$ and B_h' $(= \dot{m}/\rho_e u_e C_{HO})$.

We see that C_H/C_{HO} given by Eq. (7.1-9) decreases monotonically with increasing $\dot{m}$. On the other hand, C_H/C_{HO}, given by Eq. (7.1-8) has a minimum at a moderate value of $\dot{m}$ and after going to infinity finally takes on negative values. This anomalous behavior is due to the high specific heat

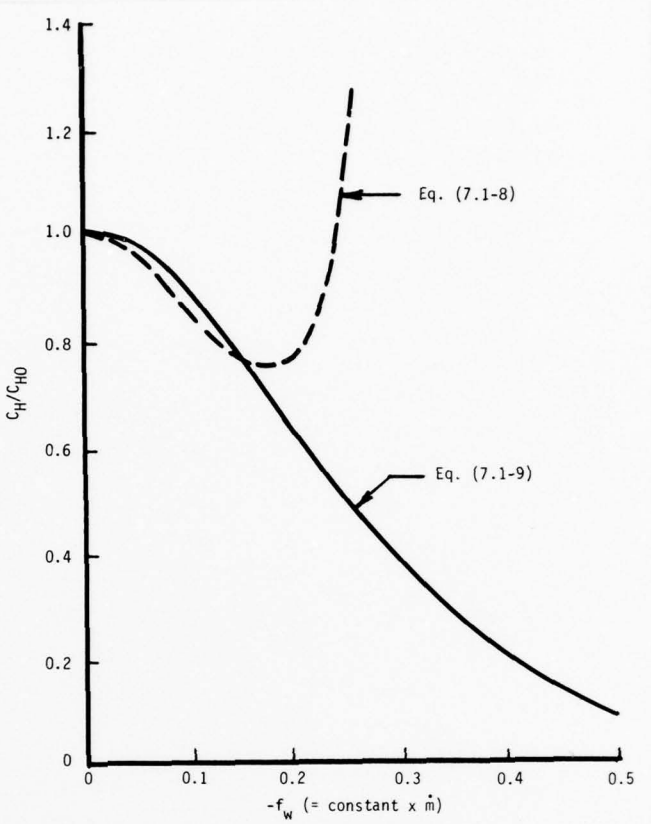

of the injectant hydrogen; at moderate blowing rates the wall enthalpy h_w becomes larger than the free stream enthalpy h_e, even though we have $T_w/T_e = 0.1$, a "cold wall" situation. The inflections in the C_H/C_{HO} curves near $\dot{m} = 0$ are real and may be explained as follows. Foreign gas injection gives values of C_H/C_{HO} different from those for air into air injection due to the effect of composition on mixture transport and thermodynamic properties, essentially through the ratio k/C_p. Now mixture values of C_p vary with mass fractions of the components whereas mixture values of k vary approximately with mole fractions. For a given mass injection rate ($-f_w$ or $\dot{m}$) the wall mole fraction of a light injectant is much larger than its mass fraction, until of course the mass fraction approaches unity. Both the k and C_p of H_2 are greater than the corresponding values for air ($k_{H_2}/k_{air} \cong 6$; $C_{pH_2}/C_{pair} \cong 14$). Thus at low injection rates the effect of composition is mainly through k, and values of C_H/C_{HO} are greater than those for air injection, while at high injection rates C_p dominates and C_H/C_{HO} is less than for air injection, i.e., more effective blockage.

Case (ii). C into air injection, $T_w/T_e = 0.1$ and 0.5

As a second example we consider injection of monatomic carbon into air, also at an axi-symmetric stagnation point. The table shows C_H/C_{HO} calculated

$-f_w$	C_H/C_{HO} for $T_w/T_e = 0.1$		C_H/C_{HO} for $T_w/T_e = 0.5$	
	Eq. (7.1-8)	Eq. (7.1-9)	Eq. (7.1-8)	Eq. (7.1-9)
0.0	1.0	1.0	1.0	1.0
0.1	0.782	0.792	0.748	0.772
0.2	0.596	0.595	0.607	0.576
0.3	0.437	0.434	0.615	0.411
0.4	0.304	0.294	0.530	0.275
0.5	0.192	0.182	0.444	0.172

according to Eqs. (7.1-8) and (7.1-9) for a "cold wall", $T_w/T_e = 0.1$, and for a somewhat hotter wall, $T_w/T_e = 0.5$. It can be seen that for $T_w/T_e = 0.1$ there is no significant difference between the values of C_H/C_{HO} calculated from the two formulae. However at $T_w/T_e = 0.5$ there is a marked difference, especially at higher blowing rates. In addition, C_H/C_{HO} calculated from Eq. (7.1-8) again does not exhibit a smooth monotonic behavior, and hence would be more difficult to correlate.

The preceding examples give some insight into the general problem, although clearly H_2 is an extreme case of a very light injectant gas. Also the enthalpy datum state is 0°R in these calculations and recall that C_H/C_{HO} given by Eq. (7.1-8) is dependent on the datum state. Different numerical values would be obtained if the JANAF datum state, 298.15°K, were used. If the datum state was chosen to be T_w then Eq. (7.1-8) would give a result identical to that given by Eq. (7.1-9), even for $Le \neq 1$.

We conclude that C_H/C_{HO} calculated from Eq. (7.1-9), i.e., based on the conduction component of the wall energy flux only, is better behaved and hence easier to correlate than C_H/C_{HO} calculated from Eq. (7.1-8), i.e., based on the total diffusive flux. It follows that for boundary layers which are inert, or for which gas phase reactions are of minor importance, the

surface energy balance in the form of Eqs. (7.1-6) or (7.1-7) is to be preferred since the correlations of C_H/C_{HO} are easier to develop. However, use of $C_M/C_H = Le^{2/3}$ in Eq. (7.1-6) is not satisfactory if variable property effects are important; rather C_{Mi} can be correlated as a function of injectant molecular weight. Such correlations will be developed in Chapter 8. On the other hand, when gas phase reactions are significant, the mass transfer Stanton numbers C_{Mi} can behave erratically and use of the surface energy balance in the form of Eq. (7.1-4) is the only feasible approach, and C_H/C_{HO} is more difficult to correlate. In addition, care must be taken to use the same enthalpy datum state for developing the correlations as will be used in the ablation calculations though, in a given problem, experience might show that errors introduced by use of inconsistent datum states are negligible.

7.3 THE SURFACE ENERGY BALANCE FOR TUNGSTEN OXIDATION

To illustrate the concepts introduced in Sections 7.1 and 7.2 we shall examine in detail the results of BLIMP calculations for tungsten oxidation at 6600°R, i.e., just below the melt temperature of W* (6625.8°R). The Aerotherm BLIMP code solves exactly the nonsimilar boundary layer equations for equilibrium chemically reacting laminar or turbulent flows over an ablating surface. The calculations were performed for a sphere-cone geometry with nose radius 0.725 inch and cone half angle of 11°. The stagnation pressure and total enthalpy are 147.06 atm and 7403.6 Btu/lb, respectively. Transition was taken to occur at a momentum thickness Reynolds number of 50. The boundary layer edge gases were assumed to expand isentropically. For the non-ablating flow with equal diffusion coefficients (nae) the chemical species considered were O_2, N_2, O, N and NO. For ablating flows with equal (edc) and unequal (udc) diffusion coefficients the additional species were W, WO, WO_2, WO_3, W_2O_6, W_3O_8, W_3O_9, W_4O_{12} and W*. The pressure distribution around the vehicle was obtained from the SAANT [6] code.

Case	B'_h	$\dot{m}$	$\rho_e u_e C_H$	h_w	q_{diff}	q_{tot}	$k \left.\frac{\partial T}{\partial y}\right\|_w$	$\dot{m} h_w$	$\Sigma j_i h_{i\,w}$	$\Sigma n_i h_{i\,w}$	$\Sigma n_i h_{i\,u}$	$\Sigma n_i \Delta h_{f,T_w}$
		$lb/ft^2 sec$	$lb/ft^2 sec$	Btu/lb	$Btu/ft^2 sec$	→	→	→	→	→	→	→
nae	0	0	1.505	2002	8129	8129	5247	0	-2882	-2882	0	-2882
edc	.8693	1.014	1.167	448.9	8116	7660	5726	456	-2390	-1934	279	-2193
udc	1.132	1.203	1.063	-115	7990	8128	5274	-138	-2716	-2854	331	-3185

Case	w-surface mole fraction x 10^2											
	O_2	N_2	O	NO	W	WO	WO_2	WO_3	W_2O_6	W_3O_8	W_3O_9	W_4O_{12}
nae	15.42	73.66	3.01	7.90	0	0	0	0	0	0	0	0
edc	.077	90.87	.213	.621	$.432 \times 10^{-4}$	.023	.388	.270	6.96	.409	.153	.0031
udc	.108	76.5	.251	.674	$.432 \times 10^{-4}$	.028	.540	.448	19.2	1.58	.700	.024

Case	ρ_w lb/ft^3	$\mu_w \times 10^6$ lb/ft sec	C_w	C_{pw} Btu/lb R	$k_w \times 10^6$ Btu/sec ft R	Pr_w	Sc_w	M_w
nae	.5373	58.60	1.60	.3155	26.79	.6901	.6974	28.53
edc	1.198	60.10	3.66	.1847	22.22	.4995	.7039	63.26
udc	2.431	63.75	7.87	.1315	17.08	.4910	.7338	212.86

a. Laminar boundary layer: $s = 3.8\times10^{-2}$ ft, $P_e = 91.10$ atm, $h_e = 6814.5$ Btu/lb, $M_e = 0.9712$. Detailed tabulations follow.

First let us reconstruct the surface energy balance in the form of Eq. (7.1-2), viz.,

$$k \left.\frac{\partial T}{\partial t}\right|_u = k \left.\frac{\partial T}{\partial y}\right|_w - \Sigma n_i h_i|_w + \dot{m}_g h_g + \dot{m}_c h_c$$

but $\dot{m}_c h_c = \Sigma n_i h_i|_u$ and $\dot{m}_g h_g = 0$,

thus $$k \left.\frac{\partial T}{\partial y}\right|_u = k \left.\frac{\partial T}{\partial y}\right|_w - \Sigma n_i h_i|_w + \Sigma n_i h_i|_u$$

$$k \left.\frac{\partial T}{\partial y}\right|_u = 5726 - (-1934) + 279$$

$$= 5726 + 2193 = 7939 \text{ Btu/ft}^2 \text{ sec}$$

the conduction into the heat shield. Note also that $-\Sigma n_i h_i|_w + \Sigma n_i h_i|_u = 2193 = -\Sigma n_i \Delta h_{f,T_w}$. Alternatively, let us use the form given by Eq. (7.1-4), noting that in the BLIMP code $\rho_e u_e C_H \equiv q_{diff}/(H_e - h_w)$.

$$k \left.\frac{\partial T}{\partial y}\right|_u = \rho_e u_e C_H (H_e - h_w) = \dot{m} h_w + \dot{m}_g h_g + \dot{m}_c h_c$$

for the edc case,

$$k \left.\frac{\partial T}{\partial y}\right|_u = 1.167(7403.6 - 448.9) = 456 + 279 = 7939 \text{ Btu/ft}^2 \text{ sec}$$

Also let us check the definition of q_{tot},

$$q_{tot} = k \left.\frac{\partial T}{\partial y}\right|_w + \Sigma j_i h_i|_w - \dot{m} h_w \left(= k \left.\frac{\partial T}{\partial y}\right|_w - \Sigma n_i h_i|_w\right)$$

For the edc case,

$$q_{tot} = 5726 + 2390 - 456 = 7660 \text{ Btu/ft}^2 \text{ sec}$$

Note that, in contradistinction to $k(\partial T/\partial y)|_w$, q_{tot} depends on choice of enthalpy base states.

Next let us compare the edc and nae results. We see that the Stanton number is reduced by 22%. Recall that $\rho_e u_e C_H \equiv q_{diff}/(H_e - h_w)$, and observe

that q_{diff} changes but slightly even though h_w decreases considerably; this is the expected blowing effect. However, the conductive heat flux $k(\partial T/\partial y)\big|_w$ actually increases by 9%, even though the thermal conductivity at the wall decreases by 17%. This anomally is possibly due to (i) variable property effects, or (ii) gas phase reactions, and cannot be simply explained. We also see that heat liberated at the wall $-\Sigma n_i \Delta h_{f,T_w}$ actually decreases from the nae case to the edc case, even though in the latter case we have exothermic heterogeneous tungsten oxidation. The reason for this behavior lies in the formation of NO at the wall in the nae case; this latter reaction is strongly exothermic and the mole fraction of NO at the wall is relatively large (7.9%). In the edc case the tungsten preferentially consumes the oxygen in a less strong exothermic reaction and the mole fraction of NO at the wall decreases to 0.62%.

Next let us compare the udc results with the edc results. First observe that the mole fraction of W_2O_6 at the wall increases from 7% to 19% when we account for multicomponent diffusion; since the heavy W_2O_6 molecule has a low effective binary diffusion coefficient, a higher concentration at the wall is required for the W_2O_6 to diffuse away as fast as it is formed. The rate of formation of W_2O_6 is of course limited by the rate at which O_2, O and NO can diffuse to the wall, since these species have higher than the average effective binary diffusion coefficients, the rate of formation of tungsten oxides is 19% higher for the udc case. The blowing associated with the higher mass lass rate reduces the Stanton number to 9% less than the edc case. However care must be taken to account for variable properties in interpreting these trends since we wee that C_w more than doubles as we go from edc to udc.

Finally let us compare the various values calculated for $k(\partial T/\partial y)\big|_u$ the conduction into the heat shield. For the nae case this is simply

q_{diff} = 8.29 Btu/ft^2 sec; for the edc case we have already calculated a value of 7939 Btu/ft^2 sec. For the udc case,

$$k \left.\frac{\partial T}{\partial y}\right|_u = k \left.\frac{\partial T}{\partial y}\right|_w - \Sigma n_i h_i|_w + \Sigma n_i h_i|_u$$

$$= 5274 - (-2854) + 331$$

$$= 8459 \text{ Btu/ft}^2 \text{ sec}$$

i.e., an increase of 7% over the edc case and 4% over the nae case. This last comparison of heat shield conduction values is the most significant for engineering purposes.

7.4 UNEQUAL DIFFUSION COEFFICIENT EFFECTS FOR GRAPHITE ABLATION

As another illustration of the concepts introduced in §7.1 and §7.2, and for the purpose of investigating some unequal diffusion coefficient effects, we will examine in detail some calculations of graphite ablation. The K-BLIMP code [7] was used and results obtained for the following conditions: total enthalpy = 7000 Btu/lb, wall temperature = 8450°R, pressure = 140 atm, nose radius = 0.5 inch. Four runs were made: a) air, equal diffusion coefficients, (b) air, unequal diffusion coefficients, c) carbon ablation with equal diffusion coefficients, and d) carbon ablation with unequal diffusion coefficients. The results of the stagnation point are summarized in the Tables.

Effect of unequal diffusion coefficients for the air boundary layers.

First let us check the Stanton number values:

edc: $$\rho_e u_e C_H = \frac{k \left.\frac{\partial T}{\partial y}\right|_w - \Sigma j_i h_i|_w}{H_e - h_w} = \frac{4980-(-4740)}{7000-3010} = 2.44$$

udc: $$\rho_e u_e C_H = \frac{k \left.\frac{\partial T}{\partial y}\right|_w - \Sigma j_i h_i|_w}{H_e - h_w} = \frac{4670-(-4740)}{7000-3050} = 2.62$$

which check. The heat flux into the heat shield for the edc case is

Case	$k(\partial T/\partial y)$ Btu/ft^{2}s	$\Sigma j_i h_i$ →	$\Sigma n_i h_i$ →	$\dot{m}h$ →	$\dot{m}h_{C*}$ →	$\rho_e u_e C_H$ lb/ft^{2}s	h Btu/lb	ρ lb/ft^3	$\mu x10^5$ lb/ft	C	C_p Btu/lb F	$kx10^5$ Btu/ft F	Pr	M
air (edc)	4980	-4740	4740	0	0	2.44	3010	0.616	6.91	1.42	0.320	3.19	0.692	27.2
air (udc)	4670	-5670	5670	0	0	2.60	3050	0.615	6.92	1.42	0.319	3.19	0.693	27.1
edc	6190	1290	5343	4053	3431	1.89	4410	0.658	7.01	1.54	0.345	3.44	0.704	29.0
udc	6460	250	4376	4126	3431	2.48	4490	6.59	7.02	1.55	0.346	3.44	0.704	29.1

Case	N_2	O_2	O	NO	C	C_2	C_3	CO	CN	C_2N_2
air (edc)	67.9	9.1	11.9	11.0	-	-	-	-	-	-
air (udc)	65.3	10.4	12.7	11.5	-	-	-	-	-	-
edc	44.3	-	-	-	1.1	2.2	9.4	29.3	10.5	3.0
udc	42.7	-	-	-	1.1	2.3	10.1	30.1	10.5	3.0

4980-(-4760) = 9720 Btu/ft^2 s, and for udc it is 7.4% higher. This result is to be compared with the conclusions reached by Bartlett and Grose [8], who performed calculations with an earlier version of the BLIMP code for P = 0.1-100 atm, H_e = 2000-13,000 Btu/lb, T_w = 1000-8000°R, and R_N = 1 and 0.5 inch. They found that $\rho_e u_e C_H$ is increased by 3 to 4 percent except at low enthalpies and low pressures where the effect is less. Thus it appears that K-BLIMP predicts more marked udc effects than those reported earlier.

Effect of unequal diffusion coefficients for graphite ablation.

The mass loss rates may be calculated from the data in the Tables. For edc $\dot{m}$ = 0.919 lb/ft^2 s and for udc it is identical. Thus unequal diffusion coefficients have negligible effect on the rate at which the carbon containing species diffuse from the surface.

The heat flux into the heat shield is given by

$$k \left.\frac{\partial T}{\partial y}\right|_u = \rho_e u_e C_H (H_e - h_w) - \dot{m} h_w + \dot{m} h_{C^*}$$

which is evaluated for edc and udc as follows:

edc: $$k \left.\frac{\partial T}{\partial y}\right|_u = 1.89(7000-4410) - 4053 + 3431 = 4273 \text{ Btu/ft}^2 \text{ s}$$

udc: $$k \left.\frac{\partial T}{\partial y}\right|_u = 2.48(7000-4490) - 4126 + 3431 = 5530 \text{ Btu/ft}^2 \text{ s}$$

so we see that the heat flux into the heat shield for udc is 29% higher than for edc. Looking at the tables we see that this increase is mainly due to the decrease in $\Sigma j_i h_i|_w$ from 1290 for edc to 250 for udc.

Comparison with Scala and Gilbert [9]

It is of interest to compare the K-BLIMP results with the correlations based on the Scala and Gilbert [9] multicomponent diffusion analysis. First the mass fraction of element carbon at the w-surface is given by

$$\tilde{K}_{C,w} = 0.15 + 2.4\text{x}10^{6}(P_e \text{ atm})^{-.67}\exp[11.1 \text{ x } \frac{10^4}{T_w(^\circ R)}]$$

$$= 0.15 \text{ x } 2.4\text{x}10^{6}(140)^{-.67}\exp[11.1 \text{ x } \frac{10^4}{8450}]$$

$$= 0.3228 \qquad \text{c.f. } \textit{0.342} \text{ for K-BLIMP}$$

Next we calculate the heat flux into the heat shield for the diffusion controlled regime,

$$k \left.\frac{\partial T}{\partial y}\right|_u^D (R_N/P_e)^{1/2} = 33.3 + 0.0333[H_e - h_{w,air}]$$

$$k \left.\frac{\partial T}{\partial y}\right|_u^D (0.5/12\text{x}140)^{1/2} = 33.3 + 0.0333[7000-3050]$$

hence $$k \left.\frac{\partial T}{\partial y}\right|_u^D = (165)(57.96) = 9563.4$$

The mass loss in the sublimation regime is given by

$$\dot{m} = \tilde{K}_{C,w}(P_e/R_N)^{1/2}(0.04235)$$

$$= (0.3228)(57.96)(0.04235)$$

$$= 0.839 \text{ lb/ft}^2 \text{ s} \qquad \text{c.f. } \textit{0.919} \text{ for K-BLIMP}$$

Finally the heat flux into the heat shield is given by

$$k \left.\frac{\partial T}{\partial y}\right|_u = k \left.\frac{\partial T}{\partial y}\right|_u^D \{1-s(\tilde{K}_{C,w}-0.15)\}$$

$$s = a + bH_e + cH_e^2 + dH_e^3 + eH_e^4 + fH_e^5$$

$$a = 1.868\text{x}10 \qquad d = 1.146\text{x}10^{-12}$$

$$b = -4.418\text{x}10^{-3} \qquad e = -2.057\text{x}10^{-15}$$

$$c = 3.945\text{x}10^{-7} \qquad f = 8.333\text{x}10^{-20}$$

For H_e = 7000 Btu/lb, s = 3.93, thus

$$k \left.\frac{\partial T}{\partial y}\right|_u = 9563.4\{1-3.93(0.3228-0.015)\}$$

$$= (9563.4)(0.321)$$

$$= 3066 \text{ Btu/ft}^2 \text{ s}$$

This value is only 55% of the BLIMP udc result. The discrepancy must be attributed to differences in the thermochemical model, thermodynamic and transport properties, and the treatment of multicomponent diffusion.

Comparison with Bartlett and Grose [8]

In the K-BLIMP calculations described above the udc case was calculated for steady state ablation and the edc case subsequently calculated for the same wall temperature obtained in the udc case. In this manner udc effects correction factors for use in coupled flow field-in depth conduction codes are correctly obtained. Bartlett and Grose [8] however calculated both the udc and edc cases assuming steady state ablation so that the wall temperatures differed, being typically 50-75°R higher for udc. The ablation rates were found to typically increase 2 to 8 percent, while the diffusive heat flux increased 3 to 10 percent, with the largest effect occurring at high pressures and moderate to high enthalpies.

A comparison with the Bartlett and Grose results was made by making a set of BLIMP-K runs for identical parameter values and steady state ablation. The total enthalpy was 13,000 Btu/lb and the nose radius 1 inch. A comparison of the results is shown in the Table which follows. Looking first at the mass loss rate we see that both Bartlett and K-BLIMP predict an increase in $\dot{m}$ due to udc, though Bartlett predicts a 2-4% increase and K-BLIMP a 5-6% increase. However the Bartlett $\dot{m}$ values are consistently about 12-15% higher than K-BLIMP.

The comparison of heat transfer conductance predictions is more complex. K-BLIMP predicts increases in $\rho_e u_e C_H$ for udc of 7 to 20% while Bartlett predicts decreases from $\sim$0 to 13%. For edc the K-BLIMP values are consistently about 13% less than those of Bartlett, but for udc, as a consequence of the above mentioned discrepancy, K-BLIMP values range from 9% lower than Bartlett at 0.01 atm to 21% higher at 30 atm.

P	edc		udc	
atm	Bartlett	K-BLIMP	Bartlett	K-BLIMP
	Mass loss rate m $lb/ft^2 s$			
.01	2.49-3	2.22-3	2.55-3	2.33-3
.1	8.81-3	7.69-3	9.33-3	8.19-3
1	5.18-2	4.38-2	5.48-2	4.71-2
10	2.33-1	1.99-1	2.42-2	2.12-1
30	4.43-1	3.76-1	4.56-1	3.99-1
100	8.71-1	7.39-1	8.90-1	7.70-1
	Heat transfer conductance $\rho_e u_e C_H$ $lb/ft^2 s$			
.01	1.41-2	1.22-2	1.43-2	1.30-2
.1	4.44-2	3.85-2	4.44-2	4.11-2
1	1.23-1	1.10-1	1.13-1	1.24-1
10	3.66-1	3.18-1	3.22-1	3.80-1
30	6.19-1	5.39-1	5.40-1	6.54-1
100	1.12	9.72-1	9.62-1	1.19
	Diffusive heat flux $k(\partial T/\partial y)\|_w - \Sigma j_i h_i\|_w$			
.01	177	154	187	163
.1	524	460	554	486
1	1211	1080	1290	1160
10	2882	2560	3111	2820
30	4582	4050	4972	4500
100	7859	6880	8545	7700

The source of the discrepancies discussed above is thought to be due to differences in thermophysical properties since there is no good reason for questioning the numerical accuracy of the calculations. Unfortunately nowhere in the Bartlett and Grose report do they document their values or sources of thermophysical property data; based on the date of the report (May 1968) it can be presumed that the original version of BLIMP was used. On the other hand K-BLIMP has thermophysical properties identical to those of a later version, BLIMP-C which incorporated a number of improvements in the methods used to calculate properties. There are also improvements in the JANAF data and data curve fits incorporated in currently used thermodynamic property tables.

7.5 THE GENERAL SURFACE ENERGY BALANCE

To complete §7 we need to extend the discussion of the surface energy balance to include other than stagnation regions, thermal radiation, and mechanical surface removal.

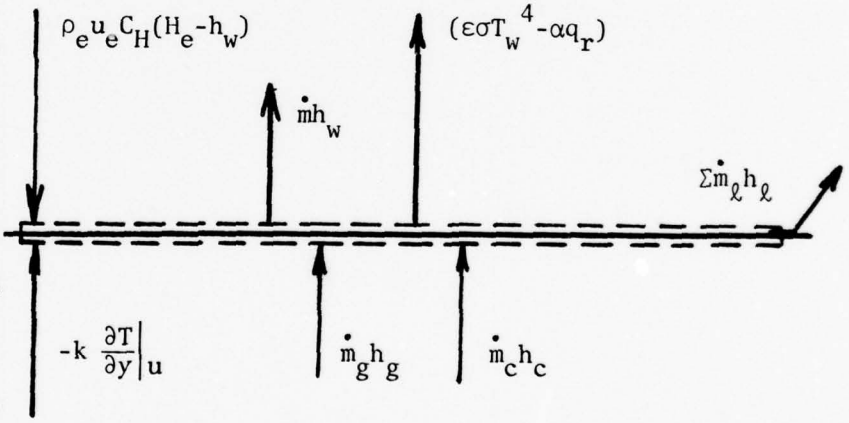

(i) Recovery enthalpy

The recovery enthalpy concept was introduced in §6.5: the textbook approach to calculate heat transfer in high speed flows is to replace the static enthalpy h_e by the recovery enthalpy h_r in the driving potential for convective heat transfer, to write

$$k\left.\frac{\partial T}{\partial y}\right|_w - \Sigma j_i h_i\Big|_w = \rho_e u_e C_H(h_r-h_w) \qquad (7.5\text{-}1)$$

Although the recovery factor is relatively easily correlated for air

boundary layers, even when thermophysical properties vary appreciably across the boundary layer, e.g., [10], it is a function of pressure gradient, and more important is a strong function of blowing rate (see §6.5 and also [10]). With foreign gas injection the adiabatic wall temperature, and hence the recovery enthalpy, is significantly affected by diffusional conduction: since by definition $q_w = 0$ for an adiabatic wall, this usually second-order contribution to q_w becomes important. Also foreign gas injection is usually associated with ablation and transpiration cooling and associated large wall heat fluxes. Thus there have been very few reliable calculations of recovery enthalpy with foreign gas injection; also pertinent experimental data is almost non-existent.

In light of the above there have been few attempts to develop engineering correlations of heat transfer data for high-speed boundary layers with foreign gas injection using the recovery enthalpy concept. Rather, common practice [11, 12] has been to develop correlations of C_H based on the edge gas total enthalpy H_e, as

$$k \left.\frac{\partial T}{\partial y}\right|_w - \Sigma j_i h_i \Big|_w = \rho_e u_e C_H (H_e - h_w) \qquad (7.5\text{-}2)$$

In so doing the discrepancy between H_e and h_r is absorbed in the resulting expression for C_H.

(ii) Thermal radiation

Thermal radiation is usually included in the surface energy balance on a gray body basis, with an appropriate emissivity and absorptivity. Since a finite depth of material is required for emission and absorption, these processes take place *below* the u-surface, and the radiative fluxes are unchanged between the w- and u- surfaces. Rigorously, we should now define a new surface, say a m-surface, sufficiently below the u-surface such that all emission and absorption takes place between the u- and

m-surfaces: the distance between these two surfaces depends on the transmissivity of the wall material. Then the surface energy balance would result from applying the first law of thermodynamics to the control volume located between the w- and m-surfaces. However, in most practical circumstances, the wall material is sufficiently opaque for the u- and m-surfaces to essentially coincide, and thus we can simply retain the u-suffix on $\partial T/\partial y$ and the implied u-suffix on h_g and h_c, as shown in the Figure. The net radiation flux across the w-surface is

$$q_{r,net} = \varepsilon\sigma T_w^4 - \alpha\, q_r \qquad (7.5\text{-}3)$$

and will be included in the surface energy balance.

(iii) Mechanical removal of material

Material may be mechanically removed from an ablating surface either as a melt layer swept away by aerodynamic forces, as ejecta due to erosion by dust or ice particles, or by other mechanical failure modes. Such material leaves the wall at the u-surface state but does not cross the w-surface: as in §5.3 we depict mechanically removed material as leaving through the *side* of the control volume located between the w- and u-surfaces. The rate at which enthalpy leaves the control volume in this manner is thus $\Sigma\dot{m}_\ell h_\ell$, where the sum suggests that more than one distinct component of the surface could be removed mechanically. Often h_ℓ will be written h_ℓ^* to emphasize that mechanically removed material is always a condensed phase.

Eq. (7.1-4) can therefore be rewritten in the more general form as

$$k \left.\frac{\partial T}{\partial y}\right|_u = \rho_e u_e C_H (H_e - h_w) - \dot{m} h_w + \dot{m}_g h_g + \dot{m}_c h_c - \Sigma\dot{m}_\ell h_\ell - (\varepsilon\sigma T_w^4 - \alpha\, q_r) \qquad (7.5\text{-}4)$$

REFERENCES FOR CHAPTER 7

1. Aerotherm Staff, "Users' Manual: boundary layer integral matrix procedure, Version C (BLIMP C)" Aerotherm Report UM-70-20, Aerotherm Corporation, Mountain View, CA, June 1970.

2. R. A. Rindal and C. A. Powars, "Effects of carbon vapor thermochemistry uncertainties on R/V ablation predictions" AIAA Paper No. 71-414, 6th Thermophysics Conference, Tullahoma, April 26-28, 1971.

3. C. A. Powars and R. M. Kendall, "Users' Manual: Aerotherm Chemical Equilibrium (ACE) computer program" Rept. UM-69-70, Aerotherm Corporation, Mountain View, CA (1969).

4. R. Meroney and W. H. Giedt, "The effect of mass injection on heat transfer from a partially dissociated gas stream" J. Heat Transfer, 89, 205-218 (1967).

5. A. F. Mills and A. Wortman, "Two-dimensional stagnation point flows of binary mixtures" Int. J. Heat Mass Transfer, 15, 969-987 (1972).

6. Aerotherm Staff, "Passive nosetip technology (PANT) program. Users' Manual, steady-state analysis of ablating nosetips (SAANT), Vol. I: program description and sample problems" Aerotherm Report UM-73-38, Acurex Corporation, Mountain View, CA, February 1973.

7. H. Tong, A. C. Buckingham and H. L. Morse, "Nonequilibrium chemistry boundary layer integral matrix procedure" Aerotherm Rept. UM-73-67, Aerotherm Division/Acurex Corporation, Mountain View, CA, July 1973.

8. E. P. Bartlett and R. D. Grose, "The multicomponent laminar boundary layer over graphite sphere-cones" Sandia Contractor Report SC-CR-68-3665, May 1968.

9. S. M. Scala and L. M. Gilbert,"Sublimation of graphite at hypersonic speeds" AIAA Journal, 3, 1635-1644 (1965).

10. A. Wortman, A. F. Mills and G. Soo-Hoo, "The effect of mass transfer on recovery factors in laminar boundary layer flows" Int. J. Heat Mass Transfer, 15, 443-456 (1972).

11. A. D. Andersen, "BLIMP calculations of tungsten ablation" Memorandum C/N 7103.107 Aerotherm/Acurex Corporation, September 1974.

12. A. T. Wassel and A. F. Mills, "Tungsten ablation: effects of equal and unequal diffusion coefficients" SAI Inter-office Memorandum LAI-750-178, El Segundo, CA, January 1975.

CHAPTER 8

LAMINAR BOUNDARY LAYER ANALYSIS

8.1 THE CONSTANT PROPERTY BOUNDARY LAYER ON A FLAT PLATE

Laminar boundary layer convective heat and mass transfer is conveniently introduced by analyzing the constant property boundary layer on a flat plate. Attention will be restricted to the low velocity flow of an inert binary mixture. Thermal, pressure and forced diffusion as well as diffusional conduction will be ignored. The fluid properties, i.e., density, specific heat, viscosity, thermal conductivity and diffusion coefficient will be assumed constant: as a consequence there can be no energy transport by interdiffusion. The particular physical problem to be considered is the same as that of §4.1, namely evaporation or sublimation. The porous plate is taken to be isothermal, and liquid 1 is supplied at a rate just sufficient to maintain a wet surface. A mixture of gas and vapor flows over the the plate; gas 2 is assumed to be insoluble in liquid 1. With these restrictions the conservation equations in boundary layer form reduce to:

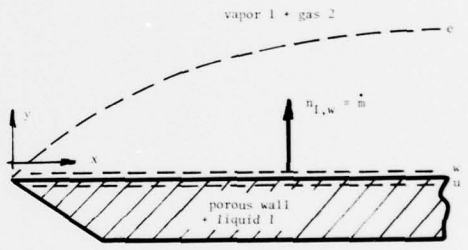

mass conservation
$$\frac{\partial u}{\partial x} + \frac{\partial v}{\partial y} = 0 \tag{8.1-1}$$

momentum conservation
$$u \frac{\partial u}{\partial x} + v \frac{\partial u}{\partial y} = \nu \frac{\partial^2 u}{\partial y^2} \tag{8.1-2}$$

energy conservation
$$u \frac{\partial T}{\partial x} + v \frac{\partial T}{\partial y} = \alpha \frac{\partial^2 T}{\partial y^2} \tag{8.1-3}$$

species conservation
$$u \frac{\partial K_1}{\partial x} + v \frac{\partial K_1}{\partial y} = \mathcal{D}_{12} \frac{\partial^2 K_1}{\partial y^2} \tag{8.1-4}$$

The boundary conditions are:

At $y = \infty$ or $x \leq 0$: $u = u_e$; $T = T_e$; $K_1 = K_{1,e}$ (8.1-5)

At $y = 0$: $u = 0$; $T = T_w$; $K_1 = K_{1,w}$; $n_{2,w} = 0$ (8.1-6)

where $K_{1w} = K_{1,w}(T_w,P)$ from vapor pressure data, and $n_{2,w} = 0$ follows from the requirement that gas 2 is insoluble in the liquid.

Eqs. (8.1-1 through 4) are partial differential equations; Eq. (8.1-2) is nonlinear, and the boundary condition $n_{2,w} = 0$ leads to a nonlinear coupling of Eq. (8.1-2) to Eqs. (8.1-3 and 4). No direct analytical solution is possible. One method of attack is to attempt to find a transformation which will reduce the equations to ordinary differential equations. An appropriate transformation is suggested by the scaling of the Navier-Stokes equations which lead to the boundary layer equations under consideration. Recall that the boundary layer thickness δ at location x is of order

$$\delta = xRe_x^{-\frac{1}{2}} = (\nu x/u_e)^{\frac{1}{2}} \tag{8.1-7}$$

and variations in the y direction scale according to y/δ, where, of course, $\delta = \delta(x)$. We suspect that in some situations the dependent variables such as u, T and K_1 suitably normalized if necessary, are functions of y/δ only, irrespective of x location. Thus the coordinate transformation $x,y \rightarrow s,\eta$ will be made, where $s = x$ and $\eta = y(u_e/2\nu x)^{\frac{1}{2}}$: the factor of $2^{\frac{1}{2}}$ has been introduced for future convenience. The mass conservation equation will be automatically satisfied if we use a stream function:

$$\text{let } u = \frac{\partial \psi}{\partial y} \quad v = -\frac{\partial \psi}{\partial x}$$

$$\text{then } \frac{\partial u}{\partial x} + \frac{\partial v}{\partial y} = \frac{\partial^2 \psi}{\partial y \partial x} - \frac{\partial^2 \psi}{\partial x \partial y} = 0$$

The required differential operators are

$$\frac{\partial}{\partial x} = \frac{\partial}{\partial s}\Big|_\eta \frac{\partial s}{\partial x} + \frac{\partial}{\partial \eta}\Big|_s \frac{\partial \eta}{\partial x} = \frac{\partial}{\partial x}\Big|_\eta - \frac{\eta}{2x}\frac{\partial}{\partial \eta}\Big|_x$$

$$\frac{\partial}{\partial y} = \frac{\partial}{\partial s}\Big|_\eta \frac{\partial s}{\partial y} + \frac{\partial}{\partial \eta}\Big|_s \frac{\partial \eta}{\partial y} = 0 + \left(\frac{u_e}{2\nu x}\right)^{\frac{1}{2}} \frac{\partial}{\partial \eta}\Big|_x$$

Now let $\psi = g(x)f(\eta)$

$$u = \frac{\partial u}{\partial y} = g(x)\left(\frac{u_e}{2\nu x}\right)^{\frac{1}{2}} f'(\eta)$$

Then if $g(x)$ is set equal to $(2u_e\nu x)^{\frac{1}{2}}$, $\frac{u}{u_e} = f'(\eta)$ (8.1-8)

$$\psi = (2u_e\nu x)^{\frac{1}{2}} f(\eta) \quad (8.1\text{-}9)$$

Also $\frac{\partial u}{\partial y} = u_e\left(\frac{u_e}{2\nu x}\right)^{\frac{1}{2}} f''$; $\frac{\partial u}{\partial x} = -u_e \frac{\eta}{2x} f''$

$$\frac{\partial^2 u}{\partial y^2} = u_e\left(\frac{u_e}{2\nu x}\right) f''' \quad ; \quad v = \left(\frac{u_e \nu}{2x}\right)^{\frac{1}{2}} (\eta f' - f)$$

Substituting in Eq. (8.1-2) and rearranging gives

$$f''' + ff'' = 0 \quad (8.1\text{-}10)$$

If the normalized variables $\theta = (T-T_e)/(T_w-T_e)$ and $\phi = (K_1-K_{1,e})/(K_{1,w}-K_{1,e})$ are introduced, Eqs. (8.1-3 and 4) similarly transform into

$$\theta'' + Pr\, f\, \theta' = 0 \quad (8.1\text{-}11)$$

$$\phi'' + Sc\, f\, \phi' = 0 \quad (8.1\text{-}12)$$

where $Pr = \nu/\alpha$ is the Prandtl number, and $Sc = \nu/\mathcal{D}_{12}$ is the Schmidt number. Notice that there is no x-dependence in Eqs. (8.1-11 and 12), a consequence of T_e, T_s. $K_{1,e}$, and $K_{1,w}$ being independent of x. The boundary conditions become:

As $\eta \to \infty$; $f' = 1$; $\theta = 0$; $\phi = 0$ (8.1-13)

At $\eta = 0$; $f' = 0$; $\theta = 1$; $\phi = 1$; $f(0) = \frac{K_{1,e}-K_{1,w}}{K_{1,w}-1} \frac{\phi'(0)}{Sc}$ (8.1-14)

The last condition is derived as follows:

$$n_{1,w} = K_1 \rho v_w - \rho \mathcal{D}_{12} \left.\frac{\partial K_1}{\partial y}\right|_w$$

but $n_{2,w} = 0$, thus $\rho v_w = n_w = n_{1,w} + n_{2,w} = n_{1,w}$, hence

$$v_w = \frac{-\mathcal{D}_{12}}{1-K_{1,w}} \left.\frac{\partial K_1}{\partial y}\right|_w \quad (8.1\text{-}15)$$

Equation (8.1-15) expresses the coupling between the momentum and species equations, and shows how the net mass transfer across the w-surface gives

rise to a blowing effect on the boundary layer. In terms of the transformed variables:

$$\frac{\partial K_1}{\partial y} = (K_{1,w}-K_{1,e})\ \frac{\partial \phi}{\partial y} = (K_{1,w}-K_{1,e})\left(\frac{u_e}{2\nu x}\right)^{\frac{1}{2}}\phi' \quad \text{hence}$$

$$v_w = -\left(\frac{u_e \nu}{2x}\right)^{\frac{1}{2}} f(0)$$

thus $$-\left(\frac{u_e \nu}{2x}\right)^{\frac{1}{2}} f(0) = -\frac{\mathcal{D}_{12}}{1-K_{1,w}}\,(K_{1,w}-K_{1,e})\left(\frac{u_e}{2\nu x}\right)^{\frac{1}{2}}\phi'(0)$$

or

$$f(0) = \frac{K_{1,e}-K_{1,w}}{K_{1,w}-1}\,\frac{\phi'(0)}{Sc} \tag{8.1-16}$$

In the notation of Chapter 4, $f(0) = \frac{B'}{Sc}\,\phi'(0)$ where B' is the mass transfer driving force, and is a constant as consequence of $K_{1,e}$ and $K_{1,w}$ being independent of x.

We see that the mathematical problem has been reduced to the solution of a set of ordinary differential equations containing two parameters, Pr and Sc, with a third parameter B' in the boundary conditions. For prescribed values of Pr, Sc and B' the equations must be integrated numerically. As an end result we are interested in rates of mass and heat transfer, and the wall shear stress:

$$\rho u_e C_M = \frac{j_{1,w}}{K_{1,w}-K_{1,e}} = -\frac{-\rho\mathcal{D}_{12}\left.\frac{\partial K_1}{\partial y}\right|_w}{K_{1,w}-K_{1,e}} = -\rho\mathcal{D}_{12}\phi'(0)\left(\frac{u_e}{2\nu x}\right)^{\frac{1}{2}}$$

Rearranging, $$C_M = \frac{-\phi'(0)}{\sqrt{2}\ Re_x^{\frac{1}{2}} Sc} \tag{8.1-17}$$

$$\rho u_e C_H = \frac{-k\left.\frac{\partial T}{\partial y}\right|_w}{C_p(T_w-T_e)} = -\frac{k}{C_p}\,\theta'(0)\left(\frac{u_e}{2\nu x}\right)^{\frac{1}{2}}$$

Rearranging, $C_H = \dfrac{-\theta'(0)}{\sqrt{2}\ Re_x^{\frac{1}{2}}\ Pr}$ (8.1-18)

$$(\frac{1}{2}\rho u_e^2)C_F = \tau_w = \mu \left.\frac{\partial u}{\partial y}\right|_0 = \mu u_e f''(0)\,(\frac{u_e}{2\nu x})^{\frac{1}{2}}$$

Rearranging

$$C_F/2 = \frac{f''(0)}{\sqrt{2}\ Re_x^{\frac{1}{2}}} \qquad (8.1\text{-}19)$$

Thus we require C_M, C_H and C_F as functions of B', Sc and Pr.

To effect the numerical solution of the ordinary differential equations it is convenient to uncouple the set and consider first the solution of Eq. (8.1-10) for various values of f(0). For f(0) = 0 we have of course the classical Blasius problem. Solutions for a range of values of f(0) were first obtained in 1953 by Emmons and Leigh [1] and are commonly referred to as solutions of the laminar boundary layer equations with blowing or suction. A number of numerical methods have subsequently been used for this problem: since the boundary conditions are split, integration using a Runge-Kutta technique requires guessing f'(0) and adjusting the guess until the condition f' = 1 as $\eta \to \infty$ is attained. Such "shooting" methods are simple and quite adequate for this problem: however, for more complex boundary layers, involving pressure gradients and property variations, shooting methods are troublesome, and are not recommended. Superior methods include finite differencing of the quasi-linearized equation [2],or formal integration followed by iteration [3]. The last mentioned method is particularly simple: rearranging Eq. (8.1-10),

$$\frac{f'''}{f''} = -f$$

integrating, $$f'' = C_1 e^{-\int_0^\eta f d\eta}$$

integrating, $$f' = C_1 \int_0^\eta e^{-\int_0^\eta f d\eta}\, d\eta + C_2$$

at $\eta = 0$, $f' = 0$, thus $C_2 = 0$

as $\eta \to \infty$, $f' \to 1$, thus $1 = C_1 \int_0^\infty e^{-\int_0^\eta f d\eta} d\eta$

$$f' = \frac{\int_0^\eta e^{-\int_0^\eta f d\eta} d\eta}{\int_0^\infty e^{-\int_0^\eta f d\eta} d\eta} \tag{8.1-20}$$

integrating,

$$f = \frac{\int_0^\eta \int_0^\eta e^{-\int_0^\eta f d\eta} d\eta\, d\eta}{\int_0^\infty e^{-\int_0^\eta f d\eta} d\eta} + f(0) \tag{8.1-21}$$

and

$$f'' = \frac{e^{-\int_0^\eta f d\eta}}{\int_0^\infty e^{-\int_0^\eta f d\eta} d\eta} \tag{8.1-22}$$

The calculation procedure can be set up as follows:

1. Choose a value of η_{max}, less than ∞ (say 10), a number of integration steps (say 100), and hence a step size $\Delta\eta = 0.1$.
2. Specify f(0).
3. Choose an initial guess, e.g., $f'' = 0$, $f' = 1$ and $f = \eta$.
4. Evaluate $e^{-\int_0^\eta f d\eta}$ at each step from $\eta = 0$ to $\eta = \eta_{max}$.
5. Evaluate $\int_0^\infty e^{-\int_0^\eta f d\eta} d\eta$ using the trapezoidal rule.
6. Evaluate f'' at each step using Eq. (8.1-22).
7. Evaluate f' at each step using Eq. (8.1-20).
8. Evaluate f at each step using Eq. (8.1-21).

9. Use the new values of f in (4) and repeat (4) through (9) until convergence is attained.

For a specified value of f(0) and the corresponding solution of the momentum equation, the solutions of the energy and species equations are found by direct integration. For example Eq. (8.1-11) becomes

$$\frac{\theta''}{\theta} = -Pr\ f$$

integrating,

$$\theta' = C_1 e^{-Pr_0 \int^{\eta} f d\eta}$$

integrating,

$$\theta = C_1 \int_0^{\eta} e^{-Pr_0 \int^{\eta} f d\eta} d\eta + C_2$$

at $\eta = 0$, $\theta = 1$, thus $C_2 = 1$

as $\eta \to \infty$, $\theta \to 0$, thus $0 = C_1 \int_0^{\infty} e^{-Pr_0 \int^{\eta} f d\eta} d\eta + 1$

$$\text{then } 1 - \theta = \frac{\int_0^{\eta} e^{-Pr_0 \int^{\eta} f d\eta} d\eta}{\int_0^{\infty} e^{-Pr_0 \int^{\eta} f d\eta} d\eta} \qquad (8.1\text{-}23)$$

or using Eq. (8.1-10), $f = -f'''/f''$, then

$$1 - \theta = \frac{\int_0^{\eta} (f'')^{Pr} d\eta}{\int_0^{\infty} (f'')^{Pr} d\eta} \qquad (8.1\text{-}24)$$

Similarly,

$$1 - \phi = \frac{\int_0^{\eta} (f'')^{Sc} d\eta}{\int_0^{\infty} (f'')^{Sc} d\eta} \qquad (8.1\text{-}25)$$

If Pr = Sc = 1 then $f' = \theta = \phi$. That is, for a given value of f(0) the shapes of the velocity, temperature and concentration profiles are identical. Typical

temperature (or concentration) profiles are shown in the Figure: there is a set of profiles for each value of Prandtl or Schmidt number. The thickness of the thermal/diffusion boundary layer decreases with increasing Pr/Sc. Since for gas mixtures both Pr and Sc are of order unity, a value of η_{max} suitable for the accurate solution of the momentum equation is also satisfactory for solution of the energy and species equations.

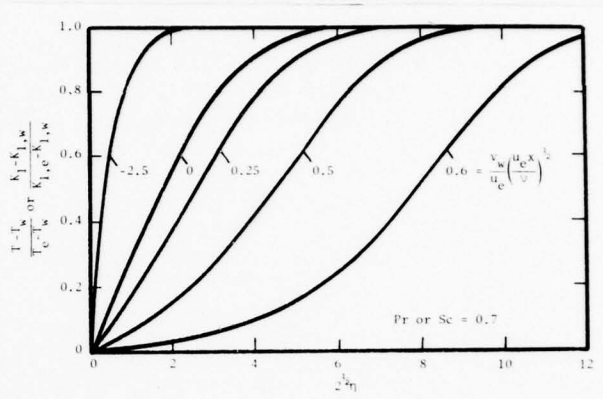

The numerical solution therefore gives

$f''(0)$ = function of $f(0)$; ($\simeq .4696$ for $f(0) = 0$)

$\theta'(0)$ = function of $f(0)$, Pr

$\phi'(0)$ = function of $f(0)$, Sc

in tabular or graphical form. In some problems the mass transfer rate $\dot{m} = \rho v_w$ may be specified, and from the derivation preceding Eq. (8.1-16),

$$f(0) = -\frac{\dot{m}}{\rho u_e} Re_x^{\frac{1}{2}} / 2^{\frac{1}{2}} \qquad (8.1\text{-}26)$$

Then the appropriate value of $f(0)$ may be evaluated using Eq. (8.1-26) and $f''(0)$, $\theta'(0)$ and $\phi'(0)$ obtained. However for the evaporation problem under consideration $\dot{m}$ is an unknown, and hence an iterative procedure appears to be required to obtain a solution. The pioneering paper of Hartnett and Eckert [4] proposed such a procedure. However it is clear that such an iterative procedure should be performed once and for all, and the results presented in a convenient form. Eq. (8.1-16), viz., $f(0) = \frac{B'}{Sc} \phi'(0)$ connects $f(0)$ with the specified data of the evaporation problem, since with $K_{1,e}$ and $K_{1,w}$ given, $B' = (K_{1,e} - K_{1,w})/(K_{1,w} - 1)$ is known. Combining Eqs. (8.1-16, 17 and

26) gives

$$\dot{m} = \rho u_e C_M B' \tag{8.1-27}$$

$$= \rho u_e C_{MO} B' \left(\frac{C_M}{C_{MO}}\right) \tag{8.1-28}$$

$$\frac{C_M}{C_{MO}} = \frac{\phi'(0)}{\phi'(0)\Big|_{f(0)\,=\,0}} \tag{8.1-29}$$

$$C_{MO} \simeq 0.332\, Re_x^{-1/2}\, Sc^{-2/3} \tag{8.1-30}$$

where we have used our analysis of §4.1 to indicate a convenient form of presentation. Eq. (8.1-29) is shown in the Figure for various values of the Schmidt number. The Couette flow model of §4.1 of course gave

$$\frac{C_M}{C_{MO}} = \frac{\ell n(1+B')}{B'}$$

which is also shown in the Figure. Negative values of B' (corresponding to suction) are not shown in the Figure. The effect of Sc is seen to be small for values of Sc characterizing gas mixtures (0.2-2.0). Furthermore, as will be seen later in Chapter 8, the effects of variable properties on C_M/C_{MO} for real gas mixtures are considerably larger than the Sc effect; thus any discussion of the effect of Sc on C_M/C_{MO} is of academic interest only.

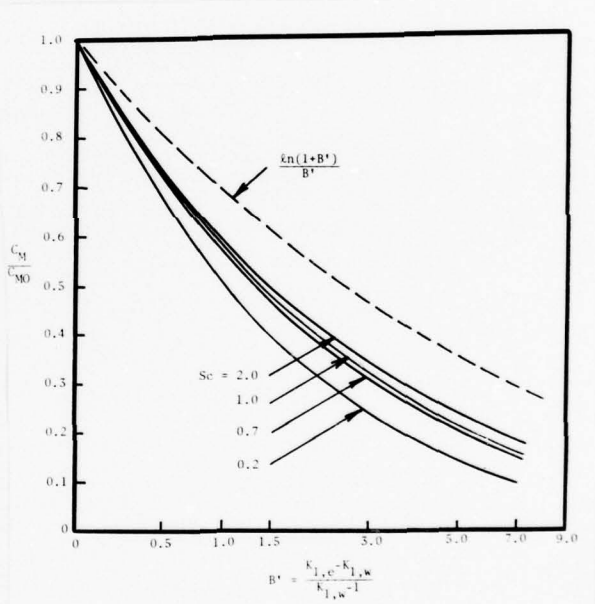

Example 8.1

Rework Example 8.1 using the exact boundary layer solution to obtain C_M/C_{MO}.

B' was evaluated to be 1.09; from the Figure $C_M/C_{MO} \simeq 0.52$ for Sc = 0.56.

Also C_{MO} was evaluated as 0.0054. Thus

$$\dot{m} = \rho u_e C_{MO} B' \left(\frac{C_M}{C_{MO}}\right)$$

$$= (0.0272 \text{ lb/ft}^3)(300 \text{ ft/s})(0.0054)(1.09)(0.52)$$

$$= 0.025 \text{ lb/ft}^2\text{s}$$

8.2 THE HOWARTH AND MANGLER TRANSFORMATIONS

The Howarth Transformation

Due to large differences in temperature between the free-stream and wall, real gas boundary layers on re-entry vehicles have large thermophysical property variations, particularly that of density. Before attempting numerical solution of the equations governing such boundary layers, it is advantageous to make use of a transformation usually attributed to Howarth or Dorodnitsyn. To demonstrate the underlying principle we will consider again the boundary layer on a flat plate, for which the mass and momentum conservation equations are

$$\frac{\partial}{\partial x}(\rho u) + \frac{\partial}{\partial y}(\rho v) = 0 \tag{8.2-1}$$

$$\rho u \frac{\partial u}{\partial x} + \rho v \frac{\partial u}{\partial y} = \frac{\partial}{\partial y}\left(\mu \frac{\partial u}{\partial y}\right) \tag{8.2-2}$$

to be solved subject to the boundary conditions,

$$\begin{aligned} &y = 0: \; u = 0, \; v = 0 \\ &x = 0, \; y \to \infty: \; u = u_e \end{aligned} \tag{8.2-3}$$

Mass conservation is satisfied by introducing a stream function ψ such that $\rho u = (\partial\psi/\partial y)$; $\rho v = -(\partial\psi/\partial x)$. Then we let

$$\psi = \rho_e (2 u_e \nu_e x)^{\frac{1}{2}} \; f(\xi)$$

$$d\xi = (\rho/\rho_e) d\eta$$

$$\eta = y(u_e/2\nu_e x)^{\frac{1}{2}}$$

where now ψ and η have been defined in terms of free-stream properties. The differential operators for the transformation $x, y \to x, \xi$ are

$$\frac{\partial}{\partial x} = \frac{\partial}{\partial x}\bigg|_{\xi} - \frac{\eta}{2x}\frac{\rho}{\rho_e}\frac{\partial}{\partial \xi}\bigg|_{x}$$

$$\frac{\partial}{\partial y} = \frac{\rho}{\rho_e}\left(\frac{u_e}{2\nu_e x}\right)^{\frac{1}{2}}\frac{\partial}{\partial \xi}\bigg|_{x}$$

After some rearrangement the transformed momentum equation is

$$\left(\frac{\rho\mu}{\rho_e\mu_e} f_{\xi\xi}\right)_{\xi} + f f_{\xi\xi} = 0 \qquad (8.2\text{-}4)$$

For gases $\rho \sim T^{-1}$ and $\mu \sim T^{0.7}$ approximately, so that $\rho\mu/\rho_e\mu_e \sim T^{-0.3}$, a rather weak dependence. Thus taking $\rho\mu/\rho_e\mu_e$ = a constant C (the Chapman constant) was a procedure followed in early analyses of variable property boundary layers. Then Eq. (8.2-4) becomes

$$C\, f_{\xi\xi\xi} + f f_{\xi\xi} = 0 \qquad (8.2\text{-}5)$$

Now let $d\zeta = C^{-\frac{1}{2}} d\xi$

$F(\zeta) = C^{-\frac{1}{2}} f(\xi)$, then Eq. (8.2-5) becomes

$$F_{\zeta\zeta\zeta} + F F_{\zeta\zeta} = 0 \qquad (8.2\text{-}6)$$

The wall shear stress is then obtained as

$$\tau_w = \mu\frac{\partial u}{\partial y}\bigg|_0 = \mu\,\frac{\partial u}{\partial \zeta}\frac{\partial \zeta}{\partial \xi}\frac{\partial \xi}{\partial \eta}\frac{\partial \eta}{\partial y}\bigg|_0 = \frac{1}{2}\rho_e u_e^{\,2} C_F$$

thus

$$\rho_e u_e^{\,2}\frac{C_F}{2} = \mu_w u_e F_{\zeta\zeta}\bigg|_0 C^{-\frac{1}{2}}\,\frac{\rho_w}{\rho_e}\left(\frac{u_e}{2\nu_e x}\right)^{\frac{1}{2}}$$

$$\frac{C_F}{2} = \left(\frac{\rho_w\mu_w}{\rho_e\mu_e}\right)\frac{0.4696}{\sqrt{2}\, C^{\frac{1}{2}}\, Re_{x,e}^{\frac{1}{2}}} \qquad (8.2\text{-}7)$$

and

$$\frac{C_F}{C_{Fi}} = \frac{\tau_w}{\tau_{wi}} = \left(\frac{\rho_w\mu_w}{\rho_e\mu_e}\right)C^{-\frac{1}{2}} \qquad (8.2\text{-}8)$$

where i refers to constant property flow. If it is reasoned that property variations are more important near the wall then $C = \rho_w\mu_w/\rho_e\mu_e$ would be a good approximation, then

$$\frac{C_F}{C_{Fi}} = \left(\frac{\rho_w \mu_w}{\rho_e \mu_e}\right)^{1/2} = \left(\frac{T_w}{T_e}\right)^{-0.15} \qquad (8.2\text{-}9)$$

that is, the shear stress will increase as the wall is cooled below the free-stream temperature. Eq. (8.2-9) also suggests a correlation scheme for exact numerical solutions, as will be seen in §8.4.

The Mangler Transformation

Mangler in 1945 discovered a transformation which results from a general equivalence of axisymmetric and planar boundary layers. For the axisymmetric boundary layer mass and momentum conservation equations are:

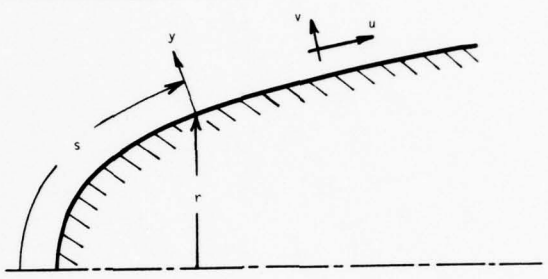

$$\frac{\partial}{\partial s}(\rho u r) + \frac{\partial}{\partial y}(\rho v r) = 0 \qquad (8.2\text{-}10)$$

$$\rho u \frac{\partial u}{\partial s} + \rho v \frac{\partial u}{\partial y} = -\frac{dP}{ds} + \frac{\partial \tau}{\partial y} \qquad (8.2\text{-}11)$$

where u, v, s, y are the axisymmetric flow variables for a given dP/ds and r(s), as shown in the Figure. The mass conservation equation is satisfied by introducing a stream function ψ such that,

$$\rho u r = \frac{\partial \psi}{\partial y}; \quad -\rho v r = \frac{\partial \psi}{\partial s}$$

Let $y' = \frac{r}{L} y$ where L is a reference length, and transform variables $s, y \rightarrow s', y'$ where s' is as yet undefined except $s' \neq f(y)$. Then

$$\rho u r = \frac{\partial \psi}{\partial s'}\frac{\partial s'}{\partial y} + \frac{\partial \psi}{\partial y'}\frac{\partial y'}{\partial y} = \frac{r}{L}\frac{\partial \psi}{\partial y'}$$

$$-\rho v r = \frac{\partial \psi}{\partial s'}\frac{\partial s'}{\partial s} + \frac{\partial \psi}{\partial y'}\frac{\partial y'}{\partial s} = \frac{\partial \psi}{\partial s'}\frac{ds'}{ds} + \frac{y}{L}\frac{dr}{ds}\frac{\partial \psi}{\partial y'}$$

Now let $\psi' = \frac{\psi}{L}$, then $\rho u = \frac{\partial \psi'}{\partial y'}$; $-\rho v = \frac{L}{r}\frac{\partial \psi'}{\partial s'}\frac{ds'}{ds} + \frac{y}{r}\frac{dr}{ds}\frac{d\psi'}{dy'}$

Substituting in the convective operator and rearranging gives

$$\rho u \frac{\partial u}{\partial s} + \rho v \frac{\partial u}{\partial y} = \left(\frac{\partial \psi'}{\partial y'} \frac{\partial}{\partial s'} - \frac{\partial \psi'}{\partial s'} \frac{\partial}{\partial y'}\right) \frac{ds'}{ds} \tag{8.2-12}$$

which suggests the definitions $\rho u' = \frac{\partial \psi'}{\partial y'}$; $\rho v' = -\frac{\partial \psi'}{\partial s'}$; then the momentum equation becomes

$$\left(\rho u' \frac{\partial u}{\partial s'} + \rho v' \frac{\partial u}{\partial y'}\right) \frac{ds'}{ds} = -\frac{dP}{ds'} \frac{ds'}{ds} - \frac{r}{L} \frac{\partial \tau}{\partial y} \tag{8.2-13}$$

For laminar flow $\tau = \mu \frac{\partial u}{\partial y} = \mu \frac{r}{L} \frac{\partial u}{\partial y'}$. Hence if we let

$\frac{ds'}{ds} = \left(\frac{r}{L}\right)^2$; $u = u'$, then

$$\rho u' \frac{\partial u'}{\partial s} + \rho v' \frac{\partial u'}{\partial y'} = -\frac{dP}{ds'} + \frac{\partial}{\partial y'} \left(\mu \frac{\partial u'}{\partial y'}\right) \tag{8.2-14}$$

and the transformation is successful since the planar form of the momentum equation has been obtained. For constant property flow and using the Euler relation $dP/\rho = -u_e du_e$

$$u' \frac{\partial u'}{\partial s} + v' \frac{\partial u'}{\partial y'} = u_e \frac{du'_e}{ds'} + \nu \frac{\partial^2 u'}{\partial y'^2} \tag{8.2-15}$$

Summarizing, the Mangler transformation can be written:

$$s' = \frac{1}{L^2} \int_0^s r^2 ds \qquad y' = \frac{r}{L} y$$

$$u' = u \qquad v' = \frac{L}{r} \left(v + \frac{yu}{r} \frac{dr}{ds}\right) \tag{8.2-16}$$

As a particular example consider constant property flow over a cone, Evans [5] gives the details of the potential flow past a cone of half angle ϕ: the freestream velocity is of the form

$$u_e = C s^n \tag{8.2-17}$$

where values of n for various values of ϕ are shown in the Table opposite. There is not a simple relation between ϕ and n, as there is for Falkner-Skan wedge flows, viz.,

n	ϕ, deg
0.0	0.0
0.1	27.73
0.2	40.33
0.3	50.11
0.4	58.22
0.5	65.20
0.6	71.31
0.7	76.84
0.8	81.60
0.9	86.00
1.0	90.00

$$\phi = \frac{m\pi}{1+m} \qquad \text{for } u_e = Cs^m$$

For a cone $r = s \sin\phi$, and the Mangler transformation gives

$$s' = \frac{s^3 \sin^2\phi}{3L^2}$$

that is $s \alpha s'^{1/3}$. Since $u_e \alpha s^n$ for a cone, $u_e' \alpha s'^{n/3}$ for the equivalent planar flow. For $n = 1$ we have the important case of axisymmetric stagnation point flow: the corresponding wedge flow is therefore $u_e' \alpha s'^{1/3}$, i.e., $m = 1/3$.

8.3 THE GENERAL EQUATIONS

Calculation of convective heat and mass transfer to heat shields requires analysis of the boundary layer flow over the heat shield. The starting point for such analysis is taken to be the equations of conservation of mass, momentum chemical species, and energy, all in boundary layer form. The Figure shows the coordinate system, and the equations are:

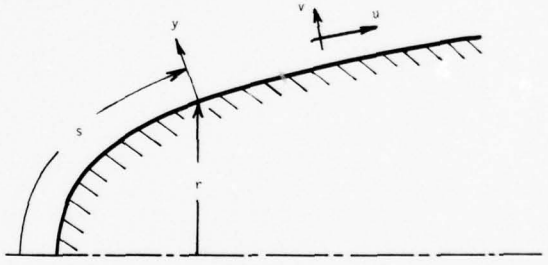

$$\frac{\partial \rho}{\partial t} + \frac{\partial}{\partial s}(\rho u r^{\varepsilon}) + \frac{\partial}{\partial y}(\rho v r^{\varepsilon}) = 0 \qquad (8.3\text{-}1)$$

where $\varepsilon = 0$ for a planar flow, $\varepsilon = 1$ for an axisymmetric flow.

momentum conservation:

$$\rho \frac{\partial u}{\partial t} + \rho u \frac{\partial u}{\partial s} + \rho v \frac{\partial u}{\partial y} = -\frac{dP_e}{ds} + \frac{\partial}{\partial y}(\tau_{sy}) \qquad (8.3\text{-}2)$$

species conservation:

$$\rho \frac{\partial K_i}{\partial t} + \rho u \frac{\partial K_i}{\partial s} + \rho v \frac{\partial K_i}{\partial y} = \frac{\partial}{\partial y}(-j_{iy}) + \dot{r}_i \; ; \quad i = 1,2,\ldots,n \qquad (8.3\text{-}3)$$

total enthalpy conservation:

$$\rho \frac{\partial H}{\partial t} + \rho u \frac{\partial H}{\partial s} + \rho v \frac{\partial H}{\partial y} = \frac{\partial}{\partial y}(-q_y + u\tau_{sy}) \qquad (8.3\text{-}4)$$

For laminar flows τ_{sy}, j_{iy} and q_y are given by diffusive flux laws obtained from the kinetic theory of gases, as described in §3. For turbulent

flows the conservation equations must be first time-averaged and the resulting turbulent diffusive fluxes modeled.

Appropriate boundary conditions for the above set of equations are

$$y \to \infty: \; u = u_e; \quad K_i = K_{i,e}; \quad H = H_e$$
$$y = 0: \; u = 0; \quad \rho v = \dot{m}; \quad H = h_w; \quad \dot{m} K_{i,tw} = \dot{m} K_{i,w} + j_{iy}\Big|_w \tag{8.3-5}$$

where the precise manner in which the transferred state mass fraction $K_{i,tw}$ is specified depends on the particular problem under consideration (see §4.3).

Transformation of the Laminar Boundary Layer Equations

For our present purpose it is convenient to assume steady laminar flow of an effective binary mixture with negligible second order diffusion effects. Upon introduction of the appropriate diffusive flux laws (see § 3) the boundary layer equations, Eqs. (8.3-1) through (8.3-4) become:

$$\frac{\partial}{\partial s}(\rho u r^{\varepsilon}) + \frac{\partial}{\partial y}(\rho v r^{\varepsilon}) = 0 \tag{8.3-6}$$

$$\rho u \frac{\partial u}{\partial s} + \rho v \frac{\partial u}{\partial y} = \rho_e u_e \frac{du_e}{ds} + \frac{\partial}{\partial y}\left(\mu \frac{\partial u}{\partial y}\right) \tag{8.3-7}$$

$$\rho u \frac{\partial K_i}{\partial s} + \rho v \frac{\partial K_i}{\partial y} = \frac{\partial}{\partial y}\left(\rho \mathcal{D}_{im} \frac{\partial K_i}{\partial y}\right) + \dot{r}_i \qquad i = 1,2,\ldots,n \tag{8.3-8}$$

$$\rho u \frac{\partial H}{\partial s} + \rho v \frac{\partial H}{\partial y} = \frac{\partial}{\partial y}\left[\frac{\mu}{Pr} \frac{\partial H}{\partial y} + \mu\left(1 - \frac{1}{Pr}\right) \frac{\partial}{\partial y}\left(\frac{u^2}{2}\right)\right.$$
$$\left. + \sum_{i=1}^{n} \left(1 - \frac{1}{Le_i}\right) h_i \rho \mathcal{D}_{im} \frac{\partial K_i}{\partial y}\right] \tag{8.3-9}$$

where the Euler equation, $(1/\rho)(dP/ds) = u(du/ds)$, has been applied at the boundary layer edge to obtain Eq. (8.3-7).

A first step in obtaining solutions to the above system of partial differential equations is to investigate the possibility of obtaining self-similar solutions. Thus we seek a transformation which will yield a system of ordinary differential equations. The most commonly used has been a combination of the Levy and Mangler transformations with the Howarth-Dorodnitsyn transformation, in a form suggested by Lees. A variety of names have been

used for this transformation, and also slightly different forms have been used. We shall use the designation "Lees transformation". The new coordinate system (ξ,η) is related to the original system (s,y) by the relations

$$\xi = \int_0^s u_e \rho_e \mu_e r^{2\varepsilon} ds \tag{8.3-10a}$$

$$\eta = \frac{r^{\varepsilon} u_e}{(2\xi)^{\frac{1}{2}}} \int_0^y \rho dy \tag{8.3-10b}$$

(sometimes $(\rho_e\mu_e)$ is replaced by $(\rho_w\mu_w)$ in the definition of ξ, e.g. [6]). The associated differential operators are:

$$\frac{\partial}{\partial y} = \frac{\partial}{\partial \xi} \cdot \frac{\partial \xi}{\partial y} + \frac{\partial}{\partial \eta} \cdot \frac{\partial \eta}{\partial y} = \frac{\rho u_e r^{\varepsilon}}{(2\xi)^{\frac{1}{2}}} \frac{\partial}{\partial \eta} \tag{8.3-11a}$$

$$\frac{\partial}{\partial s} = \frac{\partial}{\partial \xi} \cdot \frac{\partial \xi}{\partial s} + \frac{\partial}{\partial \eta} \cdot \frac{\partial \eta}{\partial s} = \frac{\partial \xi}{\partial s} \left(\frac{\partial}{\partial \xi} + \frac{\partial \eta}{\partial \xi} \cdot \frac{\partial}{\partial \eta}\right)$$

$$= \rho_e \mu_e u_e r^{2\varepsilon} \left[\frac{\partial}{\partial \xi} + \frac{\partial \eta}{\partial \xi} \cdot \frac{\partial}{\partial \eta}\right] \tag{8.3-11b}$$

We choose a stream function $\psi(\xi,\eta) = (2\xi)^{\frac{1}{2}} f(\xi,\eta)$; the velocity components are then obtained as

$$\rho u r^{\varepsilon} = \frac{\partial \psi}{\partial y} = \frac{\rho u_e r^{\varepsilon}}{(2\xi)^{\frac{1}{2}}} \frac{\partial \psi}{\partial \eta} = \frac{\rho u_e r^{\varepsilon}}{(2\xi)^{\frac{1}{2}}} (2\xi)^{\frac{1}{2}} \frac{\partial f}{\partial \eta} \; ; \quad \text{or } u = u_e f' \tag{8.3-12}$$

$$-\rho v r = \frac{\partial \psi}{\partial s} = \frac{\partial}{\partial s} \left[(2\xi)^{\frac{1}{2}} f(\eta,\xi)\right]$$

$$= \rho_e u_e r^{2\varepsilon} \left\{\frac{\partial}{\partial \xi} \left[(2\xi)^{\frac{1}{2}} f\right] + \frac{\partial \eta}{\partial \xi} \cdot \frac{\partial}{\partial \eta} \left[(2\xi)^{\frac{1}{2}} f\right]\right\}$$

$$\text{or} \qquad \rho v = -\rho_e u_e \mu_e r^{\varepsilon} \left\{(2\xi)^{\frac{1}{2}} \frac{\partial f}{\partial \xi} + f(2\xi)^{-\frac{1}{2}} + \frac{\partial \eta}{\partial \xi} (2\xi)^{\frac{1}{2}} f'\right\} \tag{8.3-13}$$

The convective operator is therefore

$$\rho u \frac{\partial}{\partial s} + \rho v \frac{\partial}{\partial y} = \rho u_e f' \rho_e u_e \mu_e r^{2\varepsilon} \left[\frac{\partial}{\partial \xi} + \frac{\partial \eta}{\partial \xi} \cdot \frac{\partial}{\partial \eta}\right]$$

$$- \rho_e u_e \mu_e r^{\varepsilon} \left[(2\xi)^{\frac{1}{2}} \frac{\partial f}{\partial \xi} + f(2\xi)^{-\frac{1}{2}} + \frac{\partial \eta}{\partial \xi} (2\xi)^{\frac{1}{2}} f'\right] \left[\frac{\rho u_e r^{\varepsilon}}{(2\xi)^{\frac{1}{2}}} \frac{\partial}{\partial \eta}\right]$$

$$\text{or} \quad \rho u \frac{\partial}{\partial s} + \rho v \frac{\partial}{\partial y} = \rho \rho_e u_e^2 \mu_e r^{2\varepsilon} [f' \frac{\partial}{\partial \xi} - (\frac{\partial f}{\partial \xi} + \frac{f}{2\xi}) \frac{\partial}{\partial \eta}] \tag{8.3-14}$$

and the diffusive operator for any coefficient $\Gamma(s,y)$ is

$$\frac{\partial}{\partial y} (\Gamma \frac{\partial}{\partial y}) = \frac{\rho u_e r^{\varepsilon}}{(2\xi)^{\frac{1}{2}}} \frac{\partial}{\partial \eta} (\Gamma \frac{\rho u_e r^{\varepsilon}}{(2\xi)^{\frac{1}{2}}} \frac{\partial}{\partial \eta}) = \frac{\rho u_e^2 r^{2\varepsilon}}{2\xi} \frac{\partial}{\partial \eta} (\rho \Gamma \frac{\partial}{\partial \eta}) \tag{8.3-15}$$

In order to transform the momentum equation, Eq. (8.3-7), we first note that $(du_e/ds) = \rho_e u_e \mu_e r^{2\varepsilon} (du_e/d\xi)$ since $u_e = u_e(\xi)$ alone. Substituting in Eq. (8.3-7) with Eqs. (8.3-14 and 15) and rearranging gives,

$$(Cf'')' + ff'' + \beta[\frac{\rho_e}{\rho} - (f')^2] = 2(f' \frac{\partial f'}{\partial \ln \xi} - \frac{\partial f}{\partial \ln \xi} f'') \tag{8.3-16}$$

where $C \equiv \rho\mu/\rho_e\mu_e$, $\beta = 2(d\ln u_e/d\ln\xi)$. Next we define a dimensionless mass fraction $z_i = K_i/K_{i,w}$, and substituting in Eq. (8.3-8) with Eqs. (8.3-14 and 8.3-15), and rearranging gives

$$(\frac{C}{Sc} z_i')' + f z_i' = 2(f' \frac{\partial z_i}{\partial \ln \xi} - z_i' \frac{\partial f}{\partial \ln \xi}) + 2f' z_i \frac{d\ln K_{i,w}}{d\ln \xi} - \frac{2\xi \dot{r}_i}{\rho u_e K_{i,w} (d\xi/ds)} \tag{8.3-17}$$

Finally we define a dimensionless total enthalpy, $g = H/H_e$, and substituting in Eq. (8.3-9) with Eqs. (8.3-14 and 15), and rearranging gives

$$(\frac{C}{Pr} g')' + f g' + \frac{u_e^2}{2H_e} [2C(1 - \frac{1}{Pr}) f' f'']' + [\frac{C}{Pr} \sum_{i=1}^{n} (Le_i - 1) g_i K_{i,w} z_i']' = 2(f' \frac{\partial g}{\partial \ln \xi} - g' \frac{\partial f}{\partial \ln \xi}) + 2f' g \frac{d\ln H_e}{d\ln \xi} \tag{8.3-18}$$

Notice that the residual viscous work term is scaled by $u_e^2/2H_e \equiv E$ which may be viewed as an Eckert number. Alternatively, for a perfect gas we have the relation

$$E = \frac{u_e^2}{2H_e} = \frac{1}{(1 + \frac{2}{(\gamma-1)M_e^2})}$$

and E may be viewed as a Mach number parameter.

The right-hand sides of Eqs. (8.3-16 through 18) contain derivatives with respect to ξ. For self-similar solutions we require the dependent variables f, z_i and g to be functions of η alone, and thus the ξ derivatives must be zero. In real flows this condition is only satisfied generally at planar and axi-symmetric stagnation points. The condition is also met for hypersonic attached flows over a cone or wedge for which P_e and u_e are constant [7]: however, such flows are turbulent under conditions of importance to reentry vehicle aerodynamic heating, thus the laminar flow is of little concern to us. Notwithstanding the above limitations, many essential characteristics of laminar boundary layers can be profitably examined by simply setting the ξ-derivatives equal to zero to get a family of mathematically self-similar solutions. The ξ-derivatives have been retained in Eqs. (8.3-16 through 18) for future use, because the complete equations form the basis of the Hartree-Wormersley method of solving non-similar boundary layers numerically: the ξ-derivatives are approximated by finite difference forms and a set of ordinary differential equations solved at each step of a forward marching procedure.

The species generation term in Eq. (8.3-17) requires special attention, since it too must depend on η alone. Since $\dot{r}_i$ depends only on the local thermodynamic variables, P, T and z_i, this condition may be met in three distinct ways: (i) $\dot{r}_i = 0$, i.e., frozen flow; (ii) $K_{i,w}$ = constant and $u_e d\ln\xi/ds$ = constant, which is met at a stagnation point; or (iii) the reaction rates are fast enough to maintain conditions sufficiently close to chemical equilibrium, in which case the reaction conductivity method may be used, or more generally, the species equations may be reduced to conservation equations for the chemical elements.

For self-similar solutions the boundary conditions Eq. (8.3-5) transform into

$$\eta \to \infty : f' = 1 \; ; \quad z_i = \frac{K_{i,e}}{K_{i,w}} \; ; \quad g = 1 \tag{8.3-19}$$

$$\eta = 0 : f' = 0 \; ; \quad f = f_o \; ; \quad g = g_o \; ; \quad K_{i,w} = \frac{K_{i,tw} f_o}{f_o + \left(\frac{C}{Sc} z_i'\right)_o}$$

The Reaction Conductivity Method [8,9,10,11]

The reaction conductivity method was widely used in the 1960's for the analysis of laminar hypersonic air boundary layers. Two assumptions are necessary: (i) the air is in local thermodynamic equilibrium, and (ii) the elemental composition is invariant. In addition it is usually assumed that pressure diffusion, thermal diffusion, and diffusional conduction are negligible. With these assumptions the multicomponent heat flux vector, Eq. (3.5-6), may be written in the form

$$\underline{q} = -(k+k_r)\nabla T \tag{8.3-20}$$

where k_r is called the reaction conductivity and accounts for the interdiffusion contribution; $k_{eq} = k+k_r$ is called the equilibrium or total thermal conductivity.

The underlying principle is simply that local thermodynamic equilibrium and invariant elemental composition implies $K_i = K_i(T,P)$, and thus $\nabla K_i = (\partial K_i/\partial T)\nabla T$. Furthermore, for the elemental composition to be invariant all the binary diffusion coefficients must be equal, thus

$$\begin{aligned} \underline{q} &= -k\nabla T + \sum_i \underline{j}_i h_i \\ &= -k\nabla T - \rho \mathcal{D} \sum_i h_i \nabla K_i \\ &= -k\nabla T - \rho \mathcal{D} \nabla T \sum_i h_i \frac{\partial K_i}{\partial T} \\ &= -\left(k + \rho \mathcal{D} \sum_i h_i \frac{\partial K_i}{\partial T}\right)\nabla T \end{aligned} \tag{8.3-21}$$

The reaction conductivity $k_r = \rho \mathcal{D} \Sigma_i h_i (\partial K_i / \partial T)$ may be evaluated once and for all as a function of T and P.

With this approach the species equation Eq. (8.3-3) is not required and the total energy equation, Eq. (8.3-4) for steady laminar flow, becomes

$$\rho u \frac{\partial H}{\partial s} + \rho v \frac{\partial H}{\partial y} = \frac{\partial}{\partial y} \left[k_{eq} \frac{\partial T}{\partial y} + \mu u \frac{\partial u}{\partial y} \right]$$

Rearranging with $Pr_e = C \ \mu/k$ gives,

$$\rho u \frac{\partial H}{\partial s} + \rho v \frac{\partial H}{\partial y} = \frac{\partial}{\partial y} \left[\frac{\mu}{Pr_{eq}} \frac{\partial H}{\partial y} + \mu \left(1 - \frac{1}{Pr_{eq}}\right) \frac{\partial}{\partial y} \left(\frac{u^2}{2}\right) \right] \qquad (8.2\text{-}18)$$

The total or equilibrium Prandtl number Pr_{eq} must be defined in terms of the equilibrium specific heat, which is derived as follows.

$$h = \Sigma_i k_i h_i \ ; \quad h_i = h_i^\circ + \int_{T^\circ}^{T} C_{pi} dT$$

$$C_{peq} \equiv \frac{dh}{dT}$$

$$= \Sigma_i h_i \frac{dK_i}{dT} + \Sigma_i K_i C_{pi}$$

$$= \Sigma_i h_i \frac{dK_i}{dT} + C_p$$

where C_p is the conventional "frozen" specific heat. Tabulations of $\mu(T,P)$ and $Pr_{eq}(T,P)$ for air are given by Hansen [10] and Bennet et al. [11].

It is important to note that the assumption of invariant elemental composition is only valid for a true binary mixture in the absence of mass addition at the wall of a gas mixture of different elemental composition. Thus the reaction conductivity method cannot be used for general ablation and transpiration cooling analyses. However for the dissociated air boundary layer it has proven to be quite adequate.

8.4 STAGNATION POINT HEAT TRANSFER

Of considerable importance in the aerothermochemical analysis of reentry is the calculation of heat transfer at the stagnation point of the reentry vehicle. Since the flow is laminar and the boundary layer self-similar, analysis is relatively straightforward and reliable. In addition to direct use in design procedures, the results of such analysis are also used, for example, to calibrate arc-jet test facilities. On a typical missile trajectory significant heating occurs only in a regime where the boundary layer temperatures and pressures are high enough to make chemical equilibrium a good assumption. Thus most of the analyses found in the literature assume chemical equilibrium, and many exploit this assumption by using the reaction conductivity method. There have been a variety of approaches and representative examples follow.

1. Ideal Gas. The undissociated air boundary layer may be simply modeled by assuming $\rho \propto h^{-1}$, $\mu \propto h^{\omega}$ and Pr = constant. The governing equations for axisymmetric stagnation point flow then reduce to

$$(Cf'')' + ff'' = \frac{1}{2}(f'^2 - g) \tag{8.4-1}$$

$$\left(\frac{C}{Pr} g'\right)' + fg' = 0 \tag{8.4-2}$$

$$\eta = 0 : \quad f = 0 , \quad f' = 0 , \quad g = g_o$$

$$\eta \to \infty : \quad f' = 1 , \quad g = 1$$

For Pr = 0.7 exact numerical solutions were obtained by Dewey and Gross [6] and Wortman [12,13] for ω = 0.5, 0.7 and 1.0, and $0.05 < g_o = h_w/H_e < 1.1$. The **Figure** shows the results for $g_o < 1$, which are well correlated by

$$(Nu/\sqrt{Re})_w = 0.665(\rho_e \mu_e / \rho_w \mu_w)^{0.43} \tag{8.4-3}$$

where $$Nu_w = \frac{q_w s}{(\mu_w/Pr_w)(H_e - h_w)} ; \quad Re_w = \frac{\rho_w u_e s}{\mu_w} ; \quad u_e = \left.\frac{du_e}{ds}\right|_o s$$

If we assume a $Pr^{0.4}$ dependence for Nu based on constant property solutions [14], then

$$(Nu/\sqrt{Re})_w = 0.767 Pr_w^{0.4} \times (\rho_e \mu_e / \rho_w \mu_w)^{0.43} \qquad (8.4\text{-}4)$$

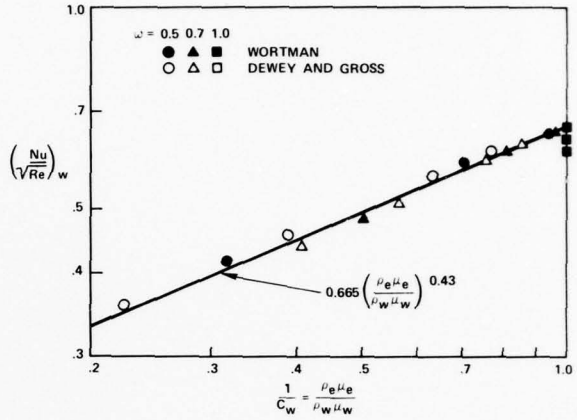

The corresponding value of the heat transfer rate is

$$q_w = 0.767 Pr_w^{-0.6} (\rho_w \mu_w)^{0.07} \times (\rho_e \mu_e)^{0.43} (H_e - h_w)(du_e/ds)_o^{\frac{1}{2}} \qquad (8.4\text{-}5)$$

Notice that the freestream values, rather than the wall values, have the dominant effect on heat transfer. Equation (8.4-4) should be compared to the familiar solution for a constant property wedge flow with $\beta = 0.5$; from [14] $Nu/\sqrt{Re} = 0.76 Pr^{0.4}$.

2. Fay and Riddell, 1958 [15]. This work considered both the equilibrium and non-equilibrium dissociated air boundary layer. In the former case solutions were first obtained for Le = 1 with Pr = 0.71, a constant. For Le ≠ 1 solutions were obtained using a model gas comprising of "air" molecules and "air" atoms only, with an appropriate average heat of formation. Pertinent parameter values were: Le = 1.0, 1.4, 2.0; $5{,}800 < U_\infty < 22{,}800$ ft/s; 25,000 < altitude < 120,000 ft; $540 < T_w < 5400$ R. Equilibrium air properties were based on NBS data. The numerical results were correlated as

$$(Nu/\sqrt{Re})_w = 0.76 Pr^{0.4} (\rho_e \mu_e / \rho_w \mu_w)^{0.4} [1 + (Le^{0.52} - 1) \frac{h_D}{H_e}] \qquad (8.4\text{-}6)$$

where h_D is the enthalpy of dissociation of the free stream. The corresponding value of the heat transfer rate is

$$q_w = \frac{0.76}{Pr^{0.6}} (\rho_w \mu_w)^{0.1} (\rho_e \mu_e)^{0.4} [1+(Le^{0.52}-1) \frac{h_D}{H_e}] (H_e - h_w) (du_e/ds)_o^{\frac{1}{2}} \qquad (8.4\text{-}7)$$

For a frozen boundary layer with a fully catalytic wall the only change in the correlation is in the Lewis number exponent, which becomes 0.63. For a finite recombination rate and a non-catalytic wall the heat transfer is considerably reduced when the reaction time becomes much longer than the time for an atom to diffuse through the boundary layer. The ratio of these times depends on the altitude and nose radius.

Convenient use of the Fay and Ridell correlations requires formulae and/or graphs for H_e, h_w, $(\rho\mu)$, h_D, Pr and Le. Some examples in British units follow.

Total enthalpy H_e

$$H_e = h_\infty + U_\infty^2/2g_oJ = 0.25T_\infty + U_\infty^2/50{,}100 \text{ Btu/lb} \quad \begin{matrix} T(R) \\ V_\infty(ft/s) \end{matrix} \qquad (8.4\text{-}8)$$

Wall enthalpy h_w

A Curve fit to the NBS data [16], which is also in agreement with the calculations of Moeckel and Weston [17], is

$$h_w = T_w(0.234 + 0.01 \frac{T_w}{1000}) \; ; \quad T_w < 5000 \text{ R} \qquad (8.4\text{-}9)$$

Density-viscosity product $(\rho\mu)$

The data of [10,16,17] has been used to develop a correlation of $(\rho\mu)$ with h,

$$\frac{(\rho\mu)}{P} = 52.06\text{x}10^{-10} h^{-0.358} \text{ slug}^2/\text{ft}^4 \cdot \text{s} \cdot \text{atm} \qquad (8.4\text{-}10)$$

where h is in Btu/lb. The correlation is valid for $10^2 < h < 2.5\text{x}10^4$ Btu/lb, and $0.1 < P < 100$ atm.

Dissociation enthalpy h_D

In order to estimate h_D, the dissociation enthalpy per unit mass of air in the free stream, the following assumptions are made (i) prior to dissoci-

ation air is comprised of 21% O_2 and 71% N_2 by volume, (ii) the heats of reaction are 6650 Btu/lb for $O_2 \rightleftarrows 2O$ and 14,400 Btu/lb for $N_2 \rightleftarrows 2N$, (iii) dissociation of O_2 is complete prior to any dissociation of N_2, (iv) no ionization occurs. Then

$$h_D = 6650(K'_{O_2} - K_O) \quad \text{for} \quad K_N = 0$$

and $$h_D = 6650K'_{O_2} + 14{,}400(K'_{N_2} - K_{N_2}) \quad \text{for} \quad K_{O_2} = 0$$

where K' and K are the mass fractions at the boundary layer edge prior to, and after, dissociation. Thus $K'_{O_2} = 0.233$ and $K'_{N_2} = 0.767$.

$$\frac{1}{M} = \sum_i \frac{K_i}{M_i}$$

and $M = 28.84/z$ where z is the compressibility factor and 28.84 is the molecular weight of undissociated air. Thus

$$\frac{z}{28.84} = \sum_i \frac{K_i}{M_i}$$

where $$K_{O_2} = 1.342 - \frac{32}{28.84} z \; ; \quad K_{N_2} = 1.942 - \frac{28}{28.84} z$$

Complete dissociation of O_2 and N_2 occurs at $z = 1.21$ and $z = 2.00$, respectively. The final expressions for h_D are:

$$\begin{aligned} h_D &= 738(z-1) \text{ Btu/lb} && z \leq 1.21 \\ &= 1550 + 13{,}980(z-1.21) && 1.21 < z \leq 2 \\ &= 12{,}595 && z > 2 \end{aligned} \qquad (8.4\text{-}11)$$

$z = z(h,P)$ can be obtained from the Figure and is based on the tables of Hansen [10].

Partial Prandtl and Lewis numbers, Pr, Le

These may be read from the Figure, which is based mainly on Hansen [10].

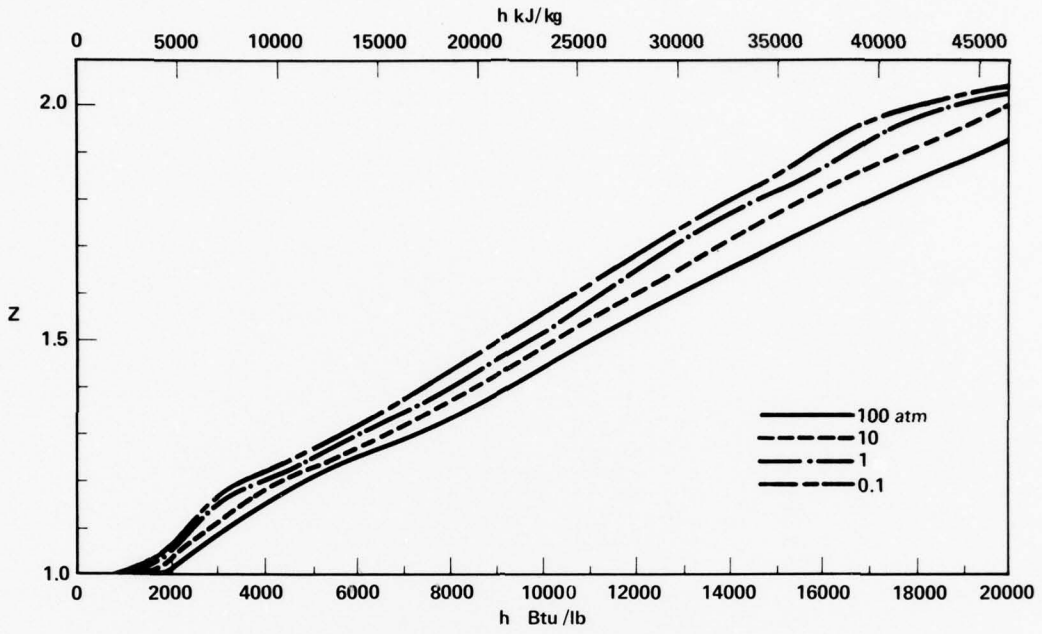
h kJ/kg
0
5000
10000
15000
20000
25000
30000
35000
40000
45000
2.0
1.5
1.0
Z
100 atm
10
1
0.1
0
2000
4000
6000
8000
10000
12000
14000
16000
18000
20000
h Btu /lb

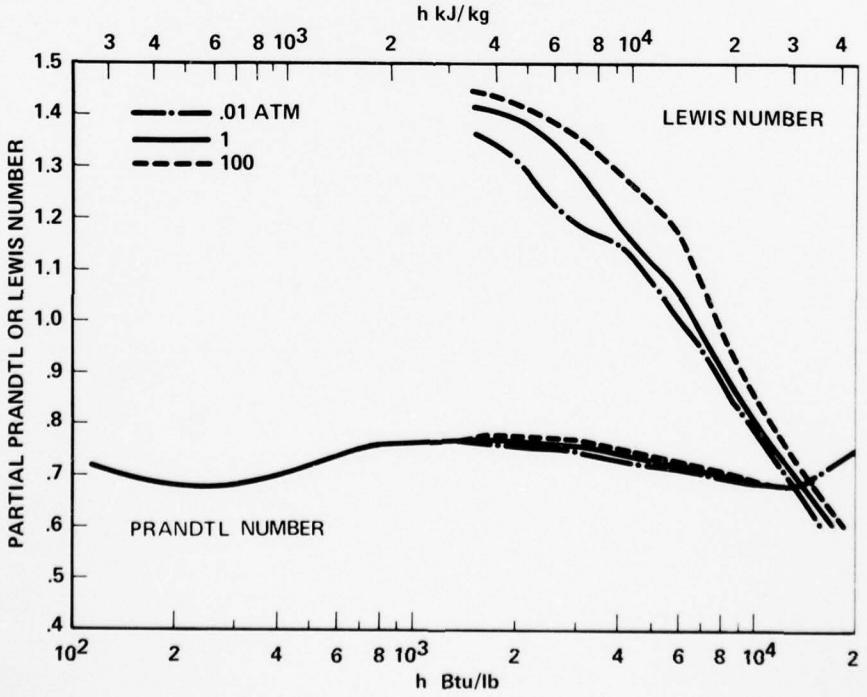
h kJ/kg
3
4
6
8 10^3
2
4
6
8 10^4
2
3
4
1.5
1.4
1.3
1.2
1.1
1.0
.9
.8
.7
.6
.5
.4
PARTIAL PRANDTL OR LEWIS NUMBER
.01 ATM
1
100
LEWIS NUMBER
PRANDTL NUMBER
10^2
2
4
6
8 10^3
2
4
6
8 10^4
2
h Btu/lb

The Figure shows a comparison of predictions using the Fay and Riddell theory and shock tube data for stagnation point heat transfer to a sphere of radius 0.66 cm [18]. The agreement between theory and experiment is seen to be quite satisfactory.

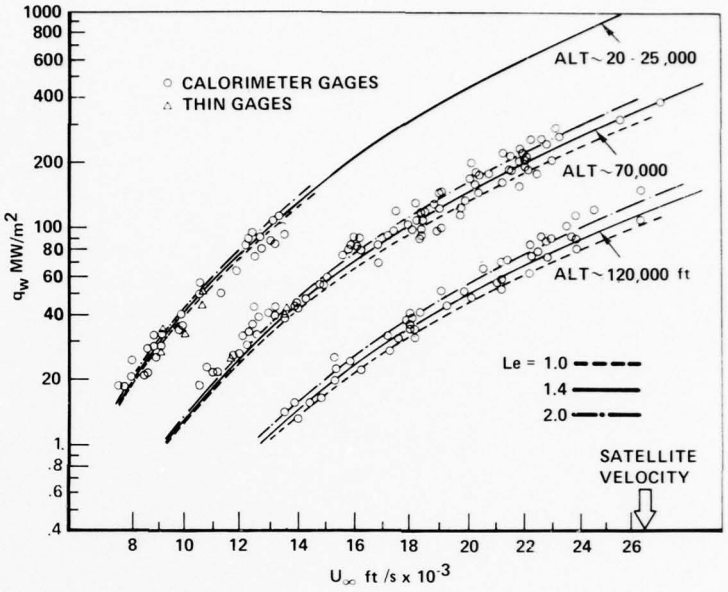

3. N. B. Cohen, 1961 [19]

An equilibrium air boundary layer was assumed and the reaction conductivity method used. For $U_\infty < 29{,}000$ ft/s the properties are from [20] and are based on the 1956 NBS data [16] incorporating the Sutherland viscosity law. For $29{,}000 < U_\infty < 41{,}000$ ft/s the properties of Hansen [10] were used. The wall temperature was in the range $540 < T_w < 3150$ R. Cohen first assumed Le = 1 and obtained for $U_\infty < 29{,}000$ ft/s,

$$(Nu/\sqrt{Re})_w = 0.767 Pr_w^{0.4} (\rho_e \mu_e)/(\rho_w \mu_w)^{0.43} \qquad (8.4\text{-}12)$$

which is identical to Eq. (8.4-4). Correspondingly,

$$q_w = 0.766 Pr_w^{-0.6} (\rho_w \mu_w)^{0.07} (\rho_e \mu_e)^{0.43} (H_e - h_w)(du_e/ds)_o^{1/2} \qquad (8.4\text{-}13)$$

Cohen investigated the effect of Le $\neq 1$. Le > 1 increases q_w, while Le < 1 decreases q_w. However Le varies from 1.4 at low enthalpies, to 0.6 at the enthalpy for complete dissociation, i.e., across the boundary layer in a typical situation. Cohen found a weak Le dependence: $q_w/q_w(\text{Le}=1)$ varied between 0.98 to 1.08, which he concluded was a negligible effect.

For $29{,}000 < U_\infty < 41{,}000$ ft/s Cohen was able to correlate his results by multiplying Eqs. (8.4-12 and 13) by

$$[1 + 0.075(\frac{H_e(\text{Btu/lb})}{8468} - 2)^2] \qquad (8.3\text{-}14)$$

4. Hoshizaki, 1962 [16]. An equilibrium boundary was assumed and the reaction conductivity method used with Hansen's properties [10]. Pertinent parameter values included: $6000 < U_\infty < 50{,}000$ ft/s; $540 < T_w < 5400$ R; $0.001 < P_e < 100$ atm. Hoshizaki correlated the heat transfer rate directly as

$$q_w = 4.24\text{x}10^4 (T_w(\text{R})/1000)^{0.2} (U_\infty(\text{ft/s})/10^4)^{1.69} (1 - \frac{h_w}{H_e})$$

$$\times (\rho_w \mu_w \left.\frac{du_e}{ds}\right|_{s=0} \text{slugs}^2/\text{ft}^4 \cdot \text{s}^2)^{\frac{1}{2}} \qquad (8.4\text{-}15)$$

and is independent of altitude. One cannot obtain a correlation for $Nu/\sqrt{Re}$ which corresponds exactly to Eq. (8.4-15); specific values may however be calculated. Fay [22] suggested an approximate correlation for $Nu/\sqrt{Re}$ based on Hoshizaki's results, viz.,

$$(Nu/\sqrt{Re})_w = 0.478(T_w(\text{R})/900)^{0.2} (U_\infty(\text{ft/s})/10^4)^{-0.31} \qquad (8.4\text{-}16)$$

which is accurate to within 5%.

5. BLIMP, 1968 [23]. Mills and Gomez [24] used the Boundary Layer Integral Matrix Procedure (BLIMP) code developed by Bartlett and Kendall [23], to solve the laminar boundary layer equations for a multicomponent gas mixture. Multicomponent diffusion is modeled using the bifurcation approximation described in §3.7. Chemical equilibrium is calculated at each node point of the finite difference grid. The formulae used for the transport properties in this early version of BLIMP are based on the Lennard-Jones potential model but involve a number of approximations. Two options are available: (a) equal diffusion coefficients, which suppresses multicomponent diffusion effects, and yields a constant elemental composition across the boundary layer; and (b) unequal diffusion coefficients accounting

for multicomponent diffusion. Sample calculations showed differences of the order of 1% in $Nu/\sqrt{Re}$ using the two options so that the results presented here were obtained with option (a) only. Selected results are shown in Table 8.1. The nose radius was 1 ft and the stagnation point velocity gradient was calculated using modified Newtonian theory as discussed in § ; however $Nu/\sqrt{Re}$ is essentially independent of these quantities.

Table 8.1 $(Nu/\sqrt{Re})_w$ calculated using the equal diffusion coefficients of the BLIMP code [24]; R_N = 1.0 ft.

U_∞	T_w = 540 R		T_w = 4000 R	
	P_e = 1	P_e = 0.1	P_e = 1	P_e = 0.1
ft/s	atm	atm	atm	atm
10,000	.444	.446	.607	.607
20,000	.356	.360	.497	.502
30,000	.302	.304	.426	.428
40,000	.272	.276	.385	.392

Comparison of the analyses

The Figure shows a comparison of predictions of $(Nu/\sqrt{Re})_w$ according to the various analyses described above. The pressure is 1 atm and the wall temperatures are 4000 R and 540 R. The analyses of Cohen, and Fay and Ridell for Le = 1, give essentially the same re-

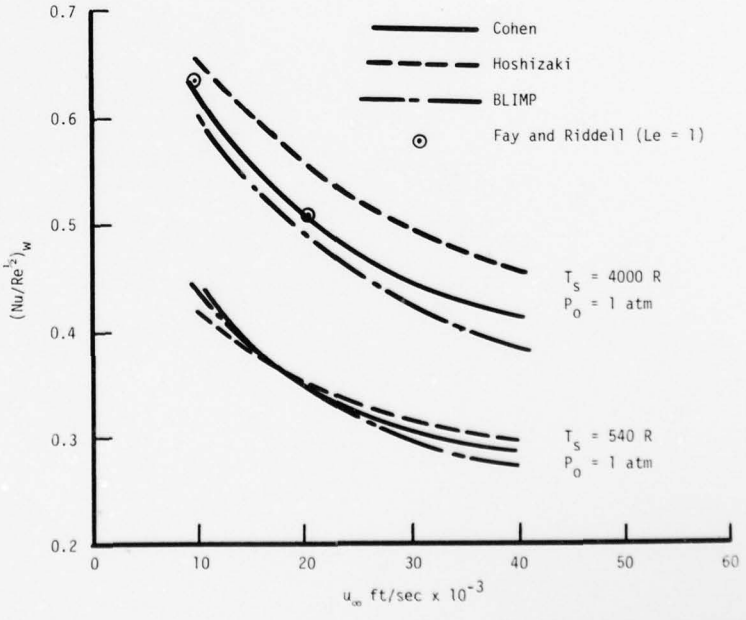

AD-A064 943 CALIFORNIA UNIV LOS ANGELES SCHOOL OF ENGINEERING A--ETC F/G 20/13
CONVECTIVE HEAT AND MASS TRANSFER TO RE-ENTRY VEHICLES.(U)
DEC 78 A F MILLS AFOSR-76-2931

UNCLASSIFIED UCLA-ENG-7982 AFOSR-TR-79-0030 NL

3 OF 3
AD A064943

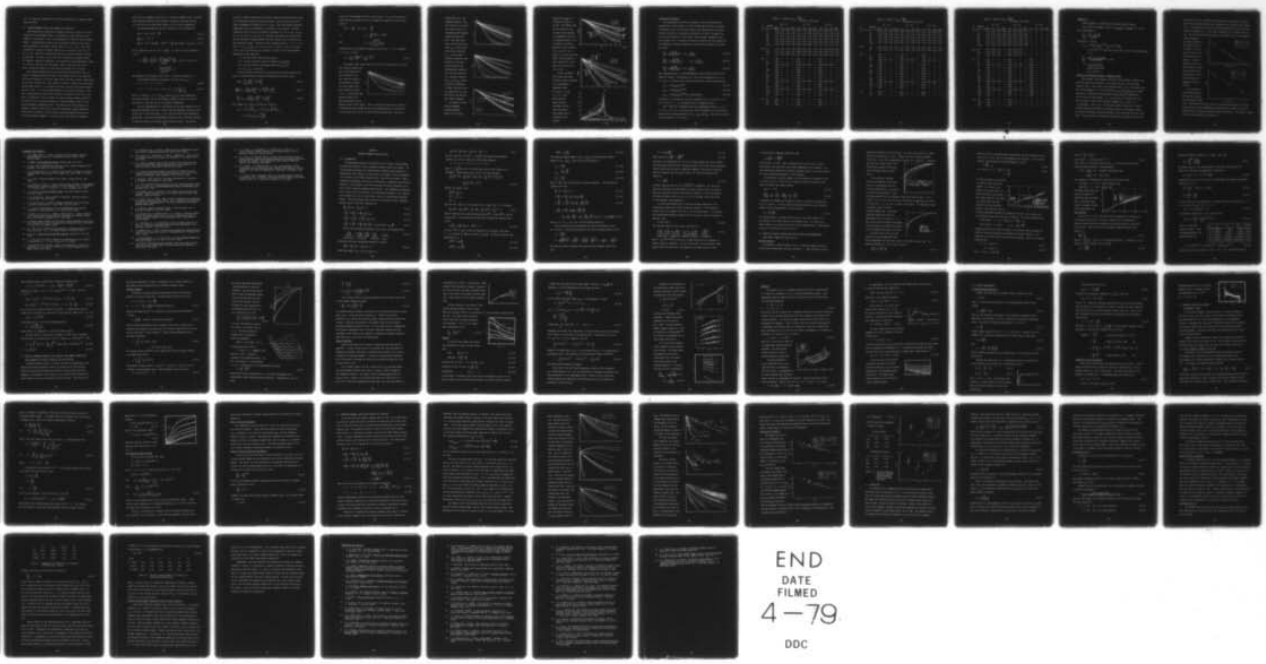

END
DATE FILMED
4-79
DDC

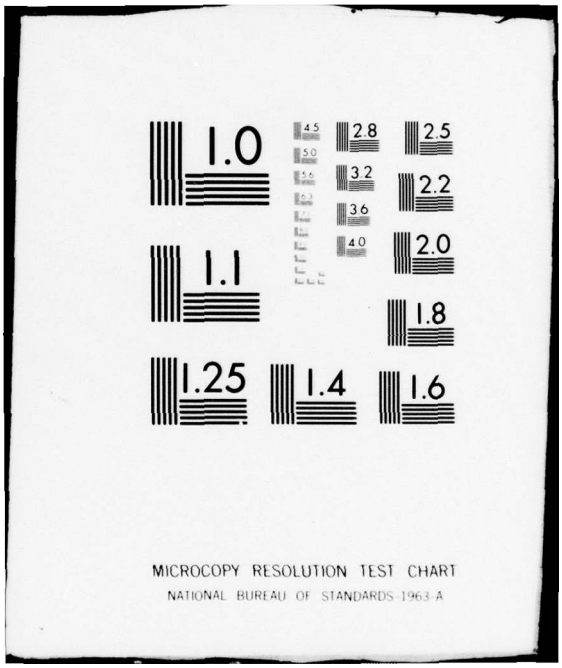
1.0
1.1
1.25
1.4
1.6
1.8
2.0
2.2
2.5
2.8
3.2
3.6
4.0
4.5
5.0
5.6
6.3
MICROCOPY RESOLUTION TEST CHART
NATIONAL BUREAU OF STANDARDS-1963-A

sult. At high wall temperatures the Hoshizaki prediction is somewhat higher than the others.

8.5 LAMINAR BOUNDARY LAYERS WITH FOREIGN GAS INJECTION

Both ablation and transpiration thermal protection systems rely on mass injection into the boundary layer to significantly reduce convective heat transfer to the vehicle: often this phenomenon is called the "heat blockage" effect. A graphite heat shield in the sublimation regime will have injectant mass mainly in the form of carbon vapor, C_1, C_2, C_3, etc. For a charring ablator a variety of chemical species may be involved, such as H_2, H, CO, C_1, etc., while for transpiration cooling the injectant might be He gas or H_2O vapor. Of course, even in the case of oxidation to gaseous oxides, for example, oxidation of graphite, or of tungsten at high temperatures, there is a net mass injection into the boundary layer, since the mass flux of oxides leaving the surface is larger than the incident flux of oxygen.

Thus laminar boundary layers with foreign gas injection have been the subject of numerous analytical studies, with primary focus on the reduction, due to mass injection, of the wall shear stress, the mass transfer conductances and the heat transfer rate. The simplest situation is that of an inert binary mixture where species 1 is injected at the wall, and the free-stream contains species 2 only: it is this problem which has received most attention. However a considerable portion of the literature is devoted to flow over a flat plate, a geometry of little relevance to reentry vehicle thermal protection. In practice we are interested primarily in laminar boundary layers at and near axisymmetric stagnation points. Thus here we will first examine axisymmetric stagnation point flows, and then subsequently examine additional effects due to changes in β (the pressure gradient parameter) and non-zero E (the Mach number parameter), as the flow moves away from the stagnation

point until it undergoes transition to a turbulent boundary layer. We shall ignore thermal diffusion and diffusional conduction since many studies, e.g. [25,26,27] have shown their effects to be of little consequence.

The governing equations are then, from Eqs. (8.3-16 through 18),

$$(Cf'')' + ff'' = \beta(f'^2 - \frac{\rho_e}{\rho}) \tag{8.5-1}$$

$$(\frac{C}{Sc} z_1') + fz_1' = 0 \tag{8.5-2}$$

$$(\frac{C}{Pr} g') + fg' = E[2C(\frac{1}{Pr} - 1)f'f'']' + [\frac{C}{Sc}(g_1 - g_2)(\frac{1}{Le} - 1)K_{1,w} z_1']' \tag{8.5-3}$$

At the stagnation point we set $E = u_e^2/2H_e = 0$, and β for the axisymmetric case is

$$\beta = 2\frac{d\ln u_e}{d\ln \xi} = \frac{2\xi}{u_e}\frac{du_e}{d\xi} = \frac{2\int_o^s \rho_e \mu_e u_e r^{2\varepsilon} ds}{\rho_e \mu_e u_e^2 r^{2\varepsilon}} \frac{du_e}{ds}, \text{ with } \varepsilon=1,\ u_e=\alpha s,\ r=s,$$

$$= \frac{2\rho_e \mu_e (s^4/4)\alpha^2}{\rho_e \mu_e \alpha^2 s^2 s^2} = \frac{1}{2}$$

and similarly for the planar case, with $\varepsilon = 0$ there is obtained $\beta = 1$.

The boundary conditions are from Eq. (8.2-16) with $K_{1,tw} = 1$,

$$\eta \to \infty : \quad f' = 1,\ z_1 = 0,\ g = 1 \tag{8.5-4}$$

$$\eta = 0 : \quad f' = 0,\ f = f_o,\ \theta = \theta_o,\ K_{1,w} = \frac{f_o}{f_o + (\frac{C}{Sc} z_1')_o} \tag{8.5-5}$$

where $\theta = T/(H_e/C_{p\,e})$ i.e., T/T_{total} where T_{total} is total temperature of the free stream. Use of this boundary condition allows the study of the effect of injection rate at a fixed wall temperature.

The most comprehensive set of solutions to the above equation set was obtained by Wortman [12,13,28]. Some of the more important features of his results will be discussed here, as will their correlation for engineering application. The mixture thermodynamic properties were calculated assuming an ideal gas mixture and constant species specific heats. The species

viscosity, thermal conductivity and binary diffusion coefficients were based on a rigid sphere molecular interaction model, and the mixture rules were those recommended by Hirschfelder et al. [29]. With these model properties, temperature level is eliminated as a parameter of the problem. The free-stream gas was air while the injectants included H, H_2, He, C, CH_4, O, H_2O, Ne, air, Ar, CO_2, Xe, CCl_4 and I_2. Synthetic injectants were also constucted by arbitrarily varying specific heat and collision cross-section for a fixed molecular weight. Parameter values considered were θ_o = 0.1, 0.5, 0.9 (for E = 0, $\theta_o = T_w/T_e$); β = 1.0, 0.5, 0.25, 0; and E = 0, 0.5, 0.9, 0.95. In all, over 1500 solutions were obtained. In [12] can be found complete tabulations of the quantities

(i) the wall shear stress function $C_w f''_w$;

(ii) the wall conductive heat flux function $C_w C_{pw} \theta'_w / Pr_w$;

(iii) the mass transfer conductance function $C_w z'_{1,w} / Sc_w$;

(iv) $K_{1,w}$, C_w, Pr_w and Sc_w.

The skin friction coefficient, and heat and mass transfer Stanton numbers, are obtained from the tabulated dimensionless functions using

$$C_w f''_w = \frac{\tau_w}{\rho_e u_e^2} \frac{(2\xi)^{1/2}}{r^{\varepsilon} \mu_e} = \frac{C_F}{2} \frac{(2\xi)^{1/2}}{r^{\varepsilon} \mu_e} \tag{8.5-6}$$

$$\frac{C_w C_{pw}}{Pr_w} \theta'_w = \frac{q_w}{\rho_e u_e H_e} \frac{(2\xi)^{1/2}}{r^{\varepsilon} \mu_e} = C_H \frac{(H_e - h_{ew})}{H_e} \frac{(2\xi)^{1/2}}{r^{\varepsilon} \mu_e} \tag{8.5-7}$$

$$\frac{C_w}{Sc_w} z'_{1,w} = \frac{-j_{1,w}}{\rho_e u_e z_{1,w}} \frac{(2\xi)^{1/2}}{r^{\varepsilon} \mu_e} = C_M \frac{(2\xi)^{1/2}}{r^{\varepsilon} \mu_e} \tag{8.5-8}$$

(For example, Eq. (8.5-8) is derived as follows:

$$j_{1,w} = -\left(\rho \mathcal{D}_{12} \frac{\partial K_i}{\partial y}\right)_{y=0} = -\left(\rho \mathcal{D}_{12} K_{1,w} \frac{\partial z_1}{\partial \eta} \frac{\partial \eta}{\partial y}\right)_{y=0}$$

$$= -(\rho \mathcal{D}_{12})_w K_{1,w} z'_{1,w} \frac{r^{\varepsilon} u_e \rho_w}{(2\xi)^{1/2}}$$

which can be rearranged into the required form.) It is also necessary to relate the mass transfer rate to f_o through the definition of the stream function

$$\rho v r^{\varepsilon} = -\frac{\partial \psi}{\partial s}, \quad \text{thus} \quad \dot{m} r^{\varepsilon} = -\frac{\partial \psi_o}{\partial s}$$

or

$$\psi_o = -\int_0^s \dot{m} r^{\varepsilon} ds = (2\xi)^{\frac{1}{2}} f_o$$

thus

$$-f_o = \frac{\int_o^s \dot{m} r^{\varepsilon} ds}{(2\int_o^s \rho_e \mu_e u_e r^{2\varepsilon} ds)}$$

Evaluation for an axisymmetric stagnation point with $\varepsilon = 1$, $\dot{m}$ = constant, $r = s$, $u_e = \alpha s$ gives

$$-f_o = \frac{\dot{m}}{\rho_e u_e} \left(\frac{\rho_e u_e s}{2\mu_e}\right)^{\frac{1}{2}} = \frac{\dot{m}}{\rho_e u_e} \left(\frac{Re_s}{2}\right)^{\frac{1}{2}} \qquad (8.5\text{-}9)$$

The Figures which follow show the skin friction coefficient, heat and mass transfer Stanton numbers, each normalized by their respective zero mass injection values at an axisymmetric stagnation point under "cold wall" conditions ($T_w/T_e = 0.1$). In [13] Mills and Wortman present a detailed explanation of the behavior shown in the Figures. Here it suffices to note that (i) there is a dominant molecular weight effect on the reductions due to injection of C_F, C_H and C_M, and (ii) for C_H the injectant specific heat also plays a

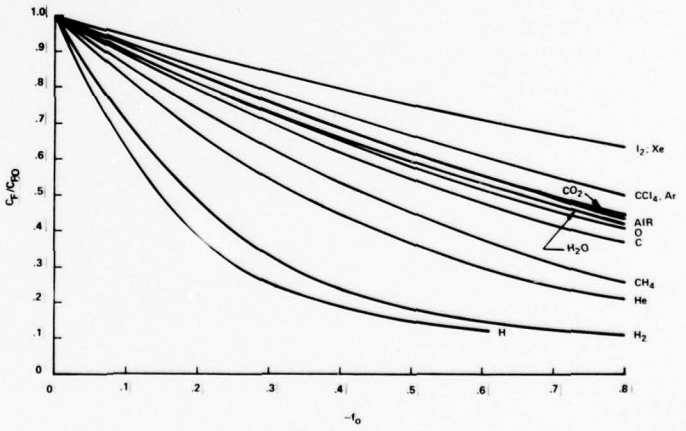

significant role. The anomalous behavior of C_H for H and H_2 at low injection rates is due to an increased mixture thermal conductivity near the wall. For light injectants the wall mole fraction $x_{1,w}$ is much larger than the mass fraction $K_{1,w}$: since mixture transport properties vary essentially with mole fraction whereas the thermodynamic properties vary with mass fraction, k_w is markedly affected while ρ_w and $C_{p,w}$ remain essentially unaffected. At higher injection rates $K_{1,w}$ approaches $x_{1,w}$ and the density and specific heat effects dominate.

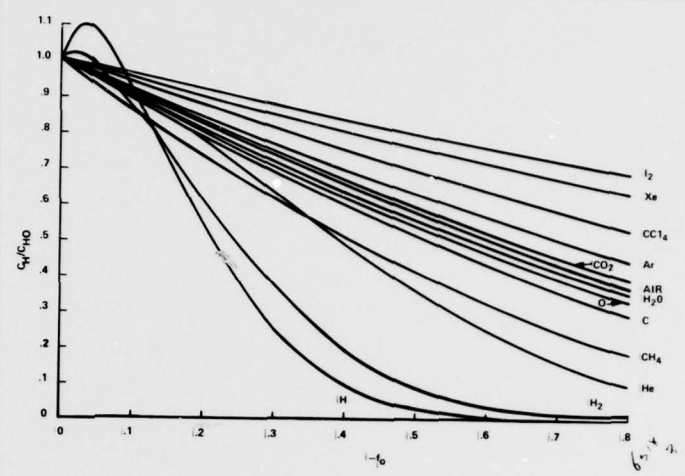

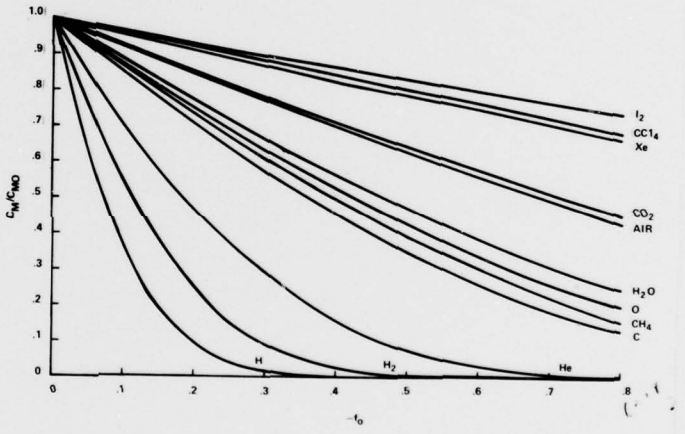

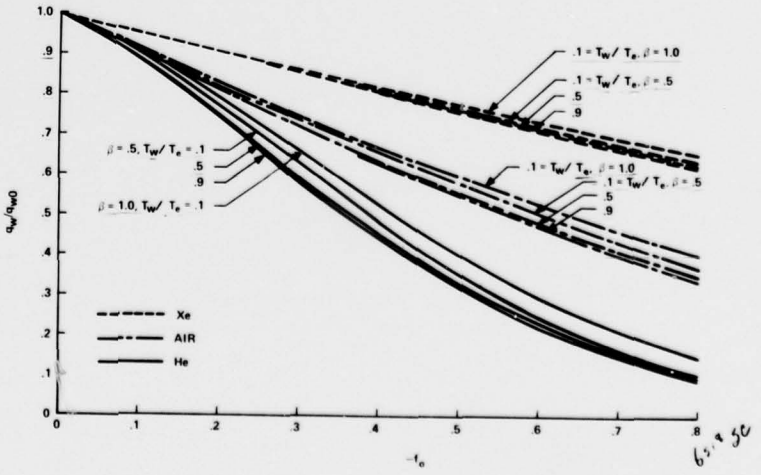

The effects of wall cooling, pressure gradient and Mach number (E) on C_F/C_{FO},

C_H/C_{HO} and C_M/C_{MO} are discussed in detail in [13,28]. The Figures show (i) the effect of wall cooling on heat transfer at axisymmetric and planar stagnation points, (ii) the effect of pressure gradient on heat transfer for a cold wall (E = 0, T_w/T_e = 0.1), and (iii) the effect of Mach number on heat transfer for a flat plate and cold wall (β = 0, θ_o = 0.1).

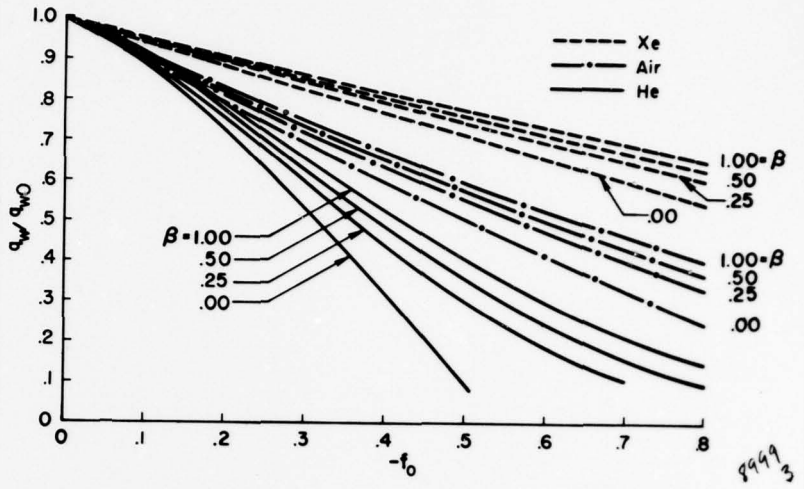

Finally the Figure below shows some representative velocity profiles at an axisymmetric stagnation point for T_w/T_e = 0.5 and $-f_o$ = 0.5. Note that there are marked velocity overshoots for the light injectants, even though there is substantial wall cooling.

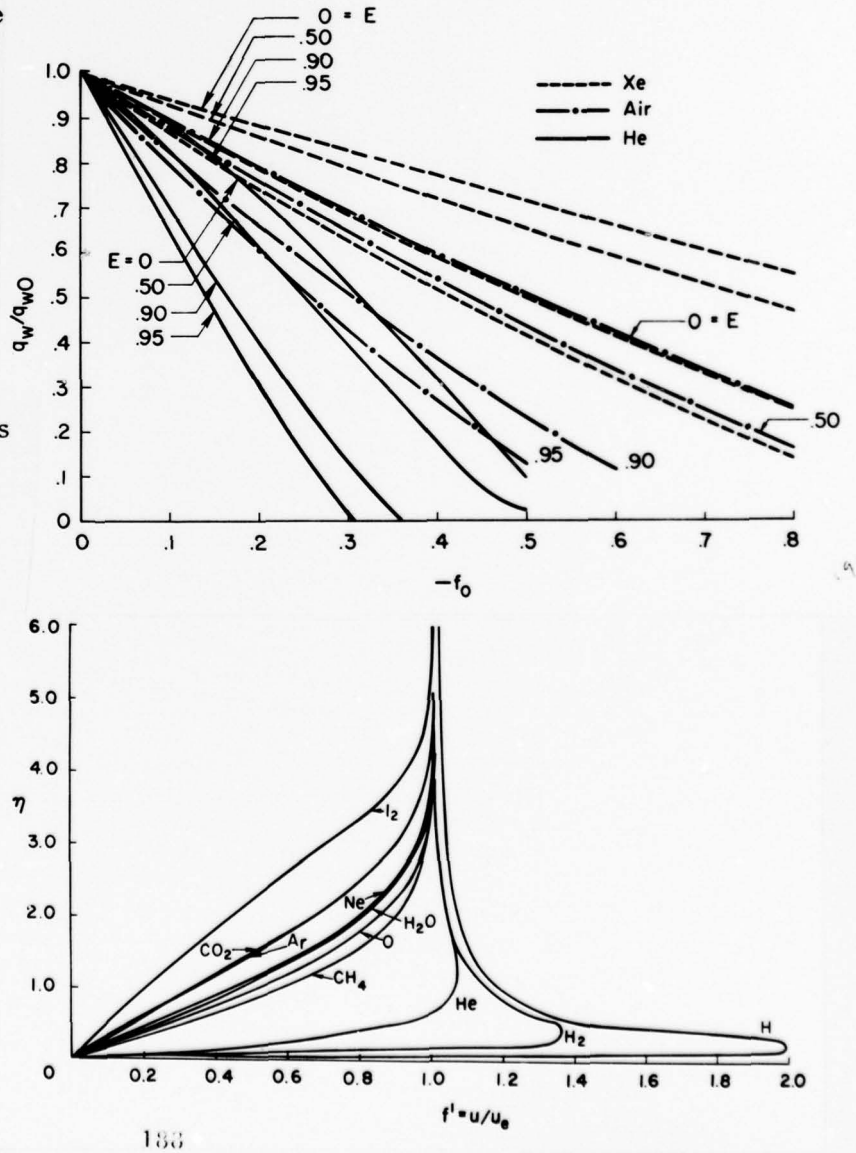

Correlation of Results

The engineering calculation of boundary layers over ablation and transpiration cooled surfaces is often accomplished by first calculating the boundary layer for zero mass transfer, and subsequently the effects of mass injection are accounted for through use of local "blockage" factors for the reduction in shear stress, mass transfer conductances and heat transfer rate. Convenient correlation functions for this purpose are the exponential functions suggested by Couette flow modeling of the boundary layer:

$$\frac{C_F}{C_{FO}} = \frac{a_{F,i}B_F}{\exp(a_{F,i}B_F)-1} \; ; \quad B_F = \frac{\dot{m}}{\rho_e u_e C_{FO}} \tag{8.5-10}$$

$$\frac{C_{Mi}}{C_{MiO}} = \frac{a_{M,i}B_{Mi}}{\exp(a_{M,i}B_{Mi})-1} \; ; \quad B_{Mi} = \frac{\dot{m}}{\rho_e u_e C_{MiO}} \tag{8.5-11}$$

$$\frac{C_H}{C_{HO}} = \frac{a_{H,i}B_H}{\exp(a_{H,i}B_H)-1} \; ; \quad B_H = \frac{\dot{m}}{\rho_e u_e C_H} \tag{8.5-12}$$

The weighting factors 'a' were determined by least square fitting of the numerical results. Correlations for a were first developed for $\beta = 0.5$, $E = 0$, $\theta_o = 0.1$ which is the situation of greatest engineering importance.

$$a_{F,i} = 1.38(M_{air}/M_i)^{5/12} \tag{8.5-13}$$

$$a_{M,i} = 1.65(M_{air}/M_i)^{10/12} \tag{8.5-14}$$

$$a_{H,i} = 1.30(M_{air}/M_i)^{3/12}(C_{P,i}/(5/2)(\mathcal{R}/M_i)) \tag{8.5-15}$$

In fact Eqs. (8.5-13 and 14) are quite adequate for $\theta_o = 0.5$ and 0.9, as well as for $\beta = 1$, i.e., for general use at stagnation points.

Next, values of a normalized with the corresponding value at $\beta = 0.5$, $E = 0$, $\theta_o = 0.1$, i.e., as given by Eqs. (8.5-13 through 15) were calculated. Denoting the resulting functions as $G_{F,i}$, $G_{M,i}$ and $G_{H,i}$, the values are tabulated in Tables 8.2, 8.3 and 8.4.

Table 8.2 Values of $G_{F,i} = \frac{a_{F,i}}{a_{F,i}|\beta=0.5,\ E=0,\ \theta_o=0.1}$

β	Species	θ_o = 0.1				θ_o = 0.5				θ_o = 0.9			
		E=0	.5	.9	.95	0	.5	.9	.95	0	.5	.9	.95
0	H	1.30	1.32	1.42	1.44	1.64	1.74	1.88	1.38	1.79	1.90	1.81	1.72
	H_2	1.19	1.21	1.19	1.22	1.44	1.44	1.63	1.59	1.49	1.59	1.79	1.62
	He	1.34	1.33	1.33	1.31	1.49	1.51	1.55	1.56	1.56	1.58	1.62	1.69
	Air	1.22	1.24	1.29	1.35	1.27	1.27	1.37	1.43	1.27	1.27	1.41	1.44
	Xe	1.38	1.40	1.48	1.50	1.35	1.39	1.41	1.43	1.34	1.34	1.39	1.43
	CCl_4	1.00	1.05	1.07	1.09	1.03	1.03	1.08	1.09	1.03	1.04	1.10	1.15
0.25	He	1.13	1.19	1.24	1.24	0.89	1.93	1.01	1.01	0.72	0.78	0.85	0.85
	Air	1.07	1.11	1.16	1.17	0.99	1.04	1.10	1.12	0.94	0.98	1.01	1.02
	Xe	1.11	1.16	1.28	1.31	1.08	1.10	1.16	1.18	1.06	1.09	1.14	1.14
0.5	H	1.00	--	--	--	0.62	--	--	--	0.45	--	--	--
	H_2	1.00	--	--	--	0.70	--	--	--	0.62	--	--	--
	He	1.00	1.09	1.15	--	0.66	0.74	0.84	--	0.56	0.63	0.69	--
	C	1.00	--	--	--	0.79	--	--	--	0.69	--	--	--
	CH_4	1.00	--	--	--	0.88	--	--	--	0.84	--	--	--
	O	1.00	--	--	--	0.79	--	--	--	0.70	--	--	--
	H_2O	1.00	--	--	--	0.82	--	--	--	0.73	--	--	--
	Ne	1.00	--	--	--	0.83	--	--	--	0.75	--	--	--
	Air	1.00	1.02	1.12	--	0.87	0.95	0.99	--	0.82	0.90	0.94	--
	A	1.00	--	--	--	0.93	--	--	--	0.91	--	--	--
	CO_2	1.00	--	--	--	0.96	--	--	--	0.94	--	--	--
	Xe	1.00	1.08	1.16	--	0.96	1.05	1.10	--	1.05	1.05	1.08	--
	CCl_4	1.00	--	--	--	1.03	--	--	--	1.07	--	--	--
	I_2	1.00	--	--	--	1.02	--	--	--	1.05	--	--	--
1.0	He	0.85	--	--	--	0.53	--	--	--	0.47	--	--	--
	Air	0.94	--	--	--	0.84	--	--	--	0.81	--	--	--
	Xe	0.90	--	--	--	0.93	--	--	--	0.95	--	--	--

Table 8.3 Values of $G_{M,i} = \frac{a_{M,i}}{a_{M,i}|\beta=0.5,\ E=0,\ \theta_o=0.1}$

β	Species	θ_o = 0.1				θ_o = 0.5				θ_o = 0.9			
		E=0	.5	.9	.95	0	.5	.9	.95	0	.5	.9	.95
0	H	1.14	1.12	1.23	1.32	1.36	1.40	1.59	1.72	1.47	1.53	1.69	1.72
	H_2	1.03	1.04	1.16	1.21	1.25	1.32	1.53	1.58	1.36	1.45	1.66	1.63
	He	1.05	1.08	1.12	1.15	1.18	1.23	1.36	1.43	1.25	1.30	1.47	1.54
	Xe	1.21	1.26	1.42	1.40	1.13	1.19	1.36	1.32	1.15	1.19	1.25	1.25
	CCl_4	1.03	1.10	1.25	1.23	0.95	1.13	1.28	1.30	1.00	1.18	1.23	1.18
0.25	He	1.08	1.07	1.07	1.17	1.12	1.15	1.28	1.33	1.12	1.15	1.29	1.34
	Xe	1.02	1.06	1.17	1.23	0.94	0.98	1.06	1.06	0.91	0.92	0.96	1.00
0.5	H	1.00	--	--	--	1.04	--	--	--	1.09	--	--	--
	H_2	1.00	--	--	--	1.06	--	--	--	1.06	--	--	--
	He	1.00	1.04	1.11	--	1.04	1.09	1.20	--	1.03	1.09	1.20	--
	C	1.00	--	--	--	1.01	--	--	--	1.00	--	--	--
	CH_4	1.00	--	--	--	1.01	--	--	--	1.00	--	--	--
	O	1.00	--	--	--	0.98	--	--	--	0.97	--	--	--
	H_2O	1.00	--	--	--	1.01	--	--	--	1.00	--	--	--
	Ne	1.00	--	--	--	1.00	--	--	--	0.98	--	--	--
	A	1.00	--	--	--	0.97	--	--	--	0.94	--	--	--
	CO_2	1.00	--	--	--	0.97	--	--	--	0.95	--	--	--
	Xe	1.00	1.00	1.04	--	0.98	0.92	0.92	--	0.96	0.87	0.89	--
	CCl_4	1.00	--	--	--	0.90	--	--	--	0.83	--	--	--
	I_2	1.00	--	--	--	0.91	--	--	--	0.85	--	--	--
1.0	He	0.96	--	--	--	0.98	--	--	--	0.98	--	--	--
	Xe	0.92	--	--	--	0.87	--	--	--	0.83	--	--	--

Table 8.4 Values of $G_{H,i} = \frac{a_{H,i}}{a_{H,i}|\beta=0.5,\ E=0,\ \theta_o=0.1}$

β	Species	θ_o = 0.1				θ_o = 0.5				θ_o = 0.9			
		E=0	.5	.9	.95	0	.5	.9	.95	0	.5	.9	.95
0	H	1.15	1.22	1.57	1.64	1.32	1.92	2.85	3.43	--	--	--	--
	H_2	1.07	1.20	1.22	1.28	1.30	1.52	2.05	2.07	--	--	--	--
	He	1.18	1.25	1.32	1.34	1.32	1.53	1.78	1.85	--	--	--	--
	Air	1.17	1.13	1.10	1.14	1.21	1.11	1.08	1.10	--	--	--	--
	Xe	1.19	1.24	1.33	1.34	1.18	1.20	1.20	1.20	--	--	--	--
	CCl_4	1.04	1.06	1.09	1.09	1.04	1.04	1.02	0.99	--	--	--	--
0.25	He	1.02	1.19	1.34	--	1.05	1.59	2.32	--	--	--	--	--
	Air	1.05	1.04	1.01	--	1.03	0.99	0.97	--	--	--	--	--
	Xe	1.04	1.10	1.20	--	0.98	1.05	1.15	--	--	--	--	--
0.5	H	1.00	--	--	--	0.94	--	--	--	0.54	--	--	--
	H_2	1.00	--	--	--	1.00	--	--	--	1.01	--	--	--
	He	1.00	1.14	1.36	--	1.00	1.70	2.62	--	0.95	--	--	--
	C	1.00	--	--	--	0.99	--	--	--	0.97	--	--	--
	CH_4	1.00	--	--	--	1.00	--	--	--	1.00	--	--	--
	O	1.00	--	--	--	0.98	--	--	--	0.95	--	--	--
	H_2O	1.00	--	--	--	1.00	--	--	--	0.99	--	--	--
	Ne	1.00	--	--	--	0.97	--	--	--	0.95	--	--	--
	Air	1.00	0.99	0.99	--	0.99	0.97	0.95	--	0.97	--	--	--
	A	1.00	--	--	--	0.96	--	--	--	0.95	--	--	--
	CO_2	1.00	--	--	--	0.99	--	--	--	0.97	--	--	--
	Xe	1.00	1.05	1.14	--	1.06	1.04	1.19	--	0.99	--	--	--
	CCl_4	1.00	--	--	--	0.96	--	--	--	0.93	--	--	--
	I_2	1.00	--	--	--	0.97	--	--	--	0.94	--	--	--
1.0	He	0.93	--	--	--	0.91	--	--	--	--	--	--	--
	Air	0.96	--	--	--	0.94	--	--	--	--	--	--	--
	Xe	0.96	--	--	--	0.93	--	--	--	--	--	--	--

Example 8.2

Rework Example 6.1 accounting for variable property effects.

$B_h' = 0.608$ is unchanged. With $\dot{m} = \rho_e u_e C_{HO} B_H = \rho_e u_e C_H B_h'$, Eq. (8.5-12) may be rearranged as

$$\frac{C_H}{C_{HO}} = \frac{\ell n(1 + a_{H,i} B_h')}{a_{H,i} B_h'}$$

and from Eq. (8.5-15),

$$a_{H,i} = 1.30(M_{air}/M_{He})^{3/12}(C_{p\,He}/(5/2)(R/M_{He}))$$

$$= 1.30\ (29/4)^{3/12} \text{ since the second term is unity for a monatomic gas.}$$

$$= 2.13.$$

$$\frac{C_H}{C_{HO}} = \frac{\ell n(1 + (2.13)(0.608))}{(2.13)(0.608)} = 0.642$$

$$\dot{m} = \rho_e u_e C_{HO}(C_H/C_{HO}) B_h'$$

$$= (120)(0.642)(0.608)$$

$$= 46.8\ \text{lb/ft}^2\ \text{hr}$$

Alternative Correlation Schemes: Reference States

The reference state approach, wherein constant property solutions are used with properties evaluated at some reference state, has been often boundary layers. Baron [30], and subsequently Gross et al. [31] showed that for a given geometry ($\beta = 0$) and injectant, C_F/C_{FO} and C_H/C_{HO} was a unique function of a modified flowing parameter $(\dot{m}/\rho_e u_e)(Re_s/C_r^{\frac{1}{2}})$ irrespective of wall cooling or Mach number. $C_r = (\rho_r \mu_r)/(\rho_e \mu_e)$ is evaluated for the free stream gas at the Eckert reference enthalpy, $h_r = 0.5(h_w + h_e) + 0.22 r_0 (u_e^2/2)$. Gross et al. [31] and more recently Simon et al. [32,33] further correlated the effect of injectant species by introduction empirical factors involving the molecular weights of the injectant and free stream gases. Thus the final correlations for foreign gas injection are not truly

the result of using a reference state approach since property variations due to mixture composition are not included in the reference state formulation. To illustrate the success of the $C_r^{\frac{1}{2}}$ approach for air injection the results of Wortman for $\beta = 0$ are shown correlated in the Figures that follow. For skin friction the correlation is excellent for all the parameter values calculated.

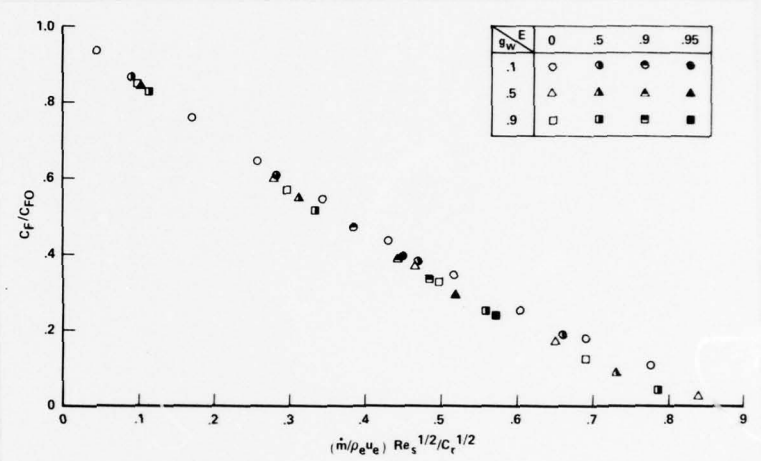

For heat transfer the data points for $\theta_o = 0.9$ and E = 0.5, 0.9 and 0.95 did not correlate and have been omitted. At these parameter values the heat transfer is small and can change sign with blowing: the resultant behavior of C_H/C_{HO} can be quite erratic.

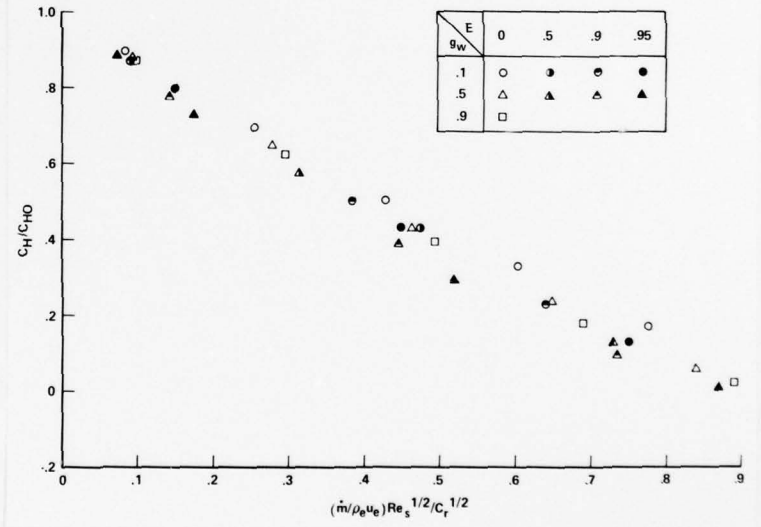

A true reference state formulation for foreign gas injection was developed by Knuth [34]. The reference state was based on a Couette flow analysis of foreign gas injection in which thermodynamic properties were allowed to vary with composition, but transport properties were held constant. For species 1 injection and a free-stream of pure species 2,

$$h_r = 0.5(h_w+h_e) + 0.2r_{Or}(u_e^2/2) + 0.1[B_{Hr}-2B_{Mr}) \frac{C_{P1}-C_{Pr}}{C_{Pr}}](h_w-h_e) \qquad (8.4\text{-}16)$$

$$K_{1r} = 1 - \frac{M_2}{M_1-M_2} \ell n[M_2/M_w(K_{1,w}/K_{1,w}-1)] \qquad (8.4\text{-}17)$$

At the time this formulation was developed (1965) the numerical data with which to evaluate it, was sparse. The numerical data obtained by Wortman [12] can now be used for a more thorough test of the formulation. The Figures show an evaluation, of skin friction and heat transfer respectively, for a flat plate with air into air injection. It is seen that the correlation is much inferior to the $C_r^{\frac{1}{2}}$ scheme shown in the Figures. It seems that the model is an inadequate representation of the blown high speed laminar boundary layer.

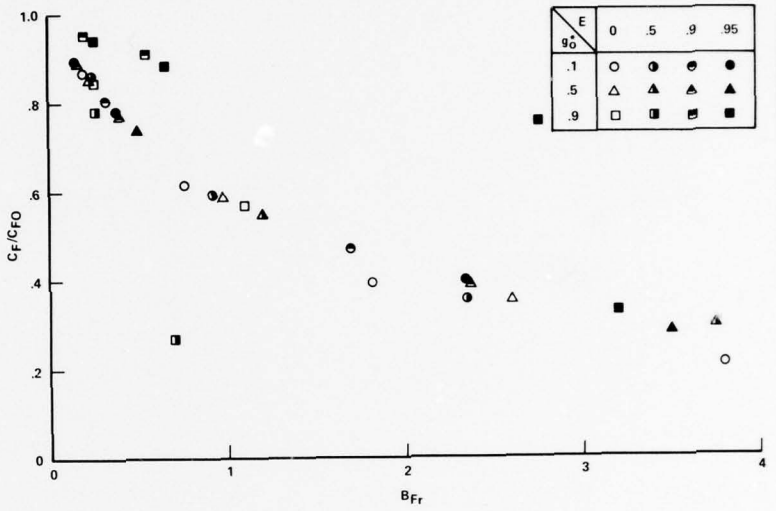

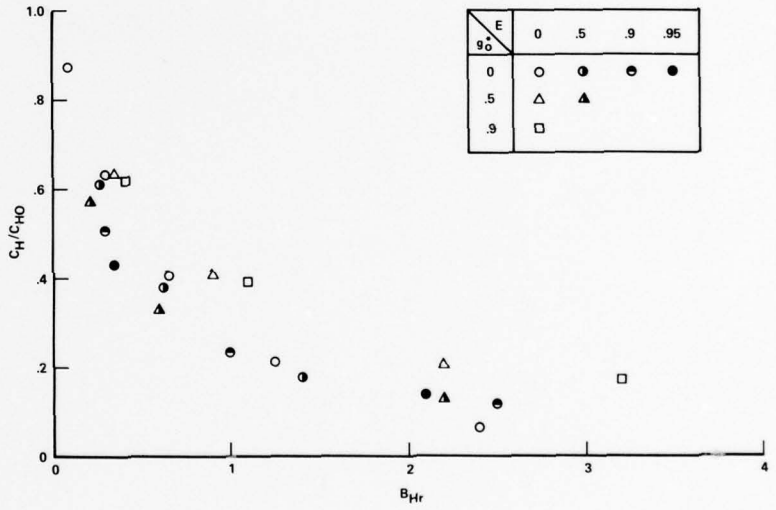

The reference state approach has the attractive feature that the reference state should be independent of the precise property data used, and independent of the combination of injectant and free-stream species. On the other hand the resulting calculation method is somewhat complex since

the wall composition must be used: in the case where this is known from thermodynamic considerations the problem is straightforward, but for inert gas injection $K_{l,w}$ must be obtained using a correlation of C_{Ml}, i.e., an iterative scheme is required.

REFERENCES FOR CHAPTER 8

1. H. W. Emmons and D. C. Leigh, "Tabulation of the Blasius function with blowing and suction", Aeronautical Research Council, Rept. FM 1915 (1953).

2. J. Newman, Electrochemical Systems, Prentice-Hall, NJ (1973).

3. H. Weyl, "On the differential equations of the simplest boundary-layer problems", Ann. Math. 43, 381-407 (1942).

4. J. P. Hartnett and E. R. G. Eckert, "Mass transfer cooling in a laminar boundary layer with constant fluid properties", Trans ASME, 79, 247-254 (1957).

5. H. L. Evans, "Laminar Boundary-Layer Theory", Addison-Wesley, Mass. (1968).

6. C. F. Dewey, Jr. and J. F. Gross, "Exact similar solutions of the laminary boundary-layer equations", Advances in Heat Transfer, Vol. 4, edited by J. P. Hartnett and T. F. Irvine, Jr., p. 317, Academic Press (1967).

7. F. K. Moore, in Theory of Laminar Flows, Princeton University Press, Princeton (1964).

8. J. O. Hirschfelder, "Heat transfer in chemically reacting mixtures", J. Chem. Phys., 26, 274 (1957).

9. J. N. Butler and R. S. Brokaw, "Thermal conductivity of gas mixtures in chemical equilibrium", J. Chem. Phys. 26, 1636 (1957).

10. C. F. Hansen, "Approximations for the thermodynamic and transport properties of high temperature air", NASA TR R-50 (1959).

11. S. Bennet, J. M. Yos, C. F. Knapp, J. Morris and W. L. Bade, "Theoretical and experimental studies of high temperature gas transport properties", Final Report AVCO/RAD-TR-67-7, May (1965).

12. A. Wortman, "Mass transfer in self-similar laminar boundary layer flows", Ph.D. Dissertation, School of Engineering and Applied Science, University of California, Los Angeles (1969).

13. A. F. Mills and A. Wortman, "Two-dimensional stagnation point flows of binary mixtures", Int. J. Heat Mass Transfer 15, 969-987 (1972).

14. W. M. Kays, Convective Heat and Mass Transfer, McGraw-Hill, New York (1966).

15. J. A. Fay and F. R. Ridell, "Theory of stagnation point heat transfer in dissociated air", J. Aero. Sciences 25, 73 (1958).

16. J. Hilsenrath and C. Beckett, "Tables of thermodynamic properties of argon-free air to 15,000 K", AEDC-TN-56-12, Arnold Engineering Development Center, USAF (1956).

17. W. E. Moeckel and K. C. Weston, "Composition and thermodynamic properties of air in chemical equilibrium", NACA TN 4265 (1958).

18. R. W. Detra, N. H. Kemp and F. R. Ridell, "Addendum to: Heat transfer to satellite vehicles re-entering the atmosphere", Jet Propulsion 27, 1256 (1957).

19. N. B. Cohen, "Boundary-layer similar solutions and correlation equations for laminar heat transfer distribution in equilibrium air at velocities up to 41,100 ft/s", NASA TR R-118 (1961).

20. N. B. Cohen, "Correlation formulas and tables of density and some transport properties of equilibrium dissociating air for use in solutions of the boundary layer equations", NASA TN D-194 (1960).

21. H. Hoshizaki, "Heat transfer in planetary atmospheres at supersatellite speeds", ARS Journal 32, 1544 (1962).

22. J. A. Fay, "Hypersonic heat transfer in the air laminar boundary layer", in W. C. Nelson, ed., The High Temperature Aspects of Hypersonic Flow, Pergamon Press (1962).

23. R. M. Kendall and E. P. Bartlett, "Non-similar solution of the multicomponent laminar boundary layer by an integral matrix method", AIAA Journal 6, 1039-1047 (1968).

24. A. F. Mills and A. V. Gomez, "Heat transfer correlations for hypersonic axisymmetric stagnation point flows. Part I, Comparison of predictions and provisional recommendations", TRW IOC 68-3324.10-4, TRW Systems, Redondo Beach (1968).

25. J. R. Baron, "Thermal diffusion effects in mass transfer", Int. J. Heat Mass Transfer 6, 1025-1033 (1963).

26. E. M. Sparrow, W. J. Winkowycz and E. R. G. Eckert, "Diffusion-thermo effects in stagnation-point flow of air with injection of gases of various molecular weights into the boundary layer", AIAA Journal 2, 652-659 (1964).

27. A. F. Gollnick, Jr., "An experimental study of thermal diffusion effects on a partially porous mass transfer cooled hemisphere", Int. J. Heat Mass Transfer 7, 699-708 (1964).

28. A. Wortman and A. F. Mills, "Accelerating compressible laminar boundary layer flows of binary gas mixtures", Archiwum Mechaniki Stosowanej 26, 479-497 (1974).

29. J. O. Hirschfelder, C. F. Curtiss and R. B. Bird, Molecular Theory of Gases and Liquids, 2nd ed., Wiley, New York (1964).

30. J. R. Baron, "The binary-mixture boundary layer associated with mass transfer cooling at high speeds, MIT Naval Supersonic Laboratory", Tech. Report 190 (1956).

31. J. F. Gross, J. P. Hartnett, D. J. Masson and C. Gazley, Jr., "A review of binary laminar boundary layer characteristics", Int. J. Heat Mass Transfer 3, 198-221 (1961).

32. C. S. Liu, J. P. Hartnett and H. A. Simon, "Mass transfer cooling of laminar boundary layers with hydrogen injected into nitrogen and carbon dioxide free streams", III International Heat Transfer Conference, Paper No. 83, Chicago, ASME (1966).

33. H. A. Simon, J. P. Hartnett and C. S. Liu, "Transpiration cooling correlations for air and non-air free streams", AIAA Paper No. 68-758, presented at the AIAA 3rd Thermophysics Conference, Los Angeles, June (1968).

34. E. L. Knuth, "Use of reference states and constant property solutions in predicting mass-, momentum-, and energy-transfer rates in high speed laminar flows", Int. J. Heat Mass Transfer 6, 1-22 (1963).

CHAPTER 9

TURBULENT BOUNDARY LAYER ANALYSIS

9.1 INTRODUCTION

The engineering analysis of turbulent flows is based on time-averaged conservation equations of mass, momentum, chemical species and energy. The time-averaging procedure for variable density boundary layer equations is algebraically very complex, as can be seen, for example, in the developments of van Driest [1] and Cebeci and Smith [2]. Here we will present a rather simplified development, which will be sufficient to illustrate some essential features of the procedure, and allow discussion of results pertinent to re-entry vehicle turbulent boundary layer analysis. The simplifying assumptions are (i) binary inert gas mixture, (ii) zero pressure gradient, (iii) hydraulically smooth wall, (iv) no body forces, and (v) no second-order diffusion effects. Then the boundary layer forms of the equations of mass, momentum, chemical species and static enthalpy, are

$$\frac{\partial \rho}{\partial t} + \frac{\partial}{\partial x}(\rho u) + \frac{\partial}{\partial y}(\rho v) = 0 \tag{9.1-1}$$

$$\rho \frac{\partial u}{\partial t} + \rho u \frac{\partial u}{\partial x} + \rho v \frac{\partial u}{\partial y} = \frac{\partial}{\partial y}(\tau_{xy}) \tag{9.1-2}$$

$$\rho \frac{\partial K_1}{\partial t} + \rho u \frac{\partial K_1}{\partial x} + \rho v \frac{\partial K_1}{\partial y} = \frac{\partial}{\partial y}(-j_{1y}) \tag{9.1-3}$$

$$\rho \frac{\partial h}{\partial t} + \rho u \frac{\partial h}{\partial x} + \rho v \frac{\partial h}{\partial y} = \frac{\partial}{\partial y}[(-q_y^c) + (-j_{1y})(h_1 - h_2)] + \tau_{xy} \frac{\partial u}{\partial y} \tag{9.1-4}$$

Each of the conservation equations can be cast in the general form

$$\underbrace{\rho \frac{\partial \phi}{\partial t}}_{\text{accumulation}} + \underbrace{\rho u \frac{\partial \phi}{\partial x} + \rho v \frac{\partial \phi}{\partial y}}_{\text{convection}} = \underbrace{\frac{\partial}{\partial y} F}_{\text{diffusion}} + \underbrace{S}_{\text{source}} \tag{9.1-5}$$

Multiplying the mass conservation equation by ϕ gives

$$\phi \frac{\partial \rho}{\partial t} + \phi \frac{\partial}{\partial x}(\rho u) + \phi \frac{\partial}{\partial y}(\rho v) = 0 \tag{9.1-6}$$

which when added to Eq. (9.1-5) results in

$$\frac{\partial}{\partial t}(\rho\phi) + \frac{\partial}{\partial x}(\rho u\phi) + \frac{\partial}{\partial y}(\rho v\phi) = \frac{\partial}{\partial y} F + S \tag{9.1-7}$$

Now for simplicity we take ρ = constant and express each dependent variable as a sum of a mean and a fluctuating component,

$$\phi = \bar{\phi} + \phi'; \quad u = \bar{u} + u', \; v = \bar{v} + v', \text{ etc.}$$

where $\bar{\phi} = \frac{1}{\tau}\int_0^\tau \phi dt$, and τ is sufficiently long for the average to be meaningful. Substituting in Eq. (9.1-7) and time-averaging,

$$\overline{\frac{\partial}{\partial t}\rho(\bar{\phi} + \phi')} + \overline{\frac{\partial}{\partial x}\rho(\bar{u} + u')(\bar{\phi} + \phi')} + \overline{\frac{\partial}{\partial y}(\bar{v} + v')(\bar{\phi} + \phi')}$$

$$= \overline{\frac{\partial}{\partial y}(\bar{F} + F')} + \overline{\bar{S} + S'} \tag{9.1-8}$$

Noting, for example, that

$$\overline{\frac{\partial}{\partial x}\rho\bar{u}} = \frac{\partial}{\partial x}\rho\bar{u}$$

$$\overline{\bar{u}u'} = \bar{u}\,\overline{u'} = 0$$

$$\overline{F'} = 0$$

and also that $\partial\bar{\phi}/\partial t = 0$ if the mean flow is steady, Eqn. (9.1-8) becomes

$$\frac{\partial}{\partial x}(\rho\bar{u}\bar{\phi}) + \frac{\partial}{\partial x}(\rho\overline{u'\phi'}) + \frac{\partial}{\partial y}(\rho\bar{v}\bar{\phi}) + \frac{\partial}{\partial y}(\rho\overline{v'\phi'}) = \frac{\partial}{\partial y}\bar{F} + \bar{S} \tag{9.1-9}$$

However boundary layer scaling indicates $\frac{\partial}{\partial x}(\rho\overline{u'\phi'}) \ll \frac{\partial}{\partial y}(\rho\overline{v'\phi'})$, and can be neglected. Then subtracting the mean mass conservation equation times $\bar{\phi}$ gives

$$\rho\bar{u}\frac{\partial\bar{\phi}}{\partial x} + \rho\bar{v}\frac{\partial\bar{\phi}}{\partial y} = \frac{\partial}{\partial y}(\bar{F} - \rho\overline{v'\phi'}) + \bar{S} \tag{9.1-10}$$

The term $\overline{v'\phi'}$ is often called the Reynolds flux (Reynolds stress when $\phi' = u'$) and must be modeled in order to proceed. We define turbulent eddy diffusivities as

$$-\rho\overline{u'v'} = \rho\varepsilon_M \frac{\partial\bar{u}}{\partial y} \tag{9.1-11a}$$

$$-\rho\overline{u'K'_1} = \rho\varepsilon_D \frac{\partial\bar{K}_1}{\partial y} \tag{9.1-11b}$$

$$-\rho\overline{u'h'} = \rho\varepsilon_H \frac{\partial \bar{h}}{\partial y} \tag{9.1-11c}$$

The turbulent Schmidt number is $Sc_t = \varepsilon_M/\varepsilon_D$, and the turbulent Prandtl number is $Pr_t = \varepsilon_M/\varepsilon_H$. Also flux laws are defined as

$$\bar{\tau}_{xy} = \bar{\mu} \frac{\partial \bar{u}}{\partial y} \tag{9.1-12a}$$

$$\bar{j}_{1y} = -\overline{\rho\mathcal{D}}_{12} \frac{\partial \bar{K}_1}{\partial y} \tag{9.1-12b}$$

$$\bar{q}^c_y = -\bar{k} \frac{\partial \bar{T}}{\partial y} \tag{9.1-12c}$$

where $\bar{\mu}$, $\overline{\rho\mathcal{D}}_{12}$ and $\bar{k}$ are molecular transport properties. The conservation equations are then

$$\frac{\partial}{\partial x}(\rho u) + \frac{\partial}{\partial y}(\rho v) = 0 \tag{9.1-13}$$

$$\rho u \frac{\partial u}{\partial x} + \rho v \frac{\partial u}{\partial y} = \frac{\partial}{\partial y}\left[(\mu+\rho\varepsilon_M)\frac{\partial u}{\partial y}\right] \tag{9.1-14}$$

$$\rho u \frac{\partial K_1}{\partial x} + \rho v \frac{\partial K_1}{\partial y} = \frac{\partial}{\partial y}\left[\left(\frac{\mu}{Sc} + \frac{\rho\varepsilon_M}{Sc_t}\right)\frac{\partial K_1}{\partial y}\right] \tag{9.1-15}$$

$$\rho u \frac{\partial h}{\partial x} + \rho v \frac{\partial h}{\partial y} = \frac{\partial}{\partial y}\left[\left(\frac{\mu}{Pr} + \frac{\rho\varepsilon_M}{Pr_t}\right)\frac{\partial h}{\partial y}\right]$$
$$+ \frac{\partial}{\partial y}\left\{\left[\left(\frac{\mu}{Sc} + \frac{\rho\varepsilon_M}{Sc_t}\right) - \left(\frac{\mu}{Pr} + \frac{\rho\varepsilon_M}{Pr_t}\right)\right]\frac{\partial K_1}{\partial y}(h_1-h_2)\right\} + (\mu+\rho\varepsilon_M)\left(\frac{\partial u}{\partial y}\right)^2 \tag{9.1-16}$$

where u, v, k, h, ρ, etc. are now time-averaged quantities.

Some controversy exists concerning the viscous dissipation term in Eq. (9.1-16). In the time-averaging of the static enthalpy equation we had

$$S = \mu\left(\frac{\partial u}{\partial y}\right)^2$$

$$\bar{S} = \mu\overline{\left[\frac{\partial(\bar{u}+u')}{\partial y}\right]^2} = \mu\left[\overline{\left(\frac{\partial \bar{u}}{\partial y}\right)^2} + 2\,\overline{\frac{\partial \bar{u}}{\partial y}\frac{\partial u'}{\partial y}} + \overline{\left(\frac{\partial u'}{\partial y}\right)^2}\right] = \mu\left(\frac{\partial \bar{u}}{\partial y}\right)^2 + \mu\overline{\left(\frac{\partial u'}{\partial y}\right)^2}$$

Most previous workers studying high speed turbulent boundary layers have used

$$\bar{S} = (\mu+\rho\varepsilon_M)\left(\frac{\partial\bar{u}}{\partial y}\right)^2 \tag{9.1-17}$$

which implies $\rho\varepsilon_M \left(\frac{\partial\bar{u}}{\partial y}\right)^2 = \mu\overline{\left(\frac{\partial u'}{\partial y}\right)^2}$ (9.1-18)

Van Driest [1] established Eq. (9.1-17) by time-averaging the total enthalpy equation rather than the static enthalpy equation, and in the process neglected several terms based on order of magnitude arguments, and physical intuition. Rubin [3] proposed that the proper form of the viscous dissipation term should be

$$\bar{S} = \mu\left(\frac{\partial\bar{u}}{\partial y}\right)^2 \tag{9.1-19}$$

therefore implying that the term $\mu\overline{(\partial u'/\partial y)^2}$ is negligible. But this term physically represents the dissipation of kinetic energy stored in turbulent eddies by molecular viscosity, and cannot be ignored. In fact calculations by Landis [4] show that use of Eq. (9.1-19) in boundary layer flows leads to poor agreement with experiment.

A clearer understanding can be obtained through examination of the conservation equation for kinetic energy of turbulence. This equation is obtained (see, for example, Hunt [5]) in the following manner. Let M denote the instantaneous momentum equation, and K the kinetic energy of turbulence equation, then

$$K = \overline{uM} - \bar{u}\bar{M} = 0 \tag{9.1-20}$$

The resulting equation can be cast in the form [6]

$$\underbrace{\rho\bar{u}\frac{\partial k}{\partial x} + \rho\bar{v}\frac{\partial k}{\partial y}}_{\text{convection}} = \underbrace{\rho\varepsilon_M\left(\frac{\partial\bar{u}}{\partial y}\right)^2}_{\text{production}} + \underbrace{\frac{\partial}{\partial y}\left[(\mu+\rho\varepsilon_K)\frac{\partial k}{\partial y}\right]}_{\text{apparent diffusion}} - \underbrace{\mu\overline{\left(\frac{\partial u'}{\partial y}\right)^2}}_{\text{dissipation}} \tag{9.1-21}$$

where $k = \frac{1}{2}(\overline{u'^2}+\overline{v'^2}+\overline{w'^2})$, and ε_K is an eddy diffusivity for transport of kinetic energy of turbulence. It can be seen that, if the turbulent energy produced from the mean flow is dissipated at the same location in flow

(no convection or apparent diffusion), then

$$\rho\varepsilon_M \left(\frac{\partial \bar{u}}{\partial y}\right)^2 = \mu \overline{\left(\frac{\partial u'}{\partial y}\right)^2}$$

which is Eqn. (9.1-18). Such a turbulent flow is said to be in "local equilibrium", and flows near walls always approximate this condition. For the engineering calculation of turbulent boundary layers on re-entry vehicles the local equilibrium postulate is quite adequate.

An alternative, and more compact, way to represent the diffusive terms in the Eqs. (9.1-14, 15 and 16) is to define an effective viscosity, and effective Schmidt and Prandtl numbers,

$$\mu_{eff} = \mu + \rho\varepsilon_M \tag{9.1-22}$$

$$\frac{\mu_{eff}}{Sc_{eff}} = \frac{\mu}{Sc} + \frac{\rho\varepsilon_M}{Sc_t} \; ; \quad \frac{\mu_{eff}}{Pr_{eff}} = \frac{\mu}{Pr} + \frac{\rho\varepsilon_M}{Pr_t} \tag{9.1-23}$$

To complete the mathematical formulation there is required a specification of ε_M, Sc_t and Pr_t. The most widely used specifications of ε_M are based on Prandtl's mixing length model [7], which leads to

$$\varepsilon_M = C\ell_m^2 \left|\frac{\partial u}{\partial y}\right| \tag{9.1-24}$$

with ℓ_m proportional to distance from the wall in the inner region, and ℓ_m = constant in the outer region of the boundary layer. Sc_t and Pr_t are usually taken to be constants across the entire boundary layer. Specification of ε_M will be discussed in detail in §9.4.

9.2 REVIEW OF VELOCITY PROFILES AND SKIN FRICTION FOR INCOMPRESSIBLE FLOW ALONG A SMOOTH FLAT PLATE [8, 9]

Velocity Profiles

In contrast to laminar boundary layers, a turbulent boundary layer has a rather well defined edge, and hence thickness δ. When turbulent velocity

profiles are plotted in the form u/u_e vs. y/δ they do not plot as a single curve, but depend on $Re_x = u_e x/\nu$. (Recall that for a laminar boundary layer u/u_e vs. y/δ with δ appropriately scaled, viz. $\delta(u_e/\nu x)^{\frac{1}{2}}$ = constant, does plot on a single curve.) The Figure shows typical velocity profiles (including some for rough walls).

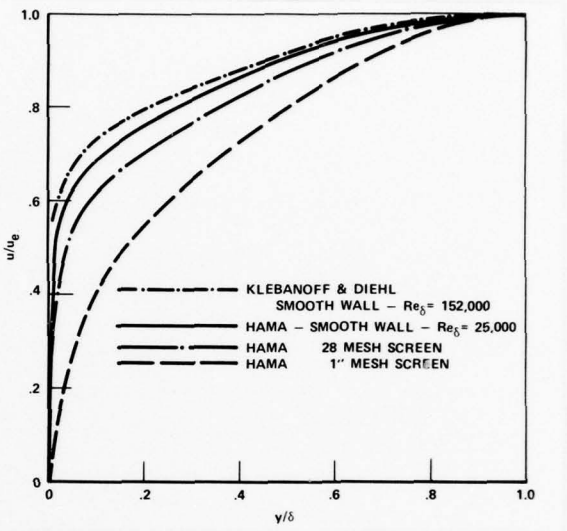

If we look for a scaling factor which depends on wall shear stress, or equivalently the skin friction coefficient $C_F = \tau_w/\frac{1}{2}\rho u_e^2$, we find that $(u/u_e)(2/C_F)^{\frac{1}{2}}$ does bring the profiles into co-incidence, except very near the wall. If $v^* \equiv (\tau_w/\rho)^{\frac{1}{2}}$ and $u^+ \equiv u/v^*$ then we find it convenient to represent this result as a plot of $u^+ - u_e^+$ vs. y/δ, as shown in the Figure. The equation of such a universal curve is called a "velocity defect law". (Note that rough and smooth walls obey the same defect law.) We term $(u_e^+ - u^+)$ and y/δ the "outer variables" and emphasize that they do not bring the profiles into co-incidence very near to the wall.

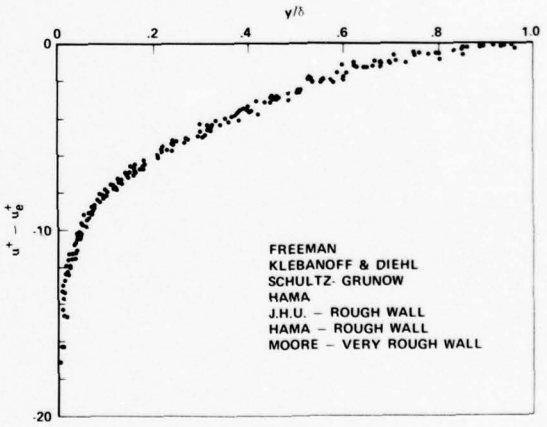

If we now turn to the near wall region we note from experiment that for an impermeable wall the shear stress is constant near the wall. The momentum equation Eq. (9.1-14) may be written

$$\rho u \frac{\partial u}{\partial x} + \rho v \frac{\partial u}{\partial y} = \frac{\partial \tau}{\partial y} \qquad (9.2\text{-}1)$$

thus we see that a constant shear stress implies that the convective terms on the l.h.s. of Eq. (9.2-1) are negligible near the wall. In the viscous sublayer, where molecular viscosity dominates, we have

$$\tau = \mu \frac{du}{dy} = \tau_w \tag{9.2-2}$$

$$\text{i.e., } u \propto y \text{ or } u^+ = y^+, \quad \text{where } u^+ = \frac{u}{v^*} \tag{9.2-3}$$

$$y^+ = \frac{y v^*}{\nu}$$

If velocity profiles are plotted in terms of these "inner variables", as is done in the Figure, we see that there is a good correlation, even outside the viscous sublayer, and indeed in a region where the outer variables also correlate the profiles, and there must thus be a unique relationship between the parameters involved. The "overlap law" can be derived using only this fact, as follows. The velocity profiles are

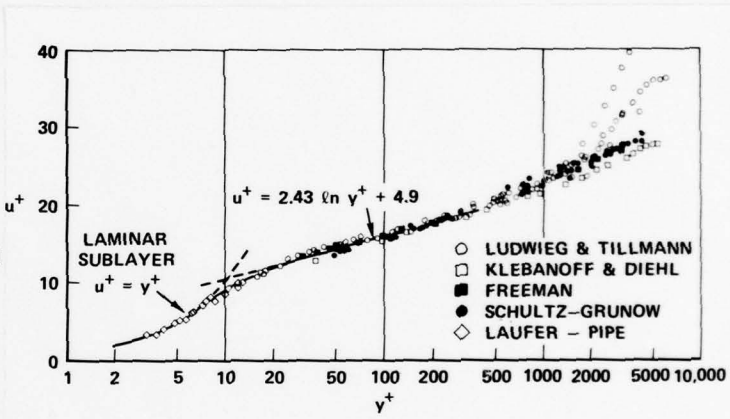

outer region: $u^+ - u_e^+ = f\left(\frac{y}{\delta}\right)$ or $u^+ = f\left(\frac{y}{\delta}\right) + u_e^+$

inner region: $u^+ = g(y^+)$ or $u^+ = g\left(\frac{y}{\delta} \cdot \frac{\delta v^*}{\nu}\right)$

Comparing the two we see that the effect of an additive factor outside the function f must be the same as an multiplicative factor inside g. The logarithm is the only function which has this property. Thus in the overlap region we have

$$u^+ - u_e^+ = A \ell n \frac{y}{\delta} + B \tag{9.2-4}$$

$$u^+ = A \ell n \, y^+ + C \tag{9.2-5}$$

and $B + u_e^+ = C + A \ell n \frac{\delta v^*}{\nu}$

But $u_e^+ = \frac{u_e}{v^*} = (2/C_F)^{\frac{1}{2}}$,

thus $(2/C_F)^{\frac{1}{2}} = A\ell n\ Re_\delta\ (C_F/2)^{\frac{1}{2}} + C - B$ (9.2-6)

and in fact it is the skin friction law $C_F = C_F\ (Re_\delta)$ which relates the inner and outer variables. From experiment,

$(A,C) \simeq (\frac{1}{0.40}, 5.5)$ Nikuradse, 1930 (pipe flow)

$\simeq (\frac{1}{0.41}, 5.0)$ Coles, 1955

The constant B is different for pipe flows and external flows:

flat plate $B \simeq -2.35$ Schultz-Grunow, 1940

pipe flow $B \simeq -0.65$ Laufer, 1951

The Figure shows flat plate velocity profiles as a function of Re_δ, and shows that a relatively small region is actually fitted by the logarithmic law.

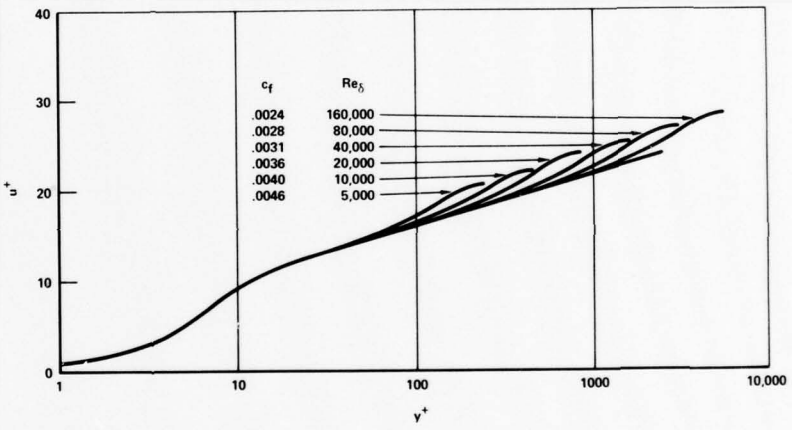

Skin Friction

Eq. (9.2-6) is a *local* skin friction law inasmuch as it relates $C_F/2$ to the local value of Re_δ. In order to obtain $C_F/2$ as a function of position along the plate, the momentum conservation equation in some form must be used. First we will use the integral momentum equation, which reduces to

$$\frac{d\theta}{dx} = \frac{C_F}{2} \tag{9.2-7}$$

where $\theta = \int_0^\infty \frac{u}{u_e}(1 - \frac{u}{u_e})\ dy$ is the momentum thickness. Refining $Re_x = u_e x/\nu$ and $Re_\theta = u_e\theta/\nu$, then Eq. (9.2-7) becomes

$$C_F = 2\ \frac{dRe_\theta}{dRe_x} \tag{9.2-8}$$

Dimensional analysis suggests $C_F = C_F(Re_\theta)$ only, thus

$$Re_x = 2\int_0^{Re_\theta} \frac{dRe_\theta}{C_F(Re_\theta)} \tag{9.2-9}$$

We require $C_F(Re_\theta)$. Our starting point is the outer region defect law which for a flat plate an appropriate correlation is

$$u^+ = A\ell n\ y^+ + C + 2.5\ \sin^2\ (\frac{\pi}{2}\frac{y}{\delta}) \tag{9.2-10}$$

Integration of Eq. (9.2-10) to give the displacement and momentum thicknesses yields, for A = 2.5,

$$\frac{\delta^*}{\delta} = \frac{3.75}{u_e^+} \quad \text{where } u_e^+ = (2/C_f)^{\frac{1}{2}} \tag{9.2-11}$$

$$\frac{\theta}{\delta} = \frac{3.75}{u_e^+} - \frac{24.8}{u_e^{+2}} \tag{9.2-12}$$

The skin friction in the form of u_e^+ is related to Re_δ by substituting $y = \delta$, $u = u_e$ in Eq. (9.2-10), for C = 5.5,

$$u_e^+ = 2.5\ \ell n\ (Re_\delta/u_e^+) + 8.0 \tag{9.2-13}$$

Eliminating δ between Eqs. (9.2-12 and 13) gives

$$Re_\theta = u_e^+\ (\frac{3.75}{u_e^+} - \frac{24.8}{u_e^{+2}})\ e^{0.4(u_e^+-8)} \tag{9.2-14}$$

Table 9.1 shows some numerical values. Power law approximations to the numerical data are:

u_e^+	C_F	Re_θ	Re_δ	$H=\delta^*/\theta$
20	0.00500	305	2,430	1.493
25	0.00320	2,480	22,450	1.359
30	0.00222	19,400	199,000	1.282
35	0.00163	149,000	1,716,000	1.233
40	0.00125	1,134,000	14,890,000	1.198

$$C_F \simeq 0.012\ Re_\theta^{-1/6} \simeq 0.018\ Re_\delta^{-1/6} \simeq 0.0128\ Re_{\delta^*}^{-1/6} \tag{9.2-15}$$

which are accurate to within 4%. Also $\delta \sim 8\delta^* \sim 11\theta$. Now substituting in

Eq. (9.2-9):

$$Re_x = 2\int_0^{Re_\theta} \frac{dRe_\theta}{0.012\ Re_\theta^{-1/6}}$$

or $$Re_\theta = 0.0142\ Re_x^{6/7} \qquad (9.2\text{-}16)$$

thus $$C_F = 0.025\ Re_x^{-1/7} \qquad (9.2\text{-}17)$$

which agrees well with experiment (a little low) in the range $10^5 < Re_x < 10^9$. Also

$$Re_\delta = 0.14\ Re_x^{6/7};\quad Re_{\delta^*} = 0.018\ Re_x^{6/7} \qquad (9.2\text{-}18,19)$$

Notice that δ, δ^* and θ grow almost linearly with x, in contrast to the laminar boundary layer growth rate of $x^{\frac{1}{2}}$.

If we now neglect the outer wake, i.e., by deleting $\sin^2(\frac{\pi}{2}\frac{y}{\delta})$ in Eq. (9.2-10), and repeat the analysis, then we obtain

$$C_F = 0.027\ Re_x^{-1/7} \qquad (9.2\text{-}20)$$

which is about 8% higher than Eq. (9.2-17). Actually the experimental data are bracketed by the two expressions, and is best represented as

$$C_F = 0.026\ Re_x^{-1/7} \qquad (9.2\text{-}21)$$

Thus for a flat plate we see that the outer wake contributes little to the skin friction calculation.

Guided by the above result which showed the wake region to be of minor importance, we now develop an approach based on the differential form of momentum conservation equation, and inner variables.

continuity: $$\frac{\partial u}{\partial x} + \frac{\partial v}{\partial y} = 0 \qquad (9.2\text{-}22)$$

momentum: $$u\frac{\partial u}{\partial x} + v\frac{\partial u}{\partial y} = \frac{1}{\rho}\frac{\partial \tau}{\partial y} \qquad (9.2\text{-}23)$$

Assume that u(x,y) is correlated by the inner variables throughout the boundary layer,

$$u^+ = \frac{u(x,y)}{v^*(x)} = g(y^+) \text{ only} \qquad (9.2\text{-}24)$$

i.e., the wake region is neglected so that δ does not appear as a parameter of the velocity profile. Then for the transformation $x,y \to x,y^+$,

$$\frac{\partial}{\partial x} = \frac{\partial}{\partial x}\frac{\partial x}{\partial x} + \frac{\partial}{\partial y^+}\frac{\partial y^+}{\partial x} = \frac{\partial}{\partial x}\bigg|_{y^+} + \frac{y^+}{v^*}\frac{dv^*}{dx}\frac{\partial}{\partial y^+}\bigg|_x$$

$$\frac{\partial}{\partial y} = \frac{\partial}{\partial x}\frac{\partial x}{\partial y} + \frac{\partial}{\partial y^+}\frac{\partial y^+}{\partial y} = \frac{v^*}{\nu}\frac{\partial}{\partial y^+}\bigg|_x$$

Using Eq. (9.2-22) and integrating by parts gives

$$v = -\int_0^y \frac{\partial u}{\partial x}\,dy = -\frac{\nu}{v^*}\int_0^{y^+} \frac{\partial}{\partial x}(v^*u^+)\,dy^+ = -\frac{\nu}{v^*}\frac{dv^*}{dx}u^+y^+$$

and $u\frac{\partial u}{\partial x} + v\frac{\partial u}{\partial y} = v^*\frac{dv^*}{dx}u^{+2}$

Eq. (9.2-23) becomes $v^*\frac{dv^*}{dx}u^{+2} = \frac{v^*}{\mu}\frac{d\tau}{dy^+}$

Integrating, $\tau - \tau_w = \frac{dv^*}{dx}\mu\int_0^{y^+} u^{+2}\,dy^+$

But as $y \to \delta$, $\tau \to 0$, $u^+ \to u_e^+$, thus

$$\tau_w = \rho v^{*2} = -\frac{dv^*}{dx}\mu\int_0^{\delta^+} u^{+2}\,dy^+ = -\mu\frac{dv^*}{dx}G(u_e^+)$$

or $v^{*2} = -\nu\frac{dv^*}{dx}G(u_e^+)$; but $u_e^+ = \frac{u_e}{v^*}$,

so that

$$\frac{u_e}{\nu} = G(u_e^+)\frac{du_e^+}{dx}$$

Separating variables and integrating assuming $\delta = 0$ at $x = 0$ gives,

$$Re_x = \frac{u_e x}{\nu} = \int_0^{u_e^+} G(u_e^+)\,du_e^+ \qquad (9.2\text{-}25)$$

We now need an expression for the velocity profile valid throughout the inner region; there are many available but Spalding's expression is

both accurate and has a particularly convenient algebraic form,

$$y^+ = u^+ + e^{-C/A}[e^{u^+/A} - 1 - u^+/A - \frac{(u^+/A)^2}{2} - \frac{(u^+/A)^3}{6}] \qquad (9.2\text{-}26)$$

where we will take A = 2.5, C = 5.5, to give $e^{-C/A} = 0.1108$. Then with $z = u_e^+/A$,

$$G(u_e^+) = \frac{1}{3} u_e^{+3} + e^{-C/A} A^2[e^z (z^2-2z+z) - 2 - \frac{z^3}{3} - \frac{z^4}{4}] \qquad (9.2\text{-}27)$$

$$Re_x = \frac{1}{12} u_e^{+4} + e^{-C/A} A^3[e^z (z^2-4z+6) - 6 - 2z - \frac{z^4}{12} - \frac{z^5}{20}] \qquad (9.2\text{-}28)$$

Eq. (9.2-28) is an implicit formula for $C_f(Re_x)$. An approximate explicit formula may be obtained if we note that in the practical range of $20 < u_e^+ < 40$,

$$G(u_e^+) \simeq 8.0\, e^{0.48u_e^+} \qquad (9.2\text{-}29)$$

Substituting in Eq. (9.2-25) and integrating gives

$$C_F = \frac{0.455}{[\ell n\ 0.06\ Re_x]^2} \qquad (9.2\text{-}30)$$

which agrees with experiment to ±2% over the whole range.

The total drag of a flat plate of length L is most easily calculated from the power law expression Eq. (9.2-21), namely $C_F = 0.026\ Re_x^{-1/7}$. Then

$$C_D = \frac{1}{L}\int_0^L C_F(x)\, dx = \frac{1}{Re_L}\int_0^{Re_L} C_F(Re_x)\, dRe_x = 0.0303\ Re_L^{-1/7} \qquad (9.2\text{-}31)$$

or $$C_D = \frac{7}{6} C_F(L) \qquad (9.2\text{-}32)$$

9.3 EFFECT OF PRESSURE GRADIENT, WALL COOLING, MACH NUMBER, BLOWING AND WALL ROUGHNESS ON VELOCITY PROFILES AND SKIN FRICTION

Turbulent boundary layers on re-entry vehicles are complicated by the presence of pressure gradients, density variations due to wall cooling, viscous dissipation and foreign gas injection, blowing effects and wall roughness. Our purpose in this section is to review briefly the effects of these factors on the velocity profile and skin friction: each factor will

be discussed separately in order to demonstrate the essential effects of each factor on the characteristics of turbulent boundary layers.

Pressure Gradient

In general a pressure gradient significantly affects the velocity profile in the outer region only. We would expect the outer law to be

$$u - u_e = f(\tau_w, \rho, y, \delta, \frac{dP}{dx})$$

or $$u^+ - u_e^+ = f(\frac{y}{\delta}, \frac{\delta}{\tau_w}\frac{dP}{dx}) \text{ by dimensional analysis} \qquad (9.3\text{-}1)$$

Clauser [8] suggested that δ be replaced by the more precisely defined δ^* to obtain

$$\beta = \frac{\delta^*}{\tau_w}\frac{dP}{dx} \quad \text{Clauser's "equilibrium" parameter} \qquad (9.3\text{-}2)$$

Clauser showed experimentally that a boundary layer with β constant was in turbulent equilibrium in the sense that all the gross properties of the layer can be scaled with a single parameter. Clauser further suggested use of the defect thickness,

$$\Delta = \int_0^\infty (u_e^+ - u^+)dy = \delta^* u_e^+ \qquad (9.3\text{-}3)$$

$$(= 3.6\delta \text{ for a flat plate})$$

for scaling velocity profiles, and a shape factor G which remains constant in an equilibrium layer,

$$G = \frac{1}{\Delta}\int_0^\infty (u_e^+ - u^+)^2\, dy \qquad (9.3\text{-}4)$$

from which it follows that $H = (1 - G/u_e^+)^{-1}$. Since $u_e^+ = u_e^+(x)$, H is not constant in an equilibrium layer. Nash developed a curve fit for G,

$$G \simeq 6.1(\beta + 1.81)^{\frac{1}{2}} - 1.7 \qquad (9.3\text{-}5)$$

The Figure shows some equilibrium velocity profiles in outer coordinates. But the curves do not have an easily recognizable shape. Coles [10] noted that the deviations of the velocity from the overlap law, when normalized by the maximum deviation (at $y = \delta$) was a function of y/δ only,

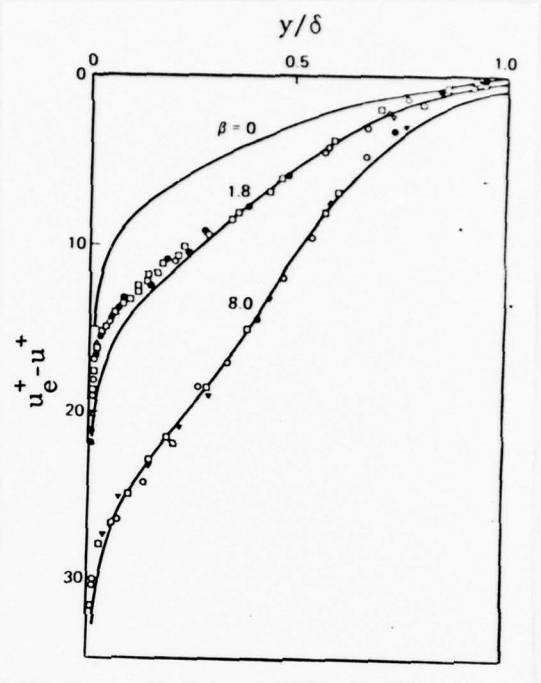

$$\frac{u^+ - 2.5\ \ell n\ y^+ - 5.5}{u_e^+ - 2.5\ \ell n\ \delta^+ - 5.5} = \frac{1}{2} W(\frac{y}{\delta}) \qquad (9.3\text{-}6)$$

W is the 'wake function' and has the value 0 at the wall and 2 at $y = \delta$. The Figure shows the original plots prepared by Coles, who proposed

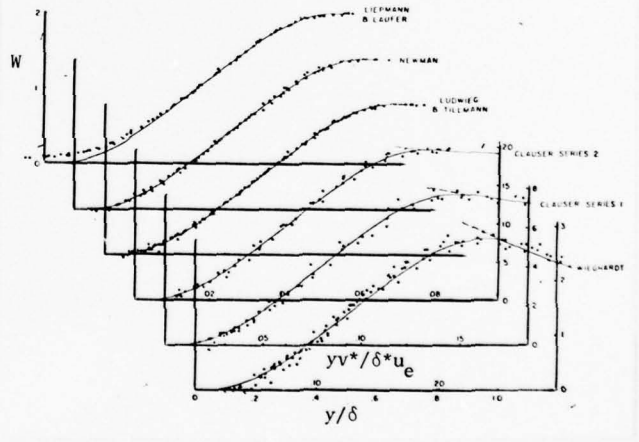

$$W(\frac{y}{\delta}) = 2 \sin^2 (\frac{\pi}{2} \frac{y}{\delta}) \qquad (9.3\text{-}7)$$

or more generally we write

$$u^+ = A\ell n\ y^+ + C + A\Pi W(\frac{y}{\delta}) \qquad (9.3\text{-}8)$$

where $\Pi = \beta/2A$; Π should be constant in an equilibrium layer, e.g., for a flat plate $\beta = 2.35$ and hence $\Pi \simeq 0.5$. A crude curve fit of experimental data gives

$$\Pi = (\frac{3}{4}\beta + \frac{3}{8})^{3/4} \qquad (9.3\text{-}9)$$

Notice that the wake vanishes for $\beta = -1/2$, which corresponds to an asympotically large favorable pressure gradient. Integrating Eq. (9.3-8) gives

$$\frac{\delta^*}{\delta} = \frac{1 + \Pi}{u_e^+/A} \tag{9.3-10}$$

$$\frac{\theta}{\delta} = \frac{1 + \Pi}{u_e^+/A} - \frac{2 + 3.179\Pi + 1.5\Pi^2}{(u_e^+/A)^2} \tag{9.3-11}$$

The essential effect of pressure gradient on skin friction can be seen in the integral momentum equation,

$$\frac{d\theta}{dx} + (2+H)\frac{\theta}{u_e}\frac{du_e}{dx} = \frac{C_F}{2} \tag{9.3-12}$$

A favorable pressure gradient accelerates the free-stream (the Euler relation gives $u_e du_e = -dP/\rho$) and hence increases C_F. However the practical problem is one in which the pressure gradient changes along the surface and we need to calculate the growth of the boundary layer by some forward marching procedure and hence find C_F. For the simple case of incompressible flow along an impermeable wall, very many calculation methods have been developed, either based on the integral or differential momentum equations: White [9] gives a good review of these methods.

Density Variation

Density variations may be caused by temperature and concentration gradients. In this section we will be concerned only with the effect of temperature gradients, which may be caused by wall cooling, or by viscous dissipation at high Mach numbers. The effect of concentration gradients, due in particular to foreign gas injection associated with ablation, will be dealt with in §9.6.

On a re-entry vehicle the wall cooling ratio T_w/T_e and Mach number vary considerably along the wall, and as a result so does the shape of the temperature profile. The Figure (on the following page) shows the observed trends where it is seen that the effect of a cold wall is to drive $u^+(y^+)$ above the incompressible logarithmic law, while the effect of

increasing M, by itself, is the opposite. Many attempts have been made to develop a compressible law of the wall, the most successful being that of van Driest [1] and White and Christoph [11]: both, however, are of complex algebraic form.

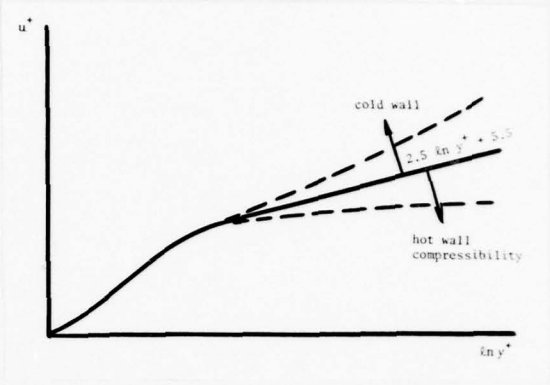

Of more interest is the effect of wall cooling and Mach number on skin friction where the essential effect is an increase of C_F with increase of density near the wall. The Figure shows calculated trends, which are in general agreement with experiment. For M = 0 an approximate correlation is [12]

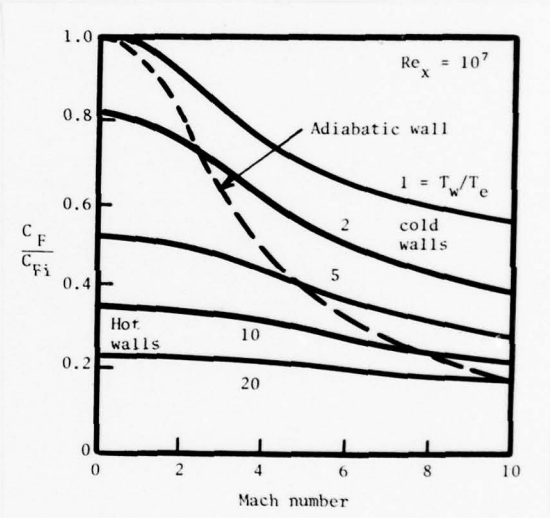

$$\frac{C_F}{C_{Fi}} \simeq \left(\frac{T_w}{T_e}\right)^{-1/3} \qquad (9.3\text{-}13)$$

Blowing

In the near wall region the Couette flow assumptions are good, so that we can write

mass: $$\frac{\partial}{\partial y}(\rho v) = 0 \qquad (9.3\text{-}14)$$

momentum: $$\rho v \frac{\partial u}{\partial y} = \frac{\partial \tau}{\partial y} \qquad (9.3\text{-}15)$$

Integrate Eq. (9.3-14): $$\rho v = \text{constant} = \rho v_w \qquad (9.3\text{-}16)$$

Substitute in Eq. (9.3-15), $$\rho v_w \frac{\partial u}{\partial y} = \frac{\partial \tau}{\partial y} \qquad (9.3\text{-}17)$$

integrating, $$\rho v_w u = \tau - \tau_w \qquad (9.3\text{-}18)$$

and the effect of blowing on the shear stress distribution is seen. To see how this shear stress distribution may affect the velocity profile consider

a simple two-layer model of the inner region. Writing $\tau = \mu_{eff} \frac{du}{dy}$ and making Eq. (9.3-18) dimensionless in the usual way gives

$$1 + v_w^+ u^+ = \frac{\mu_{eff}}{\mu} \frac{du^+}{dy^+} \tag{9.3-19}$$

In the laminar sub-layer assume $\mu_{eff} = \mu$ and integrate to obtain

$$u^+ = \frac{1}{v_w^+}(e^{v_w^+ y^+} - 1); \quad 0 < y^+ < y_a^+ \tag{9.3-20}$$

For $y^+ > y_a^+$ assume $\mu_{eff} >> \mu$, with $\frac{\mu_{eff}}{\mu} = \kappa^2 y^2 \frac{du^+}{dy^+}$, then

$$\frac{du^+}{dy^+} = \frac{1+v_w^+ u^+}{\kappa^2 y^+ 2 \frac{du^+}{dy^+}}$$

integrating, $$\frac{2}{v_w^+}[(1+u^+ v_w^+)^{\frac{1}{2}} - 1] = \frac{1}{\kappa} \ln y^+ + C \tag{9.3-21}$$

Stevenson [13] showed that experimental velocity profiles were well correlated with C taken to be the same as the unblown value. Alternatively if we let $u^+ = u_a^+$ at $y = y_a^+$ and using Eq. (9.3-20),

$$\frac{2}{v_w^+}[(1+u^+ v_w^+)^{\frac{1}{2}} - (1+u_a^+ v_w^+)^{\frac{1}{2}}] = \frac{1}{\kappa} \ln \frac{y}{y_a^+} \tag{9.3-22}$$

Simpson [14] showed that if $u_a^+ = 11$ was assumed then $y_a^+ = 11$ correlated his experimental data. The Figure on the following page, shows ϕ defined as

$$\phi = \frac{2}{v_w^+}[(1+u^+ v_w^+)^{\frac{1}{2}} - (1+11 v_w^+)^{\frac{1}{2}}] = \frac{1}{0.44} \ln \frac{y^+}{11} \tag{9.3-23}$$

for various flows measured by Simpson.

Other laws of the wall with blowing may be found in the literature, e.g., Black-Sarnecki, etc., but the differences are probably not greater than the uncertainties in the experimental data. Pimenta [15] has shown that velocity profiles on rough walls with blowing are also well correlated by Stevenson's law of the wall.

Stevenson also accounted for the variation of shear stress with blowing to develop a velocity defect law which was valid with blowing,

$$\Gamma = \frac{2}{v_w^+}\left[(1+v_w^+ u_e^+)^{\frac{1}{2}} - (1+u^+ v_w^+)^{\frac{1}{2}}\right] = \Gamma(\Pi, \frac{y}{\delta}) \qquad (9.3\text{-}24)$$

and found good agreement with experiment. Simpson found good agreement with his data for $Re_\theta > 6000$; for lower Reynolds numbers Simpson suggests K = 0.40 be replaced by $0.40(Re_\theta/6000)^{1/8}$, as in fact he recommended for the inner region law as well.

As is the case for laminar flows, blowing of course reduces skin friction. The Figure shows experimental skin friction coefficients for a flat plate for various values of the blowing parameter F (= $\dot{m}/\rho_e u_e$). The data are well correlated by

$$\frac{C_F}{C_{FO}}\bigg|_{Re_\theta} = \frac{0.7B_F}{\exp(0.7B_F) - 1};$$

$$B_F = \frac{\dot{m}}{\rho_e u_e C_{FO}} \qquad (9.3\text{-}25)$$

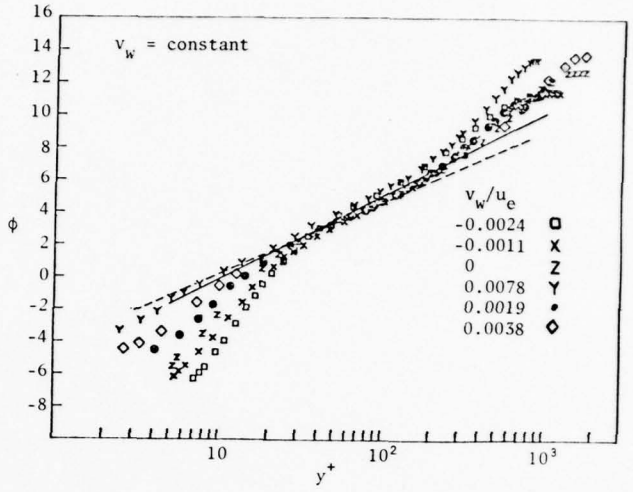

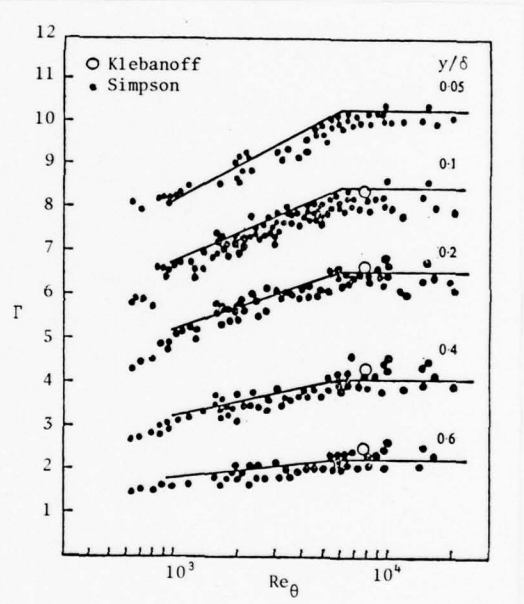

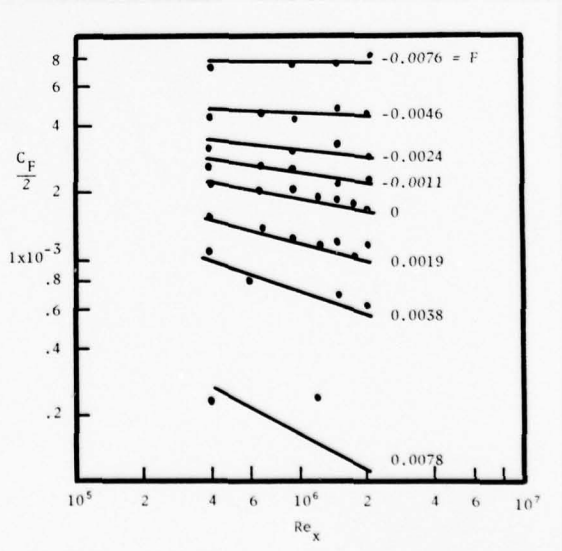

Roughness

The simplest case is a roughness pattern which can be characterized by a single size parameter, e.g., h, the mean protuberance height. Then dimensional analysis suggests that the velocity near the wall should have the following dependence:

$$u = f(y, \nu, h, \tau_w)$$

or $$u^+ = f(y^+, h^+) \qquad (9.3\text{-}26)$$

As was the case for a smooth wall, experiment shows that the inner correlation extends into an overlap region where the outer variables also correlate the velocity profiles. Also the outer region correlation has been shown to be independent of roughness. Thus it follows that the overlap region again has a logarithmic form and the slope A is identical to that for a smooth wall. Hence referring to Eq. (9.2-5), the sole effect of roughness is to change the intercept as a function of h^+; we write

$$u^+ = A\ell n\, y^+ + C - \Delta u^+(h^+) \qquad (9.3\text{-}27)$$

where Δu^+ is the vertical shift of the logarithmic portion caused by roughness. The Figure shows typical rough wall velocity profiles measured by Reda [16].

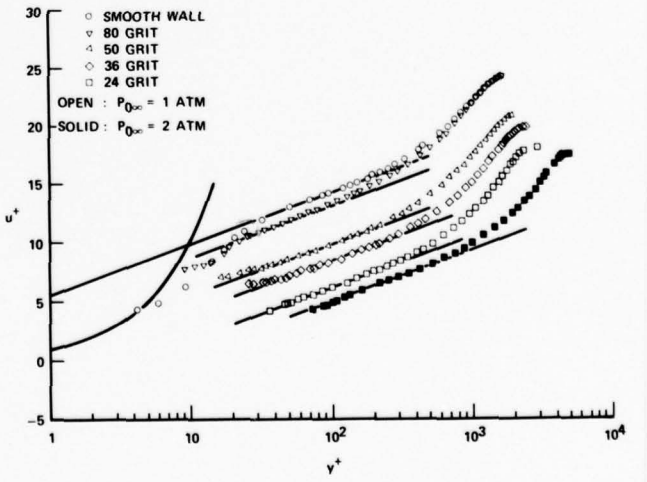

Following Nikuradse's work on pipe flow [17] a *fully* rough wall flow is defined as a flow for which C_F is independent of Re, which requires that the inner region law must be independent of viscosity. Thus Δu^+ must have a form which eliminates ν from Eq. (9.3-27), viz., $\Delta u^+ = A \log h^+ + D$, so that

$$u^+ = A\ell n\left(\frac{y}{h}\right) + C - D \quad \text{(fully rough)} \qquad (9.3\text{-}28)$$

By combining Eq. (9.3-27) with the outer region defect law we obtain the skin friction law for rough walls,

$$(2/C_F) = A\ell n\ Re_\delta\ (C_F/2)^{\frac{1}{2}} + B - C - \Delta u^+ \qquad (9.3\text{-}29)$$

which for a *fully* rough wall becomes

$$(2/C_F) = A\ \log\ (\delta/h) + B - C - D \qquad (9.3\text{-}30)$$

Notice that (C - D) can be interpreted as the velocity at y = h, u_h^+ and is often referred to as the *roughness function*. For both fully and transitionally rough walls we can write

$$u^+ = A\ell n(y/h) + u_h^+(h^+) \qquad (9.3\text{-}31)$$

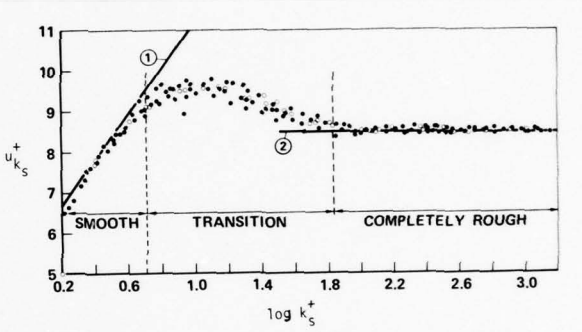

For fully rough flows over sand grain roughness of size k_s Nikuradse's velocity profiles were

$$u^+ = 2.5\ \ell n(y/k_s) + 8.5 \qquad (9.3\text{-}32)$$

The Figure above shows $u_{k_s}^+$ (k_s^+) for smooth, transitionally rough and fully rough walls as determined by Nikuradse [17]. An analytical expression for $u_h^+(h^+)$ given by White [9] is more applicable to commercially rough surfaces is

$$u_h^+ = 5.5 - A\ell n\ [h^+/(1 + 0.3h^+)] \qquad (9.3\text{-}33)$$

As was the case for the smooth flat plate, derivation of a skin friction relation $C_F = C_F(x)$ requires application of the momentum conservation form. The Figure shows results using Eq. (9.3-33) and the inner variables method.

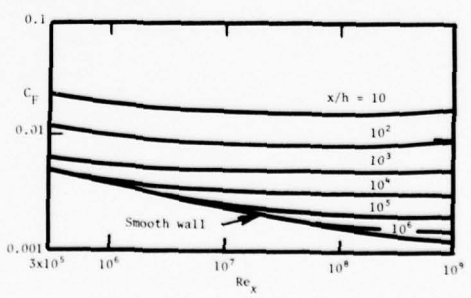

9.4 MIXING LENGTH MODELS

The Mixing Length Hypothesis

Prandtl [18] noted that the kinetic theory of gases gives [19]

$$\mu \sim \frac{1}{3} \rho \ell v \tag{9.4-1}$$

where ℓ is the mean free path and v is the mean molecular speed, and by analogy

$$\mu_t \equiv \frac{\tau_t}{\partial u/\partial y} \sim \rho \ell_m v_t \tag{9.4-2}$$

where ℓ_m, the Prandtl mixing length, is the distance a turbulent eddy is imagined to travel before it loses its identity by mixing with surrounding fluid. Also from the "Boussinesq hypothesis", Eq. (9.1-11)

$$\tau_t \alpha \frac{\partial u}{\partial y} \tag{9.4-3}$$

Prandtl further suggested that $|u'| \sim |v'|$, and that $u' \alpha \ell_m \partial u/\partial y$ (see, for example [7]): taking the proportionality constant equal to unity gives

$$v_t = \ell_m \left|\frac{\partial u}{\partial y}\right| \tag{9.4-4}$$

thus

$$\tau_t = \mu_t \frac{\partial u}{\partial y} = \rho \ell_m^2 \left|\frac{\partial u}{\partial y}\right| \frac{\partial u}{\partial y} \tag{9.4-5}$$

Finally Prandtl proposed that ℓ_m was proportional to the distance from the nearest wall.

Escudier [20] analyzed a lot of experimental data and concluded that in the turbulent core and wake ℓ_m is distributed as shown.

$$\frac{y}{\delta} \leq \frac{\lambda}{\kappa} : \quad \frac{\ell_m}{\delta} = \kappa \frac{y}{\delta} \tag{9.4-6}$$

$$\frac{y}{\delta} > \frac{\lambda}{\kappa} : \quad \frac{\ell_m}{\delta} = \lambda \tag{9.4-7}$$

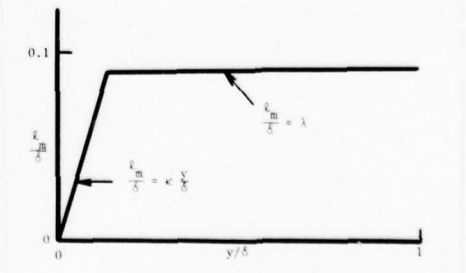

with $\kappa \simeq 0.41$, $\lambda = 0.09$. The boundary layer thickness δ is defined here to be the location where the velocity reaches 1% of the free stream value.

Very near the wall we write

$$\mu_{eff} = \mu + \rho \ell_m^2 \left|\frac{\partial u}{\partial y}\right| \tag{9.4-8}$$

van Driest [21] proposed a damping of ℓ_m close to the wall,

$$\ell_m = \kappa y \left[1 - \exp\left(-\frac{y^+}{A}\right)\right] \tag{9.4-9}$$

with A = 26. There have been many modifications of the van Driest damping factor proposed in the literature, in order to account for shear variations near the wall due to a pressure gradient of mass injection. Close to the wall streamwise convection is negligible and integration of the momentum equation gives

$$\tau = \tau_w + \rho v_w u + y \frac{dP}{dx} \tag{9.4-10}$$

Defining $\tau^+ = \frac{\tau}{\tau_w}$, $v_w^+ = \frac{v_w}{v^*}$, $P^+ = \frac{\nu}{v^* \tau_w} \frac{dP}{dx}$; various proposed arguments of the exponential in van Driest's damping factor have been:

$$\text{argument} = -\frac{y^+ \tau^{+1/2}}{A} \qquad \text{Patankar and Spalding, 1970 [22]}$$

$$= -\frac{y^+ \tau^+}{A} \qquad \text{Launder and Jones, 1969 [23]}$$

$$= -\frac{y^+}{A}\left[\frac{P^+}{v_w^+}\left(1 - e^{11.8 v_w^+}\right) + e^{11.8 v_w^+}\right] \qquad \text{Cebeci, 1970 [2]}$$

$$= -\frac{y^+}{26} e^{5 v_w^+} \qquad \text{Landis and Mills, 1972 [12]}$$

Transport of scalar quantities

Here we are concerned with the specification of Pr_t and Sc_t. Considerable research has been carried out in order to determine Pr_t. For air boundary layers $Pr_t = 0.9$ is widely used. The Figure shows data for Pr_t measured at Stanford [24]: a recommended empirical correlation is

$$Pr_t = 1.43 - 0.17\, y^{+1/4} \tag{9.4-11}$$

(if $Pr_t < 0.86$ then set equal to 0.86)

Experimental data for Sc_t in external boundary layers is extremely sparse, and common practice is to set $Sc_t = 1$ or $Sc_t = Pr_t$.

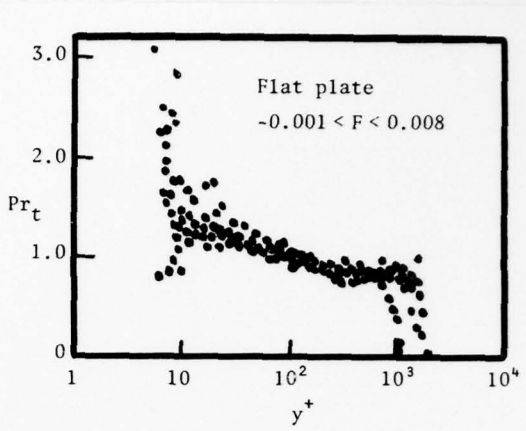

9.5 NUMERICAL CALCULATION METHODS FOR BOUNDARY LAYERS

In an external boundary layer flow there is a single predominant direction of flow, and shear stresses, heat fluxes and diffusion fluxes are significant only in a direction perpendicular to the predominant direction. Mathematically the partial differential equations are parabolic in form which implies that the equations can be solved using a forward marching procedure. Physically this means that downstream effects cannot affect upstream behavior.

A number of finite difference schemes for the numerical solution of boundary layer flows are currently in use. Four schemes in particular have been widely and successfully used, and these will be dealt with in turn.

1. A. M. O. Smith, T. Cebeci, et al. [2]

The method is one first proposed by Hartree and Womersly wherein the boundary layer equations are first transformed using the usual transformation for laminar compressible boundary layer equations given in §8.3. For example, the momentum equation becomes

$$\left[\frac{\rho\mu}{\rho_e\mu_e}\left(1 + \frac{\varepsilon_M}{\nu}\right)f''\right]' + ff'' + \beta\left[\frac{\rho_e}{\rho} - f'^2\right] = 2\xi\left(f'\frac{\partial f'}{\partial \xi} - f''\frac{\partial f}{\partial \xi}\right) \qquad (9.5\text{-}1)$$

In earlier versions of this method, the transformed equations were solved by Runge-Kutta "shooting" at each ξ location, after finite differencing the derivatives and treating these as source terms. Later shooting was replaced

by quasi-linearized finite differencing. In current versions full finite differencing using Keller's "box" method is used.

2. S. V. Patankar and D. B. Spalding [25], R. B. Landis [4], A. T. Wassel [26]

The essential feature of the numerical procedure is a normalized von Mises transformation of the independent variables before finite differencing, as follows:

$$x,y \rightarrow x,\omega \qquad \text{with} \qquad \omega = \frac{\psi-\psi_w}{\psi_e-\psi_w} = \frac{\psi-\psi_w}{\Delta\psi}$$

The conservation equations take the common form,

$$\frac{\partial\phi}{\partial x} + (a+b\omega)\frac{\partial\phi}{\partial\omega} = \frac{\partial}{\partial\omega}\left(c\frac{\partial\phi}{\partial\omega}\right) + d \qquad (9.5\text{-}2)$$

where $a = \frac{1}{\Delta\psi}\frac{d\psi_w}{dx}$ $\quad c = \frac{r^{2\varepsilon}\rho u}{\Delta\psi^2}\frac{\mu_{eff}}{\sigma_{eff}}$ $\quad \sigma_{eff} = 1,\ Pr_{eff}, Sc_{eff}.$

$b = -\frac{1}{\Delta\psi}\frac{d\Delta\psi}{dx}$ $\quad d$ = source terms

also $\frac{d\psi_w}{dx} = -r^{\varepsilon}\rho_w v_w;\ \frac{d\psi_e}{dx} = r^{\varepsilon}\dot{m}_e$

where $\dot{m}_e$ is the rate of entrainment into the boundary layer: the e-surface is located through use of an appropriate expression for the entrainment rate.

A feature of the Patankar-Spalding codes is the use of Couette flow analyses for the region adjacent to the wall, justified by the fact that streamwise convection is indeed negligible there; also in turbulent flows gradients are steep near the wall the the number of node points necessary for an accurate calculation can be reduced considerably. Actually it is difficult to apply boundary conditions at $\omega = 0$ because $\frac{\partial u}{\partial\omega} = \frac{\partial u}{\partial y}\cdot\frac{\partial y}{\partial\omega} = \frac{\Delta\psi}{\rho u}\frac{\partial u}{\partial y}$, and all higher derivatives with respect to ω, become infinite as $y \rightarrow 0$. Denny and Landis [46] showed that using the transformation

$$x,y \rightarrow x,\omega^2 \ ; \quad \omega^2 = \frac{\psi-\psi_w}{\psi_e-\psi_w} \qquad (9.5\text{-}3)$$

removed the singularity at the wall, provided $u = 0$ at the w-surface. If

$u \neq 0$ at the ω-surface, which might occur in two phase flows for example, then the ω-transformation is satisfactory, but the ω^2-transformation gives singular behavior at $\omega = 0$.

3. A. Wortman [27]

This method is very similar to Method No. 1 above. The essential difference is that the transformed equations are first formally integrated with respect to η, treating the ξ derivatives in finite difference form as source terms, and solved by iteration at each ξ-step of the forward marching procedure.

4. The Aerotherm "BLIMP" Codes [28,29]

The BLIMP series of codes developed by E. P. Bartlett, R. M. Kendall and Andersen were intended specifically for calculating boundary layers on re-entry vehicles, initially for the Apollo command module, and subsequently for general re-entry vehicles. Features which are absent in the previously mentioned schemes are an approximate treatment of multi-component diffusion using the bifurcation approach, and general equilibrium or non-equilibrium chemistry. The chemistry calculations are time consuming and are carried out at every node-point; hence a numerical scheme using a minimum number of node points was sought. The Hartree-Womersly approach is again used and the transformed equations solved using a "parametric integral" method with step weighting functions. Sets of connected cubics are used to represent velocity, enthalpy and species concentration variables: the first and second derivatives of these cubics are made continuous at the connecting points. At various times 7, 11 and 18 node-points across the boundary layer have been used.

9.6 HEAT TRANSFER

The Temperature Law of the Wall

We consider first low speed, incompressible, constant property flow, with Pr_t = constant. It follows that a law of the wall for temperature must

exist, including a logarithmic overlap layer which does however vary with molecular Prandtl number. von Karman noted that although q and τ vary across a boundary layer, their ratio remains approximately constant,

$$\frac{q}{\tau} = \frac{k+k_t}{\mu+\mu_t}\frac{dT}{du} \simeq \frac{q_w}{\tau_w} \tag{9.6-1}$$

or
$$T-T_w = \frac{q_w}{C_p \tau_w}\int_0^u \frac{\mu+\mu_t}{\frac{\mu}{Pr}+\frac{\mu_t}{Pr_t}}\,du \tag{9.6-2}$$

where q has been taken positive for a cold wall. In dimensionless form,

$$T^+ = \frac{(T-T_w)\rho C_p v^*}{q_w} = \int_0^{u^+} \frac{1+\frac{\mu_t}{\mu}}{\frac{1}{Pr}+\frac{1}{Pr_t}\frac{\mu_t}{\mu}}\,du^+$$

or
$$T^+ = \int_0^{u^+} \frac{\varepsilon^+}{\frac{1}{Pr}+\frac{1}{Pr_t}(\varepsilon^+-1)}\,du^+ \tag{9.6-3}$$

where $\varepsilon^+ = 1 + \frac{\mu_t}{\mu} = 1 + \frac{\varepsilon_M}{\nu}$.

To proceed we need a profile $\varepsilon^+(y^+)$. If we assume constant shear, which is at least valid near the wall, then

$$\tau_w = (\mu+\mu_t)\frac{du}{dy}$$

$$1 = \varepsilon^+ \frac{du^+}{dy^+}$$

i.e.,
$$\varepsilon^+ = \frac{dy^+}{du^+} \tag{9.6-4}$$

and if we use Spalding's law of the wall, Eq. (9.2-26),

$$\varepsilon^+ = 1 + (e^{-C/A}/A)\left[e^{u^+/A} - 1 - u^+/A - \frac{(u^+/A)^2}{2}\right] \tag{9.6-5}$$

The figure on the following page shows results for Pr > 0.7. The analysis fails for small Pr, since then the temperature profile extends far into a

region where ε^+ is not sufficiently accurate.

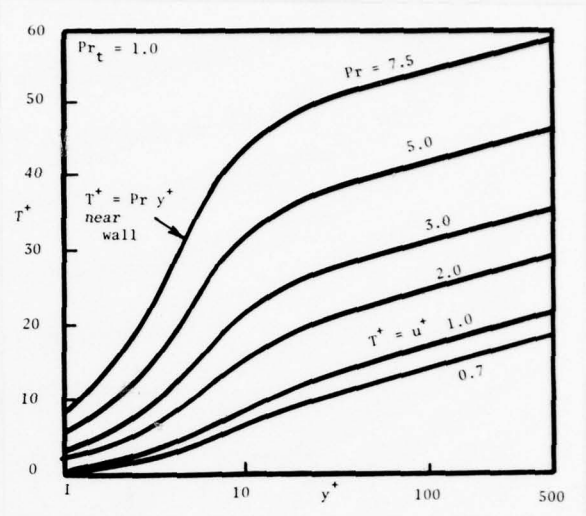

In the sub-layer where $\mu_t \to 0$,

$$T^+ = Pr\, y^+ \qquad (9.6\text{-}6)$$

while in the logarithmic region

$$T^+ = A\ell n\, y^+ + (12.8Pr^{0.68}-7.3) \qquad (9.6\text{-}7)$$

where the additive constant is from numerical data (and equals 5.5 for Pr = 1).

The Extended Reynolds Analogy

If we use inner variables only, then

$$T_e^+ = A\ell n\, \delta_t^+ + (12.8Pr^{0.68}-7.3)$$

$$u_e^+ = A\ell n\, \delta^+ + 5.5$$

For $0.7 < Pr < 10$, $\delta_t \simeq \delta$ and we can take $\ell n\, \delta_t = \ell n\, \delta$, thus

$$T_e^+ - u_e^+ = 12.8(Pr^{0.68}-1)$$

But $$C_H = \frac{q_w}{(T_w-T_e)\rho C_p u_e} = \frac{1}{T_e^+}\frac{1}{u_e^+}\,; \quad u_e^+ = (2/C_F)^{1/2}$$

thus $$\frac{1}{C_H u_e^+} - u_e^+ = 12.8(Pr^{0.68}-1)$$

or $$C_H = \frac{C_F/2}{1+12.8(Pr^{0.68}-1)(C_F/2)^{1/2}} \qquad (9.6\text{-}8)$$

However we have neglected the viscous sub-layer and buffer region: a more precise result requires use of tabulated solutions of Eq. (9.6-3), which may be found in the literature, e.g. [30].

With $C_{F,x}$ calculated for a boundary layer the Reynolds analogy gives $C_{H,x}$ directly. For flat plates or mild pressure gradients, and for slowly

varying wall temperature, Reynolds analogy methods are satisfactory for engineering use.

Effect of Pressure Gradient

The temperature law of the wall, Eq. (9.6-3) is valid only for zero or mild pressure gradients. With a pressure gradient the shear distribution τ/τ_w is different to the heat flux distribution q/q_w, and the elementary Reynolds analogy is invalid. Many approximate methods for calculating heat transfer in flows with pressure gradient have been developed, e.g., Ambrok's methods [31], but with limited success. The preferred method today is the use of finite difference calculation methods, as described in §9.5.

Effects of Wall Cooling and Mach Number

As was the case for the effect of pressure gradient, the effects of wall cooling and Mach number are best determined using finite difference calculation methods. Two results of such calculations are worthwhile mentioning here. Firstly, for the low speed boundary layer on a flat plate, an approximate correlation of the effect of wall cooling is [12]

$$\frac{C_H}{C_{Hi}} \simeq \left(\frac{T_w}{T_e}\right)^{-1/4} \tag{9.6-9}$$

Also the corresponding Reynolds analogy factor for mass transfer is approximately correlated as [12]

$$\frac{2C_M}{C_F} \simeq Sc^{-1/3} \tag{9.6-10}$$

Secondly, for high speed constant property boundary layers, the recovery factor is found to be

$$r \simeq Pr^{1/3} \tag{9.6-11}$$

9.7 TURBULENT BOUNDARY LAYERS WITH FOREIGN GAS INJECTION

As was the case with laminar boundary layers in §8.5, the primary focus of analytical studies has been to calculate the reduction, due to mass injection, of the wall shear stress, the mass transfer conductances, and the heat transfer rate. The simplest situation is that of an inert binary mixture where species 1 is injected at the wall, and the free-stream contains species 2 only. The only comprehensive study has been that of Landis and Mills [32], and their results will form the basis of this discussion. The conservation equations, Eqs. (9.1-13 through 16), are written as follows:

$$\frac{\partial}{\partial x}(\rho u) + \frac{\partial}{\partial y}(\rho v) = 0 \tag{9.7-1}$$

$$\rho u \frac{\partial u}{\partial x} + \rho v \frac{\partial u}{\partial y} = \frac{\partial}{\partial y}\left(\mu_{eff} \frac{\partial u}{\partial y}\right) \tag{9.7-2}$$

$$\rho u \frac{\partial K_1}{\partial x} + \rho v \frac{\partial K_1}{\partial y} = \frac{\partial}{\partial y}\left(\frac{\mu_{eff}}{Sc_{eff}} \frac{\partial K_1}{\partial y}\right) \tag{9.7-3}$$

$$\begin{aligned} \rho u \frac{\partial T}{\partial x} + \rho v \frac{\partial T}{\partial y} = {} & \frac{\partial}{\partial y}\left(\frac{\mu_{eff}}{Pr_{eff}} \frac{\partial T}{\partial y}\right) + \frac{1}{C_p}\left[\frac{\mu_{eff}}{Pr_{eff}} \frac{dC_p}{dT} \left(\frac{\partial T}{\partial y}\right)^2\right. \\ & + \frac{\mu_{eff}}{Sc_{eff}} (C_{p1}-C_{p2}) \frac{\partial K_1}{\partial y} \frac{\partial T}{\partial y} \\ & \left. + \mu_{eff}\left(\frac{\partial u}{\partial y}\right)^2\right] \end{aligned} \tag{9.7-4}$$

which are to be solved subject to the boundary conditions:

$$y = 0: \quad u = 0 \; ; \; \rho v\big|_w = \dot{m} \; ; \quad T = T_w \; ; \quad -\rho \mathcal{D}_{12} \frac{\partial K_1}{\partial y}\bigg|_w = \dot{m}(1-K_{1,w}) \tag{9.7-5a}$$

$$y \to \infty: \quad u \to u_e \; , \quad K_1 \to 0 \; , \quad T \to T_e \tag{9.7-5b}$$

Mixture thermodynamic properties were calculated assuming ideal gas laws. Species transport properties were calculated according to the kinetic theory of gases with the Lennard-Jones interaction potential, and mixture transport properties were estimated using Wilkie's rule, as described in §3.

Extension of incompressible turbulent boundary layer theory to compressible turbulent boundary layers with foreign gas injection is made on the

hypothesis that the momentum equation is coupled to the species and energy equations only through spatial variations of the mean density and viscosity i.e., mixing length relations established for incompressible flows are applicable. In the inner region Prandtl's mixing length law was used, together with the van Driest damping factor modified for blowing, as described in §9.4. In the outer region the mixing length expression of Simpson [14] was used. The resulting expressions for μ_{eff} are then

$$\mu_{eff}\Big|_{inner} = \mu + \rho(0.435y)^2\{1-\exp[-\frac{y^+}{26}(\exp v_s^+)^5]\}\left|\frac{du}{dy}\right| \qquad (9.7\text{-}6a)$$

$$\mu_{eff}\Big|_{outer} = \mu + \rho\{\frac{0.435}{4}\delta[1-\exp(-\frac{4y}{\delta})]\}^2\left|\frac{du}{dy}\right| \qquad (9.7\text{-}6b)$$

For the turbulent transport of the scalar quantities, $Sc_t = 0.8$ and $Pr_t = 0.9$ was used.

The flows calculated were as follows. For zero Mach number the injectants were H_2, He, CH_4, H_2O, CO, Air, CO_2, Freon 12, Xe and CCl_4 with $T_w/T_e = 0.2$ and 0.9. The effects of various problem parameters were studied for He, Air, and Xe injectants, (i) in order to study the effect of temperature ratio additional results were obtained for $T_w/T_e = 2.0$, (ii) the effect of temperature level was evaluated by obtaining $T_w/T_e = 0.9$ as both 295K/324K and 1325K/1472K, (iii) the effect of Mach number was obtained with data at M = 2.0 and 6.0 for $T_w/T_e = 2.0$, (iv) the effect of Reynolds number was obtained at $T_w/T_e = 0.2$, M = 0 by calculating as far as $Re_x = 10^8$, (v) the effect of an equilibrium injection distribution was studied for air at $T_w/T_e = 0.2$, with $\dot{m} \propto x^{-0.2}$. For all cases calculations were made at four or more injection rates. Complete tabulations of Re_θ, $C_F/2$, C_M, C_H, $K_{1,w}$, ρ_w, Sc_w and Pr_w may be found in [4].

The figures on the following page show the skin friction coefficient, the mass transfer Stanton number, and the heat transfer Stanton number, each normalized by their respective unblown values, at zero Mach number, for "cold

wall" conditions, T_w/T_e = 0.2. The main features of these results may be explained in a manner similar to which the characteristics of binary laminar boundary layers were assessed in §8.5. In [32] there is presented a detailed explanation of the behavior shown in the Figures. Here it suffices to note that the effect of injectant molecular weight is more pronounced than for the laminar case since μ_{eff} is proportional to local density. Thus $C_F/2$ is expected to be a regular function of molecular weight, and the Figure shows that, except for the heaviest injectants, the effectiveness does vary regularly with molecular weight. C_M is even more dependent on injectant molecular weight since near the wall the effect of density on Sc_{eff} augments that for

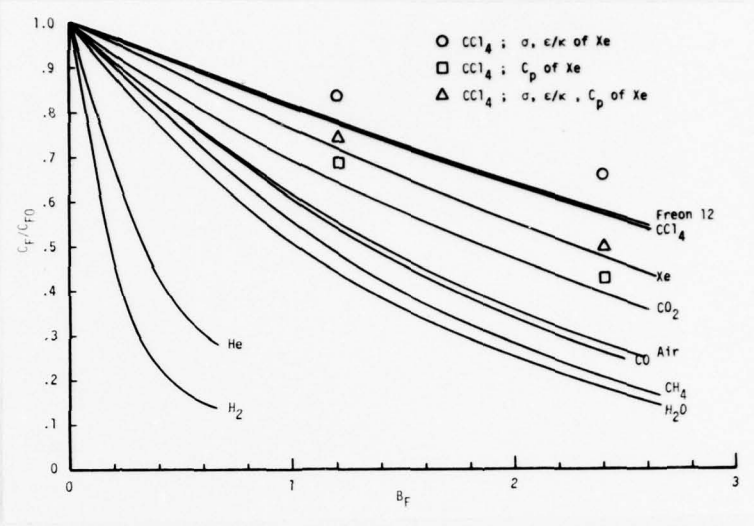

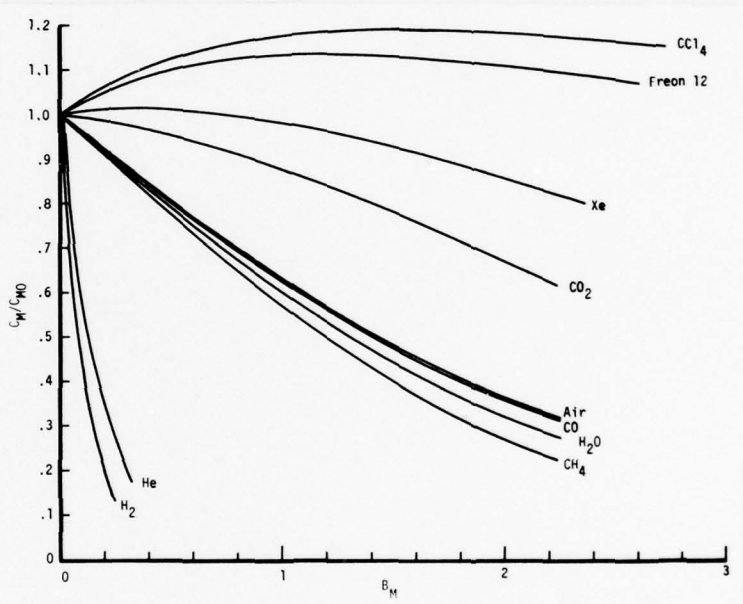

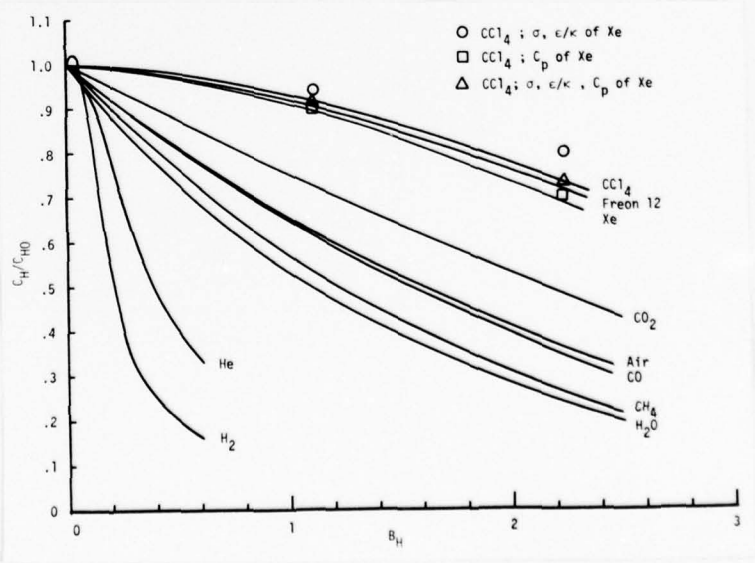

μ_{eff}. The behavior of C_H is somewhat more complex due to the dependence of Pr on k and C_p, but the essential regular dependence on molecular weight is quite apparent.

The next two Figures show comparisons with experimental data for skin friction and heat transfer in low speed flow; the agreement is reasonable.

The effect of Mach number, on the effectiveness of injection in reducing skin friction, has been the subject of some controversy. In the Figure predictions of skin friction for air injection are compared with the experimental data bands presented by Jeromin [33]. The large increase in C_F/C_{FO} with increasing M shown by the experimental data proves to be primarily an effect of T_w/T_e. An examination of the original data sources indi-

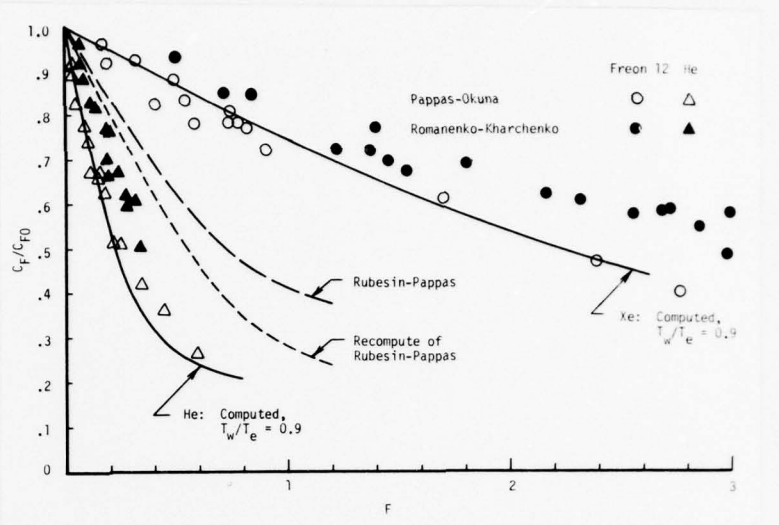

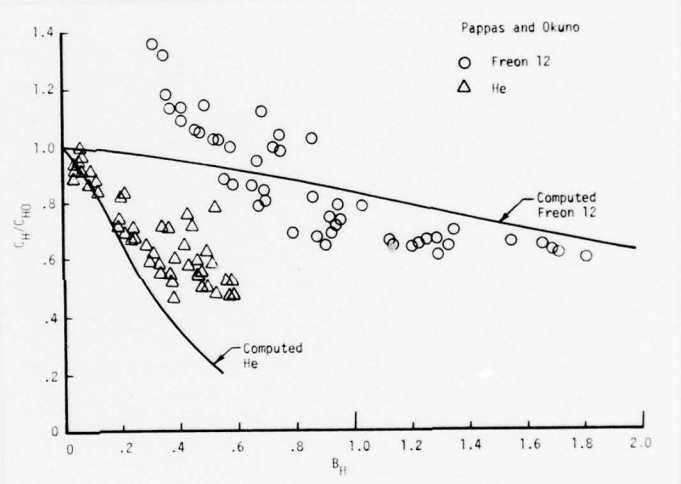

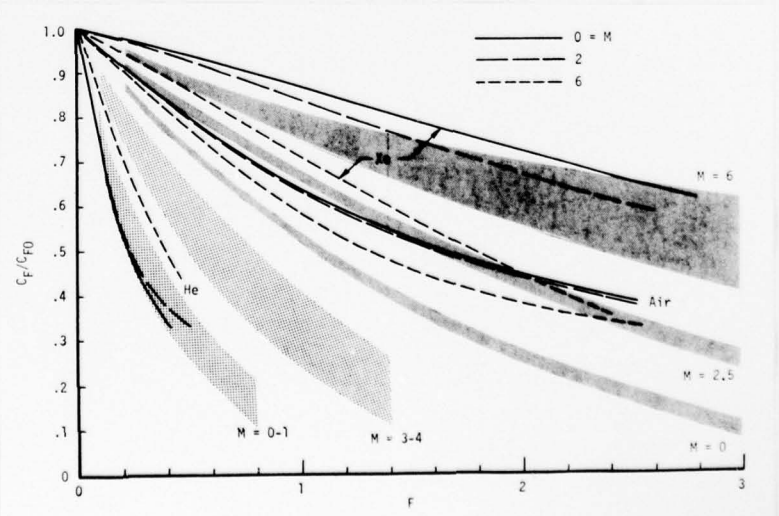

cated that for M = 0 a value of $T_w/T_e \simeq 0.9$ is typical; for M = 2, $T_w/T_e \simeq 2$; while for M = 6, T_w/T_e may lie between 4.5 and the adiabatic wall value. The Figure shows that, when appropriate temperature ratios are used the predicted effect of Mach number is consistent with experiment.

Correlation of Results

The Figures show the results for impermeable wall skin friction and heat transfer correlated by the Eckert reference enthalpy method [34]: the correlation is seen to be good and thus it is relatively simple to calculate C_{FO} and C_{HO} in practice.

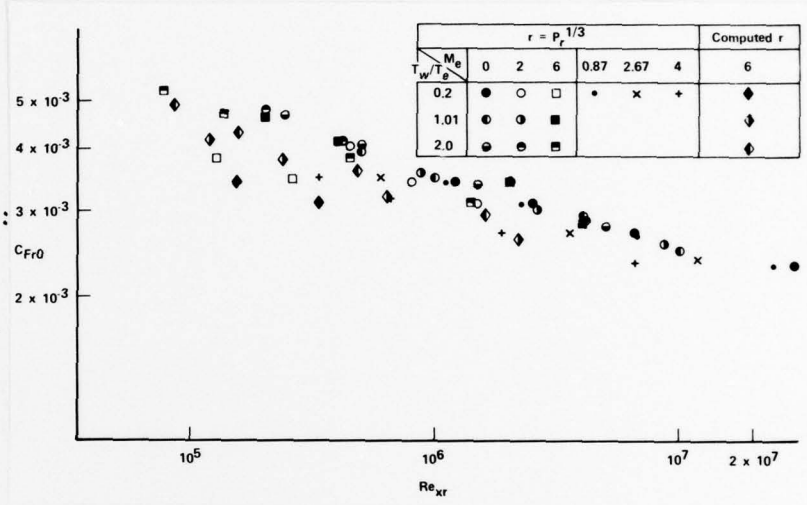

The next Figures show an attempt to use Knuth's reference state method [35] to correlate the data for air injection with $0 < M < 6$, and $0.2 < T_w/T_e < 2.0$. It can be seen that the method appears not to work, so no attempt was made to evaluate the method for foreign gas injection.

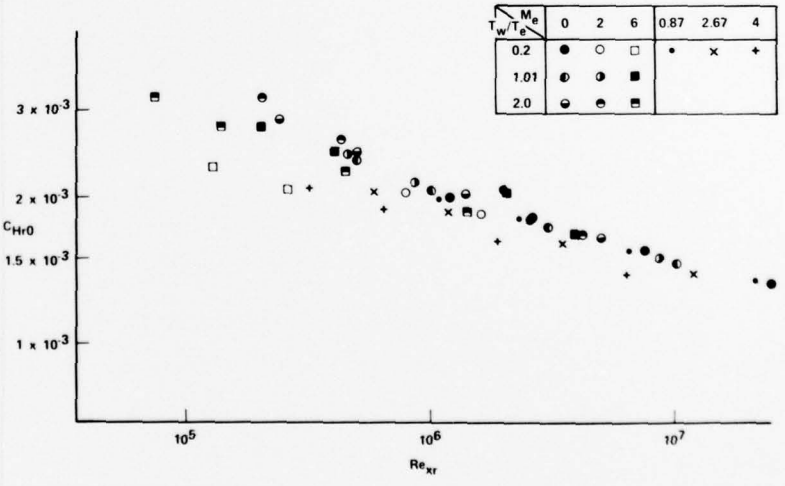

Thus the approach used was to obtain species weighting constants in exponential blockage factors, as defined in Eqs. (8.5-10 through 12) for laminar flow. The constants were correlated as

$$a_i = C(M_{air}/M_i)^n \qquad (9.7\text{-}6)$$

and the results are presented in Table 9.2 below.

All data points

	C	n
$a_{F,i}$	0.91	-0.76
$a_{M,i}$	0.79	-1.33
$a_{H,i}$	0.86	-0.73

Excluding cold walls

	C	n
$a_{F,i}$	0.87	-0.85
$a_{M,i}$	0.78	-1.45
$a_{H,i}$	0.86	-0.83

Table 9.2. Species weighting constants in exponential blockage factors for turbulent flow.

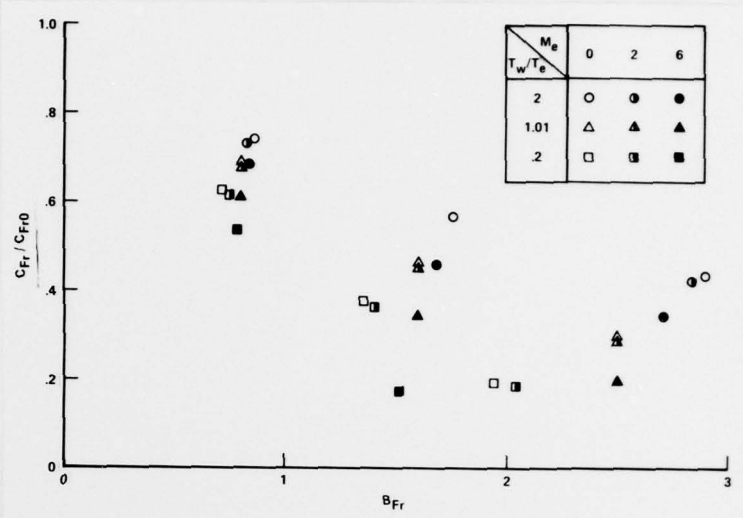

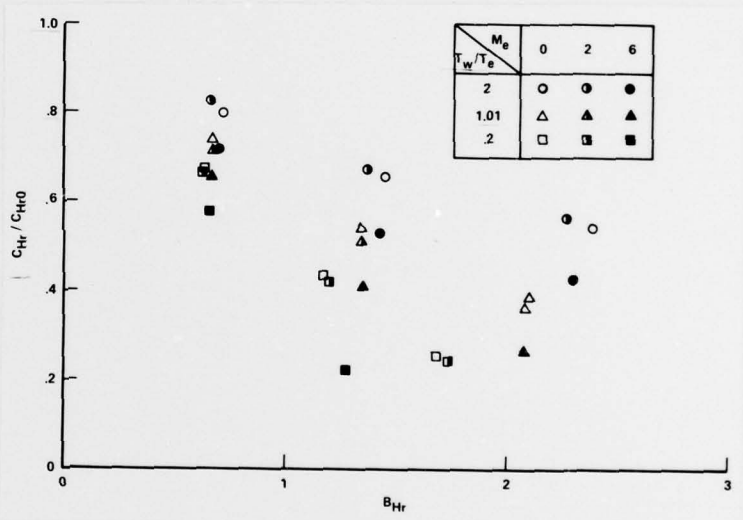

9.8 ROUGH WALLS

The effect of wall roughness on velocity profiles for incompressible flat plate flow was discussed in §9.3. In this section we outline a procedure for calculating rough wall boundary layers by finite difference methods and supply the necessary auxiliary realtions, including those required for heat transfer, and for the effects of blowing. Except in the region very close to the roughness elements, conventional modeling of turbulent transport, using for example a mixing length model, may be used. The remaining task is to characterize the turbulent transport in the vicinity of the roughness

elements. Some workers have chosen to adapt smooth wall calculation methods by simply postulating a non-zero value of the mixing length ℓ_{m0} at y = 0. For example, Healzer [36] fitted Nikuradse's sandgrain friction factor data with

$$\ell_m^+ = \sqrt{(0.4y^+)^2 + \ell_{m0}^{+2}} \; ; \quad \ell_{m0}^+ = \sqrt{[(k_s^+-46)/39]^2-0.05325} \tag{9.8-1}$$

However such an approach is a poor representation of the physics since the drag on a fully rough wall is a form drag, and not an eddy transport phenomena. Also extension to include effects of variable properties, blowing, etc., is troublesome; in particular the turbulent Prandtl number required to match heat transfer data is not of order unity, and is physically meaningless.

An alternative approach, to be followed here, is to divide the flow region at y = h, where h is of the order of the height of the roughness elements. Then for $y \geq h$ smooth wall mixing length relations may be used. For $y < h$ no attempt is made to solve the momentum equation; instead a drag coefficient is defined for the roughness elements via

$$\tau_w = C_d(\tfrac{1}{2}\rho u_h^2) \tag{9.8-2}$$

and specification of C_d gives a third kind boundary condition for the momentum equation in the domain $y \geq h$.

There is no analogy to form drag for heat transfer: some laminar sub-layer exists and constitutes a significant thermal resistance. Again, for the region $y \geq h$ the smooth wall specification of Pr_t applies and a "sub-layer" Stanton number is defined,

$$C_h = \frac{q_w}{\rho v^*(h_w-h_h)} \tag{9.8-3}$$

A definition of C_h corresponding to that for C_d would be in terms of u_h, rather than v*; however, Eq. (9.8-3) has been more widely used, and its continued use will avoid confusion. Specification of C_h provides a third kind boundary

condition for the energy conservation in the domain $y \geq h$. Boundary conditions for species conservation equations are handled in an analogous manner. The density ρ in the definitions of C_d and C_h must be evaluated at an appropriate reference value when ρ_h is significantly different to ρ_w.

The concept of representing the near wall region by auxiliary wall relations is not new. For example, Goddard [37] used the concept to explain Mach number effects on rough wall skin friction; Dipprey and Sabersky [38] correlated and interpreted their sandgrain indentation roughness heat transfer data using a sub-layer Stanton number. Jayatilleke [39] made an extensive study of the effect of roughness pattern and Prandtl number on such wall relations.

Correlations for C_d

Combining Eq. (9.8-2) with the definitions of v^* and u_h^+ gives

$$C_d = \frac{2}{u_h^{+2}} \tag{9.8-4}$$

For both transmissivity and fully rough walls the velocity profile was given by Eq. (9.3-11) as

$$u^+ = A\ell n(y/h) + u_h^+(h^+) \tag{9.8-5}$$

For example, Nikuradse found $u_h^+ = 8.5$ for fully rough sand grain roughness, which gives $C_d = 0.0277$.

Simpson [40] has correlated data for a wide variety of roughness patterns in terms of a parameter λ,

$$\lambda = \frac{\text{total surface area}}{\text{total roughness frontal area normal to flow}} \tag{9.8-6}$$

then with the height of the roughness elements as the characteristic height, for fully rough walls

$$1 \leq \lambda \leq 4.68 : \quad u_h^+ = 5.5\text{-}17.35[1.625\log\lambda\text{-}1] \tag{9.8-7a}$$

$$\lambda > 4.68 : \quad u_h^+ = 5.5\text{-}5.95[1.103\log\lambda\text{-}1] \tag{9.8-7b}$$

Note that for sandgrain roughness, $\lambda = 3.23$. The shift of the logarithmic region of the rough wall velocity profiles was used to determine B, but the actual evaluation was done by a number of different workers, and both tube flows and external boundary layers were considered. Given the scatter in the data leading to Eqs. (9.8-7), and the uncertainties in data reduction, expressions for C_d developed for the particular roughness pattern of concern should be used whenever possible.

For untested roughness patterns C_d may be at least estimated using data for the drag of individual proturberances, as was done by Lewis [41]. For transitionally rough surfaces in the absence of specific data, the expression for u_h^+ given as Eq. (9.3-33) is recommended.

Origin for the y-coordinate

A somewhat troublesome point in the preceding development is to establish where the y-coordinate should be measured from. If the origin for y is shifted, an initially straight logarithmic region will become curved. Thus in reducing experimental data the standard practice has been to adjust the origin to give the greatest extent of logarithmic region. The origin found in this manner has always proven to be between the top and bottom of the roughness elements, and to be independent of wall shear, i.e., indepedent of h^+. For example, Reda [16] found for sandgrain roughness that the origin lay at approximately half the grain-size below the tips. Pimenta, Moffat and Kays [15] showed that, for spherical ball roughness elements of equivalent sandgrain roughness of 0.031 in., the appropriate origin lay 0.006 in. below the ball tips for untranspired flow, independent of x-location or free-stream velocity.

Correlations for C_h

The commonly used correlations for the sub-layer Stanton number C_h have been developed from constant specific heat experimental data, for which Eq. (9.8-3) becomes

$$C_h = \frac{q_w}{\rho c v^* (T_w - T_h)} \tag{9.8-8}$$

The most well known correlation of C_h is that for sandgrain indentation roughness developed by Dipprey and Sabersky [38], based on measurements of pressure drop and heat transfer in tube flow. The flow region was divided into two regions with Eq. (9.8-8) characterizing heat transfer to the wall from the location y = h: the thermal resistance of the turbulent core was found by applying Reynolds analogy and assuming that the bulk velocity and bulk temperature occur at the same value of y. Summing the two thermal resistances in series gives

$$\frac{1}{C_H} = \left(\frac{2}{C_F}\right)^{1/2} \left[Pr_t (u_b^+ - u_h^+) + \frac{1}{C_h}\right] \tag{9.8-9}$$

With the assumption of $Pr_t = 1$, and noting that $u_b^+ = (2/C_F)^{1/2}$, there results

$$\frac{1}{C_h} = \left(\frac{2}{C_F}\right)^{1/2} \left[\frac{1}{C_H} - \frac{2}{C_F}\right] + u_h^+ \tag{9.8-10}$$

For fully rough flow with $u_h^+ = 8.5$, Dipprey and Sabersky obtained

$$C_h = \frac{1}{5.19} k_s^{+-0.2} Pr^{-0.44} \tag{9.8-11}$$

However, to the inherent uncertainty in the original data for heat transfer and pressure drop must be added the errors incurred by using an approximate solution of the energy conservation equation in obtaining Eq. (9.8-9). Such errors increase with roughness height, as shown in [42].

Available experimental evidence shows that the sub-layer Stanton number is quite dependent on the nature of the roughness pattern. Although considerable data exists for regular patterns of the kind used to artificially roughen surfaces, data for roughness patterns characteristic of ablating re-entry vehicles are very sparse.

Effect of blowing for fully rough walls

The only comprehensive study of the effect of blowing on rough wall boundary layers is that of Pimenta et al. [15]. Pimenta found that the effect of blowing on the logarithmic portion of the velocity profile was well represented by a Stevenson type law of the wall, Eq. (9.3-21), in the form

$$\frac{2}{u_w^+}(1+v_w^+u^+)^{1/2} = \frac{1}{\kappa}\ln\frac{y+\Delta y}{z_o} \qquad (9.8\text{-}12)$$

where z_o is defined as the value of y where $u^+ = (v_w^+)^{-1}$, y is measured from the tops of the spherical ball roughness elements, and Δy was determined to give the greatest extent of logarithmic velocity profile. For no blowing Δy = 0.006 in. while the equivalent sandgrain roughness was 0.031 in. With blowing Δy was found to increase slightly to 0.008 in. at F = $(\dot{m}/\rho_e u_e)$ = 0.002, and 0.009 in. at F = 0.004. Values of u_h^+, i.e., u^+ at $y+\Delta y = k_s$ calculated from the measured velocity profiles are presented in Table 9.3. Plate number refers to a 4 in. long segment of the total length of 8 ft. It can be seen that u_h^+ apparently decreases with increasing x, though this trend might well be due to a systematic error. Nevertheless, there is considerable evidence in the

Plate No.	7	10	13	16	19	22
F = 0.000	8.98	8.71	8.75	8.60	8.50	8.35
= 0.002	8.55	8.31	8.17	8.01	7.89	8.03
= 0.0039	8.42	8.06	7.62	6.09	7.16	(7.66)?

Table 9.3. Values of u_h^+ calculated from the velocity profiles of Pimenta et al. [15].

literature that Nikuradse's conclusion of u_h^+ = 8.5 for fully rough unblown walls irrespective of Reynolds number is not fully warranted. Table 9.4 shows averaged and derived quantities calculated from the data of Table 9.3. A

F	u_h^+	C_d	C_d/C_{d0}	B_d
0.0	8.65	0.0270	1.00	0.00
0.002	8.16	0.0300	1.11	0.15
0.0039	7.67	0.0340	1.26	0.29

Table 9.4. Roughness drag coefficient as a function of blowing; $B_d = 2F/C_{d0}$

suitable correlation for the effect of blowing is

$$\frac{C_d}{C_{d0}} \simeq 1 + 0.8B_d \tag{9.8-13}$$

Notice that the effect of blowing is to *increase* the value of C_d. This is not a surprising result if we realize that we cannot view C_d as a skin friction coefficient similar to that for a Couette flow or boundary layer: we are not prescribing the velocity at $y = h$, rather u_h results from the interaction of the form drag on the roughness elements, the effect of blowing adding zero momentum fluid to the flow, and the characteristics of the turbulent core. An analysis of the analogous problem for laminar Couette flow over a smooth wall shows that C_d does increase with blowing: we should expect the same behavior in the turbulent rough wall case as well since the first order effect in both cases arises from the addition of zero-momentum fluid to the flow.

Pimenta found that the temperature profile has a logarithmic region of about the same extent as does the velocity profile when the same virtual origin shift is used. Consequently the dimensionless temperature $(T_w-T)/(T_w-T_e)$ plotted against u/u_e is linear and is independent of the definition of virtual origin for y. The graph has a non-zero intercept with the ordinate axis indicating the expected high thermal resistance adjacent to the wall. The sublayer Stanton number C_h calculated from Pimenta's velocity profiles is shown

in Table 9.5. It is very difficult to discern any trends in C_h, and for engineering purposes it is recommended that

$$C_h = 0.10 \tag{9.8-14}$$

Plate	7	10	13	16	19	22
F = 0.000	0.12	0.11	0.11	0.11	0.11	0.11
= 0.002	0.10	0.08	0.08	0.09	0.09	0.07
= 0.0039	0.13	0.10	0.10	0.09	0.07	0.06

Table 9.5. Sub-layer Stanton number as a function of position and blowing rate.

Again, to explain why C_h is essentially independent of blowing, a laminar smooth wall Couette flow analysis gives some insight, since such an analysis shows that the variation of C_h with blowing should be only one half that of C_d; since we have already seen that variation of C_d is rather small the near constant C_h is not inconsistent.

Effect of wall boundary condition on heat and mass transfer

Burck [43] classified roughness types into two categories: (i) integral roughness, e.g., grooves cut into the surface, and (ii) overlaid roughness, e.g., wire wrap. He demonstrated that for identical geometries the overlaid roughness gave significantly lower heat transfer rates, and attributed this result to the poor thermal contact between the overlaid roughness elements and the wall. Thus the thermal conductivity of the roughness elements themselves must also have an effect on the heat transfer to the wall, and is accounted for in the sub-layer Stanton number. Dipprey and Sabersky used a nickel wall, with thermal conductivity k = 50 Btu/hr ft °F. Simple calculations [44] show that the thermal resistance of the roughness elements was of the same order as the thermal resistance of the sub-layer, and their ratio was a marked function of h^+. It follows that there could be an appreciable significant error in Eq.

(9.8-11), or in its interpretation. Also it follows that errors will be incurred when Eq. (9.8-11) is applied to a wall of lower conductivity such as a carbonaceous heat shield, or a wall of higher conductivity, such as the copper ball covered wall of the "PANT" experimental program [45].

Furthermore, once the question of the thermal path through the roughness elements is raised, it is necessary to carefully examine the ablation processes occurring on the heat shield, i.e., heat up, oxidation and sublimation, since there is no longer any simple analogy between the heat and mass transfer problem for the coupled boundary layer-wall response problem. For mass loss by oxidation or sublimation the appropriate wall material for a heat transfer experiment is one of infinite thermal conductivity, as both processes take place at the surface. Thus the choice of copper ball roughness elements in the PANT program was fortuitously appropriate.

REFERENCES FOR CHAPTER 9

1. E. R. van Driest, "Turbulent boundary layer in compressible fluids" J. Aeronaut. Sci., 18, 145-160 (1951).

2. T. Cebeci and A. M. O. Smith, Analysis of Turbulent Boundary Layers, Academic Press, NY (1974).

3. S. G. Rubin, "Compressible turbulent boundary layer equations", AIAA Journal, 5, 1919-1920 (1967).

4. R. B. Landis, "Numerical solution of variable property turbulent boundary layers with foreign gas injection" Ph.D. dissertation, School of Engineering and Applied Science, University of California, Los Angeles (1971).

5. J. N. Hunt, Incompressible Fluid Dynamics, American Elsevier Publishing Co. (1964).

6. B. E. Launder and D. B. Spalding, Mathematical Models of Turbulence, Academic Press, London (1972).

7. H. Schlichting, Boundary Layer Theory, 4th ed. McGraw-Hill Book Co. Inc., NY (1960).

8. F. H. Clauser, "The turbulent boundary layer" in Advances in Applied Mechanics, Vol. IV, Academic Press, NY (1956).

9. F. M. White, Viscous Fluid Flow, McGraw-Hill Book Co. Inc., NY (1974).

10. D. E. Coles, "The law of the wake in the turbulent boundary layer" J. Fluid Mech. 1, 191-226 (1956).

11. F. M. White and G. H. Christoph, "A simple theory for the two-dimensional compressible turbulent boundary layer", J. Basic Engr. 94, 636-642 (1972).

12. R. B. Landis and A. F. Mills, "The calculation of turbulent boundary layers with foreign gas injection" Int. J. Heat Mass Transfer, 15, 1905-1932 (1972).

13. T. N. Stevenson, "A law of the wall of turbulent boundary layers with suction or injection" The College of Aeronautics, Cranfield, Aero Report No. 166 (1963).

14. R. L. Simpson, "Characteristics of turbulent boundary layers at low Reynolds numbers with and without transpiration" J. Fluid Mech., 42, 769-802 (1970).

15. M. M. Pimenta, R. J. Moffat and W. M. Kays, "The turbulent boundary layer: an experimental study of the transport of momentum and heat with the effect of roughness" Thermosciences Division, Department of Mechanical Engineering, Stanford University, Report No. HMT-21, (1975).

16. D. C. Reda, F. C. Kelter, Jr. and C. Fan, "Compressible turbulent skin friction on rough and rough/wavy walls in adiabatic flow" AIAA Journal, 13, 553-554 (1975).

17. J. Nikuradse, "Laws of flow in rough pipes" NACA TM 1292 (1950).

18. L. Prandtl, "Bericht uber Untersuchungen zur ausgebildeten Turbulenz" ZAMM, 5, 136 (1925).

19. D. K. Edwards, V. E. Denny and A. F. Mills, Transfer Processes, 2nd ed. McGraw-Hill - Hemisphere Press, (1979).

20. M. P. Escudier, "The distribution of mixing-length in turbulent flows near walls" Imperial College, Heat Transfer Section Rep. TWF/TN/1 (1966).

21. E. R. van Driest, "On turbulent flow near a wall" J. Aero. Sci., 23, 1007 (1956).

22. S. V. Patankar and D. B. Spalding, Heat and Mass Transfer in Boundary Layers, Morgan-Grampian, London (1967).

23. B. E. Launder and W. P. Jones, "A note on Bradshaw's hypothesis for laminarization", ASME Paper 69-HT-12 (1969).

24. W. M. Kays and R. J. Moffat, "The behavior of transpired turbulent boundary layers" in Studies in Convection Vol. 1, ed. B. E. Launder, Academic Press, 1975.

25. D. B. Spalding, "GENMIX - A general computer program for two dimensional parabolic phenomena" HMT Vol. 1, Pergamon Press (1978).

26. A. T. Wassel, "A finite-difference aeroheating code for axi-symmetric re-entry vehicles" Report 75-66, Science Applications Inc. El Segundo, (1975).

27. A. Wortman and G. Soo-Hoo, "Exact operator solutions of general three-dimensional boundary layer flow equations" J. Aircraft 13, 590 (1976).

28. R. M. Kendall and E. P. Bartlett, "Non-similar solution of the multicomponent laminar boundary layer by an integral matrix method" AIAA Journal 6, 1039 (1968).

29. L. W. Anderson and H. L. Morse, "Users Manual - Boundary layer integral matrix procedure - BLIMP" AFWL TR-69-114, Vol. I, October 1971.

30. D. B. Spalding, "Contribution to the theory of heat transfer across a turbulent boundary layer" Int. J. Heat Mass Transfer, 7, 743-762 (1964).

31. W. M. Kays, Convective Heat and Mass Transfer, McGraw-Hill, NY (1966).

32. R. B. Landis and A. F. Mills, "The calculation of turbulent boundary layers with foreign gas injection" Int. J. Heat Mass Transfer 15, 1905-1932 (1972).

33. L. O. F. Jeromin, "The status of research in turbulent boundary layers with fluid injection" Progress in Aeronautical Sciences, Vol. 10, edited by D. Kuchemann, pp. 65-189, Pergamon Press, Oxford (1970).

34. E. R. G. Eckert, "Engineering relations for friction and heat transfer to surfaces in high velocity flow" J. Aero. Sci. 22, 585-587 (1955).

35. E. L. Knuth and H. Dershin, "Use of reference states in predicting transport rates in high-speed turbulent flows with mass transfer" Int. J. Heat Mass Transfer, 6, 999-1018 (1963).

36. J. M. Healzer, R. J. Moffat and W. M. Kays, "The turbulent boundary layer on a rough porous plate: experimental heat transfer with uniform blowing" Report No. HMT-18, Thermosciences Division, Dept. Mech. Eng., Stanford University (1974).

37. F. E. Goddard Jr., "Effect of uniformly distributed roughness on turbulent skin-friction drag at supersonic speeds" J. Aerospace Sci. 26, 1-15 (1959).

38. D. F. Dipprey and R. H. Sabersky, "Heat and momentum transfer in smooth and rough tubes at various Prandtl numbers" Int. J. Heat Mass Transfer, 6, 329-353 (1963).

39. C. L. V. Jayatilleke, "The influence of Prandtl number and surface roughness on the resistance of the laminar sub-layer to momentum and heat-transfer" Progress in Heat and Mass Transfer, Vol. 1, ed. U. Grigull and E. Hahne, Pergamon Press (1969).

40. R. L. Simpson, "A generalized correlation of roughness density effects on the turbulent boundary layer" AIAA Journal, 11, 242-244 (1973).

41. M. J. Lewis, "An elementary analysis for predicting the momentum - and heat-transfer characteristics of a hydraulically rough surface" J. Heat Transfer, 97, 249-254 (1975).

42. A. T. Wassel and A. F. Mills, "Calculation of variable property turbulent friction and heat transfer in rough pipes" submitted to the J. Heat Transfer.

43. E. Burck, "Influence of Prandtl number on heat transfer and pressure drop of artifically roughened channels" Warme und Stoffubertragung, 2, 87-98 (1969).

44. A. F. Mills and J. F. Courtney, "Turbulent boundary layers on rough walls" AFOSR-TR-76-1098, March 1976.

45. M. R. Wool, et al., Final Summary Report, Passive Nosetip Technology Program, Aerotherm Report 75-150, SAMSO TR-74-86, June 1975.

46. V. E. Denny and R. B. Landis, "An improved transformation of the Patankar-Spalding type for the numerical solution of two-dimensional boundary layer flows" Int. J. Heat Mass Transfer, 14, 1859-1862 (1971).